

**PREEMPTION STRATEGY FOR TRAFFIC SIGNALS AT
INTERSECTIONS NEAR HIGHWAY-RAILROAD GRADE
CROSSINGS**

A Dissertation

by

HANSEON CHO

Submitted to the Office of Graduate Studies of
Texas A&M University
in partial fulfillment of the requirements for the degree of

DOCTOR OF PHILOSOPHY

December 2003

Major Subject: Civil Engineering

**PREEMPTION STRATEGY FOR TRAFFIC SIGNALS AT
INTERSECTIONS NEAR HIGHWAY-RAILROAD GRADE
CROSSINGS**

A Dissertation

by

HANSEON CHO

Submitted to Texas A&M University
in partial fulfillment of the requirements
for the degree of

DOCTOR OF PHILOSOPHY

Approved as to style and content by:

Laurence R. Rilett
(Chair of Committee)

Thomas Urbanik II
(Member)

Don Woods
(Member)

Clifford Spiegelman
(Member)

Kevin Balke
(Member)

Paul Roschke
(Interim Head of Department)

December 2003

Major Subject: Civil Engineering

ABSTRACT

Preemption Strategy for Traffic Signals at Intersections near
Highway-Railroad Grade Crossings. (December 2003)

Hanseon Cho, B.S., Ajou University;

M.S., Ajou University

Chair Of Advisory Committee: Dr. Laurence R. Rilett

Because the operational characteristics of signalized intersections near highway-railroad grade crossings (IHRGCs) are different from those of signalized intersections located elsewhere in the traffic system, standard operational strategies do not apply. This is because safe operation at IHRGCs takes precedence over all other objectives.

Because the prime objective of the current preemption methods is to clear the crossing, secondary objectives such as safe pedestrian crossing time and minimized delay are given less consideration or ignored completely. Consequently, state-of-the-practice strategies may cause serious pedestrian safety and efficiency problems at IHRGCs. Therefore, there is a definite need for research on how to improve traffic signal preemption strategies.

An important element of preemption strategy is detection of trains and prediction of arrival times. However, because of the limitations of current detection technologies, estimation algorithms, etc., there is a wide range in these warning times. In this dissertation, a new train-arrival prediction algorithm was developed using detection equipment located farther upstream from the HRGC.

The state-of-the-art transition preemption strategy (TPS) was developed to ensure that as preemption is initiated by approaching trains, the signal display does not change in a manner that endangers either pedestrians or drivers. However, because it does not

account for the variability of predicted train arrival times, there is still a possibility of failure.

Therefore, a new transition preemption algorithm that is specifically designed to improve intersection performance while maintaining or improving the current level of safety is developed. This dissertation developed a preemption strategy (TPS3) that uses better train arrival time estimates to improve the safety and efficiency of IHRGCs. The approach was simulated on a test bed in College Station, Texas, and it was concluded that the new TPS improves the safety and operation of intersections near highway-railroad grade crossings.

ACKNOWLEDGMENTS

First of all, I would like to thank Dr. Larry Rilett not only for his technical knowledge and insight, but also for his encouragement and guidance in the preparation of this dissertation. Furthermore, I would like to thank Dr. Don Woods, Dr. Tom Urbanik, and Dr. Clifford Spiegelman for providing their technical expertise and for devoting their time to serve on my committee.

Special thanks is offered to Dr. Kevin Balke for his sincere advice and for providing support and needed facilities so that I could concentrate on my research. I would also like to express my heartfelt gratitude to Mr. Roelof Englebrect for sincere assistance in response to my continuous questions. Finally, I want to express my sincere appreciation to my mother, Heejin Kim; two brothers, Hanjoo and Hanwoo; my wife, Soyoung; and my lovely daughter, Yoonjoo, for consistently trusting and supporting me.

TABLE OF CONTENTS

	Page
ABSTRACT	iii
ACKNOWLEDGMENTS.....	v
TABLE OF CONTENTS.....	vi
LIST OF FIGURES	x
LIST OF TABLES.....	xv
 CHAPTER	
I INTRODUCTION.....	1
1.1 Problem Statement.....	1
1.2 Research Objectives.....	3
1.3 Scope of Study.....	3
1.3.1 Forecasting Train Arrival Time.....	3
1.3.2 Preemption Transition Methodology.....	4
1.3.3 Organization.....	5
II LITERATURE REVIEW.....	6
2.1 Preemption Guideline and Preemption Sequence.....	6
2.1.1 Preemption Standard and Guidelines.....	6
2.1.2 Preemption Sequence.....	9
2.1.2.1 Entry into Preemption	9
2.1.2.2 Terminating the Current Phase	10
2.1.2.3 Timing the Track Clearance Phase	11
2.1.2.4 Preemption Hold Interval	11
2.1.2.5 Return to Normal Operations	12
2.2 Timing of Track Clearance Phase.....	12
2.2.1 Queue Clearance Time.....	12
2.2.2 Clearance Time to Avoid Preempt Trap	16
2.2.2.1 Increasing the Track Clearance Green Time	21
2.2.2.2 Actuating the End of Track Clearance Green.....	22
2.2.2.3 Using Two Preempts.....	23
2.2.2.4 Controlling Variation in the Advance Preemption Time	23
2.2.2.5 Controlling Variation in the Right-of-Way Transfer Time	24
2.2.2.6 Avoiding Use of Advance Preemption.....	25

CHAPTER	Page
2.3	Train Detector Technologies 25
2.3.1	First Generation Technologies 26
2.3.1.1	Conventional Detection Systems 26
2.3.1.2	Motion Detection Systems 27
2.3.1.3	Constant Warning Time (CWT) Systems 27
2.3.1.4	Inductive Loop Systems 28
2.3.1.5	Extension of Conventional Railroad Track Circuits 29
2.3.2	Second Generation Technologies 29
2.3.2.1	Sonic 29
2.3.2.2	Doppler Radar 30
2.3.3	Third Generation Technologies 30
2.3.3.1	AVI/Radio Frequency 30
2.3.3.2	GPS 31
2.4	Transition Preemption Strategy (TPS) 31
2.5	Train Arrival Time Prediction 36
2.6	Concluding Remarks 37
III STUDY DESIGN 39	
3.1	Test Bed 39
3.1.1	Test Bed for Development of New Train Arrival Time Prediction Algorithm 39
3.2.2	Test Bed for Development of New TPS 41
3.2	Prediction Algorithm 44
3.3	TPS Algorithm 45
3.4	Micro-Simulation 48
3.5	Development of the VAP Traffic Signal Controller Logic 50
3.5.1	Permissive Coordinated Mode 51
3.5.2	Transition Modes Back to Normal Mode 52
3.6	VAP and Hardware-in-the-Loop Comparison 53
3.7	Method to Emulate Trains in Simulation 56
3.8	Simulation Design 58
3.9	Concluding Remarks 59
IV DEVELOPING A TRAIN ARRIVAL TIME PREDICTION ALGORITHM 61	
4.1	Preliminary Analysis 62
4.2	Artificial Neural Network (ANN) Model Design 76
4.2.1	Input Variables for ANN 76
4.2.2	ANN Design 77
4.2.3	ANN Results 80
4.3	Modular Artificial Neural Network (MANN) Design 81

CHAPTER	Page
4.3.1	Clustering Analysis..... 82
4.3.2	MANN Results 87
4.4	Comparison of the MANN Model with Other Approaches 90
4.5	Prediction Interval of MANN 95
4.6	Concluding Remarks..... 100
V	DEVELOPING A TRANSITION PREEMPTION STRATEGY FOR IHRGC..... 102
5.1	Overview of Current TPS (TPS1)..... 103
5.1.1	Issue 1: Inappropriate Minimum Time 104
5.1.1.1	Case 1: Case When There Is Still a Vehicle Call for the Current Phase..... 108
5.1.1.2	Case 2: Case When There is No Call for the Current Phase 110
5.1.2	Issue 2: Longer Service Times of the Dwell Phases..... 111
5.1.2.1	Case 1: When There Is Still a Call for the Current Phase (Phase 2 or 6)..... 113
5.1.2.2	Case 2: When There Is No Call for the Current Phase (Phase 2 or 6)..... 117
5.2	Developing the New TPS Algorithm (TPS2)..... 118
5.3	Modifying the New TPS Algorithm Associated with the Prediction Error Bound (TPS3) 128
5.4	Concluding Remarks..... 139
VI	SENSITIVITY ANALYSIS..... 141
6.1	Simulation Design..... 141
6.1.1	Simulation Duration..... 141
6.1.2	Estimating the Difference between CWT and Actual Arrival Time 143
6.1.3	Simulation Scenarios 150
6.2	Simulation Results (Fixed Train Arrival Times)..... 154
6.2.1	Metric 1: Truncation of Pedestrian Clearance Interval Results 154
6.2.2	Metric 2: Phase Length Results..... 161
6.2.3	Metric 3: Delay Results..... 167
6.2.3.1	Effect of TPS Algorithm 167
6.2.3.2	Effect of Pedestrians 179
6.2.3.3	Effect of Train Speed Profile..... 182
6.2.3.4	Preemption Trap..... 188
6.3	Simulation Results and Findings with Random Train Arrival 189
6.3.1	Truncation of Pedestrian Clearance Interval..... 189
6.3.2	Results..... 190
6.4	Benefit/Cost Analysis..... 190
6.5	Concluding Remarks..... 197

	Page
6.5.1	TPS Algorithm..... 197
6.5.2	Effect of Pedestrians 198
6.5.3	Effect of Train Speed Profile..... 199
6.5.4	Effect of Random Train Arrival 199
6.5.5	Benefit/Cost Analysis 199
VII	CONCLUSIONS 201
7.1	Summary 201
7.1.1	Prediction Algorithm 201
7.1.2	The Transition Preemption Strategy Algorithm..... 201
7.2	Conclusions 202
7.2.1	Predicted Arrival Time 202
7.2.2	The Transition Preemption Strategy Algorithm..... 202
7.2.3	Benefit/Cost Analysis 204
7.3	Future Research 204
	GLOSSARY 206
	NOTATIONS 213
	REFERENCES 217
APPENDIX A	AAE AND OPTIMAL NUMBER OF ITERATIONS FOR EACH ANN STRUCTURE AND EACH GROUP IN 2, 3, AND 4 GROUPINGS 222
APPENDIX B	TPS ALGORITHM FLOW CHARTS 231
APPENDIX C	FIXED TRAIN ARRIVAL TIME 237
APPENDIX D	RANDOM TRAIN ARRIVAL TIME 259
VITA 288

LIST OF FIGURES

	Page
FIGURE 2-1 Preemption Sequence and the Required Variables for Each Step.....	9
FIGURE 2-2 Crossing Clearance Geometry for Calculating t_2	16
FIGURE 2-3 Relationship between Each Element of Preemption During Simultaneous Preemption	18
FIGURE 2-4 Relationship between Each Element of Preemption During Advance Preemption	18
FIGURE 2-5 Scenario of Preempt Trap	20
FIGURE 2-6 Conventional Train Detection Systems	27
FIGURE 3-1 Map of Wellborn Corridor, College Station, Texas	41
FIGURE 3-2 Site Detail for George Bush Drive and Wellborn Road Intersection.....	42
FIGURE 3-3 Conceptualization of the Normal Preemption.....	47
FIGURE 3-4 Conceptualization of Preemption Using the TPS1 Algorithm.....	48
FIGURE 3-5 Framework of Hardware-in-the-Loop System.....	49
FIGURE 3-6 An Example of the Method to Calculate the Detector Length to Emulate the Real Train	58
FIGURE 3-7 Relationship between the Real World and the Simulation World.....	59
FIGURE 4-1 Histogram of Instantaneous Train Speed at FM 2818	63
FIGURE 4-2 Histogram of Instantaneous Train Speed at George Bush Drive	64
FIGURE 4-3 Histogram of Average Train Speed at FM 2818	64
FIGURE 4-4 Average Train Speed versus Time in Detection at FM 2818.....	66

	Page
FIGURE 4-5 Average Train Acceleration/Deceleration versus Time in Detection at FM 2818	66
FIGURE 4-6 Number of Speed Observations for Time in Detection	67
FIGURE 4-7 Histogram of Arrival Time from FM 2818 to George Bush Drive	68
FIGURE 4-8 Histogram of Train Length.....	69
FIGURE 4-9 Histogram of Time in Detection.....	70
FIGURE 4-10 Time in Detection versus Average Train Speed.....	71
FIGURE 4-11 Time in Detection versus Train Length	72
FIGURE 4-12 Average Train Speed versus Train Length.....	72
FIGURE 4-13 Train Arrival Time versus Average Train Speed	74
FIGURE 4-14 Train Arrival Time versus Time in Detection.....	75
FIGURE 4-15 Train Arrival Time versus Train Length.....	75
FIGURE 4-16 Input-Output Structure of Artificial Neural Network Model.....	79
FIGURE 4-17 Error Sum of Squares versus Group Number after 10 Seconds of Detection	83
FIGURE 4-18 Average Speed versus Time in Detection for Four Groups (Model 15: 150 seconds of detection time)	85
FIGURE 4-19 Average Speed versus Time in Detection for Three Groups (Model 15: 150 seconds of detection time).....	85
FIGURE 4-20 Average Speed versus Time in Detection for Two Groups (Model 15: 150 seconds of detection time)	86
FIGURE 4-21 A Schematic Diagram of the Bootstrap Applied to Problems with a General Data Structure $P \rightarrow x$	97
FIGURE 5-1 Signal Procedure with Current M_j	107

	Page
FIGURE 5-2 Signal Procedure with Suggested M_j	108
FIGURE 5-3 Time Frame When There Is Still a Vehicle Call for the Current Phase	109
FIGURE 5-4 Time Frame with No Vehicle Call for the Current Phase.....	111
FIGURE 5-5 Conditions to Provide Longer Service Times of the Dwell Phase	112
FIGURE 5-6 Ring Structure.....	113
FIGURE 5-7 Time Frame with a Vehicle Call for the Current Phases (Phase 2 or 6).....	114
FIGURE 5-8 Time Frame with No Vehicle Call for the Current Phase (Phase 2 or 6).....	118
FIGURE 5-9 Phase Number of Each Movement and Phase Sequence for Developing the TPS2 Algorithm.....	120
FIGURE 5-10 Time Frame of Earlier Arrival Case	129
FIGURE 5-11 Time Frame of the Late Arrival Case	132
FIGURE 5-12 Example of Histogram of Sample Means and (1-0.05) Percentile Lower and Upper Bound.....	134
FIGURE 5-13 Application of Prediction Error to Predicted Arrival Time in Case of $U < 0$	137
FIGURE 5-14 Application of Prediction Error to Predicted Arrival Time in Case of $U > 0$	137
FIGURE 6-1 Change of Volume during Simulation	142
FIGURE 6-2 Time Frame for Analysis Period and Train Arrival Time Range at the Crossing during Simulation for Fixed Train Arrival Time	143
FIGURE 6-3 Preemption Warning Time versus First Train Speed.....	145
FIGURE 6-4 Preemption Warning Time versus Last Train Speed	145

	Page
FIGURE 6-5 Preemption Warning Time versus Average Train Speed.....	146
FIGURE 6-6 Preemption Warning Time versus Difference in Train Speed	146
FIGURE 6-7 Speed Profile of the 30 Trains in Each Subgroup	153
FIGURE 6-8 Example of a Pedestrian Phase Truncation for the TPS1 (Train 3, APWT = 80 seconds).....	157
FIGURE 6-9 Example of a Pedestrian Phase Truncation for the TPS1 (Train 89, APWT = 110 seconds).....	158
FIGURE 6-10 Equivalent Annual Cost of Each Element versus Interest Rate	192
FIGURE 6-11 B/C Ratio Depending on the Probability of Accident Considering Property Only Damage as the Benefit	195
FIGURE 6-12 B/C Ratio versus Value of Time	197
FIGURE B-1 Flow Chart of the Current TPS Algorithm.....	232
FIGURE B-2 Flow Chart of the TPS2 Algorithm	233
FIGURE B-3 Flow Chart of the TPS3 Algorithm	235
FIGURE C-1 Average Delay versus APWT for each TPS Algorithm (Delay Comparison Period; Pedestrian Phase Active Scenario; and Fixed Train Arrival Time)	240
FIGURE C-2 Average Delay versus APWT for each TPS Algorithm (Analysis Period; Pedestrian Phase Active Scenario; and Fixed Train Arrival Time).....	242
FIGURE C-3 Average Delay versus APWT for each TPS Algorithm (Delay Comparison Period; Pedestrian Phase Inactive Scenario; and Fixed Train Arrival Time).....	245
FIGURE C-4 Average Delay versus APWT for each TPS Algorithm (Analysis Period; Pedestrian Phase Inactive Scenario; and Fixed Train Arrival Time).....	247

	Page
FIGURE D-1 Time Frame for Analysis Period and Train Arrival Time Range at the Crossing during Simulation for Random Train Arrival Time	260
FIGURE D-2 Average Delay versus APWT for each TPS Algorithm (Delay Comparison Period; Pedestrian Phase Active Scenario; and Random Train Arrival Time)	264
FIGURE D-3 Average Delay versus APWT for Each TPS Algorithm (Analysis Period; Pedestrian Phase Active Scenario; and Random Train Arrival Time).....	267
FIGURE D-4 Average Delay versus APWT for Each TPS Algorithm (Delay Comparison Period; Pedestrian Phase Inactive Scenario; and Random Train Arrival Time)	270
FIGURE D-5 Average Delay versus APWT for Each TPS Algorithm (Analysis Period; Pedestrian Phase Inactive Scenario; and Random Train Arrival Time).....	273

LIST OF TABLES

		Page
TABLE 3-1	Signal Control Variables at the Intersection of George Bush and Wellborn.....	43
TABLE 3-2	Signal Control Variables in Preemption Mode at the Intersection of George Bush Drive and Wellborn Road.....	44
TABLE 3-3	Signal Timing for Hardware-in-the-Loop System.....	54
TABLE 3-4	Signal Timing for VAP.....	55
TABLE 4-1	Summary Statistics at FM 2818 and George Bush.....	63
TABLE 4-2	Selected Seconds after Detection for the Input Speed.....	77
TABLE 4-3	Average Absolute Error as Function of Time in Detection.....	81
TABLE 4-4	Number of Trains in Training Set and Testing Set for Each Model Tested.....	87
TABLE 4-5	Best Group Size and AAE versus Time in Detection.....	89
TABLE 4-6	AAE for Different Linear Regression Models.....	92
TABLE 4-7	AAE for Current Method, Best MLR Model, Best ANN, and Best MANN.....	94
TABLE 4-8	Prediction Interval Depending on Significant Level and Input Data Duration with Model Refitting.....	100
TABLE 5-1	Prediction Interval Depending on Significant Level and Input Data Duration without Model Refitting.....	135
TABLE 6-1	Correlation between the Variables.....	144
TABLE 6-2	Results of the Simple Regression Models.....	147
TABLE 6-3	Correlation between the Independent Variables in Each of the Multiple Linear Regression Models.....	149

	Page
TABLE 6-4 Results of the Multiple Regression Models	149
TABLE 6-5 Number of Train Speed Observations in Each Group Depending on Time in Detection	154
TABLE 6-6 Number of Pedestrian Phase Truncations and Average Phase Abbreviation Time at the Onset of Preemption for Pedestrian Phase Active Scenario and Fixed Train Arrival Time	155
TABLE 6-7 Average TPS Duration as Function of Advance Preemption Warning Time for Pedestrian Phase Active Scenario and Fixed Train Arrival Time.....	160
TABLE 6-8 Total Phase Length for APWT and TPS Algorithms (Comparison Period for Signal Timing ¹ ; Pedestrian Phase Active Scenario; and Fixed Train Arrival Time).....	163
TABLE 6-9 Total Phase Length for APWT and TPS Algorithms (Comparison Period for Signal Timing ¹ ; Pedestrian Phase Inactive Scenario; and Fixed Train Arrival Time)	166
TABLE 6-10 Average Delay (Delay Comparison Period ¹ ; Pedestrian Phase Active Scenario; and Fixed Train Arrival Time)	168
TABLE 6-11 Results of Duncan Test between TPS Algorithms (Delay Comparison Period ¹ ; Pedestrian Phase Active Scenario; Fixed Train Arrival Time; and Pooled Test).....	171
TABLE 6-12 Average Delay (Delay Comparison Period ¹ ; Pedestrian Phase Inactive Scenario; and Fixed Train Arrival Time)	172
TABLE 6-13 Results of Duncan Test between TPS Algorithms (Delay Comparison Period ¹ ; Pedestrian Phase Inactive Scenario; Fixed Train Arrival Time; and Pooled Test).....	173
TABLE 6-14 Delays during the Comparison Period (APWT of 120 Seconds; Pedestrian Phase Active Scenario; and Fixed Train Arrival Time).....	174
TABLE 6-15 Results of Duncan Test between TPS Algorithms (Delay Comparison Period ¹ ; Pedestrian Phase Active Scenario; and Fixed Train Arrival Time)	176

	Page
TABLE 6-16 Results of Duncan Test between TPS Algorithms (Delay Comparison Period; Pedestrian Phase Inactive Scenario; and Fixed Train Arrival Time).....	178
TABLE 6-17 Results of Paired t-Test between Two Pedestrian Scenarios (Pedestrian Phase Active Scenario vs. Pedestrian Phase Inactive Scenario) for Fixed Train Arrival.....	180
TABLE 6-18 Average Delay of Each Movement During Analysis Period ¹ for Pedestrian Phase Active Scenario and Fixed Train Arrival Time.....	181
TABLE 6-19 Average Delay of Each Movement During Analysis Period ¹ for Pedestrian Phase Inactive Scenario and Fixed Train Arrival Time.....	182
TABLE 6-20 Average Delay by Train Group (Delay Comparison Period ¹ ; Pedestrian Phase Active Scenario; and Fixed Train Arrival Time).....	183
TABLE 6-21 Results of Duncan Test between Train Speed Groups (Delay Comparison Period ¹ ; Pedestrian Phase Active Scenario; and Fixed Train Arrival Time)	184
TABLE 6-22 Number of Pedestrian Phase Truncations and Average Phase Abbreviation Time at the Onset of Preemption by Train Speed Group for Pedestrian Phase Active Scenario and Fixed Train Arrival Time	185
TABLE 6-23 Average Delay by Group (Delay Comparison Period ¹ ; Pedestrian Phase Inactive Scenario; and Fixed Train Arrival Time)	186
TABLE 6-24 Results of Duncan Test between Train Speed Groups (Delay Comparison Period ¹ ; Pedestrian Phase Inactive Scenario; and Fixed Train Arrival Time).....	187
TABLE 6-25 Average Train Speed, Average Train Length, and Average Blocking Time by Each Train Group	188
TABLE 6-26 Elements of the TPS3 System and Its Cost.....	191
TABLE 6-27 Calculation of Number of Pedestrian Phase Truncations	193
TABLE 6-28 Comprehensive Costs in Police-Reported Crashes by K-A-B-C Scale Severity (1994).....	193

	Page
TABLE 6-29 Accident Cost Depending on the Probability of Accident and the Accident Severity	194
TABLE 6-30 Calculation of Annual Delay Reduced	196
TABLE A-1 AAE and Optimal Number of Iterations for Each ANN Structure and Each Group in 2 Grouping.....	223
TABLE A-2 AAE and Optimal Number of Iterations for Each ANN Structure and Each Group in 3 Grouping.....	225
TABLE A-3 AAE and Optimal Number of Iterations for Each ANN Structure and Each Group in 4 Grouping.....	228
TABLE C-1 Total Phase Length versus APWT and TPS Algorithms during Analysis Period ¹ for Pedestrian Phase Active Scenario and Fixed Train Arrival Time.....	238
TABLE C-2 Total Phase Length versus APWT and TPS Algorithms during Analysis Period ¹ for Pedestrian Phase Inactive Scenario and Fixed Train Arrival Time.....	239
TABLE C-3 Average Delay (Analysis Period ¹ ; Pedestrian Phase Active Scenario; and Fixed Train Arrival Time).....	241
TABLE C-4 Results of Duncan Test between TPS Algorithms (Analysis Period ¹ ; Pedestrian Phase Active Scenario; and Fixed Train Arrival Time).....	243
TABLE C-5 Average Delay (Analysis Period ¹ ; Pedestrian Phase Inactive Scenario; and Fixed Train Arrival Time).....	246
TABLE C-6 Results of Duncan Test between TPS Algorithms (Analysis Period ¹ ; Pedestrian Phase Inactive Scenario; and Fixed Train Arrival Time).....	248
TABLE C-7 Average Delay of Each Movement for APWT and TPS Algorithms (Analysis Period ¹ ; Pedestrian Phase Active Scenario; and Fixed Train Arrival Time)	249

	Page
TABLE C-8 Average Delay of Each Movement for APWT and TPS Algorithms (Analysis Period ¹ ; Pedestrian Phase Inactive Scenario; and Fixed Train Arrival Time)	250
TABLE C-9 Average Delay by Group and APWT (Delay Comparison Period ¹ ; Pedestrian Phase Active Scenario; and Fixed Train Arrival Time).....	251
TABLE C-10 Average Delay by Group and APWT (Analysis Period ¹ ; Pedestrian Phase Active Scenario; and Fixed Train Arrival Time).....	252
TABLE C-11 Average Delay by Group (Analysis Period ¹ ; Pedestrian Phase Active Scenario; and Fixed Train Arrival Time)	253
TABLE C-12 Results of Duncan Test between Train Speed Groups (Analysis Period ¹ ; Pedestrian Phase Active Scenario; and Fixed Train Arrival Time).....	253
TABLE C-13 Average Delay by Group and APWT (Delay Comparison Period ¹ ; Pedestrian Phase Inactive Scenario; and Fixed Train Arrival Time).....	255
TABLE C-14 Average Delay by Group and APWT (Analysis Period ¹ ; Pedestrian Phase Inactive Scenario; and Fixed Train Arrival Time).....	256
TABLE C-15 Average Delay by Group (Analysis Period ¹ ; Pedestrian Phase Inactive Scenario; and Fixed Train Arrival Time)	257
TABLE C-16 Results of Duncan Test between Train Speed Groups (Analysis Period ¹ ; Pedestrian Phase Inactive Scenario; and Fixed Train Arrival Time).....	257
TABLE D-1 Number of Pedestrian Phase Truncations and Average Phase Abbreviation Time at the Onset of Preemption for Pedestrian Phase Active Scenario and Random Train Arrival Time.....	261
TABLE D-2 Number of Pedestrian Phase Truncations and Average Phase Abbreviation Time at the Onset of Preemption for Pedestrian Phase Inactive Scenario and Random Train Arrival Time	262
TABLE D-3 Average Delay (Delay Comparison Period ¹ ; Pedestrian Phase Active Scenario; and Random Train Arrival Time)	263

	Page
TABLE D-4 Results of Duncan Test between TPS Algorithms (Delay Comparison Period ¹ ; Pedestrian Phase Active Scenario; and Random Train Arrival Time)	265
TABLE D-5 Average Delay (Analysis Period ¹ ; Pedestrian Phase Active Scenario; and Random Train Arrival Time)	266
TABLE D-6 Results of Duncan Test between TPS Algorithms (Analysis Period ¹ ; Pedestrian Phase Active Scenario; and Random Train Arrival Time).....	268
TABLE D-7 Average Delay (Delay Comparison Period ¹ ; Pedestrian Phase Inactive Scenario; and Random Train Arrival Time)	269
TABLE D-8 Results of Duncan Test between TPS Algorithms (Delay Comparison Period ¹ ; Pedestrian Phase Inactive Scenario; and Random Train Arrival Time)	271
TABLE D-9 Average Delay (Analysis Period ¹ ; Pedestrian Phase Inactive Scenario; and Random Train Arrival Time)	272
TABLE D-10 Results of Duncan Test between TPS Algorithms (Analysis Period ¹ ; Pedestrian Phase Inactive Scenario; and Random Train Arrival Time).....	274
TABLE D-11 Results of Paired t-Test between Two Pedestrian Volumes for Random Train Arrival Time.....	275
TABLE D-12 Average Delay by Group (Delay Comparison Period ¹ ; Pedestrian Phase Active Scenario; and Random Train Arrival Time)	276
TABLE D-13 Average Delay by Group and APWT (Delay Comparison Period ¹ ; Pedestrian Phase Active Scenario; and Random Train Arrival Time).....	277
TABLE D-14 Results of Duncan Test between Train Speed Groups (Delay Comparison Period ¹ ; Pedestrian Phase Active Scenario; and Random Train Arrival Time)	278
TABLE D-15 Average Delay by Group (Analysis Period ¹ ; Pedestrian Phase Active Scenario; and Random Train Arrival Time)	279

	Page
TABLE D-16 Average Delay by Group and APWT (Analysis Period ¹ ; Pedestrian Phase Active Scenario; and Random Train Arrival Time).....	280
TABLE D-17 Results of Duncan Test between Train Speed Groups (Analysis Period ¹ ; Pedestrian Phase Active Scenario; and Random Train Arrival Time).....	281
TABLE D-18 Average Delay by Group (Delay Comparison Period ¹ ; Pedestrian Phase Inactive Scenario; and Random Train Arrival Time).....	282
TABLE D-19 Average Delay by Group and APWT (Delay Comparison Period ¹ ; Pedestrian Phase Inactive Scenario; and Random Train Arrival Time).....	283
TABLE D-20 Results of Duncan Test between Train Speed Groups (Delay Comparison Period ¹ ; Pedestrian Phase Inactive Scenario; and Random Train Arrival Time)	284
TABLE D-21 Average Delay by Group (Analysis Period ¹ ; Pedestrian Phase Inactive Scenario; and Random Train Arrival Time).....	285
TABLE D-22 Average Delay by Group and APWT (Analysis Period ¹ ; Pedestrian Phase Inactive Scenario; and Random Train Arrival Time).....	286
TABLE D-23 Results of Duncan Test between Train Speed Groups (Analysis Period ¹ ; Pedestrian Phase Inactive Scenario; and Random Train Arrival Time).....	287

CHAPTER I

INTRODUCTION

1.1 PROBLEM STATEMENT

Because the operational characteristics of signalized intersections near highway-railroad grade crossings (IHRGCs) differ from those of signalized intersections elsewhere in the traffic system, standard operational strategies do not apply. With an IHRGC, safe operation takes precedence over all other objectives. When a train is detected approaching the highway-railroad grade crossing (HRGC), the normal traffic signal operation is preempted to ensure all queued vehicles on the track are cleared before the train reaches the crossing. The traffic signal operation timing plan of the IHRGC, the distance between the intersection and the HRGC, and the traffic conditions on each approach of the intersection are important factors in identifying the track clearance strategy. Important elements of the preemption strategy include detecting the train and predicting its arrival time at the crossing. Because the prime objective of the current preemption methods is to clear the crossing, secondary objectives, such as safe pedestrian crossing time and minimizing delay, are given less consideration or ignored completely. Consequently, state-of-the-practice strategies may cause serious pedestrian safety and efficiency problems at the IHRGC. Given the large number of traffic signals in close proximity to highway-railway grade crossings in the U.S., the fact that current architecture may not be adequate with respect to safety and efficiency, and the high cost of accidents, there is a definite need for research on how to improve traffic signal preemption strategies at IHRGCs.

On the surface, the preemption logic of traffic signal controllers at IHRGCs is relatively simple. That is 1) as a train approaches the crossing it must be detected a certain time before it actually reaches the crossing, and 2) the vehicles must be cleared from the

This dissertation follows the style and format of the *Transportation Research Record*.

HRGC before some set time period. This must all be accomplished in a way that does not endanger other users of the intersection such as pedestrians. However, a number of complex elements need to be considered when developing a successful preemption strategy. A key requirement to any preemption strategy is estimating the train arrival time. The estimate may be in terms of when crossing gates come down, or it may be in terms of a time headway until the train enters the HRGC. Currently, railroad companies in the U.S. are required to give a minimum of 20 seconds of warning time before their trains arrive at crossings with active warning devices. However, because of the limitations of current detection technologies, estimation algorithms, etc., a wide range of warning times occurs. For example, it has been shown in Knoxville, Tennessee, that the range in warning time varies from 20 seconds to 90 seconds with an average value of 41.7 seconds (1). The uncertainty in arrival time arises because existing prediction methods assume that the train's speed at the time of detection remains constant until the train reaches the crossing. The relatively short period of warning time occurs because the train detection equipment is located fairly close to the HRGC. As the accuracy of the predicted train arrival time improves, it would be expected that the traffic signal controller of the IHRGC will be able to initiate the preemption strategy closer to the ideal time, thus improving the safety and efficiency of the IHRGC. In addition, if the train arrival time can be predicted earlier, then more robust preemption strategies may be employed that also will increase the efficiency and safety of the IHRGC. One goal of this research is to develop new train arrival prediction algorithms using detection equipment located further upstream from the HRGC. It is anticipated that the mean arrival time and a prediction interval will be estimated, and that both will be used in the signal timing methodology.

The number of preemption strategies available depends on the arrival time estimate and its accuracy. Recently, the transition preemption strategy (TPS) was developed at the Texas Transportation Institute (2,3,4,5,6) that explicitly accounts for the current signal status at the onset of preemption. The goal of the TPS algorithm was to ensure that as

the preemption was initiated by approaching trains, the signal display did not change in a manner that endangered either pedestrians or drivers. Although the TPS algorithm provides a smooth transition to preemption, the developers did not account for the variability of predicted train arrival times when identifying the default parameters. Therefore, even though the goal of TPS is to eliminate the case where the minimum vehicle time and pedestrian clearance time will be truncated before the preemption begins, in practice this goal is not achieved successfully. Also, it does not account for overall intersection performance. That is, the TPS algorithm may operate the signal in an ineffective manner with respect to the intersection performance as a whole (1,2,3,4,5,6). Therefore, a new transition preemption algorithm that is specifically designed to improve the intersection performance while maintaining or improving the current level of safety is required. The focus of the research described in this dissertation is on developing a better preemption strategies and a better train arrival time predict methodology in order to improve the safety and efficiency of IHRGCs.

1.2 RESEARCH OBJECTIVES

The objectives of this research are to develop 1) an accurate prediction algorithm of train arrival time, which includes prediction bounds on the estimate, at the HRGC based on data from upstream detectors, and 2) a new transition preemption strategy that uses the predicted arrival time and associated prediction intervals in the transition preemption methodology to operate signalized intersections near highway-railroad crossings in a safe and efficient manner.

1.3 SCOPE OF STUDY

1.3.1 Forecasting Train Arrival Time

Better forecasting of train arrival time is essential if improved IHRGC preemption strategies are to be developed. The transition preemption methodology requires a forecast of the train arrival time that must occur sooner than required under the normal preemption strategy. To provide the earlier forecast train arrival time, the current TPS

assumes the train travels at a constant speed from the time of last detection until it arrives at the HRGC. The constant speed is equal to the last observed speed. This assumption is problematic because if the train is accelerating (decelerating), the normal preemption will begin later (earlier) than the optimal time. In addition, because the current approach uses only one speed measurement, the trend of speed change is not reflected to the prediction algorithm.

Regardless of which prediction algorithm is used, the forecast will be subject to some error. Therefore, the forecast train arrival time should be updated as new speed data are obtained in order to reduce the prediction error. The updated prediction time will be used within the transition preemption methodology. In this dissertation, a new train arrival prediction algorithm is developed using time series speed data from Doppler microwave radar. Also, the prediction error bounds are obtained, and the method to incorporate these bounds into the new transition preemption strategy is developed.

1.3.2 Preemption Transition Methodology

Because 1) state-of-the-practice preemption strategies are designed to clear queued vehicles off the tracks as quickly as possible, and 2) the preemption warning time is relatively small, the current state-of-the-practice preemption algorithm is typically operated so that the track clearance phase has the higher priority. This means that the minimum vehicle and/or pedestrian clearance length may not be provided. A direct result of this strategy is that vehicle and/or pedestrian phases that conflict with the track clearance phase can be terminated abruptly. Thus, an inadequate minimum green time may be provided to pedestrians or vehicles that have already entered the intersection. As discussed in Section 1.1, the TPS algorithm was developed to eliminate the probability that the minimum vehicle time and pedestrian clearance time will not be provided before a preemption begins. This design, however, can result in sub-optimal performance of the intersection as a whole. Furthermore, the TPS was designed to be deterministic. Because the developers did not account for variability of predicted arrival time, a

possibility still exists that the controller will truncate a minimum vehicle time or pedestrian clearance interval when preemption occurs. That is, the logic is based solely on average arrival time. Using a prediction interval about the estimated arrival time could improve the operating condition of the signal. For example, the current transition preemption algorithm may provide more green time to the main street phase, which is parallel to the railroad, even though these approaches do not have any vehicle on them before the preemption. Because these phases also are provided during the preemption, providing more green time to the phases before the preemption is not necessary. Intuitively, the transition algorithm should provide more time to the phases that are not active during preemption. Therefore, a new transition preemption strategy is needed to efficiently operate the intersection during the transition into preemption.

1.3.3 Organization

Chapter II provides a literature review of the state of the art of the main research. It includes an introduction to preemption guidelines and sequence, train detector technologies, train arrival time prediction algorithms, and the transition preemption strategy. Chapter III provides the methodology of this study. It contains the simulation methods for sensitivity analysis and a description of the test bed. A new train arrival time prediction algorithm and a new transition preemption strategy are developed in Chapters IV and V, respectively. The methodology is demonstrated on a test bed in College Station, Texas, as shown in Chapter VI. The findings of this dissertation and the future research are presented in Chapter VII.

CHAPTER II

LITERATURE REVIEW

Many steps should be followed when considering the implementation of signal preemption at the IHRGC. The first step is to determine if preemption is required at the intersection. If preemption is needed, the preemption sequence should be designed considering the specific conditions of the intersection and the crossing. In this chapter traffic signal preemption strategies at IHRGCs will be reviewed. The train detection technologies, the current transition preemption strategy, and train arrival time prediction algorithms also will be reviewed.

2.1 PREEMPTION GUIDELINE AND PREEMPTION SEQUENCE

2.1.1 Preemption Standard and Guidelines

The *Manual on Uniform Traffic Control Devices* (MUTCD) states that “On tracks where trains operate at speeds of 20 mph or higher, circuits controlling automatic flashing light signals shall provide for a minimum operation of 20 seconds before arrival of any train on such track” (7). The Association of American Railroads (AAR) *Signal Manual* states that “warning time devices shall operate for a minimum of 20 seconds before a train operating at maximum speed enters the crossing” (8,9).

To provide the appropriate warning time, the location of the train detector is critical. In North America, the detector location is based on a minimum warning time (MWT). The recommended value from the MUTCD and the AAR *Signal Manual* is 20 seconds. The product of the fastest train expected and the minimum warning time is used to identify detector location as shown in Equation 2-1 (10).

$$\Delta = \Phi \times W \quad (2-1)$$

where;

$$\Delta = \text{Detector location from the crossing (m);}$$

- Φ = Fastest allowable train speed for the track (m/s); and
 W = Minimum warning time provided to crossing users (s).

Equation 2-2 from the AAR *Signal Manual* shows all of the additive factors that should be considered when calculating the total warning time (8,10). The total warning time, W^* , is a function of the width of the crossing, equipment response time, safety buffer time, preemption time, and minimum warning time.

$$W^* = W + \chi + \phi + \beta \quad (2-2)$$

$$\chi = \text{Roundup}\left(\frac{\delta - 10.7}{3}\right) \quad (2-3)$$

where;

- W^* = Total warning time (s);
 χ = Clearance time for each additional track clearance distance (s);
 δ = Minimum track clearance distance (m);
 ϕ = Adjustment time (s); and
 β = Buffer time added for safety purposes into the minimum warning time (s).

If the minimum track clearance distance is greater than 10.7 m, additional time, known as the clearance time (χ), is provided. AAR recommends 1 second of clearance time (χ) for each additional 3.0 m of track clearance distance as shown in Equation 2-3. The adjustment time, ϕ , accounts for equipment response, motion sensing and constant warning time detectors, and automatic gate activation time. Automatic gates should activate no less than 3 seconds after the flashing light signals are started. The AAR also allows a buffer time (β) to be added for safety purposes. The β is based on engineering judgment but should be less than 25 percent of the sum of δ plus χ (8,9,10).

The MUTCD recommends that preemption should be applied when the distance between a signalized intersection and the HRGC is less than 60 m (200 ft). However, no explanation is provided on how this recommendation was identified. Generally, preemption may be required at an intersection, even when the distance is more than 60 m, if the prevailing queuing characteristics result in blockage of the HRGC. Recently, Marshall and Berg showed that preemption should be considered even if the intersection is located farther from the HRGC than the 60 m based on an analysis using macroscopic traffic flow modeling procedures (9,11). Based on the results of the study, the authors contend that preemption should be implemented wherever the possibility of collision between trains and queued vehicles exists, regardless of the distance.

Preemption warning time is often longer than the total warning time because the phase clearance time of the operation phase and track clearance time should be provided before trains arrive at the HRGC. Preemption warning time is calculated considering the time from the start of preemption to the end of the separation time after track clearance time as shown in Equations 2-4 and 2-5. If the total warning time is greater than preemption warning time, the total warning time should be used as the preemption warning time.

$$P_{WT} = \gamma + \sigma + Y_i + R_i + \tau + \Omega \quad (2-4)$$

$$P_{WT} = \text{Max}(P_{WT}, W^*) \quad (2-5)$$

where;

P_{WT} = Preemption warning time (s);

γ = Minimum green time for any vehicle phase and any pedestrian phase at the onset of the preemption (s);

σ = *Selective pedestrian clearance*: The time provided to clear a terminating walk during the transition to track green (s);

Y_i = Yellow interval of current phase i (s);

R_i = All-Red interval of current phase i (s);

τ = Track clearance time (s); and

Ω = Separation time (s).

2.1.2 Preemption Sequence

All controllers currently in use have the same basic preemption sequencing, in accordance with currently accepted practice (10,12). The normal preemption sequence and the required variables for each step are shown in Figure 2-1.

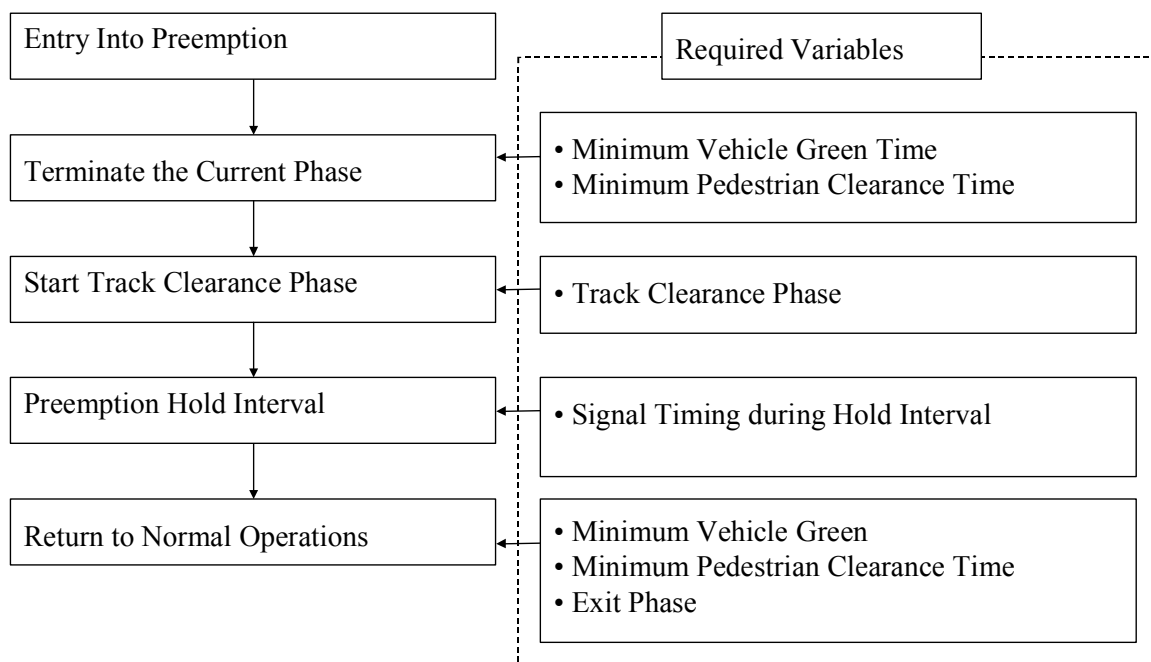


FIGURE 2-1 Preemption Sequence and the Required Variables for Each Step

2.1.2.1 Entry into Preemption

Because time available before the train arrives at the HRGC is relatively short, the signal controller usually initiates the preemption sequence immediately upon detection of an approaching train. However, several signal controllers have the ability to choose between a locking and nonlocking mode of operation, similar to that of inductive loop detectors. In the locking mode, the preemption sequences are initiated immediately and

cannot be shortened or aborted once the sequence has been initiated. The only exception is for start-up flash or external start. In the nonlocking mode, a programmable delay timer is started once the train is detected. If the preemption call is still present when the timer has expired, the preemption is initiated. If the preemption call is no longer there, as would be the case if the train had stopped and reversed direction, the preemption is not initiated and normal operation would continue (10,13,14).

2.1.2.2 Terminating the Current Phase

At certain points in the cycle, the termination can occur immediately at the onset of preemption and, thus, the track clearance phase is provided directly, that is, in the case that the minimum green time and pedestrian clearance time are already provided at the onset of preemption. At other points, however, the current phase must be extended to provide the minimum interval time prior to implementing the track clearance phase. Therefore, the point at which the difference between the start of preemption and the start of track clearance time, known as the wait time, would be the greatest must be identified in the cycle. The required wait time prior to the track clearance phase is termed the right-of-way transfer time. It is calculated based on Equation 2-6.

$$\begin{aligned}
 K &= Y_i + R_i && \text{if } c - S_i \geq \max(\gamma, \sigma) \forall i && (2-6) \\
 &= \max(\gamma, \sigma) - (c - S_i) + Y_i + R_i && \text{if } c - S_i < \max(\gamma, \sigma) \forall i
 \end{aligned}$$

where;

- K = Right-of-way transfer time (s);
- S_i = Start time of phase i in the cycle (s) ($i = 1, \dots, \text{Number of phases in the cycle}$);
- c = Time in the cycle (s);
- γ = Minimum green time for any vehicle phase and any pedestrian phase at the onset of the preemption (s);
- σ = *Selective pedestrian clearance*: The time provided to clear a terminating walk during the transition to track green (s); and

Y_i = Yellow interval of current phase i (s);

R_i = All-Red interval of current phase i (s);

The maximum right-of-way transfer time occurs when the preemption signal is received at the beginning of a phase or a pedestrian clearance interval. The wait time is added to the required preemption warning time. The clearance interval of the phase being terminated also must be considered in the required preemption warning time, as it must be provided in its entirety. If a preemption is activated during a clearance interval of any phase, the remainder of the clearance interval should be provided and the track clearance phases initiated immediately thereafter (10,13).

2.1.2.3 Timing the Track Clearance Phase

After the operation phase has been terminated and the clearance interval has been provided, a track clearance green time must be provided that is long enough to clear vehicles that may be queued over the track. The duration of the track clearance time should be based on the maximum number of queued vehicles that need to be cleared before the train arrives (10,11,13,14).

2.1.2.4 Preemption Hold Interval

The preemption hold interval occurs after the track clearance interval. It occurs when the train is near or in the crossing. Once the preemption hold interval begins, the controllers keeps it active until the train has left the detection zone. The MUTCD suggests that the signals be operated to permit vehicle movements that do not cross the tracks once the train is in the crossing. It does not mention whether it is permissible to cycle through all phases that do not conflict with the track. Many traffic signal controllers provide a function to allow the signal indication to cycle, alternately serving traffic flows that do not conflict with the train movement (2,7,10,14).

In addition, there is no apparent reason why nonconflicting pedestrian phases could not be served during the hold interval. In fact, it may be wise to do so to avoid having the pedestrians grow impatient and attempt to cross against the signal. Therefore, it is recommended that nonconflicting pedestrian movements be served during the hold intervals (2,7,10,14).

2.1.2.5 Return to Normal Operations

Once the train vacated the crossing, the traffic signal must transition back to its normal mode of operation. The first phase implemented is based on the minimum delay. Generally, most engineers permit the controller to service the approaches that were not served while the crossing was blocked. However, if vehicles from any other of the delayed movements are queue back into an adjacent intersection, some engineers permit to service these movements first to begin clearing the queues (2,10,14).

2.2 TIMING OF TRACK CLEARANCE PHASE

2.2.1 Queue Clearance Time

The length of the track clearance phase should be based on the maximum number of queued vehicles that need to be cleared before the train arrives. Queuing analysis has been applied to estimate the queued vehicles at each particular location. A methodology for this analysis was developed using macroscopic traffic flow modeling procedures (11,13).

The length of queue expected during any signal cycle is a function of the approach volume, cycle length, saturation flow rate, and green split. Although the signalized intersection capacity analysis procedures in the U.S. Highway Capacity Manual (HCM) provide for the calculation of maximum discharge rates, they do not include a storage requirement for precluding spillback into an upstream intersection (15). A simple practical method for doing this is to apply a macroscopic “continuum” model that

assumes constant arrival and discharge flow rates (16). For unsaturated conditions, the time necessary to discharge vehicles queued in a cycle is given as Equation 2-7.

$$t_0 = \frac{\lambda(C - g)}{\mu - \lambda} \quad (2-7)$$

where;

t_0 = Time necessary to discharge vehicles queued in a cycle (s);

λ = Arrival rate (veh/h);

μ = Discharge rate (veh/h);

C = Cycle length (s); and

g = Green split (s).

The maximum number of queue from stopline can then be calculated as Equation 2-8.

$$\rho = \mu t_0 = \mu \left[\frac{\lambda(C - g)}{\mu - \lambda} \right] \frac{1}{3600} \quad (2-8)$$

where;

ρ = Maximum number of queue (veh).

Assuming an average spacing of 6.7 m per vehicle, the maximum average distance that the queue will extend upstream can then be calculated as Equation 2-9.

$$\theta = \frac{\mu}{537} \left[\frac{\lambda(C - g)}{\mu - \lambda} \right] \quad (2-9)$$

where;

θ = Maximum distance of queue (m).

Because the continuum model is based on the assumption of uniform arrivals, Equations 2-8 and 2-9 represent the average queue length that will develop over many cycles.

Assuming an isolated intersection, vehicles will actually arrive in an approximately random distribution. The length of the queue during any particular cycle then will fluctuate about the mean. During some cycles, the queue may extend back over the tracks, and during other cycles, it may not. Therefore, to determine the length of track clearance time, one must first establish the probability with which queues would be expected to spill back over the tracks (13).

A methodology for estimating this probability was developed using the Poisson distribution to approximate random arrival (16). The distribution gives the probability of x vehicles arriving during a given interval as Equation 2-10.

$$P_r(x) = \frac{m^x e^{-m}}{x!} \quad (2-10)$$

where;

- x = Expected number of arrivals in a given time period (= cycle length) (veh); and
- m = Average number of arrivals in a given time period (= cycle length) (veh).

Using queuing analysis, one can estimate the maximum number of queued vehicles that need to be cleared before the train arrives. The desired number of vehicles to be cleared is equal to the expected maximum queue that is between the tracks and the upstream grade signal crossing. However, because of limited preemption warning time, track clearance time is normally set for the distance between the stopline of the intersection and the stopline of the crossing.

Once the desired distance to be cleared is fixed, the track clearance interval can be calculated as shown below. The track clearance interval normally includes two subintervals. The first subinterval is the time for the last queued vehicle to begin to clear the track. Shockwave methodology has been applied as a simplified approach to

calculate the time interval in which “the rate of queue dissipation is equal to the rate at which the starting wave moves backward through the queue” (11,13). The time interval is obtained by dividing the length of queue by the dissipation rate as shown in Equation 2-11.

$$t_l = \frac{Q}{u_w} \times 3.6, \quad u_w = \frac{2q_s}{k_j} \quad (2-11)$$

where;

- t_l = Time interval until the last vehicle in the blocking queue departs (s);
- Q = Length of queue to be cleared as measured from the intersection stopline to the point where a vehicle needing to be cleared may be stopped (m);
- u_w = Backward shockwave speed (km/h);
- q_s = Saturation flow rate (veh/h); and
- k_j = Jam density (veh/km).

The second subinterval is the time needed for the last queued vehicle to accelerate and move to a position clear of the tracks. The first step is to define the area at the tracks from which vehicles must be removed. One definition of the area that should be cleared (as well as a methodology for determining the time required for a vehicle to accelerate across this area) is found in the U.S. procedures for determining sight distance requirements at highway-railroad grade crossings (17).

Assuming the crossing geometry shown in Figure 2-2, any vehicle located within a danger zone, Γ , on either side of the tracks must be cleared completely before a train arrives at the crossing. The critical vehicle for preemption design purposes is shown in Figure 2-2, with its front located at position (a). After time t_1 the vehicle will begin to move and its rear must reach position (b) before the train arrives at the crossing. The time required for this maneuver, t_2 , is expressed in Equation 2-12 (13).

$$t_2 = \frac{v}{a} + \frac{\zeta + 2\Gamma + \Theta - \omega}{v} \quad (2-12)$$

where;

- v = Maximum speed of the design vehicle in first gear (m/s);
- a = Acceleration rate for the design vehicle in first gear (m/s^2);
- ζ = Length of the design vehicle (m);
- Γ = Clearance distance on either side of the tracks (m);
- Θ = Width of the crossing (m); and
- ω = Distance traveled while accelerating to maximum speed in first gear (m).

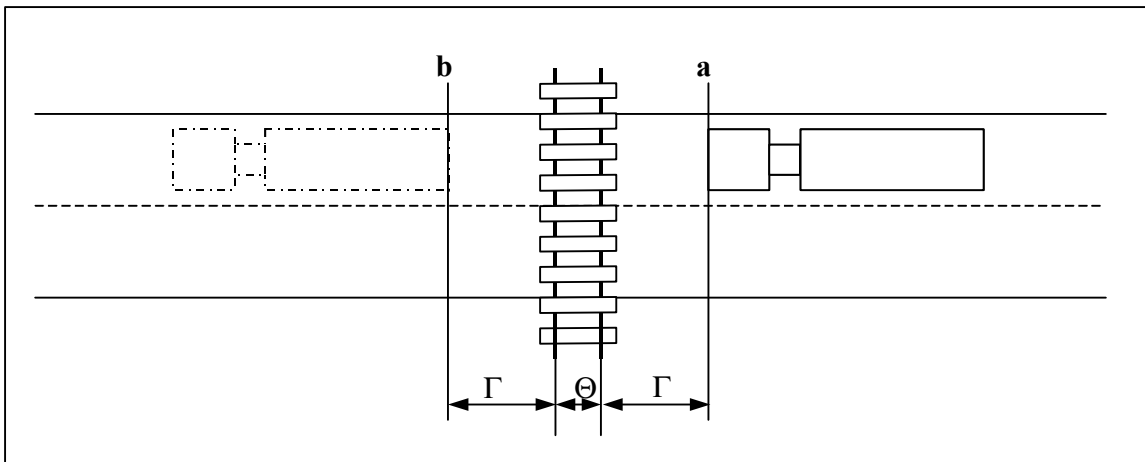


FIGURE 2-2 Crossing Clearance Geometry for Calculating t_2 (13)

2.2.2 Clearance Time to Avoid Preempt Trap

To initiate a preemption sequence, two major executes must occur: 1) the traffic signal controller must receive an electronic signal to start the preemption sequence to clear the tracks, and 2) the active railroad warning devices, including the flashing lights and gates, must be activate to provide the warning signal and stop vehicles from crossing.

The railroad warning devices should be active for a minimum time of 20 seconds before the train arrives at the crossing under normal conditions based on the federal requirements. However, if the crossing is wide or crosses multiple track, or if requested by the highway authority, a MWT longer than 20 seconds may be provided (7).

Two types of preemption are commonly used in practice: 1) simultaneous preemption, and 2) advance preemption. Under simultaneous preemption, the traffic signal controller starts the preemption sequence at the same time that the railroad crossing warning devices activate, providing at least the minimum warning time. Under advance preemption, the traffic signal controller starts the preemption sequence before the railroad crossing devices activate. Advance preemption is required if the time available under simultaneous preemption is not enough to clear the tracks safely (18).

The time difference between when the traffic signal controller starts the preemption sequence and when the railroad crossing warning devices activate is called the advance preemption time. The highway authority usually requests advance preemption time if the minimum warning time is not enough to clear traffic safely off the tracks. The advance preemption time is zero for simultaneous preemption (18,19,20).

The relationship between each element of preemption during simultaneous preemption is shown in Figure 2-3, while Figure 2-4 shows the same for advance preemption.

After the traffic signal controller receives the preempt notification, the right of way must be transferred to traffic in the approach to the intersection crossing the tracks. The required wait time prior to the track clearance phase is termed the right-of-way transfer time. The right-of-way transfer time depends on the controller state and is calculated based on Equation 2-6 in the previous section. Once the right of way is transferred, the track clearance phase is active. The track clearance green should be provided at least equal to the queue clearance time, which is the time it requires a vehicle stopped on the

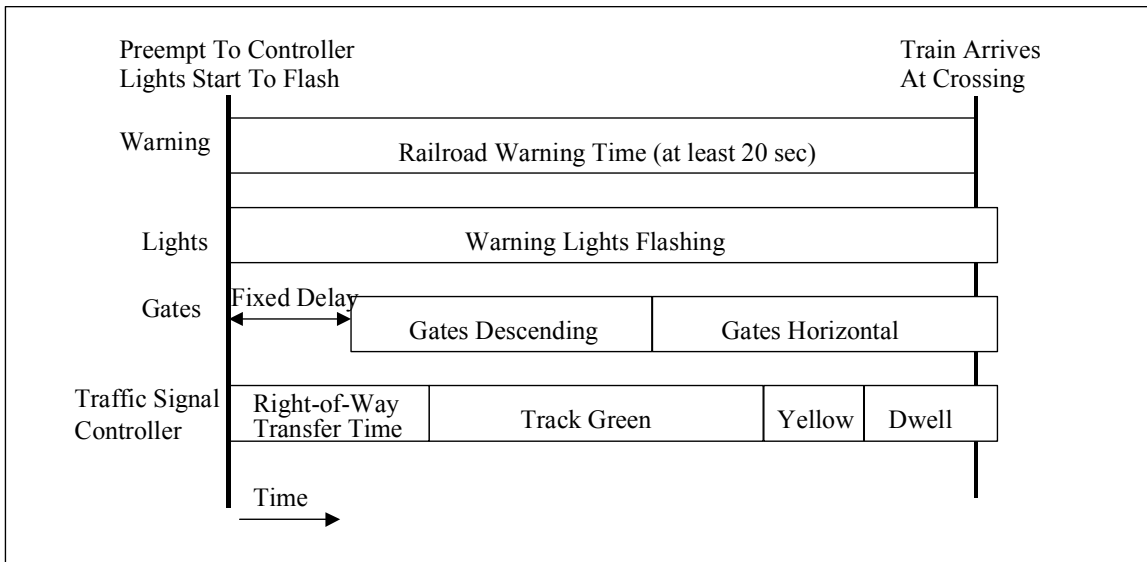


FIGURE 2-3 Relationship between Each Element of Preemption During Simultaneous Preemption (20)

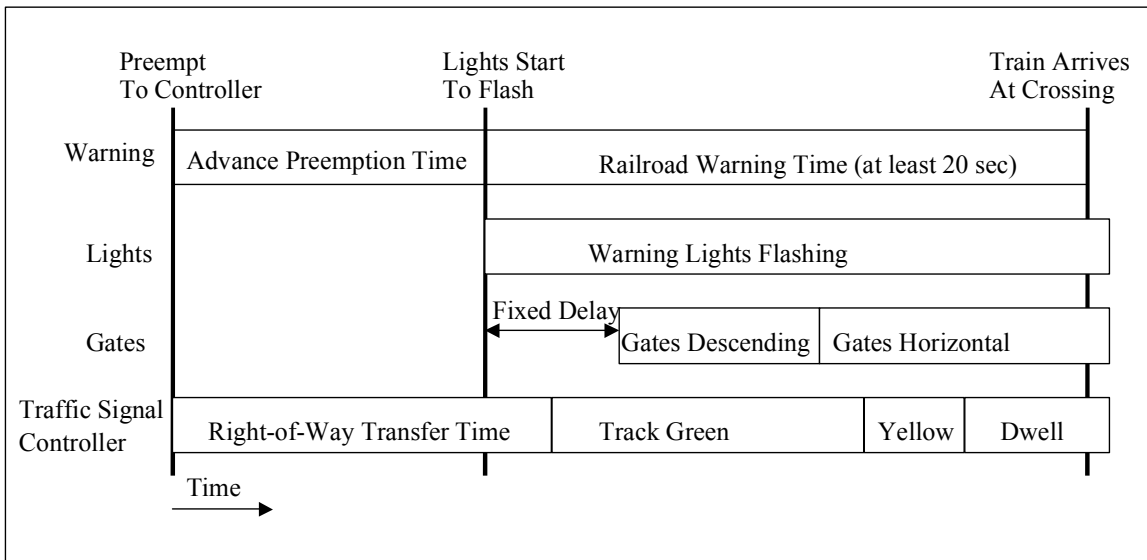


FIGURE 2-4 Relationship between Each Element of Preemption During Advance Preemption (20)

track to start up and move off the tracks (19). The queue clearance time can be calculated using queuing analysis, the distance between the railroad stopline and the intersection stopline, and so on as shown in Section 2.2.1.

From the railroad warning device perspective, first the warning lights flash for 3 to 5 seconds. This period is the “gate delay time” and is needed to warn drivers of the impending gate descent. After the gate delay time, the gates start to descend, and railroad procedures require that the gates be horizontal not less than 5 seconds before the train arrives at the crossing (7,19).

Although the preemption warning time is greater than the sum of the right-of-way transfer time and track clearance time, safe preemption operation may not be guaranteed at the crossing. If the track clearance green ends before the warning lights start to flash, vehicles may be trapped between the intersection stopline and the moving train, or even worse, trapped on the tracks in the path of the oncoming train. The condition where the track clearance green ends before the warning lights start to flash is the “preempt trap” (19).

Figure 2-5 shows an example of a preemption trap. In this example, the crossing under consideration has a maximum right-of-way transfer time of 10 seconds and the track clearance green time was 13 seconds. The median values of the preemption warning time and railroad warning time were 48 seconds and 29 seconds, respectively, from the observed data. If the right-of-way transfer time is zero in this condition, the track clearance green will end 35 seconds ($48 - 13 = 35$) before the train’s arrival at the crossing. Thus, the track clearance green will end 6 seconds ($35 - 29 = 6$) before the warning lights start to flash and 10 seconds before the gates start to descend. During the first 6 seconds after the end of the track clearance green, vehicles have no warning of the imminent preemption and will continue to cross the tracks and possibly stop on the

tracks. However, the track clearance phase has already expired, and there will be no further opportunity to clear (19,20).

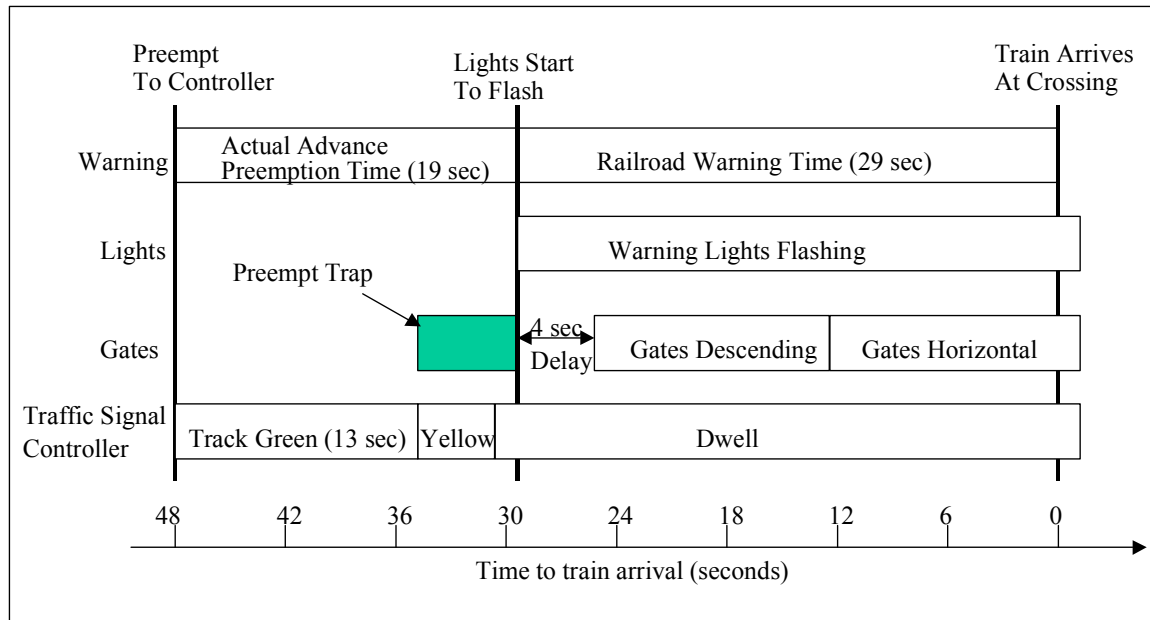


FIGURE 2-5 Scenario of Preempt Trap (20)

The preempt trap only occurs when advance preemption is used at a crossing. Because the warning lights will start to flash at the same time that the traffic signal controller initiates the preempt sequence under simultaneous preemption, the track clearance green cannot end before the lights start to flash. The main reason for the preempt trap is the “uncoupling” of the preempt notification from the warning light activation. If the track clearance green time is less than the advance preemption time, the preempt trap exists even without any warning time variability. Any variability that would increase the advance preemption time would result in a longer and more severe preempt trap. For example, if the 95 percent preemption warning time of 57 seconds occurs together with the median railroad warning time of 29 seconds, the advance preemption time will be $57 - 29 = 28$ seconds, which will result in a preempt trap of $28 - 13 = 15$ seconds. Fifteen

seconds is likely to be enough for vehicles to arrive and fill up the 65 feet of queue space and queue over the tracks thereby creating a preemption trap. As discussed below, several potential solutions exist to remove, or at least mitigate, the preempt trap.

2.2.2.1 Increasing the Track Clearance Green Time

If a track clearance green is less than the advance preemption time, the possibility exists that the track clearance green will end before the warning lights are activated, which results in the preempt trap. The situation worsens if variations in the warning time result in longer advance preemption time. Any increase of the track clearance green will reduce the probability of the preempt trap occurring.

A general rule of thumb for advance preemption is that,

The track clearance green duration should be equal to the expected advance preemption time plus 15 seconds.

This rule of thumb was suggested by Railroad Controls Limited of Fort Worth, Texas. The rationale for this rule of thumb is that the gates are guaranteed to be down 15 seconds after flashing of the warning lights. This is because federal law requires the gates be horizontal for at least the last 5 seconds of the 20 seconds minimum time. Therefore, the 15 seconds in which the gates may not be horizontal should be added to the advance preemption time. Even though this rule of thumb does not consider the variation in advance preemption time, it does contain a safety factor, because the gates do not have to be completely horizontal to block access to the tracks. In addition, the gates may reach the horizontal position less than 15 seconds after the warning lights start to flash.

At the study site intersection, the Wellborn Road and George Bush Drive intersection, College Station, Texas, the gates usually blocked access to the crossing 11 seconds after

the warning lights started to flash. Therefore, the gates reached the horizontal position 4 seconds earlier than the recommended 15 seconds. For this reason, the above-mentioned rule of thumb appears to be somewhat conservative.

For many locations, 30 seconds (19 seconds of expected advance preemption time + 15 seconds) of track clearance green is too long considering the queue clearance time of 10 seconds. Therefore, Engelbrecht, et al. proposed an alternative to the rule of thumb. This alternative involves determining the duration of the track clearance green that would reduce the probability to an acceptable target level using the probability distributions of the various components of the preemption sequence. Engelbrecht, et al. used Monte Carlo analysis to calculate the probability of three or more vehicles in the preempt trap as a function of the track clearance green time and the approach volume using the probability distributions that were observed in the study site crossing. The results show that increasing the track clearance green time results in a significant reduction in exposure to the preempt trap.

It should be noted that due to variability of the predicted train arrival time, no guarantee exists that the gates will be down when the track clearance green ends, even with an increased track clearance green time. It is always possible that the advance preemption time will exceed the track clearance green time.

The only way to completely eliminate the problem is to treat the causes of the problem: the variability in the advance preemption time together with the variability in the right-of-way transfer time. If there were no variability in either of these times, the end of the track clearance green easily could be timed to coincide with the gates descending.

2.2.2.2 Actuating the End of Track Clearance Green

The only way to completely eliminate the problem of the preempt trap is to actuate the end of the track clearance phase with a “gate down” confirmation signal. The traffic

signal controller will initiate the track clearance phase as usual, but will dwell in the track clearance phase until the “gate down” confirmation signal is received.

2.2.2.3 Using Two Preempts

Even if existing traffic signal controllers do not have the function to actuate the end of the track clearance green, one way to implement a similar approach on existing controllers is to use two preempts. This approach uses two different levels of preempt: 1) a lower priority preempt activated at the start of the preemption sequence, and 2) a higher priority preempt activated by the “gates down” confirmation signal. The first, lower priority preempt will initiate the normal preemption sequence, that is, go through the right-of-way transfer sequence without a track clearance interval and then hold the phase. The lower priority preempt will be overridden by the higher priority preempt when the “gates down” confirmation signal is received. Because the traffic signal will already be holding the track clearance phase, no right-of-way transfer would be required and the track clearance phase can start immediately. In this case, the duration of the track clearance green would be only for clearing out the area between the crossing and the intersection, which depends on the distance between the crossing and the intersection.

2.2.2.4 Controlling Variation in the Advance Preemption Time

An additional preemption input into the controller may not be allowed in certain controllers. In these cases, the possibility of preempt trap can be reduced by controlling variability in the advance preemption time and variability in the right-of-way transfer time. Because the speed of an approaching train may change from the time the preemption is activated to the time the railroad warning devices are activated, the advance preemption time can vary. Therefore, to ensure that the gates are horizontal before the end of the track clearance green is difficult. This problem was recognized by the American Railway Engineering and Maintenance-of-Way Association (AREMA) and addressed in their 2000 Edition Signal Manual (21) as follows:

Where advance preemption is utilized, a timing circuit should be employed to maintain a maximum time interval between the initiation of the advance preemption and operation of the warning system for a train move where speed is decreasing. It should be noted, however, that this maximum time interval will decrease in the event train speed is increasing.

Even if a “not-to-exceed” timer is used to control the maximum advance preemption time, it may not be able to prevent shorter advance preemption times. However, because only long advance preemption times result in the preempt trap, this railroad timing solution can be very successful in preventing long advance preemption times, thereby helping to remove the preempt trap.

While the “not-to-exceed” timer can control advance preemption time variation, variation in the right-of-way transfer time can cause a preempt trap, also, and should be controlled as well.

2.2.2.5 Controlling Variation in the Right-of-Way Transfer Time

Right-of-way transfer time can have more variation than advance preemption time, especially when pedestrian clearances are provided. Even though, a maximum value of right-of-way transfer time exists, it can range between zero and a maximum value that depends on the state of the traffic signal controller at the onset of preemption.

One source of variability is that vehicle clearance may or may not be required, depending on whether the controller is in the track clearance phase at the onset of preemption. If it is possible to force the controller to always go through a “clearance time” regardless of the status of the controller, the variation in right-of-way transfer time

could be reduced by the duration of the clearance interval. This actually can be achieved on controllers with a spare phase and by overlapping phases.

2.2.2.6 Avoiding Use of Advance Preemption

If, for some reason, these variance reduction methods cannot be applied, a final treatment for the cause of the preempt trap is to not use advance preemption. The only way to completely eliminate the effects of variability in advance preemption time is to only use simultaneous preemption, as is currently done by the State of Illinois. In this case the minimum warning time may be increased for safe preemption, which usually is more than the minimum time of 20 seconds. The drawback of this approach is that if the railroad warning time is excessively long, the gates may be down for an extended period of time before the train arrives at the crossing, and this can encourage drivers to drive around the gates.

2.3 TRAIN DETECTOR TECHNOLOGIES

Once a train is detected, the detection system sends an electric signal to the traffic signal controller to activate the preemption sequence. A number of detection technologies have been developed for this task. The most common detector system uses the tracks as part of a circuit. When no trains are present, a uniform signal in the form of white noise is sent to the controller. When a train is present, the circuit is completed and a different signal is sent to the controller. Because these systems send only detection information to the traffic signal controller, they can only measure the presence of a train and are therefore referred to as first-generation technology. In contrast, second-generation technologies are capable of providing estimated time of arrival (ETA) information in addition to basic detection information. Generally, these systems are not part of the railway operations and are installed adjacent to the railway. Third-generation technologies go one step further to provide continuously updated train information typically acquired using on-board global positioning systems (GPS) (2,3).

2.3.1 First Generation Technologies

2.3.1.1 Conventional Detection Systems

In these systems, the rails are used as conductors of energy supplied by a battery. The relay remains energized as long as no train is present in the circuit. When a train enters the circuit between the battery and the relay, the train axles shunt the circuit, causing the relay to de-energize. When the relay is de-energized, automatic warning devices are activated and the traffic signal controller near the intersection receives the notification that a train is approaching through a separate interconnection circuit (10,22).

To allow the detection of trains operating in both directions over any single track, conventional train detection systems are composed of three isolated circuits along the track. As shown in Figure 2-6, these include a circuit for each approach on either side of the HRGC and a circuit at the middle of the crossing. These three circuits are separated electronically to provide an isolated circuit in each part. Each circuit is used to detect the presence of a train. Based on the order in which the circuits are actuated the train direction can be ascertained. Considerable variability in actual train arrival time exists because: 1) the track circuit must be long enough to provide a minimum warning time for the fastest train expected on the given site, and 2) the system assumes train speed is constant (3,10,23).

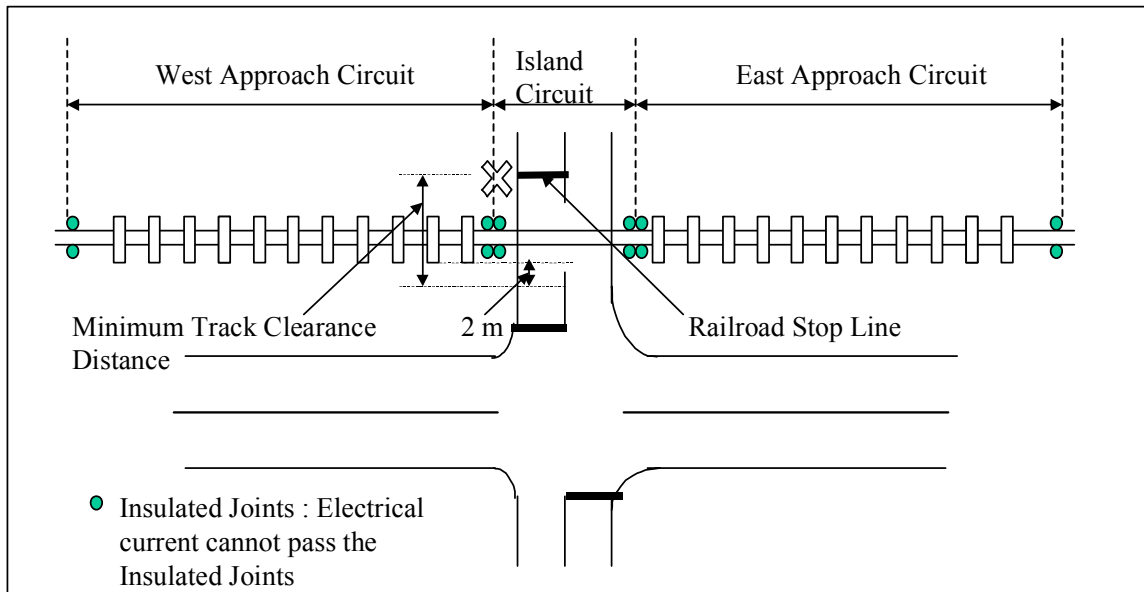


FIGURE 2-6 Conventional Train Detection Systems (10,20)

2.3.1.2 Motion Detection Systems

Motion detection systems employ an alternating current voltage across the two running rails and, therefore, the insulated joints that are needed in the conventional systems, are not required. This system is designed to determine the presence and the direction of motion of a train by continuously measuring the track circuit impedance. If the track circuit is unoccupied or no train is moving within the approach, the impedance of the track circuit is relatively constant. If a train is moving toward the crossing, the track circuit impedance decreases. An increasing track circuit impedance indicates that a train is moving away from the crossing. If the train subsequently stops, the impedance will remain at a constant value. Thus, if a train stops on the approach or moves away from the crossing, the warning device would deactivate (10,23).

2.3.1.3 Constant Warning Time (CWT) Systems

Constant warning time systems utilize advance motion-detection systems to continuously measure the rate of change of the circuit impedance to determine the speed

of the train. Once the position and speed of the train are estimated, the arrival time can be estimated using Equation 2-13 (10).

$$W = \frac{\psi}{V} \quad (2-13)$$

where;

W = Warning time (s);

ψ = Estimated distance from the head of train to the crossing (m); and

V = Train speed (m/s).

The goal is to provide a constant warning time to the controller. Note that it is assumed that the train speed is constant. CWT systems are designed to establish an arrival time prediction at the crossing within the first 15 percent of the approach circuit. Predicted arrival time at the crossing is based on the speed of the train as it enters the circuit, even though the train may accelerate or decelerate after entering a detection circuit. Therefore, there is still some variability in warning time (3,10,23,24).

2.3.1.4 Inductive Loop Systems

Inductive loop detectors are currently being used in a four-quadrant gate system to detect vehicles that may be trapped between the gates. The use of this system is being evaluated as a means of providing a more fail-safe design for four-quadrant gate systems (24). Loop detectors have also been applied to detect transit trains. Several tests revealed that burying these detectors under the track ballast leads to a decrease in the effectiveness of the detector. For this reason, a loop detector that can be mounted directly on the tracks was developed. Systems of three or four detectors are often applied to detect a train approaching a HRGC and activate a preemption of the traffic signal at the IHRGC. However, this technology has similar limitations to the conventional track circuitry approach (25).

2.3.1.5 Extension of Conventional Railroad Track Circuits

It has been proposed by Jacobson, et al. that the conventional track circuits be extended to provide increasing warning time for preemption. The existing detection system would be modified to send the detection signal separately to the traffic signal controller and the railroad warning devices. Therefore, the signal sent to the traffic signal controller could be sent earlier than the signal for the railroad warning devices, which may allow for safer operation. By keeping the detection equipment on the tracks, the need to install additional equipment on the trains that use the crossing does not exist. Also, the fail-safe properties of these systems have been repeatedly tested, and they are currently considered acceptable practice. However, this system is still problematic because it does not account for speed change of approaching trains and the cases where a train may stop within the detection circuit or even reverse direction (3).

2.3.2 Second Generation Technologies

2.3.2.1 Sonic

Sonic waveform detectors have been used to detect trains in several train priority systems. Originally these systems were developed to identify the siren from an emergency vehicle so that the traffic signal controller could provide a green signal for that vehicle when it approaches the intersection. These systems have been modified for trains so that a silent emitter is placed in each locomotive to emit sonic waves that the receiver can detect but are undetectable to the human ears. When the wave is detected, a “preemption” call is sent to the traffic signal controller to activate the preemption sequence. The emitter can be disabled by the driver of the train if preemption is not necessary at the intersection. The major disadvantage of this system is that trains can be detected only within a limited distance of a HRGC. Although the detector can be placed farther away from the crossing to provide a longer warning time, the actual warning time is a function only of the location at which the emitter in the locomotive emits sonic waves (3).

2.3.2.2 Doppler Radar

The system continually measures and records train speed. From the data recorded, train acceleration or deceleration may be estimated. Prediction algorithms also have been developed using the speed, acceleration, and deceleration information. Some of the arrival time prediction algorithms that were developed use the distance of the train and detector from the HRGC along with the train speed. The prediction errors of these algorithms have been recorded to be relatively high (3). For example, a prediction time algorithm that is currently used in College Station, Texas, calculates arrival time by dividing the estimated distance between the train head and the crossing by the last observed train speed. Because this method assumes that the last observed train speed remains constant, the prediction error is approximately ± 17 seconds (12.3 percent of mean absolute percentage error) when the prediction is performed after 100 seconds of observation. More importantly, prediction intervals have not been calculated with any of these methods.

2.3.3 Third Generation Technologies

2.3.3.1 AVI/Radio Frequency

Automatic vehicle identification (AVI) systems have been applied in a number of train applications. An electronic “identification tag” containing information about the train is installed in all or a subset of the vehicles on the train. AVI readers, which are typically radio frequency antenna, are located at various locations along the train right of way. As the train passes the readers, the information from the identification tags is read. Therefore, this system provides more precise train position information than the systems discussed previously. However, because the train information is collected only at discrete locations, only space mean speed between the receiver locations can be calculated. Thus, speed change may not be accurately accounted for when predicting train arrival time, especially when the distance between the receiver locations is long (3,26).

2.3.3.2 GPS

A global positioning system uses satellites orbiting the earth to collect information on the train as it approaches the HRGC. The GPS device is located on the lead locomotive. Using this device and the satellites, the train's position on the tracks, direction of travel, and train speed at any point along the approach to the HRGC are obtained. Because the information is updated continuously, the forecast train arrival time can be updated continuously. Even though this system is superior to any other system for collecting more accurate train information, there are a number of issues. For example, the safety and operation of the system is entirely dependent on 1) access to U.S. military GPS satellite information, 2) the ability of GPS receivers on trains to remain in relatively constant radio communication with satellites, and 3) that there is a sufficient communication ability to transmit train information to the traffic management center (3,27).

2.4 TRANSITION PREEMPTION STRATEGY (TPS)

Because the general preemption sequence is designed to clear queued vehicles on the tracks as quickly as possible, the minimum vehicle and/or pedestrian phase length may not be provided. Therefore, it may be argued that the current system does not 1) generally account for the safety of pedestrian, or 2) attempt to maximize intersection efficiency. For example, the vehicular and pedestrian phase that conflicts with the track clearance phase can be truncated before the minimum phase length has been provided, which could result in "stranded" pedestrians or vehicles. However, as advance detection technologies are developed and additional preemption warning time is made available, safety issues such as "stranded" pedestrians and vehicles at the IHRGC have received increased interest. That is, new preemption strategies can be implemented if more warning time is made available, thus allowing minimum interval times at the IHRGC to be satisfied (2,3,4).

Recently the TPS was developed for vehicle and pedestrian safety using earlier preemption warning time (2,3,4) obtained from a Doppler advance warning system. TPS is initiated at the advance preemption warning time predicted using Doppler detector data, and the normal preemption is started at the normal preemption warning time predicted using the preemption warning time detector data. The difference in time between the Doppler warning activation and the activation of the preemption warning time detector is the time period provided to operate the TPS algorithm. Because both systems have variability, the advance preemption warning time can be shorter or longer than the predetermined advance preemption warning time. If normal preemption is started before TPS completes its process, the current phase during the TPS algorithm can be cut abruptly. This has the potential to create a safety problem. If normal preemption is started after TPS completes its process, the track clearance phase will continue until normal preemption is started which may result in excessive intersection delay (3,4,5,6).

The TPS system was programmed assuming an average detection of 70 seconds before train arrival at the crossing and normal preemption activation when the train was, on average, 48 seconds from the crossing. The 22-second average duration between these two times is when the TPS system can operate. TPS duration should be decided based on the features of the TPS algorithm, and advance preemption warning time is dependent on the TPS duration. These times were selected as a compromise between giving the TPS system more time to operate (i.e., more than 22 seconds would give the system more time to influence controller operation) and the increasing variability the farther in time the Doppler system gives its warning (i.e., advance preemption warning time variability increases the farther the temporal detection horizon is set with respect to train arrival at the crossing). For general application a new method is needed to find an adequate advance preemption warning time (3,4,5,6).

It was found by Engelbrecht, et al. that the number of vehicle minimum green phases that were truncated was reduced by 82 percent, which corresponded to a 40 percent

reduction in abbreviation time. In addition, the number of pedestrian clearance times that were truncated was reduced by 39 percent, which corresponded to a 77 percent reduction in abbreviation time. These results are from data sets that included inadequate advance preemption warning time (i.e., when predicted time is longer than actual arrival time). The analyses were repeated using data sets that did not include inadequate preemption warning time, and in this situation there was a 100 percent reduction of both abbreviation of vehicle minimum green and abbreviation of pedestrian clearance time. These results demonstrate that if advance preemption warning time is too long, the benefit of TPS is reduced (3,4,5,6). In other words it is important to have an accurate prediction algorithm in addition to an appropriate transition preemption algorithm.

The following variables are needed in order to use the TPS logic (3,4).

Time to Train Arrival (T): The time the train is predicted to arrive at the crossing. The estimator used to predict arrival time is a function of the track equipment and agency objective. This value is updated every t seconds as the train approaches the crossing. For all field applications in the U.S., t is 1 second.

Track Clearance Time (τ): The time at which the track clearance phase should be initiated.

Remaining Time Available ($X = T - \tau$): Effectively, a “countdown” until the track clearance time.

Extended Time (B_i): Time period added into M_j to end a vehicle phase i that has a call. That is, when there is a vehicle call for phase i , phase i is provided until $X = M_j + B_i$, instead of $X = M_j$.

From the above definitions, two other variables that are used in the TPS logic are calculated.

M_j : Minimum time necessary to service the next phase (phase $i+1$); and

M_k : Minimum time needed to service the next two phases (phase $i+1$ and phase $i+2$) when the next phase is the track clearance phase.

Once the train detection equipment has indicated that a train will arrive at the crossing within the TPS initiation time, the TPS logic monitors and, if necessary, affects controller operation. The following steps define the TPS logic. TPS logic also is shown in the flow chart of Figure B-1 in Appendix B.

Step 1:

The status of the current phase is (are) checked to determine if both the minimum green time and minimum pedestrian time have been serviced. If the minimums have not been completely serviced, the current phase remains active. Otherwise, the logic proceeds to step 2.

Step 2:

If the T at the crossing is less than the τ , the track clearance phases are initiated. The τ is the preset desired time that the track clearance phase should begin prior to the train's arrival at the crossing. This time is determined by vehicle and geometric characteristics at the crossing and is usually longer than the warning time provided by railroad equipment. Theoretically, the intersection would then be in track clearance every time the preempt call is received from the railroad equipment. This will lead to a more controlled and predictable entry into preemption.

Step 3:

The current phase is (are) checked. If the current phase is the track clearance phase, then the logic goes to step 5B-3. Otherwise, it goes to step 4.

Step 4:

The next phase is (are) checked. If the next phase is the track clearance phase, the logic goes to step 5A-1. Otherwise, it goes to step 5B-1.

Step 5A-1:

Vehicle calls for the current phase are checked. If there are still vehicle calls for the current phase, then the logic goes to step 5A-2. Otherwise, it goes to step 5A-3.

Step 5A-2:

- If $M_k + B_i \geq X \geq M_k$, the current phase is terminated and the next phase is started. The logic skips to step 6.
- If $M_k + B_i < X$ or $X < M_k$, the current phase remains. The logic skips to step 6.

Step 5A-3:

- If $X \geq M_k$, the current phase is terminated and the next phase is started. The logic skips to step 6.
- If $X < M_k$, the current phase remains. The logic skips to step 6.

Step 5B-1:

Vehicle calls for the current phase are checked. If there are still vehicle calls for the current phase, then the logic goes to step 5B-2. Otherwise, it goes to step 5B-3.

Step 5B-2:

- If $M_j + B_i < X$ or $X < M_j$, the phase is held green. The logic skips to step 6.

- If $M_j + B_i \geq X \geq M_j$, the current phase will be terminated and the next phase will begin timing. The logic skips to step 6.

Step 5B-3:

- If $X < M_j$, the phase is held green. The logic skips to step 6.
- If $X \geq M_j$, the current phase will be terminated and the next phase will begin timing. The logic skips to step 6.

Step 6:

At this point, the logic returns to step 1 to ensure that the minimum times for the current phase have been satisfied.

The above steps will be performed every time the train's predicted arrival time at the crossing is updated by the detection equipment and each time a new signal phase becomes active.

2.5 TRAIN ARRIVAL TIME PREDICTION

The ultimate goal of the detection is to predict the train arrival time at the HRGC so that preemption is initiated at the most appropriate time. The train arrival time prediction is important because it is the major input to the preemption strategy. The deciding factor of the arrival time forecast is a function of the detector technology, the prediction algorithm, and the detector location with respect to the HRGC.

CWT systems, which are used most commonly today, use the train's detection position and the assumption that the train's speed will remain constant to predict the train arrival time at the crossing. However, because the train speed can vary considerably as it approaches the crossing, the predicted time is subject to error.

Recently Estes and Rilett used modular multiple linear regression to predict the train arrival time based on upstream train speed data. Their model predicted the arrival time of a train to within ± 20 seconds of its true arrival time when most trains are between 100 and 200 seconds away from the crossing. For earlier predictions (e.g., trains between 200 and 300 seconds from the crossing) the prediction achieved an accuracy of ± 60 seconds (28).

If a more advanced preemption strategy, such as the transition preemption algorithm, is considered before the normal preemption is initiated, the prediction of train arrival time should be performed earlier. Because prediction accuracy will decrease as the detector is located farther from the crossing, more sophisticated detector and prediction algorithms will be required for the advanced preemption strategy.

2.6 CONCLUDING REMARKS

The general preemption sequence is designed to clear queued vehicles on the tracks as quickly as possible. As discussed in this chapter, it is argued that the current preemption strategy does not generally account for the safety of pedestrians and vehicles at the intersection, or the intersection performance as a whole. However, as advance detection technologies are developed and additional preemption warning time is made available, safety issues at the IHRGC has received increased interest. That is, new preemption strategies can be implemented if more warning time is made available, thus allowing minimum interval times at the IHRGC to be satisfied.

Recently a transition preemption strategy was developed for vehicle and pedestrian safety using earlier preemption warning time obtained from a Doppler advanced warning system. TPS is initiated at the advance preemption warning time predicted by Doppler detector, and the preemption is started at the preemption warning time predicted by CWT. However, because both systems have variability, it is difficult to expect that the TPS algorithm achieves its goal properly. Therefore, it is important to have an accurate

train arrival prediction algorithm in addition to an appropriate transition preemption algorithm. A new train arrival time prediction algorithm is developed in Chapter IV, and a new transition preemption strategy is developed to improve intersection safety and performance in Chapter V.

CHAPTER III

STUDY DESIGN

In Chapter II, the basic signal preemption logic at an IHRGC was introduced. As discussed in the previous two chapters, a new train arrival time prediction algorithm and a new TPS algorithm are needed to improve the safety and performance of an IHRGC. In the first section of this chapter, the test bed for this study will be discussed. Subsequently, the methodologies used to develop these two new algorithms will be introduced. The new train arrival time prediction algorithm and the new TPS algorithm will be developed in Chapters IV and V, respectively.

The evaluation of a TPS algorithm requires information on each individual unit (i.e., vehicle and pedestrian) that behaves stochastically. Because of the difficulty in obtaining empirical information, a behavior and periodic-scan based micro-simulation model was utilized. For the topics covered in this dissertation the simulation model also is required to simulate vehicles, trains, and pedestrians. The VISSIM micro-simulation model satisfies the above criteria. More importantly the VISSIM micro-simulation model has an ability to control the user-defined traffic signal logic with a function called vehicle actuated programming (VAP), which is an optional add-on module for the simulation of programmable, phase- or stage-based, and traffic-actuated signal controls (29). Therefore, the new TPS logic can be implemented along with the traffic signal controller logic in VISSIM using the VAP module. The VISSIM micro-simulation model and VAP will be evaluated in this chapter. The methodologies to emulate the actual train in the simulation and simulation procedure also are introduced.

3.1 TEST BED

3.1.1 Test Bed for Development of New Train Arrival Time Prediction Algorithm

The test bed chosen for this study was the Wellborn Road corridor in College Station, Texas, as shown in Figure 3-1. The corridor is approximately 2.2 km in length and is

located between FM 2818 and George Bush Drive. An arrival time forecast is required at George Bush Drive because the Wellborn Road-George Bush Drive intersection is the test bed for traffic signal preemption research. Currently train volume in the corridor is between 20 and 30 trains per day. The train speed limit is 95 km/h (60 mi/h) south of Rock Prairie Road, which is a rural environment, while the speed limit is 50 km/h (30 mi/h) inside the city limits. A dual track alignment exists north of the test site that allows for train switching and passing. Several depots where the trains may stop for loading and unloading also exist north of University Drive. Thus, northbound trains tend to experience greater speed variations because of the lower speed limit and the possibility of having to wait for the switching station to clear (28). Because of the wide range in operating speeds, the northbound trains were used in the research. Doppler radar detectors have been installed at every major crossing (Rock Prairie Road, FM 2818, George Bush Drive, and University Drive) along the Wellborn Road corridor as part of the TransLink Train Monitoring Project in College Station, Texas. In this dissertation, information from 683 trains was collected at George Bush Drive and FM 2818 during the period from April 18, 2001, to September 30, 2001.

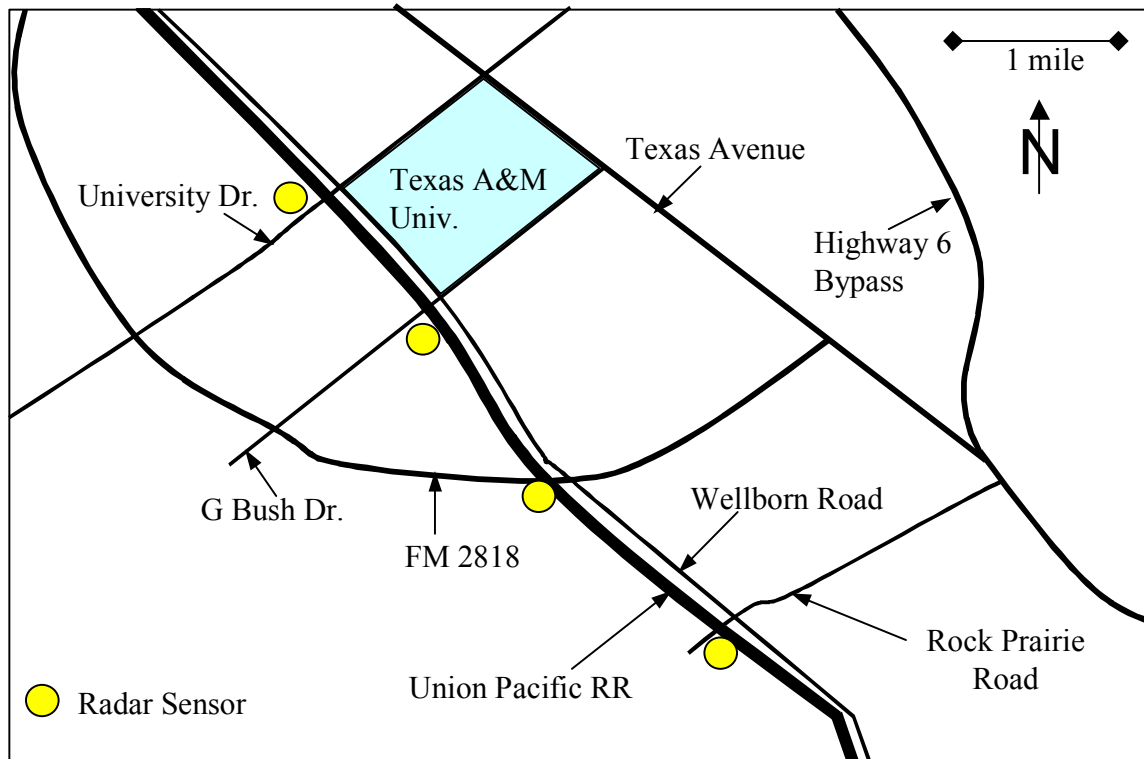


FIGURE 3-1 Map of Wellborn Corridor, College Station, Texas

3.2.2 Test Bed for Development of New TPS

The signalized intersection of George Bush Drive and Wellborn Road in College Station, Texas, along the railway corridor, which is the test site for development of a new train arrival time prediction algorithm, was chosen as the test bed for development of a new TPS algorithm. The geometric conditions for the highway-railroad grade crossing and the near intersection are shown in Figure 3-2. All approaches have one through lane, one through/right-turn shared lane and one exclusive left-turn lane with the exception of the westbound approach, which has two through lanes, one exclusive right-turn lane and one exclusive left-turn lane. The intersection has moderate to high traffic volumes during the peak hour and is regularly preempted by trains at the adjacent highway-railroad grade crossing located approximately 12 m to the west of the intersection. The railroad track detection system is designed to provide a minimum 35 seconds of

preemption warning time to the signal controller at the intersection. The clear storage distance, or the distance between the intersection stopline in the eastbound direction and the intersection-side edge of the crossing, is approximately 10 m. The storage capacity is two vehicles per lane (not including trucks). Traffic volumes were collected at the intersection between December 7, 1999 and December 13, 1999 using video cameras for 51 preemption cases, which have 15-minute period of volume. Traffic volume between 5:05 pm and 5:20 pm on December 9, 1999, was chosen as a representative peak volume and used for the analysis. The flow rates of each movement were converted to hourly volume and these are shown in Figure 3-2.

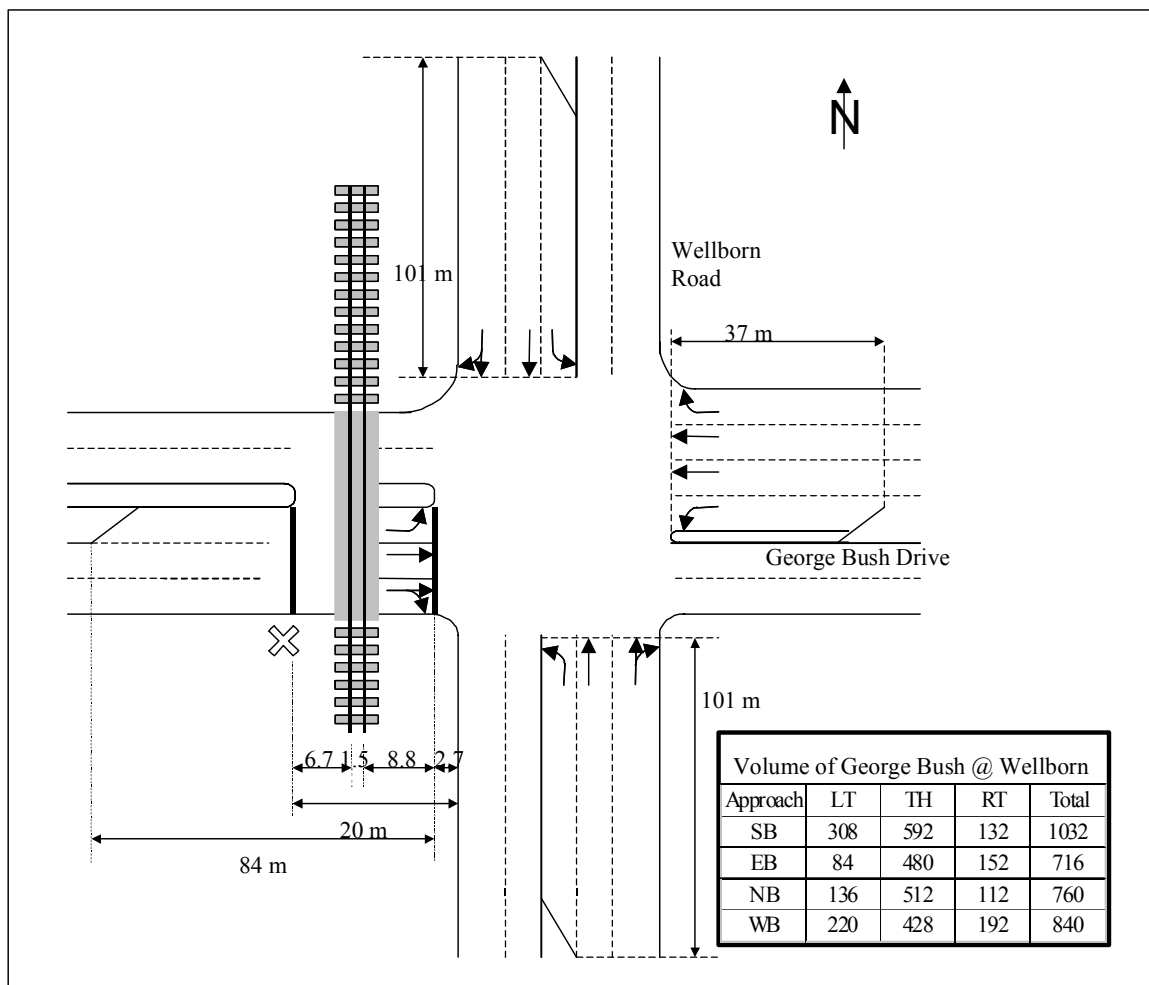


FIGURE 3-2 Site Detail for George Bush Drive and Wellborn Road Intersection

The intersection signal is operated in a coordinated mode with a 120-second cycle length, including the northbound and the southbound through, Wellborn Road, as coordinated phases. The eastbound and the westbound approaches, George Bush Drive, are individual phases. That is, the left-turn and through movements operate together. The signal control variables in normal mode and preemption mode are shown in Tables 3-1 and 3-2, respectively.

TABLE 3-1 Signal Control Variables at the Intersection of George Bush and Wellborn

	Movement	NB LT	SB TH	EB	WB	SB LT	NB TH
	Phase	Phase 1	Phase 2	Phase 3	Phase 4	Phase 5	Phase 6
Normal Mode	PASS	2	4.5	3	3	4	4.5
	MIN	7	10	8	8	7	10
	MAX	25	65	32	55	30	60
	YEL	4	4	4	4	4	4
	RED	1	1	1	1	1	1
	WALK	0	4	4	4	0	4
	PED CLR	0	15	15	15	0	15
Coordinated Mode	TIME	24	41	30	25	18	47
	MODE	3	1	3	3	3	1

Mode 1: Coordinated phase

Mode 3: MAX REC - the phase will operate as an actuated phase with coordination modifier of MAXIMUM RECALL within the pattern defined

Note: All values in table are expressed in seconds.

TABLE 3-2 Signal Control Variables in Preemption Mode at the Intersection of George Bush Drive and Wellborn Road

Variable	Time (seconds)	Variable	Time (seconds)
MIN GRN/WLK	5		
SEL PED CLR	0	TRK RED/10	10
SEL YEL/10	40	RET PED CLR	15
SEL RED/10	10	RET YEL/10	40
TRK PED CLR	0	RET RED/10	10
TRK YEL/10	40	TRACK GREEN	22
Track Green	Phase 3	EXIT	Phase 3
Cycle	Phase 2 & 6 – Max. REC. and Phase 5 – Min. REC.		

MIN GRN/WLK: Minimum Green Time for any vehicle phase and any pedestrian phase at the onset of the preemption. This time (0-999 seconds) must have been displayed prior to its termination for a transition to the preemption.

SEL PED CLR (Selective Pedestrian Clearance): This sets the time (0-99 seconds) that will be provided to clear a terminating Walk during the transition to Track Green.

SEL YEL/10 (Selective Yellow Change): This sets the time (0-999 tenth seconds) that will be provided to clear a terminating Green during the transition to Track Green.

SEL RED/10 (Selective Red Clear): This sets the time (0-999 tenth seconds) that will be provided to clear a terminating Yellow during the transition to Track Green.

TRACK GREEN: This sets the time (0-99 seconds) that will be provided as a Track Green interval.

TRK PED CLR (Track Pedestrian Clear): This sets the time (0-99 seconds) that will be provided to clear a terminating Walk during the transition to Dwell Green.

TRK YEL/10 (Track Yellow Change): This sets the time (0-999 seconds) that will be provided to clear a terminating Green during the transition to Dwell Green.

TRK RED/10 (Track Red Clear): This sets the time (0-999 seconds) that will be provided to clear a terminating Yellow during the transition to Dwell Green.

RET PED CLR: This sets the time (0-99 seconds) that will be provided to clear a terminating Walk during the transition to Normal Operation.

RET YEL/10 (Return Yellow Change): This sets the time (0-999 tenth seconds) that will be provided to clear a terminating Green during the transition to Normal Operation.

RET RED/10 (Return Red Clear): This sets the time (0-999 tenth seconds) that will be provided to clear a terminating Yellow during the transition to Normal Operation.

3.2 PREDICTION ALGORITHM

The ability to forecast train arrival time at highway-railroad grade crossings is essential for the accurate preemption of traffic signals at an IHRGC. However, because of the limitation of current detection technologies and estimation algorithms, a wide range in warning times exists. The uncertainty in arrival time arises because the existing prediction methods assume that the train's speed at the time of detection will remain

constant until the train reaches the crossing. If the train is accelerating or decelerating, the preemption will begin later or earlier than the preemption warning time.

The preemption warning time depends on several characteristics of the site including the distance between the intersection and the crossing, traffic signal timing, longest vehicle allowed on the roadway, pedestrian volume, and other factors. Generally the preemption warning time is longer than the minimum warning time. With the recent advances in train detection technology, the potential exists for placing additional equipment in the field that will allow for earlier detection of on-coming trains. The goal of the proposed approach is to supplement, not replace, the current system. Therefore, if the system is designed correctly, safety can only increase, or, at worse, remain constant.

In this dissertation, artificial neural network (ANN) models are applied to handle the nonlinear relationship between the train speed profile and arrival time. A modular artificial neural network (MANN) also is applied to model the situation where trains with markedly different speed profiles may have the same arrival time. The current prediction method and five multiple linear regression (MLR) models also will be evaluated for comparison purposes. Because the artificial neural network model is a non-parametric method, a bootstrap technique, which is a computer-based method for assigning measures of accuracy to statistical estimates, is used to obtain the prediction interval. The mean predicted arrival time and associated prediction interval will be combined in the transition preemption strategy in order to reduce the effect of the error in the arrival time prediction. The new prediction algorithm will be developed in Chapter IV.

3.3 TPS ALGORITHM

When a train is detected by CWT detector and the predicted arrival time is the same as the pre-determined preemption warning time, a preemption signal is sent to the traffic signal controller. The traffic controller uses this information and any information from

inductive loop detectors and pedestrian push button to control the preemption. After a while, when the predicted arrival time is the same as the pre-determined crossing warning time, the train detector also provides a signal to the gate controller so that the gate will begin to descend. The conceptualization of the normal preemption method is shown in Figure 3-3. As discussed in Chapters I and II, the traffic signal can operate in unsafe ways (i.e., abrupt truncation of pedestrian phases at the onset of preemption) in the normal preemption method.

In order to reduce the safety problem of the exist preemption logics, Venglar et al. developed a new logic called the Transition Preemption Strategy (referred to here in this dissertation TPS1). The concept of the TPS1 algorithm was to provide a smooth transition from normal mode to preemption mode by controlling the time period before the normal preemption begins (3,4,5,6). The TPS1 algorithm is initiated by the advance preemption warning time (APWT) from the Doppler detector. The TPS1 algorithm is operated until the traffic signal controller receives the preemption signal from the CWT detector. Once the traffic signal controller receives the preemption signal from the CWT detector, the TPS1 logic is terminated and the normal preemption is initiated immediately regardless of the completion of the TPS1 algorithm. Therefore, unexpected phase truncations still can occur because of the variability of predicted train arrival time but their likelihood is greatly reduced. In addition, room for improvement exists because developers did not consider intersection performance in the TPS1 algorithm. Figure 3-4 shows a conceptualization of the preemption including the TPS1 algorithm.

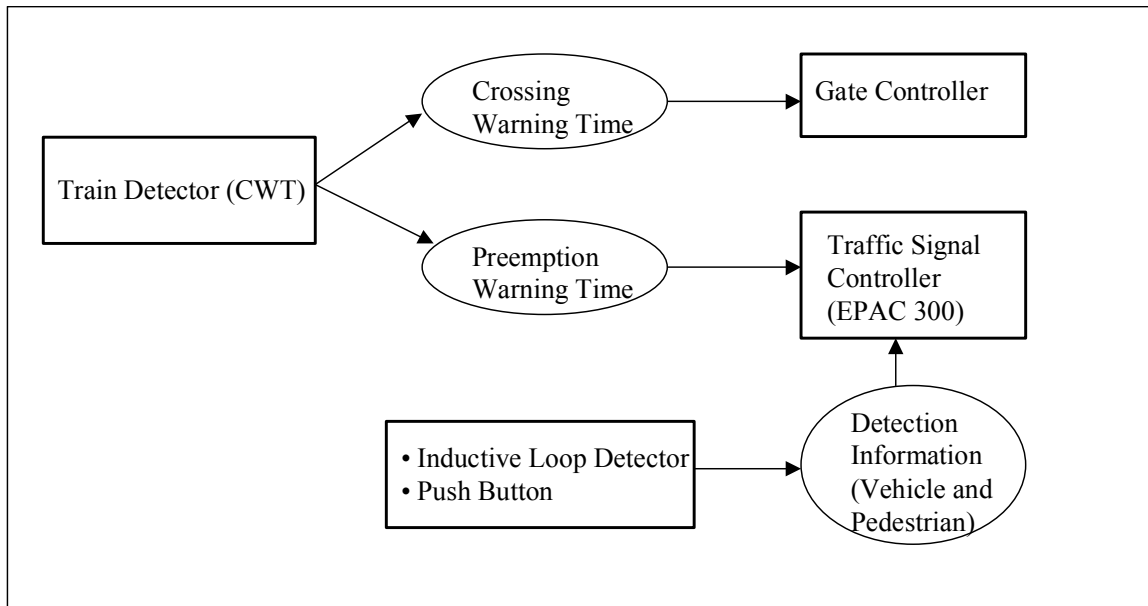


FIGURE 3-3 Conceptualization of the Normal Preemption

Therefore, a new TPS algorithm is needed to solve the above two problems. A new transition preemption method will be developed to provide more green time to the phases that are blocked during the preemption mode than phases that are served during the preemption mode. The conceptualization of the preemption including this new TPS algorithm is similar to that shown in Figure 3-4. However, the internal logic is different. The new TPS algorithm will be developed in Chapter V.

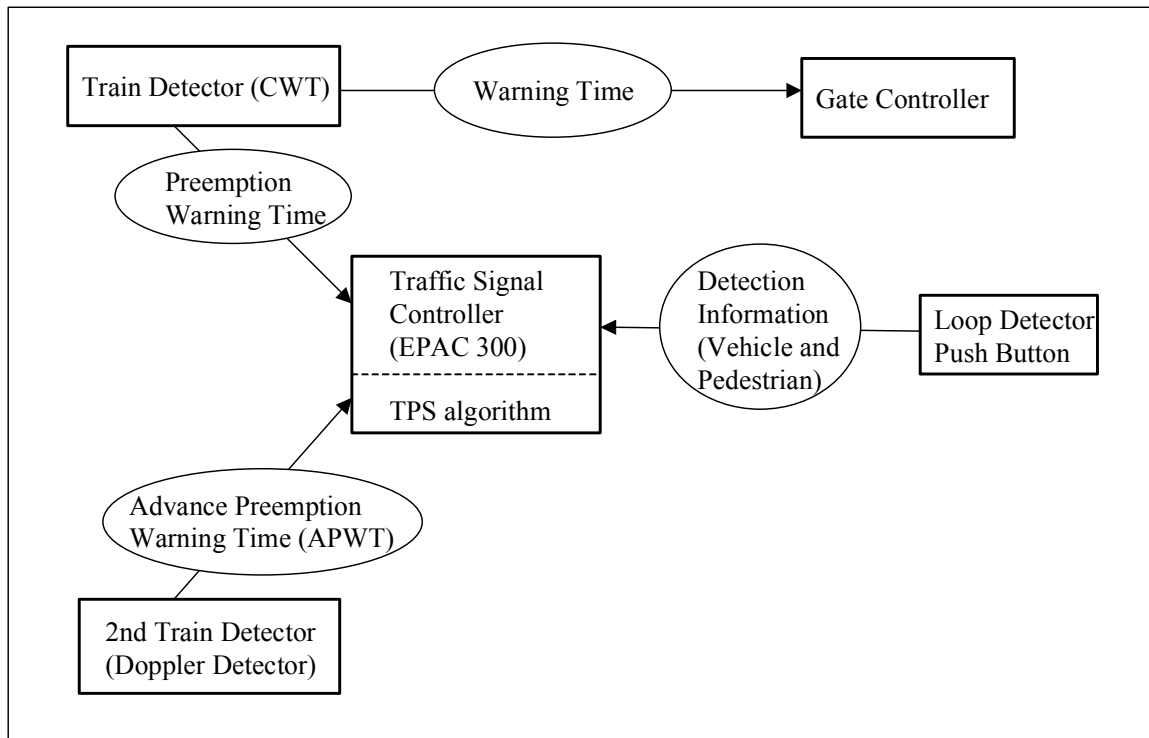


FIGURE 3-4 Conceptualization of Preemption Using the TPS1 Algorithm

3.4 MICRO-SIMULATION

The evaluation of a TPS algorithm requires information on each individual unit (i.e., vehicle and pedestrian). Therefore, a behavior and periodic-scan based micro-simulation model is required for this simulation study. Preemption and TPS logic needs to operate in the simulation as close as possible to the way they operate in the field. First, a hardware-in-the-loop system was examined. Hardware-in-the-loop systems were developed to enhance the advantage of software-only traffic simulation by replacing the traffic control component of the simulation with real traffic signal control hardware. It has several advantages over regular traffic simulation models that rely on internal controller emulation logic. These advantages include adding realism to the simulation and allowing the testing and use of advanced signal control strategies and vendor-specific controller capabilities in the simulation. However, because hardware-in-the-loop systems, by their nature, can run in real time only, the same number of simulations

takes longer to perform than with regular traffic simulation models. Moreover, because the simulation model is connected to a real traffic signal controller, some communication errors may occur (30).

Figure 3-5 shows a diagram of the hardware-in-the-loop system used in this dissertation. It can be seen that there are three main components. Component 1 is a simulation model that gives the detection information to the controller. The traffic signal in the simulation model is operated based on the signal information received from the controller. Component 3 is the traffic signal controller, which gives the signal information to the simulation model based on the detector information received from the simulation model. Component 2 is the controller interface device (CID), which allows a computer to communicate with the traffic controller (30). Any number of micro-simulation models, including CORSIM, TEXSIM, and VISSIM, can be used. The traffic controller was the Eagle EPAC 300, which was used at the test site.

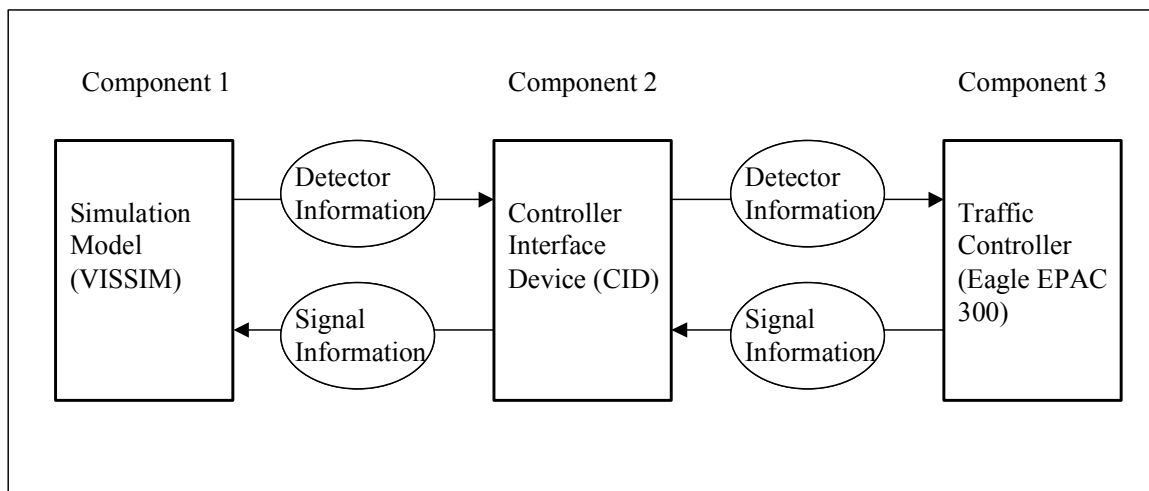


FIGURE 3-5 Framework of Hardware-in-the-Loop System

Most existing microscopic traffic simulation models such as CORSIM (31) do not provide all the traffic signal functions that the vendor-specific controllers have. Consequently the hardware-in-the-loop system has been the only viable solution for accurate simulation of functions in the controller. Recently the development of new simulation models, including the VISSIM microscopic traffic model have increased the realism of traffic signal control. VISSIM provides VAP, which is an optional add-on module for the simulation of programmable, phase- or stage-based, traffic-actuated signal controls (29). Therefore most functions in the vendor-specific controllers can be modeled with software-only traffic simulation rather than hardware-in-the-loop. All signal functions including transition preemption strategy logic, which is developed in this dissertation, as well as preemption and the transition back to normal after preemption, which are available in the controller, can be programmed using VAP. Because the VISSIM model also has the capability to simulate vehicles, trains, and pedestrians that behave stochastically, it was chosen as the microscopic traffic simulation model for this study.

In this dissertation, different VAP codes were developed for each of the traffic signal preemption algorithms that were developed. The traffic signal logic was based on an Eagle EPAC 300 controller, which is currently used in the study site. The simulations are not constrained to run in real time and many more simulations can be run. Therefore, more scenarios can be tested and statistical inference of the results can be applied.

3.5 DEVELOPMENT OF THE VAP TRAFFIC SIGNAL CONTROLLER LOGIC

The features of the Eagle EPAC 300 signal controller were studied under a hardware-in-the-loop system environment to develop the VAP traffic signal controller code in VISSIM. Some of the complicated logics such as, the coordinated mode and transition mode back to normal mode, were obtained from the SIEMENS Energy & Automation,

Inc., who developed the traffic signal controller. The VAP codes were developed by module for each control mode. There are four signal modes required to emulate the controller: 1) coordinated actuated mode, 2) fully actuated mode, 3) preemption mode, and 4) transition mode back to the coordinated mode. In the normal condition at the study site (i.e., the absence of trains), the permissive coordinated mode is operated. The control mode is changed to the preemption mode at the onset of preemption. After preemption, the controller returns to the coordinated mode through the transition mode, which includes the fully actuated mode.

The permissive coordinated actuated mode and the transition mode will be reviewed in this section. Special attention is required to code these two traffic signal control modes because the detailed processes of these two modes are not discussed in the literature.

3.5.1 Permissive Coordinated Mode

The permissive coordinated mode is designed to provide a safeguard against an excessive early release from the coordinated phases. This mode controls the release period, called the permissive period, to each of the non-coordinated phases in the sequence. The permissive period is the time during which the controller can release the coordinated phases to serve non-coordinated phases. The length of the permissive period is determined based on the split time and the minimum time for each phase. The permissive period for each phase opens and closes in sequence based on where the phase occurs in the cycle (32).

When the coordinated phases are terminated to serve a non-coordinated phase during its permissive period, all subsequent phases can be served in their normal order before returning to the coordinated phases. That is, once the controller has left the coordinated phases, it will leave a non-coordinated phase to serve another non-coordinated phase normally (32).

The beginning of the permissive period for each phase is the point that the controller could leave the coordinated phase and run the entire split time for that phase and all subsequent phases before the end of the cycle. The end of the permissive period for each phase is the last point that the controller could leave the coordinated phase and run the minimum time for that phase and the split time for all subsequent phases before the end of the cycle. That is, it is guaranteed that once the controller leaves to serve a phase, at least the minimum time for that phase will be served. It also ensures that any phase that occurs after the phase will have the full split time to be served. A complete description of the permissive coordinated mode may be found elsewhere (32).

3.5.2 Transition Modes Back to Normal Mode

Four transition methods are provided in the Eagle EPAC 300 controller. The SWY (Shortening Dwell) option provides an offset correction either by shortening the cycle length or by dwelling based on a shortest way calculation. This option automatically takes into consideration minimum times. Note that each phase length during the transition can be different and is a function of the vehicle calls. Because the time period of interest in this dissertation is before the preemption, it is desirable that the time frame for each scenario is the same in order to observe any difference between the scenarios.

In addition, even though DWL (Dwell) mode may produce higher delay, it was chosen for simplicity of coding in VAP. While it can take a few cycles to return to normal mode with the SWY transition method, the DWL transition method needs only one cycle to return to normal cycle. The signal is run with the fully actuated mode for the first cycle after the preemption. During the second cycle the controller identifies its offset with the other traffic signal in the system at the same time it runs with the coordinated mode. In the third cycle after preemption, the signal controller transitions to the default offset by increasing the coordinated phase length (32).

To verify if the VAP emulates the Eagle EPAC 300 controller correctly, the signal status for both the VAP and the hardware-in-the-loop system during the simulation including a normal preemption were collected and compared under several scenarios. The simulations for the comparison were performed under both the permissive coordinated mode and the fully actuated mode with three different random number seeds.

It was found that each function in the VAP emulated the controller logic correctly. It should be noted that some differences in signal timing existed between the two methods during simulation. These differences are considered to be caused by a communication problem. This problem will be examined in detail in the Section 3.6.

3.6 VAP AND HARDWARE-IN-THE-LOOP COMPARISON

The signal status for both the hardware-in-the-loop system and the VAP during the simulation including a normal preemption were collected and compared under the fully actuated mode including a preemption. Tables 3-3 and 3-4 show the signal status including each phase start time and duration during the simulation as an example for both the hardware-in-the-loop system and the VAP, respectively.

Table 3-3 shows that the preemption occurred at 541 seconds during the simulation under the hardware-in-the-loop system. Table 3-4 shows that the preemption occurred at 540 seconds during the simulation under the VAP. There is a 1-second difference in the duration of phase 1 during cycle 5 (i.e., at the 437 seconds of the simulation time). That is, the hardware-in-the-loop system gave phase 1 16 seconds and the VAP give it 17 seconds. From this point on, the start times of most phases in the VAP were shifted 1 second later than in the hardware-in-the-loop system and the duration of some phases were changed by 1 second. Interestingly, by time 949 the two are back in synchronization. However, after 1089 seconds of the simulation time, the durations of phase 1 are quite different from each other. It can be seen in Tables 3-3 and 3-4 that at 1089 seconds the length of phase in the hardware-in-the-loop system was 10 seconds

TABLE 3-3 Signal Timing for Hardware-in-the-Loop System

Cycle	Phase 6		Phase 2		Phase 3		Phase 4		Phase 1		Phase 5	
	ST*	Duration	ST*	Duration	ST*	Duration	ST*	Duration	ST*	Duration	ST*	Duration
1	1	10	1	10	16	19	40	19	64	9	64	7
2	76	21	78	19	102	22	129	19	153	11	153	7
3	165	23	169	19	193	19	217	19	241	16	241	7
4	253	30	262	21	288	19	312	19	336	19	336	7
5	348	34	360	22	387	19	411	21	437	16	437	7
6	449	28	458	19	482	19	506	21	(532)	(9)	(532)	(9)
7					(546)	(13)						
8			(564)	(171)							(564)	(7)
9	(576)	(60)									(641)	(9)
10	(655)	(60)									(720)	(7)
11					740	19	764	21	790	25	790	7
12	802	37	820	19	844	22	871	19	895	25	895	7
13	907	37	925	19	949	19	973	22	1000	12	1000	7
14	1012	24	1017	19	1041	19	1065	19	1089	10	1089	7
15	1101	22	1104	19	1128	21	1154	19	1178	7	1178	7
16	1190	19	1190	19	1214	20	1239	21	1265	7	1265	10
17	1280	23	1277	26	1308	19	1332	19	1356	25	1356	7
18	1368	49	1386	31	1421	19	1445	19	1469	17	1469	9
19	1483	27	1491	19	1515	24	1544	0	0	0	0	0
Sum		504		452		312		277		208		128

ST* : Phase start time during simulation

() : Preemption period

Bold: Critical checking point

while the length of phase in the VAP system was 25 seconds. After checking the animation files and detection information file, an error was found in the hardware-in-the-loop system. That is, the controller did not “recognize” a vehicle at the corresponding detector. This detection error of one vehicle caused the difference of 15 seconds in phase duration. This large difference is possible when the characteristics of actuated mode operation are considered. For example, if there is no vehicle call for a phase at a certain time, the phase can “gap out.” This means that once the minimum amount of green time is provided and there are no more vehicle calls the phase is terminated.

However, if there is a vehicle call for the phase at that time, the phase will be extended for the vehicle detected. The phase may be further extended for other vehicles that are detected until the length of the phase reaches the maximum phase length. Therefore, even a small error in detection can change the signal status considerably.

TABLE 3-4 Signal Timing for VAP

Cycle	Phase 6		Phase 2		Phase 3		Phase 4		Phase 1		Phase 5	
	ST*	Duration	ST*	Duration	ST*	Duration	ST*	Duration	ST*	Duration	ST*	Duration
1	1	10	1	10	16	19	40	19	64	9	64	7
2	76	21	78	19	102	22	129	19	153	11	153	7
3	165	23	169	19	193	19	217	19	241	16	241	7
4	253	30	262	21	288	19	312	19	336	19	336	7
5	348	34	360	22	387	19	411	21	437	17	437	7
6	449	29	459	19	483	19	507	20	(532)	(8)	(532)	(8)
7					(545)	(13)						
8			(563)	(171)							(563)	(7)
9	(575)	(60)									(640)	(9)
10	(654)	(60)									(719)	(7)
11					739	19	763	21	789	25	789	7
12	801	37	819	19	843	22	870	19	894	25	894	7
13	906	38	924	20	949	19	973	22	1000	12	1000	7
14	1012	24	1017	19	1041	19	1065	19	1089	25	1089	7
15	1101	41	1119	23	1147	20	1172	19	1196	15	1196	10
16	1211	24	1216	19	1240	20	1265	21	1291	11	1291	9
17	1305	21	1307	19	1331	20	1356	19	1380	25	1380	7
18	1392	40	1410	22	1437	23	1465	25	1495	9	1495	9
19	1509	19	1509	19	1533	19	1557	0	0	0	0	0
Sum		511		441		311		282		227		129

ST* : Phase start time during simulation

() : Preemption period

Bold: Critical checking point

Note that all signal timings following time 1089 seconds were affected by this small error. This error was considered a communication problem between the simulation

model and the controller. Several more tests were performed under the same condition but different random number seeds. For most of the tests, this type of error (i.e., non-recognition of simulated vehicles by hardware-in-the-loop) was found. Therefore, the hardware-in-the-loop system with VISSIM cannot be used for this simulation without fixing the communication problem.

3.7 METHOD TO EMULATE TRAINS IN SIMULATION

Because trains often change their speed continuously, it is not possible to emulate the train speeds exactly in VISSIM. This would be true even if continuous data on the train's speed throughout its journey were available. Emulation of the real situation in VISSIM can be achieved by adjusting the placement of the train detector on the tracks (i.e., detector length) and the average train speed of each train according to the following steps:

- Step 1: From the field identify the time (X) when the advance preemption warning time is predicted as a specific time and the real time (Y) when the preemption warning time is predicted as 35 seconds.
- Step 2: Set the detector lengths for X and Y for the given train using the average speed of each train at FM 2818.

Because the TPS is designed to begin at a specific time before the train arrives at the crossing, it is necessary to accurately predict this arrival time. However, it is not possible to predict the train arrival time with 100 percent accuracy regardless of how often the algorithm is updated. In this dissertation, a new predicted arrival time will be forecast every 10 seconds. Therefore, it should be acknowledged that the TPS algorithm does not have to be started at a specific desired time ahead of the arrival time. For this simulation study, once the predicted arrival time is equal to or less than the desired arrival time prediction, the TPS algorithm is started.

Once the predicted arrival time is determined, the detector length can be calculated according to the predicted arrival time and the actual arrival time. An example of the method to calculate the detector length to emulate the real train is shown in Figure 3-6. This example is the case where the TPS algorithm is started when the predicted arrival time is equal to or less than 100 seconds and the preemption is started when the predicted arrival time is equal to 35 seconds. The actual arrival time and the predicted arrival time are shown in Figure 3-6. For example, when the actual arrival time is 100 seconds, the predicted arrival time is 106 seconds. Because the predicted arrival time is more than 100 seconds, the TPS algorithm will not start. When the prediction is performed again after 10 seconds, the predicted arrival time is 95 seconds and the TPS algorithm is started immediately. Therefore, the detector length for the TPS algorithm should be 1000 m ($= 90 \text{ (seconds)} \times 40 \text{ (km/h)} \times (1000/3600)$) assuming a 40 km/h train speed. Afterward the prediction is updated every 10 seconds. If the preemption is started when the actual arrival time is 42 seconds, the detector length for the preemption should be 467 m ($= 42 \text{ (seconds)} \times 40 \text{ (km/h)} \times (1000/3600)$).

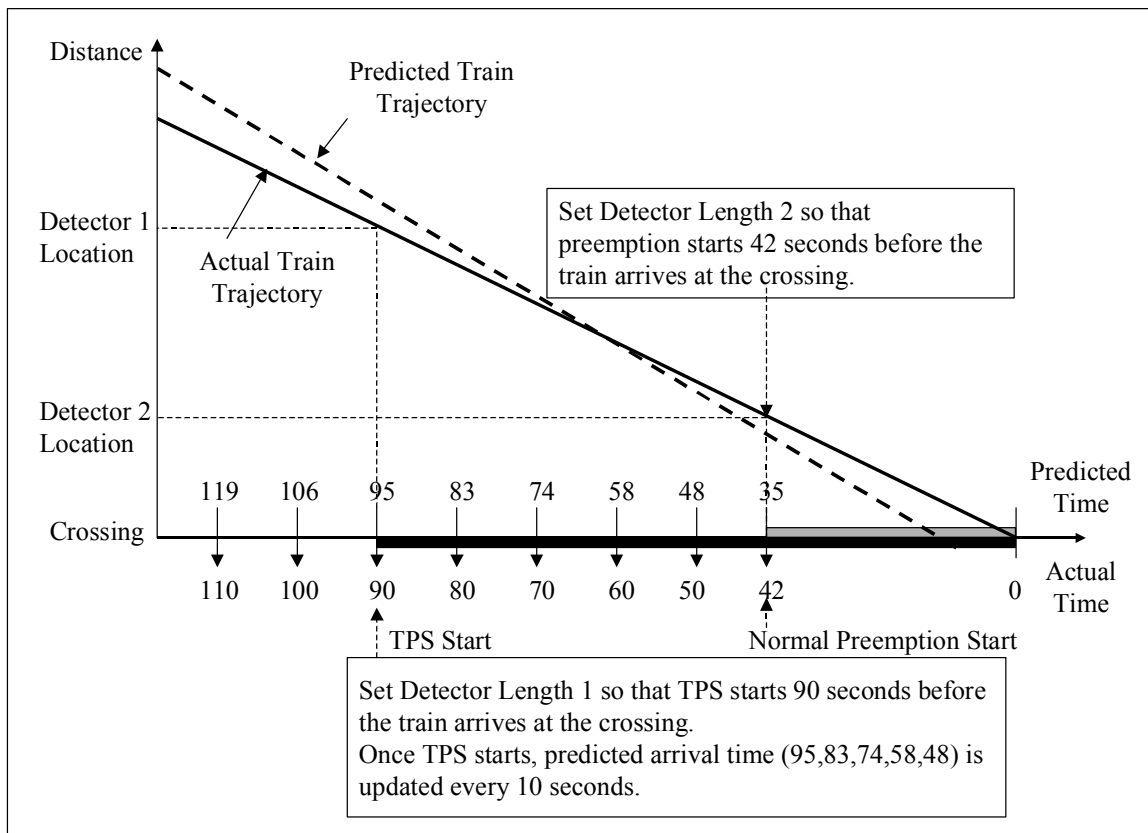


FIGURE 3-6 An Example of the Method to Calculate the Detector Length to Emulate the Real Train

3.8 SIMULATION DESIGN

As discussed in previous sections, in order to perform simulations various input data are required. The required data for the simulation and the relationship between the real world and the simulation world are shown in Figure 3-7. Simulation will be performed according to the following steps:

- Step 1: Collect train speed data, actual preemption warning time, and actual advance preemption warning time from the CWT detector and the Doppler detector.
- Step 2: Calculate detector length 1 based on actual preemption warning time and

the average train speed, and detector length 2 based on actual advance preemption warning time and the average train speed.

- Step 3: Predict the train arrival time (using the model developed in Chapter IV and the train speed data).
- Step 4: Input the detector lengths and the average train speed into the VISSIM model.
- Step 5: Input the train arrival time into the VAP cord.
- Step 6: Run the simulation.

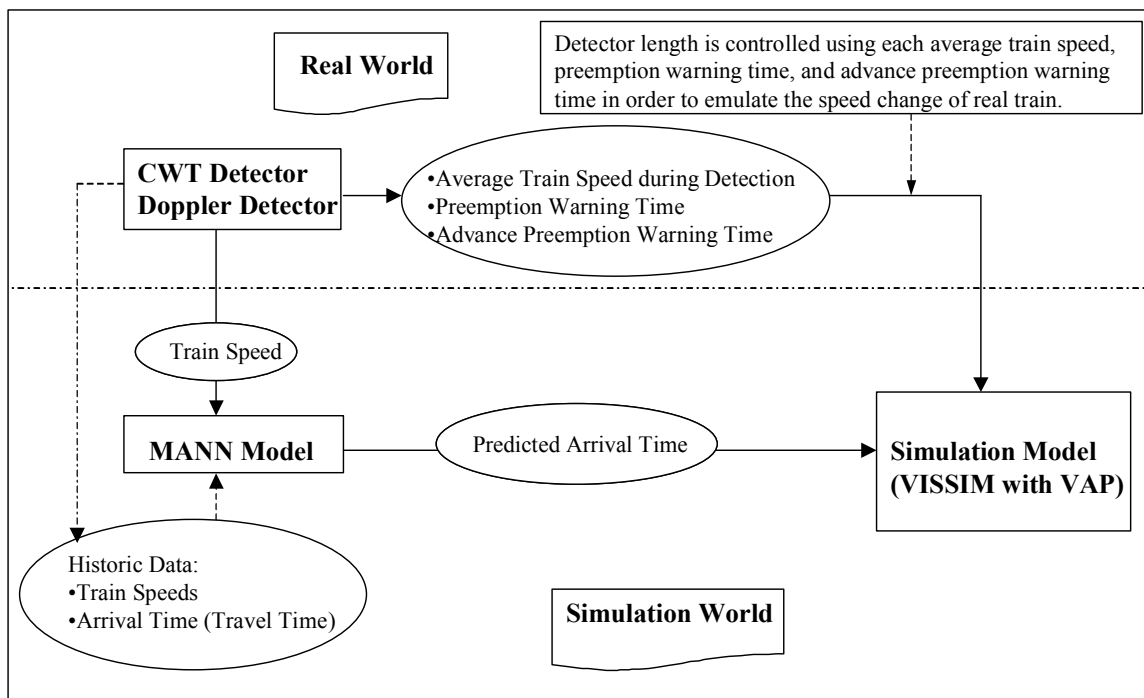


FIGURE 3-7 Relationship between the Real World and the Simulation World

3.9 CONCLUDING REMARKS

The methodologies to develop a new train arrival time prediction algorithm and new TPS algorithm were introduced in this chapter. The new prediction algorithm will be

developed using an artificial neural network and modular technology in Chapter IV. The new TPS algorithm, where the phases that are blocked during the preemption are given more importance than phases that are served during the preemption, will be developed in Chapter V.

Because the VISSIM micro-simulation model is a behavior and periodic-scan based micro-simulation model and has the capability to simulate vehicles, trains, and pedestrians, it was chosen as the microscopic traffic simulation model for this study. Moreover, because VISSIM provides VAP (vehicle actuated programming), which is an optional add-on module for the simulation of programmable, phase- or stage-based, and traffic-actuated signal controls (29), the functions in the vendor-specific controllers could be modeled within the simulation environment. All signal functions for this study including permissive coordinated mode, fully actuated mode, preemption mode, and the transition mode back to normal after preemption, which are available in the traffic signal controller, were programmed in VAP.

The test bed chosen for the train arrival time prediction algorithm was the Wellborn Road corridor in College Station, Texas. The corridor is approximately 2.2 km in length and is located between FM 2818 and George Bush Drive. The signalized intersection of George Bush Drive and Wellborn Road in College Station, Texas, along the railway corridor was chosen as the test bed for the development of 1) the new train arrival time prediction algorithms, and 2) the new TPS algorithm.

CHAPTER IV

DEVELOPING A TRAIN ARRIVAL TIME PREDICTION ALGORITHM

The ability to forecast train arrival time at highway-railroad grade crossings is essential for the accurate preemption of traffic signals at IHRGCs. However, because of limitations in detection technologies and the train arrival time prediction algorithms, a wide range exists in predicted arrival times. The uncertainty in arrival time arises because the existing prediction methods assume that the train's speed at the time of prediction will remain constant until the train reaches the crossing.

Generally two different arrival time predictions are needed at the site of interest in this dissertation: 1) the warning time for the HRGC, and 2) the preemption warning time for the IHRGC preemption. This predictions are calculated using the constant warning time detector.

With the recent advances in train detection technology, the potential exists for placing additional equipment in the field that will allow for earlier detection of oncoming trains, which is required for the TPS algorithm. In this chapter, a new train arrival time prediction algorithm will be developed based on train data obtained using Doppler microwave radar, which is one of the second-generation detector technologies. This new predicted arrival time will be updated continuously. Once the train arrival prediction equals to the APWT, the TPS algorithm starts. To predict the train arrival time, the train speed, acceleration rate, train length, time in detection, etc. can each be the candidate for the independent variable. A preliminary analysis for the variables will be undertaken in order to provide insight regarding the data structure, the distribution, and the relationship between the variables.

A new prediction algorithm will be developed using the artificial neural network because of the complexity of a series of speed data and the nonlinear relationship between the speed and arrival time. The study will identify the optimal number of neurons in the hidden layer and the optimal number needed for training, as well as the parameters in the models. Because trains can exhibit a wide range of behavior, a modular approach will be used. The chosen model will update the forecasted train arrival time at 10-second intervals. The current prediction method for the current TPS algorithm and five Multiple Linear Regression (MLR) models also will be evaluated for the purpose of comparison. A bootstrap technique will be used to obtain the prediction interval.

As discussed in Chapter III, the test bed was a railway corridor located in College Station, Texas. Doppler radar equipment was utilized to measure train speed and direction approximately 2.2 km from the HRGC. Because the detector is located relatively far from the crossing, the prediction at the detector location is subject to error. Even though the prediction algorithm will be developed using the train data at a specific test bed, the methodology can be applied to any other place where the speed data of trains are available.

4.1 PRELIMINARY ANALYSIS

In this section, the relationship among the variables and the characteristics of the variables, including train speed, train arrival time, train length, and time in detection, observed or estimated from the detectors of FM 2818 and George Bush Drive, were studied in order to implement them into the train arrival time prediction algorithm.

The average speed was obtained taking the average of all observed speeds per second. The average train speed during detection in the direction from FM 2818 toward George Bush Drive was 42.1 km/h and the standard deviation was 10.0 km/h. The distribution of the average train speed follows the normal distribution based on a chi-square test performed at the 95 percent significance level. The entering speeds of trains at FM 2818

ranged from 9.5 to 88.4 km/h. The average train entering speed was 47.2 km/h with 15.7 km/h of the standard deviation. The crossing speeds of trains at George Bush Drive ranged from 12.9 to 85.3 km/h. The average train crossing speed was 39.0 km/h with 8.2 km/h of the standard deviation. These are shown in Table 4-1 and the histograms of those speeds are shown in Figures 4-1, 4-2, and 4-3.

TABLE 4-1 Summary Statistics at FM 2818 and George Bush

	Average Train Speed (km/h)	Speed at FM 2818 (km/h)	Speed at George Bush (km/h)	Train Arrival Time (s)	Train Length (m)	Time in Detection (s)
Average	42.1	47.2	39.0	206	1363	128
Standard Deviation	10.0	15.7	8.2	44.8	564.0	59.9
Maximum	81.6	88.4	85.3	472	2327	405
Minimum	11.4	9.5	12.9	99	83	10

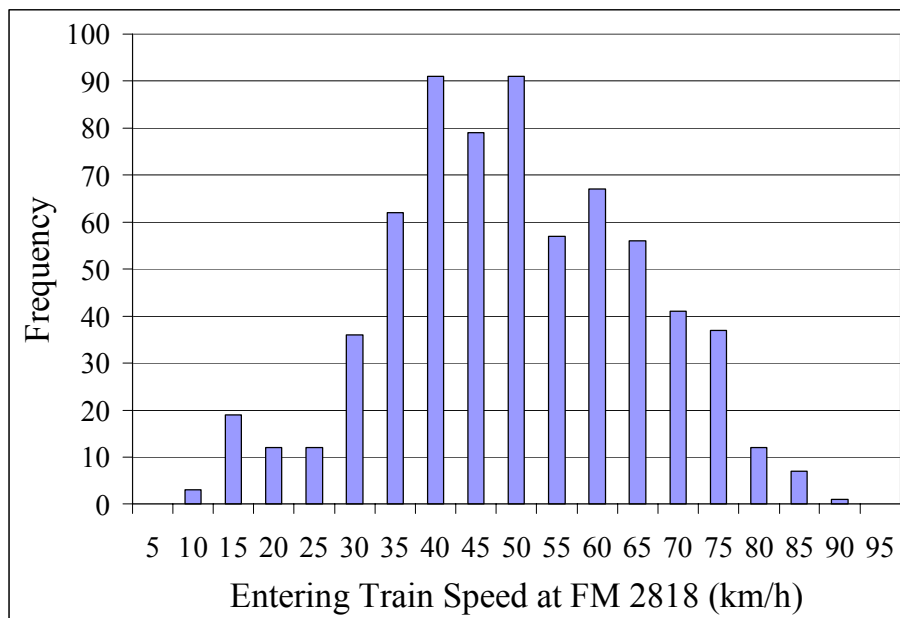


FIGURE 4-1 Histogram of Instantaneous Train Speed at FM 2818

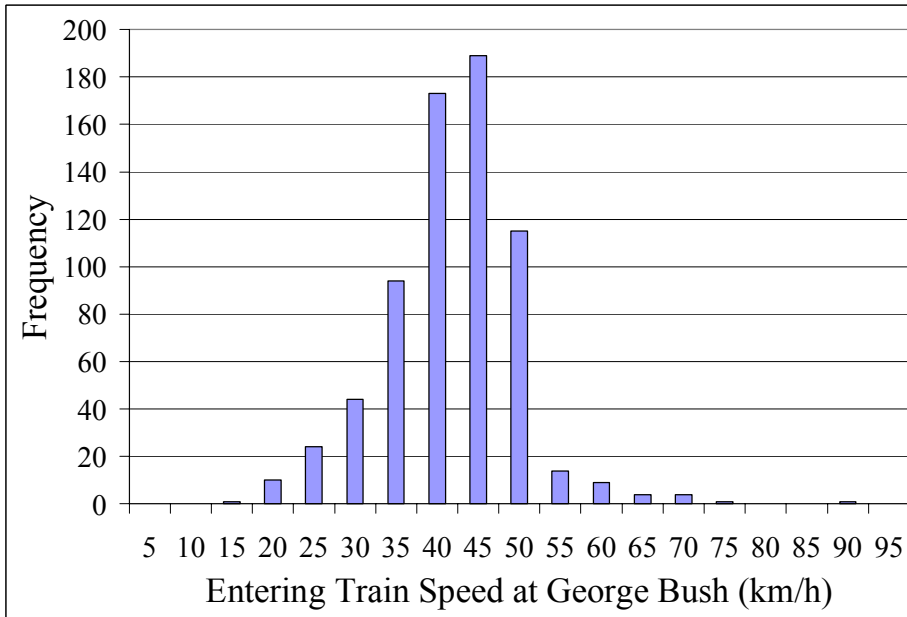


FIGURE 4-2 Histogram of Instantaneous Train Speed at George Bush Drive

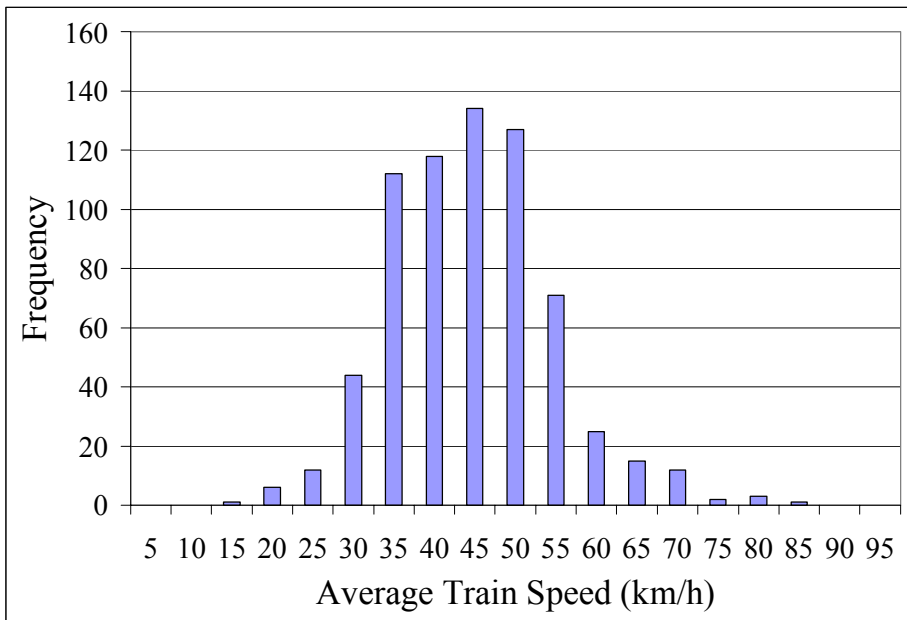


FIGURE 4-3 Histogram of Average Train Speed at FM 2818

The average train speed decreases as the trains pass the FM 2818 crossing as shown in Figure 4-4. However, the minimum speed is getting higher as time in detection increases as shown in Figures 4-1 and 4-2, and Table 4-1. It can be seen that the average train speed is lower at George Bush Drive than at FM 2818 and the variability of speed at George Bush Drive is less than at FM 2818 as shown in Table 4-1. Therefore, trains are typically experiencing a deceleration during their time in detection shown in Figure 4-5. This is consistent with Figure 4-4.

Note that the Doppler detector does not provide the acceleration/deceleration rate. However, the acceleration/deceleration rate may be estimated using Equation 4-1.

$$A_{cc} = \bar{S}_i - \bar{S}_{i-1} \quad (4-1)$$

where;

- A_{cc} = Acceleration/deceleration rate of train (km/h/s); and
- \bar{S}_i = Average train speed at i seconds after the detection (km/h) ($i = 2, 3, \dots, 240$).

The estimate acceleration/deceleration rate, in km/h/s, at FM 2818 detector location are shown in Figure 4-5. It may be seen that as trains approach the George Bush Drive crossing, the rate of deceleration decreases. Whereas most of the trains tend to decelerate generally, some slow trains tend to accelerate. This characteristic may cause trains that have different speed profiles to have the same arrival time. This is problematic for many estimation procedures.

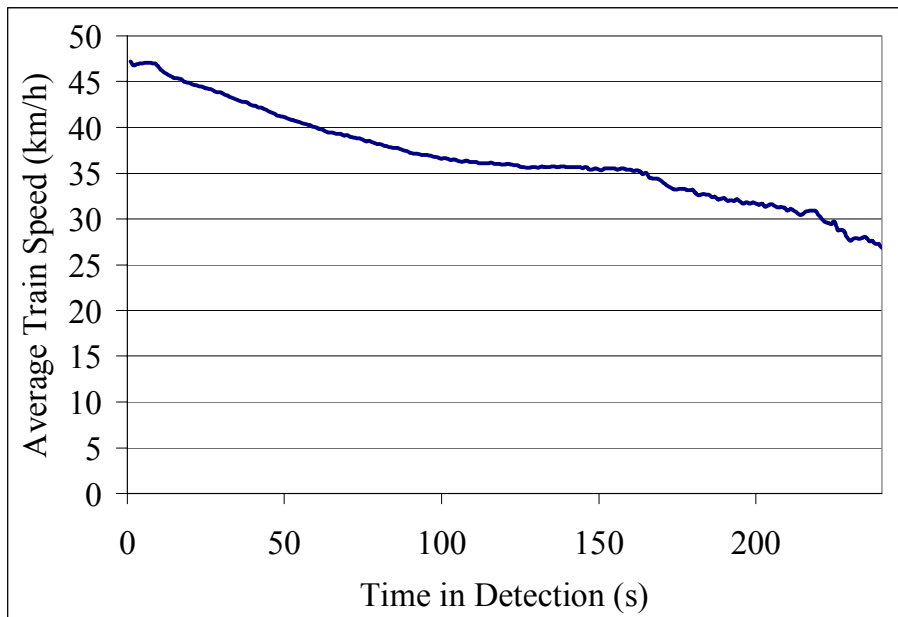


FIGURE 4-4 Average Train Speed versus Time in Detection at FM 2818

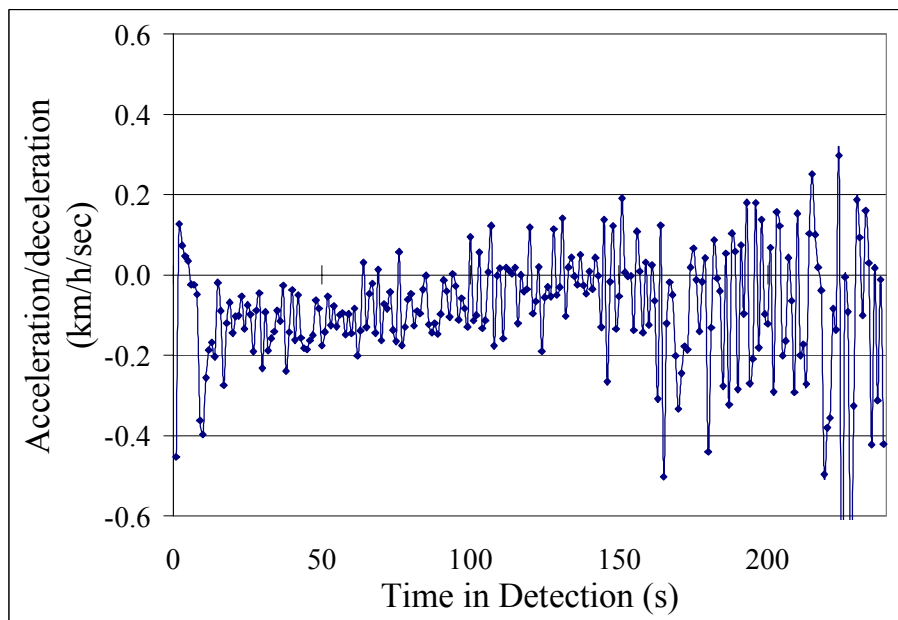


FIGURE 4-5 Average Train Acceleration/Deceleration versus Time in Detection at FM 2818

The number of speed observations is dependent on the train speed and the train length. The number of speed observations is shown in Figure 4-6. It shows that the number of speed observations decreases as time in detection increases.

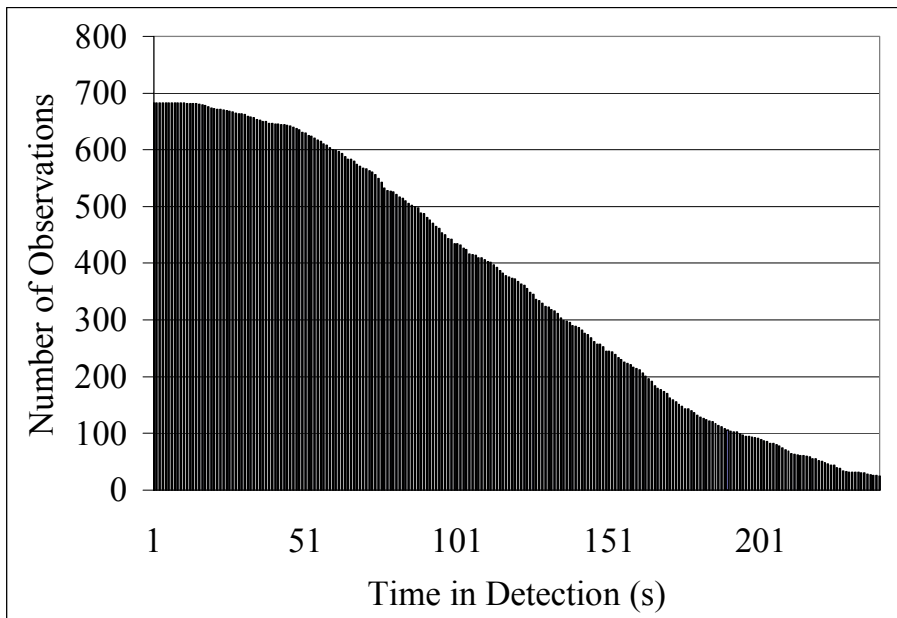


FIGURE 4-6 Number of Speed Observations for Time in Detection

Figure 4-7 shows the histogram of the train arrival time at George Bush Drive after detection at FM 2818. The average train arrival time was 206 seconds, and the standard deviation was 44.8 seconds as shown in Table 4-1.

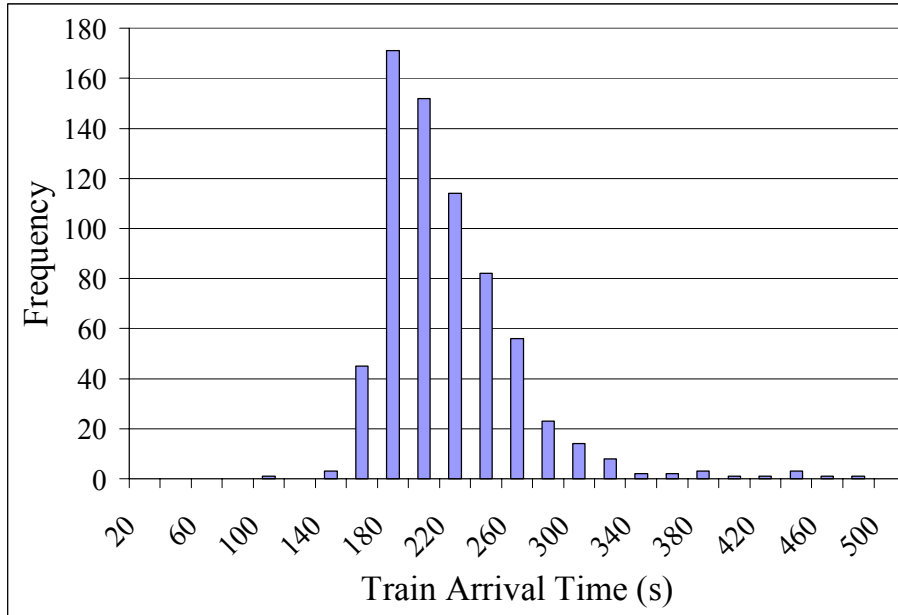


FIGURE 4-7 Histogram of Arrival Time from FM 2818 to George Bush Drive

Figure 4-8 shows the histogram of estimated train length. The average estimated train length was 1363 m and the standard deviation was 564.0 m as shown in Table 4-1. The train length was estimated using the speed observation and the time in detection as shown in Equation 4-2.

$$\xi = \sum_{i=1}^H V_i \quad (4-2)$$

where;

- ξ = Estimated train length (m); and
- V_i = Observation train speed at i seconds after the detection (m/s); and
- H = Time in detection (s).

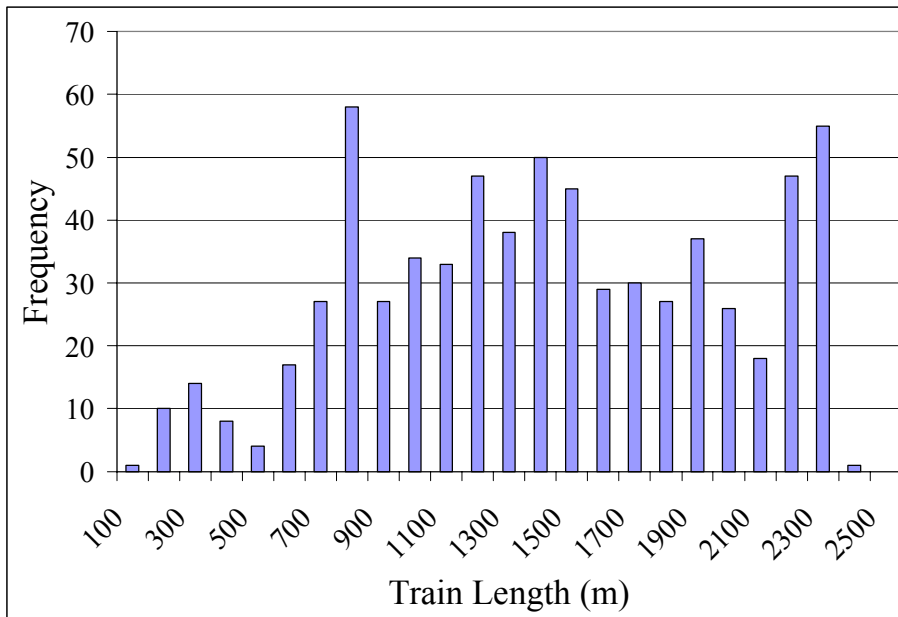


FIGURE 4-8 Histogram of Train Length

Figure 4-9 shows the histogram of the time in detection. The average time in detection was 128 seconds, and the standard deviation was 59.9 seconds as shown in Table 4-1.

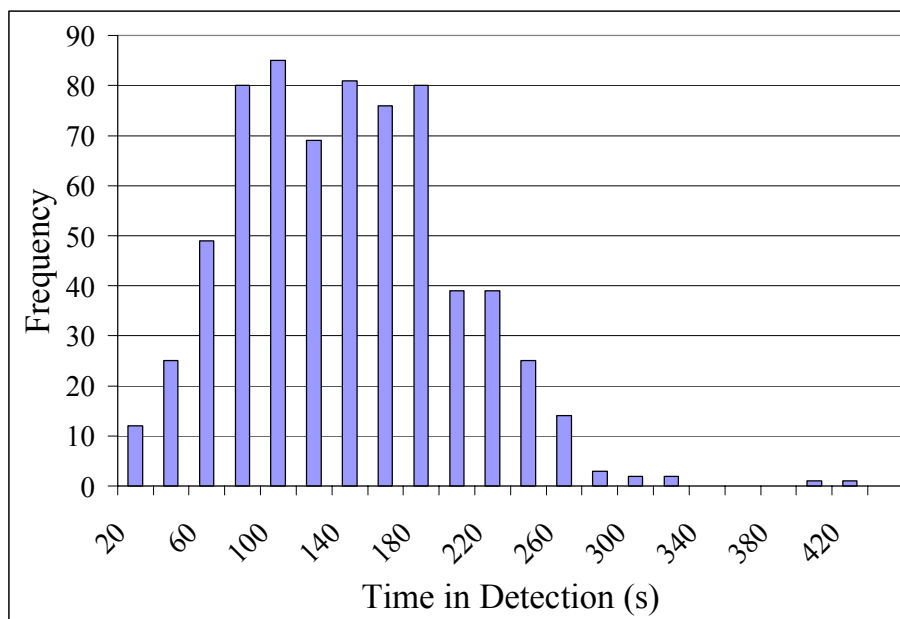


FIGURE 4-9 Histogram of Time in Detection

A series of two-dimensional graphs of different combinations of the four variables (average speed, time in detection, train length, and train arrival time) were created to help visualize the relationships. It was found that as time in detection increases, the average speed of trains decreases as shown in Figure 4-10. The correlation coefficient of this graph is -0.5526 . This negative relationship was expected from Figure 4-4, because there is general decreasing (negative) trend in average train speed as time in detection increases.

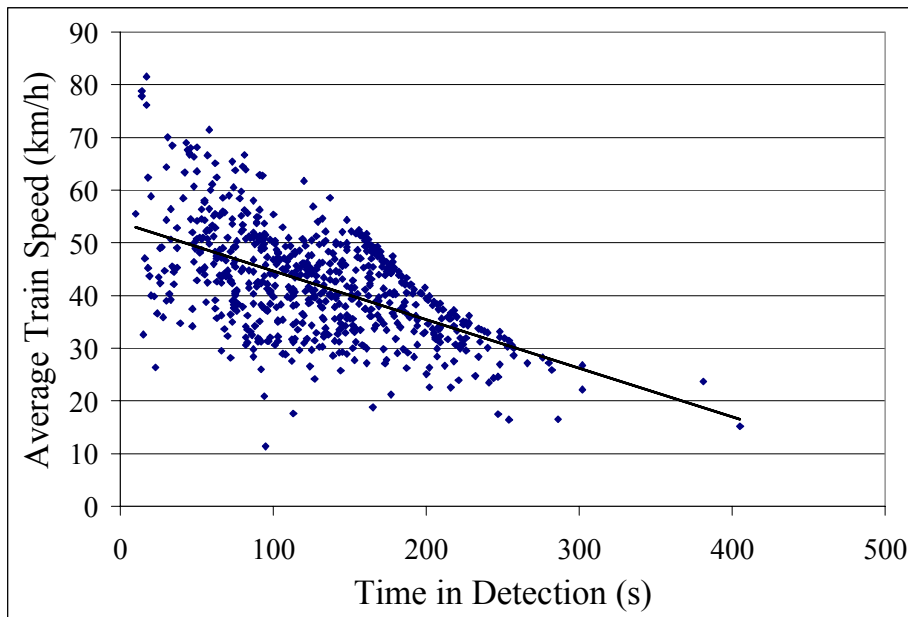


FIGURE 4-10 Time in Detection versus Average Train Speed

It was found that as the train length increases, time in detection increases as shown in Figure 4-11. The correlation coefficient was a relatively high 0.8367. It also was found that as train length increases the variance in time in detection increases. Therefore, it is hypothesized that as train length increases then the variation of the train speed increases and this accounts for the observed behavior.

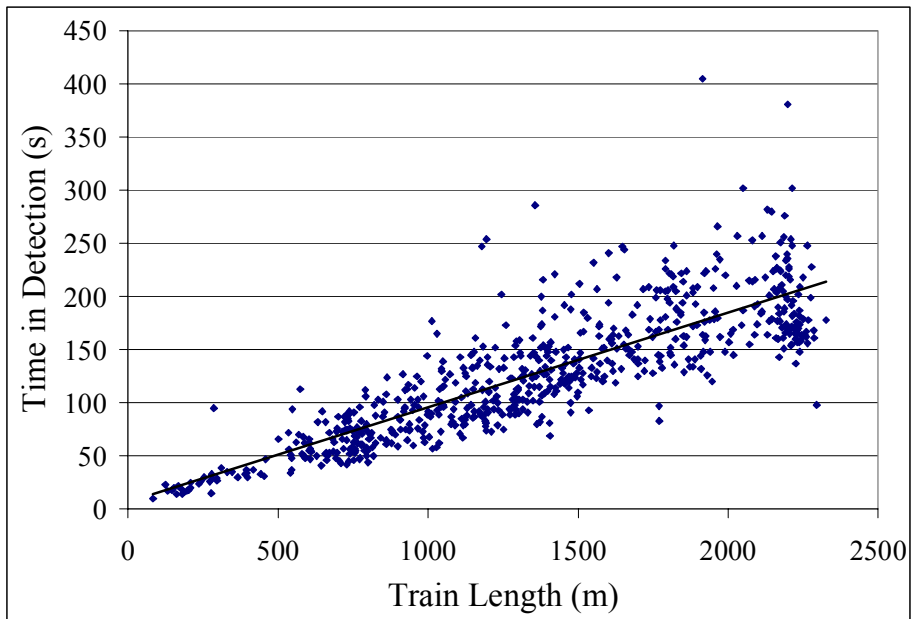


FIGURE 4-11 Time in Detection versus Train Length

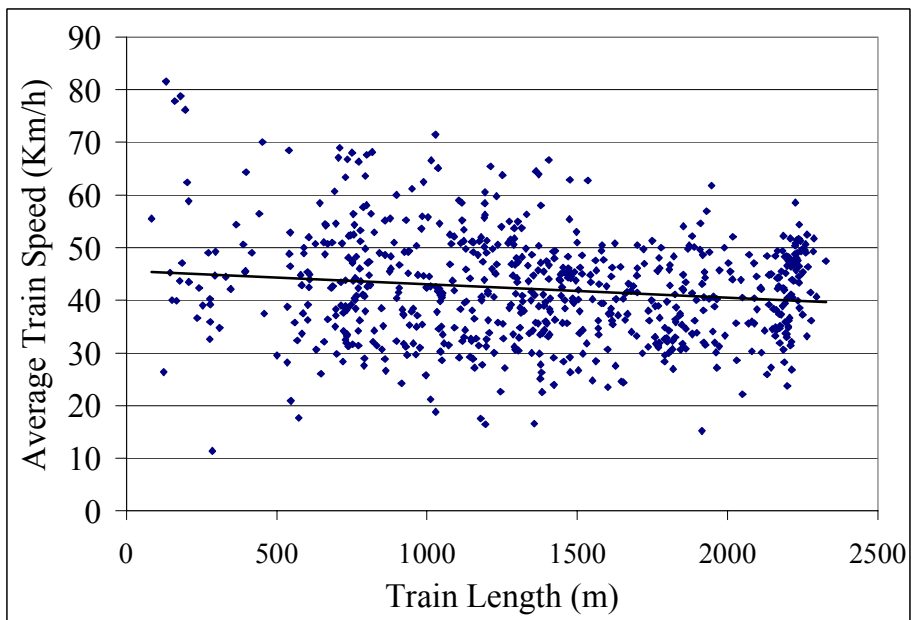


FIGURE 4-12 Average Train Speed versus Train Length

It was found that as the train length increases, the average train speed decreases slightly as shown in Figure 4-12. The correlation coefficient was a relatively small -0.1417 . From Figure 4-10 and 4-11, it would be expected that the relationship between train length and average speed would be negative. That is, the following relationships were found from Figure 4-10 and 4-11;

- 1) As the train speed increase, time in detection decrease.
- 2) As the train length increase, time in detection increase.

If the inverse relationship for each of two relationships is always satisfied, it is easy to derive the relationship between the average train speed and the train length. However, the inverse relationship of 1 and 2 may not be true for individual trains. For example, large values of time in detection can occur when (1) train length is long and train speed is high and (2) train length is short and train speed is low. Therefore, there is no clear relationship between any train speed and train length as shown in Figure 4-12.

It was found that as average speed increases, the train arrival time at George Bush Drive crossing decreases as shown in Figure 4-13. The correlation coefficient was a relatively high -0.7914 , illustrating a relatively high linear relationship. However, it can be seen in the figure that, the relationship is a power function, then the actual correlation could be even higher. Therefore, the speed could be used as an input variable for prediction of arrival time.

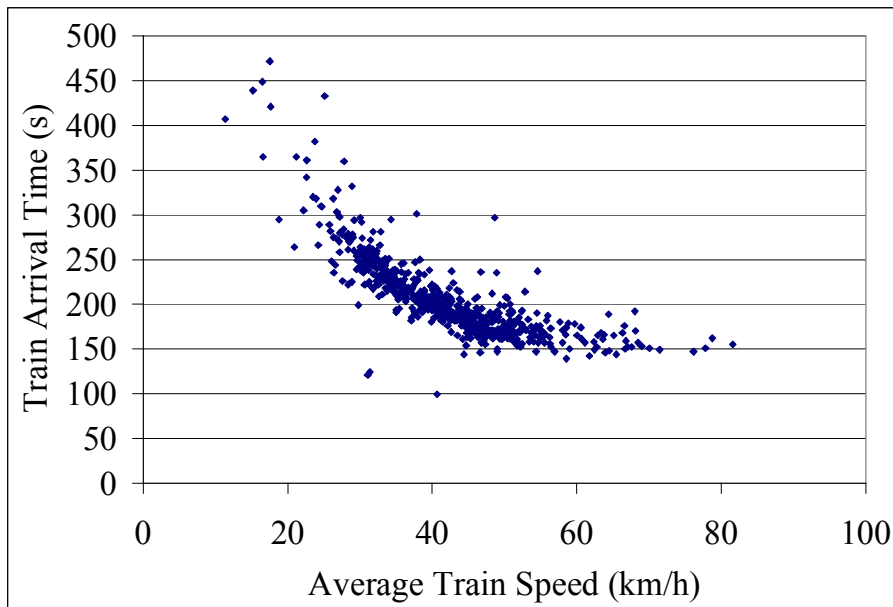


FIGURE 4-13 Train Arrival Time versus Average Train Speed

It was found that as time in detection increases, arrival time increases as shown in Figure 4-14. The correlation coefficient was 0.4877. It was found that time in detection is a function of train speed and train length. That is, as train speed increases, the time in detection decreases. As train length increases, the time in detection increases. As train speed increases, the arrival time decreases and there is no relationship between train length and arrival time. Therefore, the relationship between time in detection and train arrival time can be explained by the “hidden” variable train speed. On the other hand, there is no discernible relationship between the arrival time and the train length as shown in Figure 4-15. The correlation coefficient was a relatively low -0.0024 .

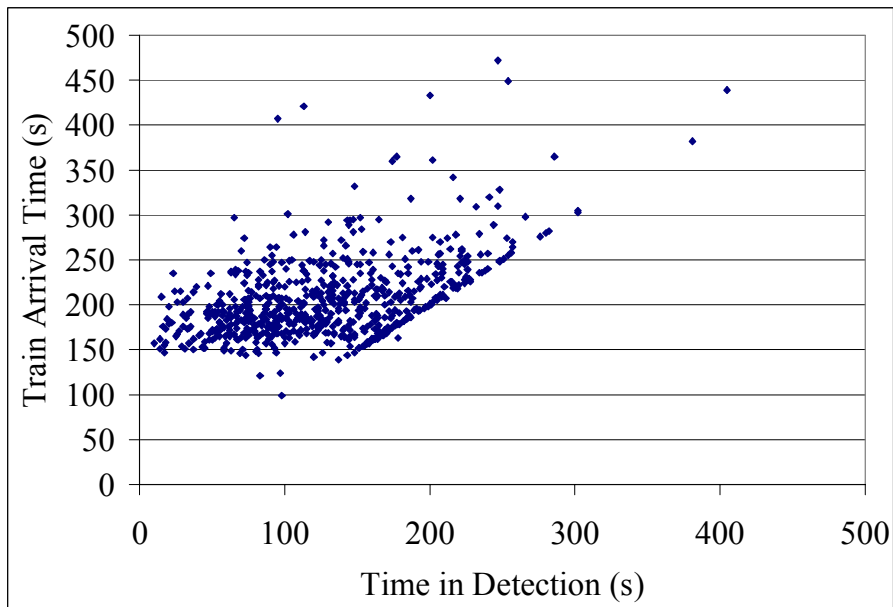


FIGURE 4-14 Train Arrival Time versus Time in Detection

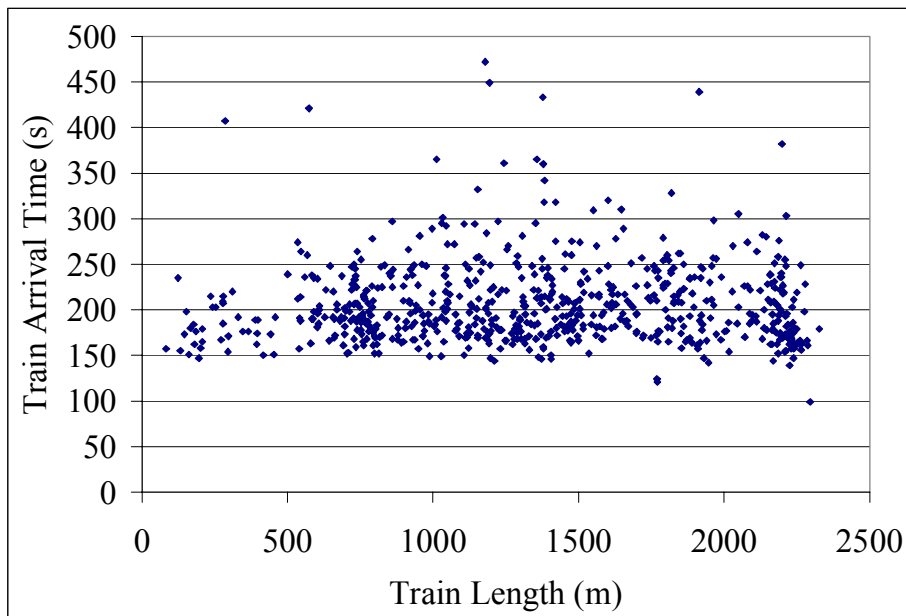


FIGURE 4-15 Train Arrival Time versus Train Length

4.2 ARTIFICIAL NEURAL NETWORK (ANN) MODEL DESIGN

4.2.1 Input Variables for ANN

An ANN model was used to model the relationship between train arrival time at George Bush Drive and the train speed at FM 2818. An ANN architecture was adapted because there is a nonlinear relationship between the independent variables such as train speed profile and the dependent variable such as train arrival time at the crossing as discussed in the preliminary analysis. Because a forecast arrival time is required every 10 seconds after the train is first detected, a series of ANNs is required. Note that as the time in detection increases the number of observations increases and, therefore, all else being equal, so would the accuracy of the prediction. While the best input would be the entire speed profile, 1-second speed measurements would be too complex for training an ANN. Consequently a speed profile consisting of 10 speed observations was used as input for each of the 24 forecasting models (i.e., a different model for every 10 seconds for 240 seconds). For example, for model 10 (i.e., 100 seconds after first detection) the input speed profile consisted of 10 observations starting at 10 seconds and proceeding in increments of 10 seconds. The exact time the speed information was collected is shown in Table 4-2.

TABLE 4-2 Selected Seconds after Detection for the Input Speed

Model	TID*	Selected Seconds after Detection for the Input Speed (s)									
1	10	1	2	3	4	5	6	7	8	9	10
2	20	2	4	6	8	10	12	14	16	18	20
3	30	3	6	9	12	15	18	21	24	27	30
4	40	4	8	12	16	20	24	28	32	36	40
5	50	5	10	15	20	25	30	35	40	45	50
6	60	6	12	18	24	30	36	42	48	54	60
7	70	7	14	21	28	35	42	49	56	63	70
8	80	8	16	24	32	40	48	56	64	72	80
9	90	9	18	27	36	45	54	63	72	81	90
10	100	10	20	30	40	50	60	70	80	90	100
11	110	11	22	33	44	55	66	77	88	99	110
12	120	12	24	36	48	60	72	84	96	108	120
13	130	13	26	39	52	65	78	91	104	117	130
14	140	14	28	42	56	70	84	98	112	126	140
15	150	15	30	45	60	75	90	105	120	135	150
16	160	16	32	48	64	80	96	112	128	144	160
17	170	17	34	51	68	85	102	119	136	153	170
18	180	18	36	54	72	90	108	126	144	162	180
19	190	19	38	57	76	95	114	133	152	171	190
20	200	20	40	60	80	100	120	140	160	180	200
21	210	21	42	63	84	105	126	147	168	189	210
22	220	22	44	66	88	110	132	154	176	198	220
23	230	23	46	69	92	115	138	161	184	207	230
24	240	24	48	72	96	120	144	168	192	216	240

*: Time since train was first detected

4.2.2 ANN Design

Because of the complexity of the function estimated, a fully connected multilayer neural network, rather than a single-layer ANN, was chosen for this study. The backpropagation algorithm was used to train the multilayer neural networks. The backpropagation algorithm is a generalization of the least mean square algorithm, and both algorithms use mean square error. The chain rule is employed in the backpropagation algorithm in order to compute the derivatives of the squared error with respect to the weights and biases in the hidden layers. However, when the

backpropagation algorithm converges, there is no guarantee the optimum solution is found. Consequently, it is best to try several different initial conditions to increase the possibility of finding a global optimum solution (33). Therefore, all ANNs tested in this dissertation were run 50 times with different initial parameters to find the parameters that gave the best results.

Several nonlinear optimization algorithms including the steepest-descent algorithm, Newton's method, and conjugate-gradient algorithm are generally used to minimize the squared error during training (33). The Levenberg-Marquardt algorithm, which is a variation of Newton's method, was used in this dissertation. The Levenberg-Marquardt algorithm was designed for minimizing functions that are sums of squares of other nonlinear functions. This algorithm is very well suited to neural network training. A hyperbolic tangent sigmoid was used as neuron transfer functions in this dissertation (33).

The number of neurons used is related to the complexity of the function that is approximated. Because a way to find the feature of the function does not exist, the number of neurons used in the hidden layer was identified based on a sensitivity analysis. Five different architectures, consisting of one, five, ten, twenty, and thirty hidden neurons were tested for each model and the average absolute error was used as the performance index. The input-output structure of the ANN model used in this dissertation is shown in Figure 4-16. A preliminary test indicated that 10 iterations were sufficient for identifying the initial ANN parameters. A complete description of ANN theory may be found elsewhere (33,34,35,36,37).

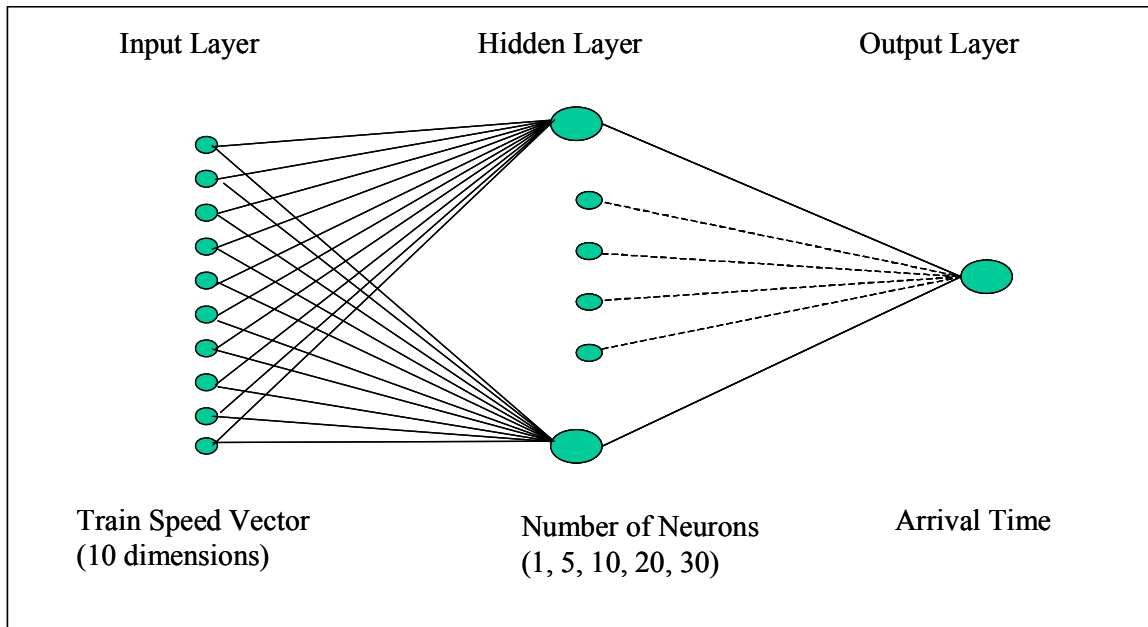


FIGURE 4-16 Input-Output Structure of Artificial Neural Network Model

The average absolute error of the testing set is used as the performance index for this study. The average absolute error of testing set is calculated as shown in Equation 4-3.

$$AAE_k = \frac{\sum_{i=1}^{N_k} |O_{ki} - P_{ki}|}{N_k} \quad (4-3)$$

where;

AAE_k = Average absolute error in testing set at time index k ($k = 10, 20, \dots, 240$);

O_{ki} = Observed arrival time for train i at time index k ($k = 10, 20, \dots, 240$);

P_{ki} = Predicted arrival time for train i at time index k ($k = 10, 20, \dots, 240$);

and

N_k = Number of trains in testing set i at time index k ($k = 10, 20, \dots, 240$).

4.2.3 ANN Results

One hundred iterations were performed for each of the ANNs using the initial parameters identified in the preliminary testing. The results are shown in Table 4-3. For all ANNs, the average absolute error (AAE) for the training sets decreases as the number of iterations increases, while the AAE for the testing sets decreases until the critical iteration is reached, at which point the AAE begins to increase. Therefore, after a certain iteration number, the ANN model continues to perform better for training sets while it performs worse for testing sets. This behavior is a well know property of ANN (33). The optimal parameters of the ANN model are identified based on the ANN that has the minimum AAE for testing sets.

The minimum AAE and the associated critical iteration number for every prediction model (i.e., every 10 seconds) are shown in Table 4-3. It can be seen that the best number of hidden neurons tends to decrease as the time in detection increases. As would be expected, the average absolute error also tends to decrease as time in detection decreases.

TABLE 4-3 Average Absolute Error as Function of Time in Detection

Model	Time in Detection*	Number of Neurons k (ANN Structure: 10-k-1)					Min. AAE	Best Number of Neurons
		1	5	10	20	30		
1	10	21.1(9)	20.5(3)	20.8(8)	20.3(9)	20.8(10)	20.3	20
2	20	18.9(13)	18.9(10)	18.6(19)	18.6(4)	18.1(17)	18.1	30
3	30	17.6(8)	17.5(10)	17.9(10)	18.1(14)	18.4(6)	17.5	5
4	40	17.7(10)	17(13)	16.9(13)	17(28)	17.6(10)	16.9	10
5	50	17.1(8)	16.8(6)	16.8(3)	17.3(14)	17.6(5)	16.8	5
6	60	17.1(10)	16.6(9)	16.4(9)	16.5(8)	16.7(4)	16.4	10
7	70	16.8(10)	16.2(10)	16.6(10)	16.5(8)	17.5(13)	16.2	5
8	80	16(4)	15.4(6)	15.7(6)	15.6(10)	15.6(10)	15.4	5
9	90	14.6(5)	14.6(8)	14.8(10)	15(10)	15.1(6)	14.6	5
10	100	14.1(9)	13.4(8)	13(8)	14.1(9)	14.4(4)	13	10
11	110	11.4(5)	10.3(5)	10.8(4)	10.8(9)	11.1(5)	10.3	5
12	120	10.3(6)	10.5(7)	11.1(7)	11.2(5)	11.8(6)	10.3	1
13	130	10.6(10)	10.7(4)	11(6)	11.9(8)	12.4(14)	10.6	1
14	140	11.5(9)	11.7(5)	11.7(6)	13.4(15)	11.6(12)	11.5	1
15	150	11(8)	10.5(9)	10.3(5)	12.5(6)	12.1(3)	10.3	10
16	160	11.8(11)	11.5(6)	11.8(7)	12(4)	12(6)	11.5	5
17	170	11(10)	9.1(7)	9.5(12)	9.5(16)	10.5(3)	9.1	5
18	180	11.1(11)	8.9(8)	10.1(7)	10.9(16)	12.7(5)	8.9	5
19	190	12.4(10)	10.8(6)	12.1(12)	13.8(11)	14.4(8)	10.8	5
20	200	16.8(9)	13.6(11)	15.9(17)	17.1(9)	16.9(7)	13.6	5
21	210	11.2(6)	10.7(11)	9.3(13)	11.8(6)	13.3(11)	9.3	10
22	220	15.7(6)	13.9(4)	15.1(34)	17.4(8)	15.1(3)	13.9	5
23	230	19.2(9)	19.1(12)	16(17)	22.7(5)	20.4(2)	16	10
24	240	23.4(10)	20.3(14)	15.7(8)	19.7(5)	39.2(4)	15.7	10

(): Optimal number of iterations

*: Time since train was first detected

4.3 MODULAR ARTIFICIAL NEURAL NETWORK (MANN) DESIGN

In general, the trains with lower initial speeds tended to accelerate, whereas the trains with higher initial speeds tended to decelerate. Therefore, trains that have markedly

different speed profiles may have the same arrival time. Because of this characteristic, a modular approach for train forecasting was also examined.

4.3.1 Clustering Analysis

The Ward method was used to group the speed profiles of the trains in the training sets for each of the 24 models that were developed (38). The method starts off with a separate data set (i.e., speed profile represented by 10 observations) for each of the trains. At the beginning of the algorithm each train is treated as a separate group. For example, there are 499 data sets (trains) for model 1. The objective is to identify, at each iteration, the two groups that, produce the minimum increase in total within group error sum of squares (E), when the two groups are combined as shown in Equation 4-4.

$$E = \sum_{k=1}^{N_G} E_k \quad (4-4)$$

where;

$E =$	Total within group error sum of squares;
$E_k = \sum_{i=1}^n \sum_{j=1}^{m_k} (x_{ijk} - \bar{x}_{ik})^2 =$	Error sum of squares for group k ;
$\bar{x}_{ik} = \sum_{j=1}^{m_k} \frac{x_{ijk}}{m_k} =$	Sample mean of the m_k observations of element i in the k th group;
$x_{ijk} =$	Value (speed) of i th element of j th data set (speed profile) in the k th group ($i = 1, \dots, n$; $j = 1, \dots, m_k$; $k = 1, \dots, H$);
$n =$	Number of elements in data set. In this dissertation, it is set to 10 for all 24 models;
$m_k =$	Number of data sets (speed profile) in k th group ($k = 1, \dots, H$); and
$N_G =$	Number of groups at current iteration of Ward algorithm.

The error sum of squares for a given group k is the sum of Euclidian distances from each data point in group k to the mean vector of group k (i.e., the within group squared deviation about the mean for group k). The algorithm is recursive in nature where after each iteration the total number of groups is reduced by one and the corresponding error sum of squares increases. A graph of the error sum of squares versus group number for model 1 (i.e., 10 seconds of detection time) is shown in Figure 4-17. Note that this technique does not identify the optimal number of groups but rather provides information to the analyst regarding the similarity among different grouping options. There is a natural bend at approximately four groups and therefore values in this area were studied further. A detailed description of the grouping algorithm may be found elsewhere (38,39,40).

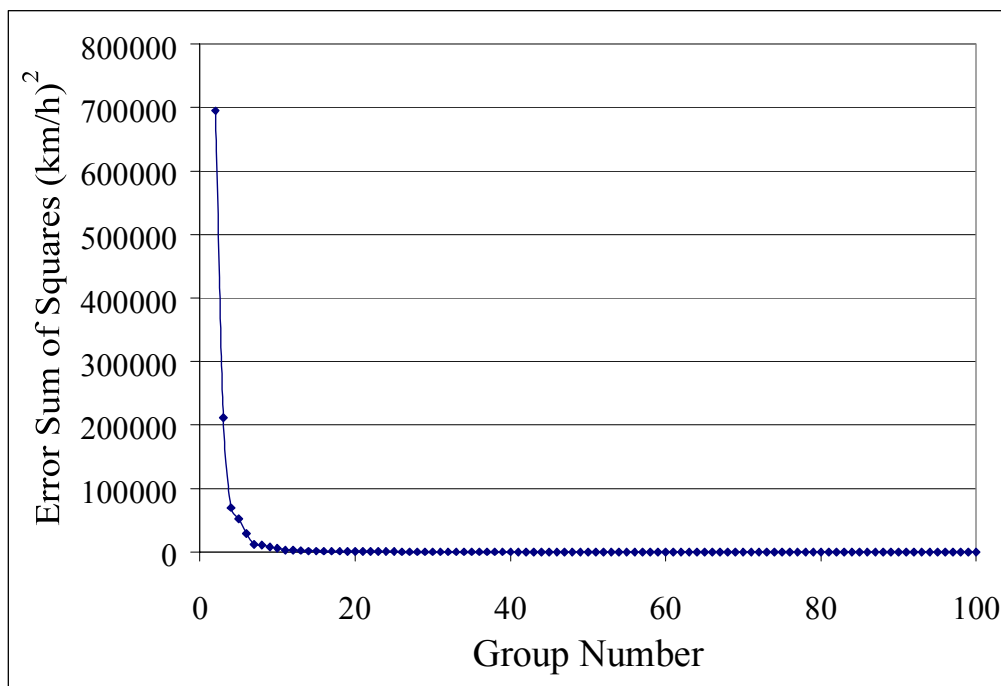


FIGURE 4-17 Error Sum of Squares versus Group Number after 10 Seconds of Detection

An empirical study was conducted to identify the best group size. Five ANN architectures, 10-1-1, 10-5-1, 10-10-1, 10-20-1, and 10-30-1 were considered in the analysis. A separate ANN was trained and tested for the trains in each group using the process described earlier. In order to compare and contrast the groups for a particular grouping option and a particular model, the average train speed for each group is calculated as shown in Equation 4-5.

$$AS_{gi} = \frac{\sum_{j=1}^{n_g} s_{gij}}{n_g} \quad \forall i=1,\dots,n; g=1,\dots,G; j=1,\dots,n_g \quad (4-5)$$

where;

- AS_{gi} = Average train speed of g th group and i th speed observation (km/h);
- s_{gij} = Speed of i th observation of j th train of group g (km/h);
- n_g = Number of data sets (trains) in group g ; and
- n = Number of elements in data set (10).

Figure 4-18 shows the relationship between the average speed and time in detection for the four groups for model 15 (i.e., 150 seconds after first detection). It can be seen that the trains in group 4 originally have slow speeds and accelerate while trains in group 2 have high speeds and decelerate. The trains in group 1 and group 3 have similar speed profiles although the trains in group 1 experience speeds that are approximately 10 km/h higher. Figures 4-19 and 4-20 show the relationship between average speed and time in detection for the three-group and two-group analyses, respectively. It can be seen that the speed profiles for the three-group analysis may be categorized as increasing, decreasing, and constant. The speed profiles in the two-group analysis may be categorized as constant and decreasing. As the number of groups decreases there is a loss in similarity in the trains in each group but a gain in the average number of observations per group. The number of trains for each group are shown in Table 4-4 depending on the group number and time in detection.

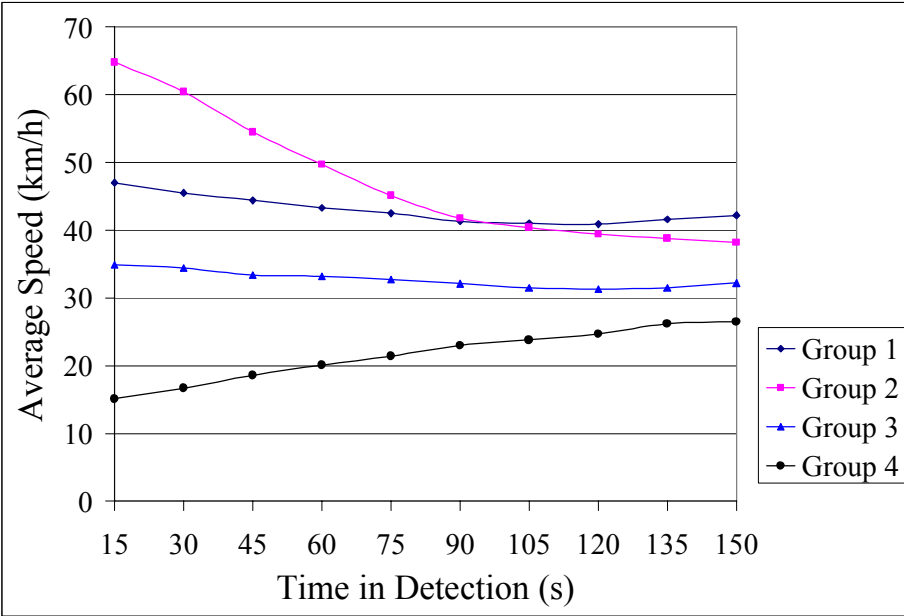


FIGURE 4-18 Average Speed versus Time in Detection for Four Groups (Model 15: 150 seconds of detection time)

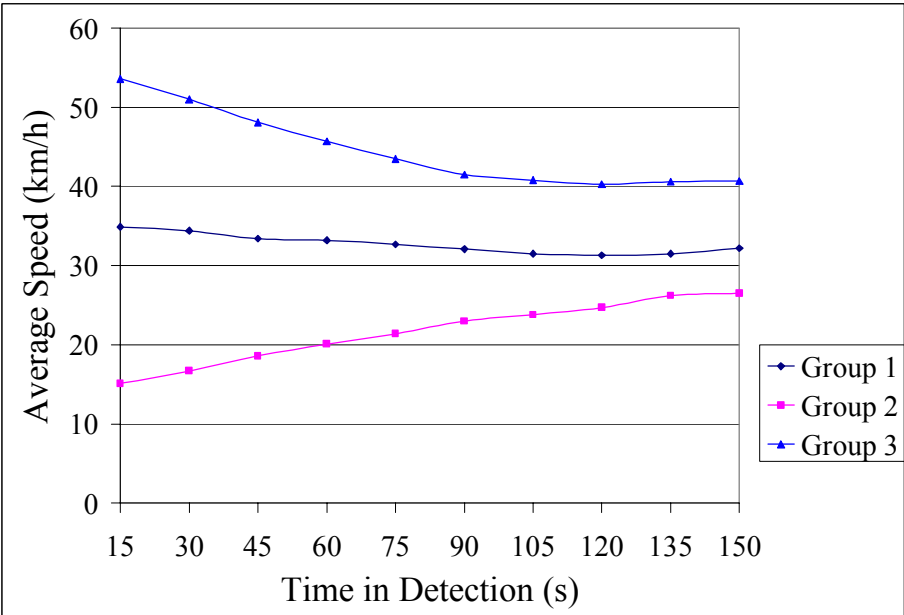


FIGURE 4-19 Average Speed versus Time in Detection for Three Groups (Model 15: 150 seconds of detection time)

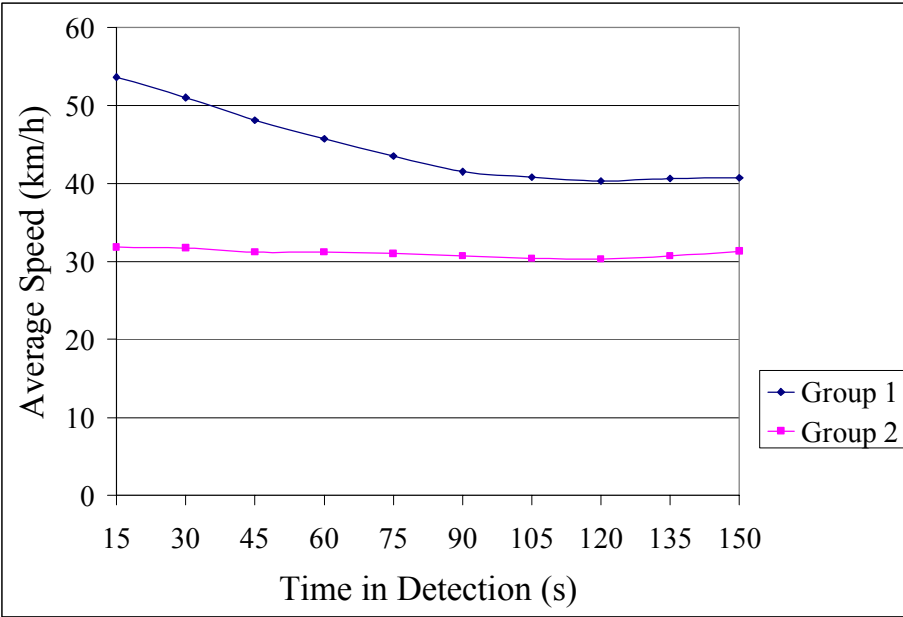


FIGURE 4-20 Average Speed versus Time in Detection for Two Groups (Model 15: 150 seconds of detection time)

TABLE 4-4 Number of Trains in Training Set and Testing Set for Each Model Tested

M ¹	TID ²	Training Set		Testing Set		Training Set			Testing Set			Training Set				Testing Set			
		G1	G2	G1	G2	G1	G2	G3	G1	G2	G3	G1	G2	G3	G4	G1	G2	G3	G4
1	10	338	161	118	66	131	207	161	49	80	55	104	27	207	161	41	13	75	55
2	20	329	163	117	65	144	185	163	51	80	51	117	27	185	163	44	14	73	51
3	30	321	166	109	67	281	40	166	95	21	60	144	137	40	166	54	56	16	50
4	40	323	155	107	62	157	166	155	53	69	47	138	19	166	155	45	13	64	47
5	50	320	147	104	60	123	197	147	44	73	47	105	42	123	197	42	14	44	64
6	60	311	134	101	54	115	196	134	42	69	44	88	46	115	196	39	13	42	61
7	70	315	110	97	46	118	197	110	44	62	37	97	21	197	110	37	11	58	37
8	80	223	173	68	62	104	119	173	35	48	47	122	51	104	119	42	16	35	37
9	90	213	154	64	56	120	93	154	49	29	42	108	46	120	93	35	16	40	29
10	100	245	83	65	42	187	58	83	50	23	34	102	85	58	83	36	29	17	25
11	110	188	121	55	42	104	84	121	41	23	33	77	44	104	84	25	13	36	23
12	120	114	169	43	46	99	70	114	32	18	39	96	18	99	70	33	9	29	18
13	130	110	134	34	46	119	15	110	41	9	30	69	41	119	15	23	10	38	9
14	140	109	113	27	40	98	15	109	34	8	25	88	21	98	15	22	5	32	8
15	150	89	98	22	36	83	15	89	28	8	22	56	33	83	15	16	6	28	8
16	160	73	88	19	34	73	15	73	28	8	17	40	33	73	15	10	6	29	8
17	170	75	53	28	14	61	14	53	23	6	13	46	7	61	14	12	1	23	6
18	180	70	29	22	11	58	12	29	19	6	8	45	13	12	29	13	6	5	9
19	190	67	13	18	8	55	12	13	15	4	7	21	34	12	13	6	11	3	6
20	200	58	12	14	7	49	9	12	14	2	5	17	32	9	12	4	11	2	4
21	210	41	11	11	5	36	5	11	11	1	4	29	7	5	11	7	5	1	3
22	220	32	9	8	3	28	4	9	8	1	2	23	5	4	9	6	2	1	2
23	230	13	10	4	4	11	2	10	4	1	3	8	2	11	2	2	2	3	1
24	240	10	9	3	3	8	2	9	3	1	2	7	2	8	2	1	2	2	1

¹: Model²: Time since train was first detected

4.3.2 MANN Results

Table 4-5 shows the smallest AAE and the number of hidden neurons for the different group sizes for all 24 models. For Model 1 the four-group scenario experienced the smallest average AAE. While the best group size is different for different models, a

group size of four was identified most often as the best. As the detection time increases, the AAE tends to decrease. A similar pattern was found for ANN. A detailed set of results are provided in Appendix A.

Note that there is a trade-off between the number of groups and the number of observations in each group. Intuitively, as the number of groups increases, the average number of samples per group will decrease. If the number of observations in a given group is small then the ANN cannot be trained adequately (33). This was not seen to be a problem in this dissertation for two reasons. Firstly, the number of groups was a control variable and the best number was identified based on the AAE of the testing set. More importantly, the groups were relatively distinct. For example, group 4, which had the lowest number of observations in the training set (Model 15), consisted of trains that had positive accelerations after 150 seconds of detection. This acceleration characteristic is non-typical for this test bed and, consequently, the fact that they are treated separately makes intuitive sense even though the groups had low numbers. That is, it is better to have two small groups with homogeneous characteristics than one large group with heterogeneous characteristics. It is hypothesized that as more data become available the number of observations per group will increase and this trade-off will cease to be an issue.

TABLE 4-5 Best Group Size and AAE versus Time in Detection

Model	2 Groups			3 Groups				4 Groups					Min. AAE	Best Group Size
	G1	G2	Ave.	G1	G2	G3	Ave.	G1	G2	G3	G4	Ave.		
1	24.3 (5)	12.2 (5)	20	34.4 (10)	15.1 (5)	11.3 (5)	19.1	27.4 (5)	42.6 (1)	15.1 (5)	10.8 (20)	18.5*	18.5	4
2	22 (5)	11.8 (1)	18.4	30.4 (5)	14.1 (5)	9.8 (5)	17.5*	25.3 (5)	37.7 (10)	14.4 (5)	9.8 (5)	17.5	17.5	3
3	21.6 (5)	10.7 (20)	17.4	18.9 (5)	28.9 (10)	9.6 (10)	16.9	23.7 (5)	13.2 (5)	31.4 (1)	8.8 (5)	16.8*	16.8	4
4	20.5 (10)	10.1 (1)	16.7	28.4 (10)	12.3 (20)	8.8 (1)	16.4	25.1 (20)	30.1 (1)	11.7 (5)	9.2 (1)	16*	16	4
5	20.7 (10)	9 (5)	16.4	25.7 (10)	14.7 (5)	8 (1)	15.8*	9.4 (1)	4.9 (5)	27.5 (5)	14.9 (5)	16	15.8	3
6	20.7 (20)	7 (10)	15.9	25.7 (10)	15 (1)	6.8 (5)	15.6*	7.5 (1)	4 (10)	26.4 (10)	16.2 (5)	15.7	15.6	3
7	19.8 (5)	8.4 (10)	16.2	23.3 (10)	14.9 (5)	7.8 (5)	15.6*	21.2 (5)	27.1 (5)	14.9 (1)	8.3 (10)	15.8	15.6	3
8	21.9 (5)	8 (5)	15.3	19.4 (1)	19.3 (5)	6.7 (10)	14.8	7.6 (20)	4.5 (5)	19.2 (1)	22.1 (5)	14.5*	14.5	4
9	19.9 (30)	6.7 (5)	13.7*	17.4 (1)	19.6 (5)	6.6 (5)	14.2	7.4 (10)	3.5 (5)	18.7 (1)	20.1 (10)	13.7	13.7	2
10	7.2 (5)	21.5 (1)	12.8	8.6 (5)	5.1 (5)	23.7 (10)	12.6*	18.8 (5)	5.9 (5)	3.2 (10)	17.9 (10)	12.6	12.6	3
11	14.3 (1)	5.6 (5)	10.5	9.2 (5)	19.8 (20)	4.8 (5)	10.2*	5.2 (1)	4.1 (5)	10.5 (10)	19.7 (5)	10.5	10.2	3
12	15.7 (1)	5.7 (5)	10.5	5.6 (10)	3.8 (5)	16.7 (1)	10.1	11.8 (5)	22.9 (5)	5.8 (20)	4.1 (10)	9.4*	9.4	4
13	4.3 (10)	14.5 (1)	10.2	10.9 (5)	24.1 (10)	4.8 (10)	10.1*	5 (10)	1.9 (10)	11.2 (5)	36.2 (1)	11.1	10.1	3
14	4.4 (5)	15.5 (1)	11*	13.4 (5)	22.2 (5)	4.7 (10)	11.2	4.6 (10)	1.7 (5)	14.8 (5)	27.4 (5)	12	11	2
15	2.8 (5)	14.6 (1)	10.1	11.1 (10)	27.9 (5)	3 (10)	10.3	3.6 (10)	2.1 (10)	9.4 (5)	25.5 (5)	9.3*	9.3	4
16	3.5 (5)	14.7 (1)	10.7	10.3 (5)	26.9 (1)	3.1 (10)	10.5*	2.9 (5)	1.8 (10)	10.2 (5)	28.4 (20)	10.6	10.5	3
17	12.5 (10)	3.2 (10)	9.4	7.9 (5)	26.4 (20)	2.7 (5)	8.9	2.8 (5)	0 (1)	7.5 (5)	22.8 (5)	8.2*	8.2	4
18	11.9 (10)	3.7 (1)	9.1	4.5 (5)	33.8 (5)	2.9 (5)	9.5	6.2 (5)	3.7 (5)	29.2 (30)	3.2 (10)	8.4*	8.4	4
19	4.6 (5)	10.8 (10)	6.5*	5.8 (10)	1 (1)	23.8 (5)	9.9	2.4 (1)	10.2 (5)	0.8 (1)	17.2 (10)	8.9	6.5	2
20	4.1 (5)	25.2 (5)	11.1	8.9 (10)	1.2 (5)	18.3 (10)	10.4	3.3 (1)	6.8 (5)	0.9 (1)	20.6 (20)	8.2*	8.2	4
21	2.6 (5)	15.5 (5)	6.6	1.9 (10)	0.4 (5)	23.8 (1)	7.3	1.8 (5)	7.1 (1)	3.6 (10)	5.5 (30)	4.3*	4.3	4
22	2.5 (1)	22.5 (10)	7.9	2.2 (5)	0.3 (20)	18.5 (30)	5	2.2 (5)	1.7 (5)	1.1 (5)	11 (20)	3.6*	3.6	4
23	5 (5)	26.1 (10)	15.6	1.4 (5)	1.4 (5)	33.6 (10)	13.5	0.4 (5)	4.9 (10)	0.3 (5)	0.8 (10)	1.6*	1.6	4
24	1.1 (1)	11.1 (10)	6.1	2.6 (5)	0.1 (1)	12 (30)	5.3*	0.1 (5)	26.1 (1)	0.8 (1)	0.2 (10)	9	5.3	3

(): Number of neuron in hidden layer

*: Minimum AAE for input data duration

4.4 COMPARISON OF THE MANN MODEL WITH OTHER APPROACHES

The ANN models and the MANN models also were compared to the current forecasting method and a series of linear regression models. The current method assumes that the most recent observed speed will remain constant until the train arrives at the crossing. The distance is calculated as the difference of the distance between FM 2818 and George Bush Drive and the current estimated train length. The predicted arrival time of the current method and the remaining distance are calculated as shown in Equation 4-6.

$$P_k = \frac{\eta_k}{V_k}, \quad \eta_k = D - \sum_{i=1}^k V_i \quad (4-6)$$

where;

- D = Distance from the detector at FM 2818 to the detector at George Bush (m);
- P_k = Predicted arrival time k seconds after detection (s);
- η_k = Estimated distance between crossing and head of train at the crossing k seconds after detection (m); and
- V_k = Train speed k seconds after detection (m/s).

Five regression models were tested and in each case the arrival time was the dependent variable. The independent variables examined included the most recent observed speed, the square of this speed, and the estimated distance between the head of the train and the HRGC.

Regression Model 1 is a simple linear regression using the last observed speed as the independent variable and the arrival time as the dependent variable.

Regression Model 2 is the polynomial regression model of degree 2 using the last observed speed as an independent variable and the arrival time as the dependent variable. This model was chosen to improve the simple linear regression model because

it was found that there is the polynomial relationship between train speed and train arrival time in the preliminary analysis (see Figure 4-12).

Regression Model 3 is a multiple linear regression using the last observed train speed and the remaining distance as independent variables and arrival time as the dependent variable. Because the remaining distance is used as the current method, the same variables were tested for the regression model.

Regression Model 4 is a combination of Regression Model 2 and Regression Model 3. The independent variables are the last observed train speed, the squared last observed train speed, and the remaining distance. The arrival time is the dependent variable.

In the current method the remaining distance is used with the form of the remaining distance divided by the last observed train speed. In order to put the relationship among the remaining distance, train speed, and train arrival time into the linear regression model, the natural logarithm is applied to both sides in Regression Model 5.

The models and corresponding AAE for each time in detection are shown in Table 4-6. Models 4 and 5 were the best regression models, based on the AAE, for the most time periods. Regression Models 4 and 5 had the best AAE for 21 of the 24 time periods. Note that both models had significant coefficients. The p-values of all the coefficients of the 24 best regression models are less than 0.033, which means they are statistically significant at the 95 percent level of confidence. The optimal coefficient of determination also is shown and, as expected, the value increases as the time in detection increases.

TABLE 4-6 AAE for Different Linear Regression Models

Model	Time in Detection ¹	Linear Reg.1	Linear Reg.2	Linear Reg.3	Linear Reg.4	Linear Reg.5	R ² of Optimal Model
1	10	23.4	22.4	23.2	22.2*	(22.2)	0.47
2	20	22.3	21.0	21.6	20.2	20.1*	0.51
3	30	20.9	19.3	20.2	18.4	18.3*	0.56
4	40	20.0	18.1	19.7	17.8	17.7*	0.61
5	50	18.8	16.9*	18.7	17.1	17.8	0.68
6	60	18.5	16.9*	(18.6)	(17.0)	(17.9)	0.71
7	70	18.7	17.5	(18.2)	17.0*	18.3	0.73
8	80	18.1	17.4	17.4	16.2*	18.1	0.77
9	90	18.1	17.5	16.3	15.0*	18.0	0.80
10	100	19.8	18.2	16.0	14.3	14.3*	0.89
11	110	18.7	15.6	14.9	12.2	11.2*	0.91
12	120	19.6	17.8	14.6	11.9*	12.4	0.90
13	130	21.0	18.8	15.3	12.1*	15.4	0.91
14	140	23.6	20.8	16.1	12.4*	14.8	0.92
15	150	25.0	21.3	16.2	12.2*	13.6	0.92
16	160	25.4	21.8	16.9	13.2*	16.9	0.92
17	170	28.5	24.3	18.3	14.3*	(11.6)	0.93
18	180	29.2	24.6	16.1	13.0	12.4*	0.96
19	190	29.6	(27.0)	18.0	16.5*	(13.3)	0.94
20	200	34.6	(34.0)	20.1	19.7	17.7*	0.94
21	210	30.7	(30.9)	16.8	16.7	13.5*	0.95
22	220	35.9	(36.4)	19.2*	19.4	(17.2)	0.92
23	230	42.7	(43.4)	22.8	(24.2)	20.8*	0.96
24	240	42.1	(41.3)	29.2	(29.5)	25.6*	0.93

*: Best regression model for input data duration

¹: Time since train was first detected

(): At least one coefficient is not significant at the 95 percent level of confidence

The regression equations are shown in Equations 4-7 through 4-11.

$$\text{Reg1: } Y_{ik} = b_{0k} + b_{1k}x_{1ik} \quad (4-7)$$

$$\text{Reg2: } Y_{ik} = b_{0k} + b_{1k}x_{1ik} + b_{2k}x_{1ik}^2 \quad (4-8)$$

$$\text{Reg3: } Y_{ik} = b_{0k} + b_{1k}x_{1ik} + b_{2k}x_{2ik} \quad (4-9)$$

$$\text{Reg4: } Y_{ik} = b_{0k} + b_{1k}x_{1ik} + b_{2k}x_{1ik}^2 + b_{3k}x_{2ik} \quad (4-10)$$

$$\text{Reg5: } \ln(Y_{ki}) = b_{0k} + b_{1k} \ln(x_{1ik}) + b_{2k} \ln(x_{2ik}) \quad (4-11)$$

where;

Y_{ik} = Estimated arrival time of train i , k seconds after detection (s)
($k=10,20,\dots,240, i=1,2,\dots,N_k$);

X_{1ik} = Instantaneous speed of train i , k seconds after detection (m/s)
($k=10,20,\dots,240, i=1,2,\dots,N_k$);

X_{1ik}^2 = Squared Instantaneous Speed of Train i , k seconds after detection
($k=10,20,\dots,240, i=1,2,\dots,N_k$);

X_{2ik} = Estimated distance between crossing and head of train i , k seconds
after detection (m) ($k=10,20,\dots,240, i=1,2,\dots,N_k$); and

N_k = Number of trains, k seconds after detection (m/s) ($k=10,20,\dots,240$).

Table 4-7 shows a comparison of the current method, the best linear regression model (from Table 4-6), the best ANN (from Table 4-3), and the best MANN (from Table 4-5). The current method had an average absolute error of 21.5 seconds across the entire analysis period. The best MLR model error was approximately 17.8 percent lower at 16.1 seconds. The best ANN model was approximately 46 percent better than the current method, and the MANN model was approximately 19.5 percent better than the simple ANN model. In summary, for this test bed the MANN gave superior results. In addition, for all the methods examined as the time in detection increases the accuracy of forecasting is improved.

TABLE 4-7 AAE for Current Method, Best MLR Model, Best ANN, and Best MANN

Model	TID*	Current Method	MLR	ANN	MANN	Diff ₁ ¹ (%)	Diff ₂ ² (%)	Diff ₃ ³ (%)	Diff ₄ ⁴ (%)	Diff ₅ ⁵ (%)	Diff ₆ ⁶ (%)
1	10	46.9	22.2	20.3	18.5	52.8	56.8	60.6	8.4	16.5	8.9
2	20	41.3	20.1	18.1	17.5	51.3	56.2	57.7	10.0	13.0	3.3
3	30	35.8	18.3	17.5	16.8	49.0	51.2	53.1	4.3	8.1	4.0
4	40	30.9	17.7	16.9	16	42.9	45.4	48.3	4.4	9.5	5.3
5	50	27.5	16.9	16.8	15.8	38.6	38.8	42.4	0.4	6.3	6.0
6	60	24.6	16.9	16.4	15.6	31.2	33.4	36.7	3.2	7.9	4.9
7	70	23.5	17.0	16.2	15.6	27.8	31.1	33.7	4.6	8.2	3.7
8	80	22.4	16.2	15.4	14.5	27.6	31.3	35.3	5.1	10.6	5.8
9	90	21.8	15.0	14.6	13.7	31.0	33.0	37.1	2.9	8.9	6.2
10	100	17.1	14.3	13	12.6	16.5	23.9	26.2	8.8	11.6	3.1
11	110	13.6	11.2	10.3	10.2	17.3	24.2	25.0	8.4	9.3	1.0
12	120	15.2	11.9	10.3	9.4	22.0	32.5	38.4	13.4	21.0	8.7
13	130	17.2	12.1	10.6	10.1	29.7	38.2	41.2	12.2	16.4	4.7
14	140	15.5	12.4	11.5	11	20.1	25.8	29.0	7.1	11.1	4.3
15	150	13.4	12.2	10.3	9.3	8.6	23.0	30.4	15.7	23.9	9.7
16	160	12.6	13.2	11.5	10.5	-4.5	8.8	16.8	12.8	20.4	8.7
17	170	12.4	14.3	9.1	8.2	-15.1	26.8	34.0	36.4	42.7	9.9
18	180	12.1	12.4	8.9	8.4	-2.2	26.4	30.5	28.0	32.0	5.6
19	190	13.6	16.5	10.8	6.5	-21.8	20.5	52.2	34.7	60.7	39.8
20	200	17.3	17.7	13.6	8.2	-2.2	21.3	52.5	23.0	53.6	39.7
21	210	14.6	13.5	9.3	4.3	7.6	36.5	70.6	31.3	68.2	53.8
22	220	19.4	19.2	13.9	3.6	1.3	28.3	81.4	27.4	81.2	74.1
23	230	20.3	20.8	16	1.6	-2.3	21.2	92.1	23.0	92.3	90.0
24	240	25.9	25.6	15.7	5.3	0.9	39.3	79.5	38.7	79.3	66.2
Average		21.5	16.1	13.6	11.0	17.8	32.2	46.0	15.2	29.7	19.5

*: Time since train was first detected

- 1.: Difference between Current method and MLR
2.: Difference between Current method and ANN
3.: Difference between Current method and MANN
4.: Difference between MLR and ANN
5.: Difference between MLR and MANN
6.: Difference between ANN and MANN

The differences between the methods are calculated as shown in Equation 4-12.

$$Diff_n^k = \frac{M_i^k - M_j^k}{M_i^k} \times 100 \quad (4-12)$$

(if n = 1, i = 1 and j = 2;
 if n = 2, i = 1 and j = 3;
 if n = 3, i = 1 and j = 4;
 if n = 4, i = 2 and j = 3;
 if n = 5, i = 2 and j = 4;
 if n = 6, i = 3 and j = 4)

where;

$Diff_1^k$ = Difference between Simple method and Regression Model, k seconds after detection;

$Diff_2^k$ = Difference between Simple method and ANN, k seconds after detection;

$Diff_3^k$ = Difference between Simple method and MANN, k seconds after detection;

$Diff_4^k$ = Difference between Regression Model and ANN, k seconds after detection;

$Diff_5^k$ = Difference between Regression Model and MANN, k seconds after detection;

$Diff_6^k$ = Difference between ANN and MANN, k seconds after detection;

M_1^k = AAE of Simple method, k seconds after detection;

M_2^k = AAE of Regression model, k seconds after detection;

M_3^k = AAE of ANN, k seconds after detection; and

M_4^k = AAE of MANN, k seconds after detection.

4.5 PREDICTION INTERVAL OF MANN

Prediction error is defined as the difference between the real arrival time and the predicted arrival time. Because the MANN is a non-parametric method, a bootstrap technique was chosen to obtain the prediction interval. The bootstrap is a computer-based method for assigning measures of accuracy to statistical estimates. In this

dissertation, the bootstrap technique is used to estimate the interval for prediction error, which provides a measure of the accuracy of the forecast. In general the narrower the interval, the more precise the prediction. This prediction interval will be used as input to the preemption algorithm.

The bootstrap is a data-based simulation method for statistical inference. Figure 4-21 is a schematic diagram of the bootstrap applied to problem with a general data structure $P \rightarrow x$. On the left is the real world, where an unknown probability mechanism P gives an observation data set $x = (x_1, x_2, \dots, x_n)$, according to the rule of construction indicated by the arrow “ \rightarrow ”; from x the statistic of interest $\hat{\theta} = s(x)$ is calculated. On the right side of the diagram is the bootstrap world. The bootstrap world is defined by the analogous quantities in the real world: the arrow in $\hat{P} \rightarrow x^*$ is defined to mean the same thing as the arrow in $P \rightarrow x$. In the bootstrap world, the estimated probability model produced by observed data generates a bootstrap sample $x_n^* = (x_1^*, x_2^*, \dots, x_n^*)$ according to the rule of construction indicated by the arrow “ \rightarrow ”; from which the bootstrap replications of the statistic of interest, $\hat{\theta}^* = s(x^*)$ are calculated. A major advantage of the bootstrap world is that as many bootstrap replications $\hat{\theta}^*$ can be calculated as desired, or at least as many as can be afforded. This allows probabilistic calculations to be calculated directly (41).

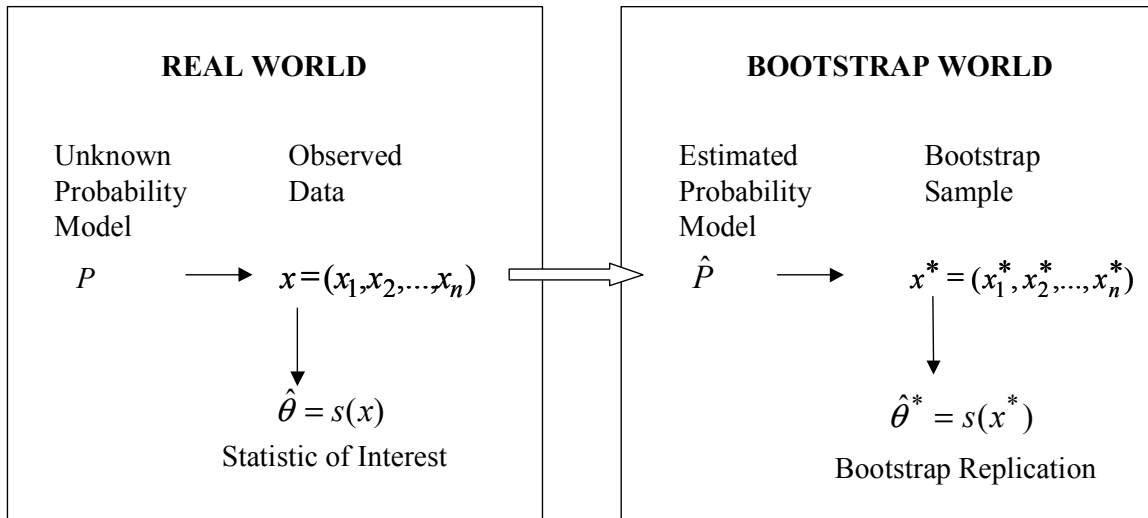


FIGURE 4-21 A Schematic Diagram of the Bootstrap Applied to Problems with a General Data Structure $P \rightarrow x$

A bootstrap data set x^* is generated by re-sampling the training set and the testing set with replacement. The MANN model is re-fitted based on the each bootstrap sample. The mean of the predicted value and the prediction interval of a train arrival time are calculated for each train based on the MANN models re-fitted. Bootstrap replications $\hat{\theta}^* = s(x^*)$ (θ = mean of the error) are computed. The sample size of both the training set and the testing set, N_i and M_i , is set equal to the size of the observed data set for the model under consideration. For example the sample sizes for model 1, N_1 and M_1 , are 499 and 184 for the training set and the testing set, respectively, while the sample sizes for model 8, N_8 and M_8 , are 396 and 130 for the training set and the testing set, respectively. Let \hat{G} be the cumulative distribution function of $\hat{\theta}^*$. The $1-2\alpha$ percentile interval is defined by the α and $1-\alpha$ percentiles of \hat{G} as shown in Equation 4-13.

$$[\hat{\theta}_{\%lo}, \hat{\theta}_{\%up}] = [\hat{G}^{-1}(\alpha), \hat{G}^{-1}(1-\alpha)] \quad (4-13)$$

Because, by definition $\hat{G}^{-1}(\alpha) = \hat{\theta}^{*(\alpha)}$, the $100 \times \alpha^{\text{th}}$ percentile of the bootstrap distribution, the percentile interval can be written as shown in Equation 4-14.

$$[\hat{\theta}_{\%lo}, \hat{\theta}_{\%up}] = [\hat{\theta}^{*(\alpha)}, \hat{\theta}^{*(1-\alpha)}] \quad (4-14)$$

Equations 4-13 and 4-14 refer to the ideal bootstrap situation in which the number of bootstrap replications is infinite. The bootstrap procedure for the prediction interval is described as follows:

- Step 1: Generate a bootstrap sample from the training set and the testing set. The size of the bootstrap sample is equal to the size of the observed data set for the model under consideration. The sampling is random and with replacement.
- Step 2: The MANN model is re-fitted based on the bootstrap sample generated in Step 1.
- Step 3: Repeat steps 1 and 2 R times.
- Step 4: Input train speed data into R MANN models. Obtain R predicted arrival time.
- Step 5: Sort the predicted arrival time in ascending order. Extract the αR^{th} and $(1-\alpha)R^{\text{th}}$ value from the ordered R Predicted arrival time. These represent the lower bound and upper bound of the $1 - 2\alpha$ percentile interval for the predicted arrival time for the train.

Therefore, the prediction interval is obtained based on each train and each time of prediction. The prediction interval is converted to the prediction error interval to check the accuracy of the models. For illustration purpose the Table 4-8 shows the intervals for the mean error over the trains in the testing set for each time period with the 90 percent and 95 percent level of significance. In this example, the MANN models were re-fitted based on the bootstrap samples using the optimal neuron number and the

optimal group size. The optimal initial parameter and the optimal number of iterations are obtained each bootstrap sample. A finite number of replications, R , was used where R was set to 20.

It should be note that in this dissertation the MANN models were re-fitted for each bootstrap sample using the optimal neuron number and the optimal group size, which were found when the MANN model was originally fitted. In fact, these two factors should also be optimized in order to re-fit the model correctly. In this case, the model re-fitting time is relatively long. It will take approximately one week to fit one replication of the MANN model. Therefore, it is not realistic to obtain the prediction interval correctly. Instead of this method, a simple method will be used to estimate the prediction error interval as will be discussed in Chapter V.

TABLE 4-8 Prediction Interval Depending on Significant Level and Input Data Duration with Model Refitting

Model	Time in Detection ¹	Error Mean	90% Bound		95% Bound	
			Lower	Upper	Lower	Upper
1	10	-1.2	-5.6	2.9	-5.6	6.2
2	20	-2.2	-5.2	0.7	-5.2	1.4
3	30	-3.1	-6.0	-0.4	-6.0	0.8
4	40	-3.3	-6.8	-1.2	-6.8	1.1
5	50	-3.6	-7.5	-1.1	-7.5	-0.8
6	60	-4.3	-8.3	-2.3	-8.3	-0.6
7	70	-3.3	-6.9	-1.1	-6.9	2.5
8	80	-4.4	-6.9	-0.9	-6.9	-0.9
9	90	-4.5	-7.2	-2.0	-7.2	-1.8
10	100	-5.2	-9.1	-1.6	-9.1	-0.5
11	110	-2.1	-6.5	1.3	-6.5	2.2
12	120	-0.5	-6.5	6.6	-6.5	11.0
13	130	-3.0	-17.9	1.4	-17.9	8.0
14	140	-3.0	-5.3	-1.2	-5.3	1.0
15	150	-4.6	-12.4	-1.0	-12.4	2.2
16	160	-2.5	-9.1	1.0	-9.1	5.3
17	170	-3.4	-8.9	4.8	-8.9	7.0
18	180	-1.8	-21.3	14.3	-21.3	20.9
19	190	-1.4	-10.6	7.4	-10.6	10.7
20	200	1.7	-15.9	12.9	-15.9	38.8
21	210	2.6	-17.3	22.7	-17.3	27.6
22	220	0.8	-7.0	9.6	-7.0	10.0
23	230	-0.4	-62.9	14.8	-62.9	17.8
24	240	-6.6	-60.0	24.7	-60.0	26.8

¹: Time since train was first detected

4.6 CONCLUDING REMARKS

The current forecasting method assumes that the last observed speed will be constant until the train arrives at the crossing. It was found that this method had the highest forecasting error. The MANN approach is promising for train arrival prediction in that it provided an average 19.5 percent improvement over a standard ANN model, an average

29.7 percent improvement over a multiple linear regression model, and an average 46 percent improvement over the current method. While the last observed speed is used to predict the train arrival time in the current method and the MLR model, the trend of speed change is used in the ANN and MANN. Therefore, it is concluded that the trend of speed change is a better explanatory variable than the last observed speed when forecasting train arrival time.

Because trains exhibit a wide range of behavior during detection, trains that have markedly different speed profiles may have the same arrival time. Because the modular ANN approach first categorizes trains into groups having similar speed profiles, these characteristics of trains can be handled in the MANN methodology. Therefore, a modular approach is appropriate for forecasting train arrival time at sites where there is a wide range in train speed profiles.

It was found that as the forecast was updated the accuracy of all models tested improved. Because a more accurate predicted arrival time is available, there is a potential for improving traffic signal preemption at IHRGCs. As well, a methodology for calculating the prediction error associated with the estimation was provided. The methodology of incorporating these forecasts and their associated prediction intervals into the traffic signal preemption algorithms will be developed in Chapter V.

CHAPTER V

DEVELOPING A TRANSITION PREEMPTION STRATEGY FOR IHRGC

In Chapter IV, a new train arrival time prediction algorithm was developed. In this chapter, a new TPS algorithm will be developed by modifying the signal logic from the current TPS algorithm to take advantage of the new train prediction model developed in Chapter IV.

First, the current transition preemption strategy will be investigated in detail and its advantages and disadvantages will be examined. From this analysis, a new transition preemption method will be developed based on the framework of the current TPS algorithm. The new algorithm has two objectives. The first is to increase safety by obtaining an earlier and more accurate warning regarding train arrivals. It is hypothesized that by including a more accurate estimate of the train arrival time and its standard error, pedestrian phase truncations can be eliminated and therefore safety will be improved. The second objective is to decrease vehicle delay. The basic idea of the new transition preemption method is to provide more time to the traffic signal phases that are blocked during the preemption mode and less time to the traffic signal phases that are served during the preemption mode. It is hypothesized that if this strategy is followed, the total intersection delay will be reduced.

As discussed in Chapters III and IV, the test bed was a signalized intersection of George Bush Drive and Wellborn Road in College Station, Texas, along the railway corridor. The intersection has four-leg approaches and is operated with a dual ring structure. Even though the new TPS algorithm is developed based on this specific test bed, the methodology developed in this dissertation can be applied to any IHRGC.

5.1 OVERVIEW OF CURRENT TPS (TPS1)

The current TPS algorithm (TPS1) was designed to reduce the probability that the minimum vehicle green time and pedestrian clearance time of a given phase will be truncated, while simultaneously guaranteeing that sufficient track clearance time was available. However, if the current system's preemption warning time is long enough to provide the minimum vehicle/pedestrian green phase and pedestrian clearance phase at the onset of preemption, there is no need to truncate the minimum vehicle green/pedestrian green phase and pedestrian clearance phase at the onset of preemption. Therefore, the TPS1 algorithm is only useful in the case that the available preemption warning time is less than the required preemption warning time.

Under certain circumstances, the TPS1 algorithm provides more green time to the phases of the parallel to the railroad (i.e., dwell phase) as compared to the normal signal mode, even if there is no vehicle call for those phases before the preemption. These cases will be explained in detail in Section 5.1.2. This extra green time may result in a higher average delay. Because the dwell phase also are provided during the preemption mode, it is not necessary to provide more green time to them in the time period immediately before the preemption. Therefore, in contrast to the current transition preemption method, the new transition preemption method is designed to provide more green time to the phases that will be blocked during a preemption, as compared to the normal traffic signal mode and TPS1.

Finally, while the primary goal is to operate the HRGC in a safe manner, an opportunity exists to increase the efficiency (e.g., reduce delay) of the IHRGC during the transition into preemption. A new transition preemption method was developed that explicitly considers the variability of the predicted train arrival time. There are two goals behind the methodology. The first is to increase safety by minimizing the number of pedestrian phase truncations while still maintaining 100% track clearance time. The second goal is to reduce overall intersection delay associated with a preemption. The proposed

transition preemption methodology was developed based on the framework of the current transition preemption strategy (2-6).

5.1.1 Issue 1: Inappropriate Minimum Time

In the current signal timing plans, the minimum time necessary to service the next phase (M_j) is calculated as the sum of Yellow + All-Red of the current phase (Y_i+R_i), the minimum green time of the next phase (G_j), and the Yellow + All-Red of the next phase (Y_j+R_j). M_k is defined as the minimum time needed to service the next two phases when the next phase is the track clearance phase. M_k is calculated as the sum of Yellow + All-Red of the current phase (Y_i+R_i), the minimum green time for the next phase (G_j), the Yellow + All-Red of the next phase (Y_j+R_j), the minimum green time of the next phase after the track clearance phase (G_k), and Yellow + All-Red of the next phase after the track clearance phase ($Y_k + R_k$). M_j and M_k can be expressed as in Equations 5-1 and 5-2.

$$M_j = Y_i + R_i + G_j + Y_j + R_j \quad (5-1)$$

$$M_k = M_j + G_k + Y_k + R_k \quad (5-2)$$

$$(i = 1, 2, \dots, n;$$

$$j = i + 1, \text{ if } i < n; \quad j = 1, \text{ if } i = n;$$

$$k = j + 1, \text{ if } j < n; \quad k = 1, \text{ if } j = n)$$

where;

Y_i = Yellow interval of current phase i (s);

R_i = All-Red interval of current phase i (s);

G_j = Minimum green time of phase $i+1$ (s);

i = Current phase;

j = Next phase after phase i ;

k = Next phase after phase j ;

M_j = Minimum time necessary to service the next phase (phase $i+1$) (s);

and

M_k = Minimum time needed to service the next two phases when the next phase is the track clearance phase (s).

Additional terms should be defined to further explain the current TPS algorithm.

Time to Train Arrival (T): The time the train is predicted to arrive at the crossing. The estimator used to predict arrival time is a function of the track equipment and agency objective. This value is updated every t seconds as the train approaches the crossing. For all field applications in the U.S., t is 1 second.

Track Clearance Time (τ): The time at which the track clearance phase should be initiated. As stated in Chapter II, this value is typically set equal to the expected advance preemption time plus 15 seconds. For the test bed it is 22 seconds.

Remaining Time Available ($X = T - \tau$): Effectively, a “countdown” until the track clearance time.

Extended Time (B_i): Time period added into M_j to end a vehicle phase i that has a call. That is, when there is a vehicle call for phase i , phase i is provided until $X = M_j + B_i$, instead of $X = M_j$.

Note that M_j (or M_k) includes the Yellow + All-Red of the next phase (or includes the Yellow + All-Red of the phase after the track clearance phase). Therefore the next phase (the phase after the track clearance phase) will be terminated when the remaining time available (X) is equal to zero and the Yellow + All-Red is initiated. That means that while M_j (or M_k) can serve the minimum time of the next phase (the minimum time of the phase after the track clearance phase), it also has an extra amount of time, equal to $Y_j + R_j$ (or $Y_k + R_k$). This feature often causes the controller not to serve the next phase even if there is enough time to serve the minimum of the next phase. Note that this can

be a problem because once X is zero the Yellow + All-red interval is provided. In other words, cases exist when the next phase could be serviced but are not. Equation 5-3 shows the problem.

$$\text{If } Y_i + R_i + G_j \leq X \leq M_j \quad (5-3)$$

then, keep current phase until $X = 0$ (problem: while there is enough time to provide the next phase, the current phase is provided until $X = 0$)

$$\text{else if } X < Y_i + R_i + G_j$$

then, keep current phase until $X = 0$

$$\text{else } X > M_j$$

then, current phase is terminated and the next phase starts

Therefore, M_j (or M_k) does not need to include the Yellow + All-Red of the next phase (or the Yellow + All-Red of the phase after the track clear phase). The problem can be solved as shown in Equation 5-4.

$$\text{If } Y_i + R_i + G_j \leq X \leq M_j \quad (5-4)$$

then, current phase is terminated and the next phase starts

The difference in signal operation between the current M_j and the reduced M_j is shown in Figures 5-1 and 5-2, respectively. Therefore, the problem can be solved by extracting Y_j+R_j (or Y_k+R_k) from the current M_j (or M_k) as shown in Figure 5-1 and Figure 5-2.

As an example, consider the situation where $G_j = 10$, $Y_i+R_i = 5$, and $B_i = 5$, M_j and M_k are 20 and 35 seconds based on the current TPS algorithm. The problem will be explained using two cases: 1) when there is still a vehicle call for the current phase, and 2) when there is no vehicle call for the current phase. Indication for the vehicle call is shown in Equation 5-5.

$$\begin{aligned} \Lambda_i = 1, & \text{ There is a call for phase } i \text{ during phase } i \\ = 0, & \text{ There is no call for phase } i \text{ during phase } i \end{aligned} \tag{5-5}$$

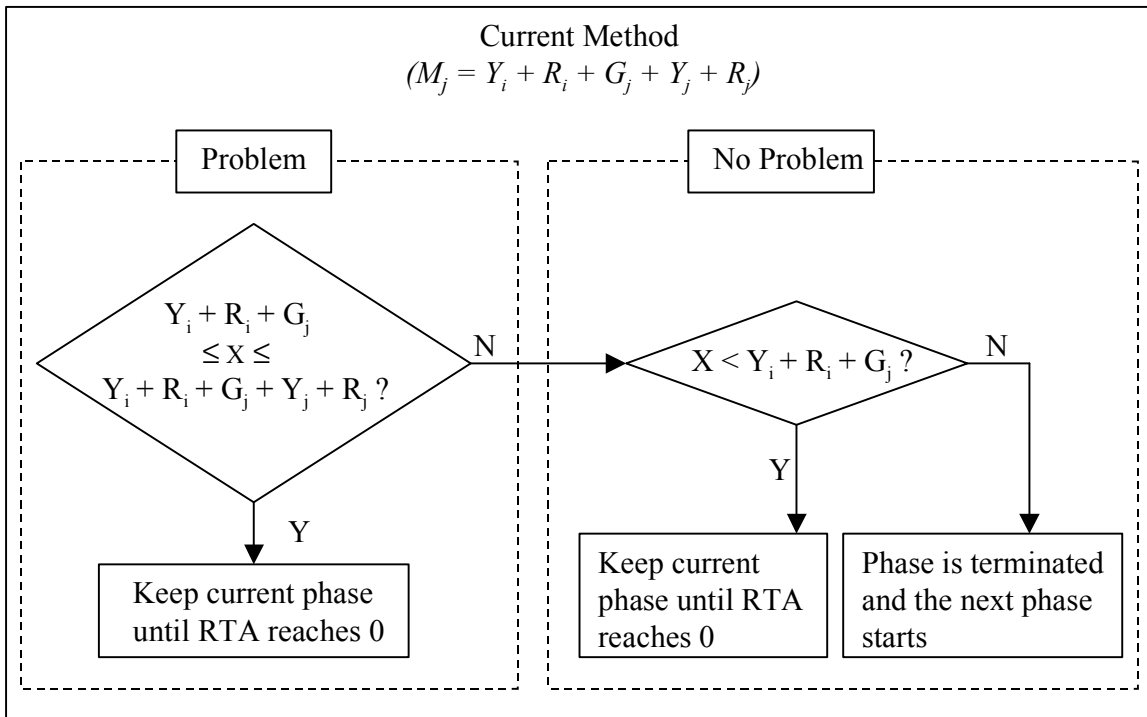


FIGURE 5-1 Signal Procedure with Current M_j

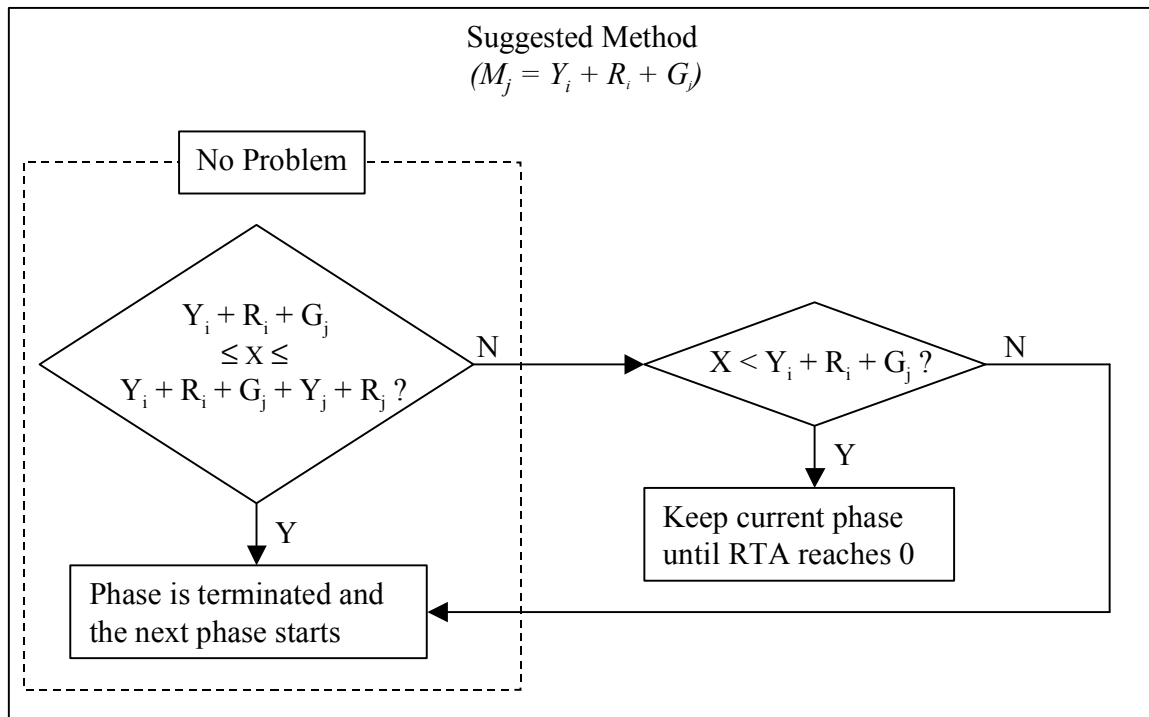


FIGURE 5-2 Signal Procedure with Suggested M_j

5.1.1.1 Case 1: Case When There Is Still a Vehicle Call for the Current Phase

When vehicle calls for the current phase and the next phase ($\Lambda_i = 1$ and $\Lambda_j = 1$) exists, the signal will be changed to the next phase only if $M_j \leq X \leq M_j + B_i$ as shown in Figure 5-3. However, when X is less than M_j , even if there is enough time to provide the minimum green time of the next phase, the signal is not changed to the next phase. Rather, the current phase remains until the preemption is initiated. That is, if X is in the period of “x1,” the signal has enough time to serve the minimum green of the next phase. However, the current phase is held until X reaches zero. Therefore, it is reasonable to reduce M_j (or M_k) to 15 seconds (or 30 seconds) in order to serve the next phase once there is enough time to serve the minimum of the next phase. When there is a call for the next phase ($\Lambda_j = 1$), and if enough time to provide the minimum green time exists, then there is no reason not to serve it. However, when M_j (or M_k) is reduced to 15 seconds (or 30 seconds), the signal changing to the next phase can occur up to “x2”

seconds later than when M_j is 20 seconds (or 35 seconds). The time of the phase change increases/decreases by the extended time. The extended time is used to adjust the time that phase i begins. Increasing the extended time increases the time that phase j begins. If the B_i time increases, the current phase may be terminated earlier. The amount by which it is terminated early is equivalent to the amount of time it was originally lengthened. The next phase will be started, which will ensure that it will take a longer time to serve the next phase. If the extended time of the current phase (B_i) is not changed, the current phase will be held more than when the B_i time increases, which is preferable for the current phase. Therefore, there is a trade-off between the length of the

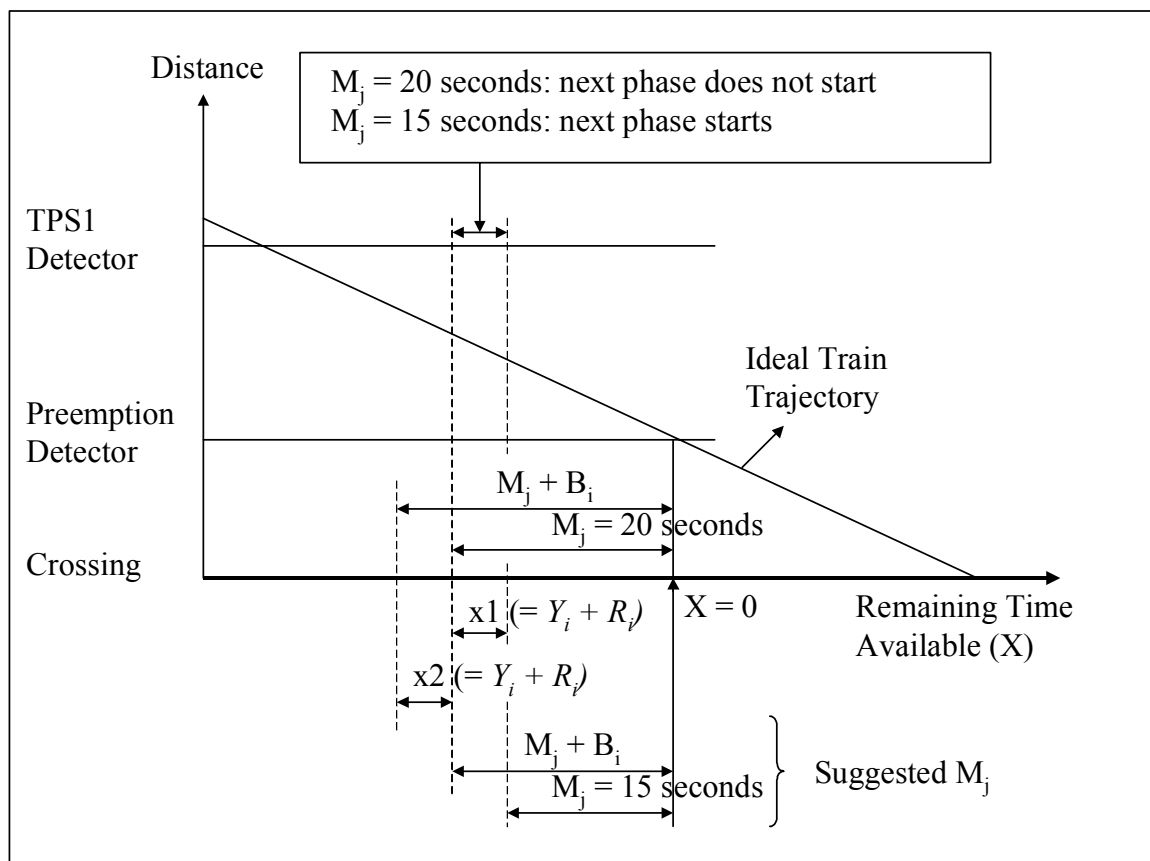


FIGURE 5-3 Time Frame When There Is Still a Vehicle Call for the Current Phase

current phase and the length of the next phase. This trade-off is represented by the extended time of the current phase (B_i).

5.1.1.2 Case 2: Case When There is No Call for the Current Phase

When there is no call for the current phase ($\Lambda_i = 0$), the signal is changed to the next phase only if $X \geq M_j$ as shown in Figure 5-4. Once X is less than M_j , the current phase will be held until X reaches zero even if there is a call for the next phase ($\Lambda_j = 1$) and there is enough time to serve it. That is, if X is in the period of “x1,” the signal has enough time to serve the minimum green of the next phase. However, the current phase is continued until X reaches zero. Therefore, it is reasonable to reduce M_j (or M_k) to 15 seconds (or 30 seconds) in order to serve the next phase once there is enough time to serve the minimum of the next phase.

This problem can be solved easily. Based on the current TPS algorithm, the phase before the track clearance phase is terminated at $X = 0$ and the Yellow + All-Red is started. Therefore, the track clearance phase is started $Y_i + R_i$ seconds after X reaches zero. However, it is desirable that the track clearance phase is started at $X = 0$. Therefore, the phase before the track clearance phase should be terminated at $X = Y_i + R_i$ and the Yellow + All-Red should be started. Even if the phase is terminated at $X = Y_i + R_i$, the minimum green time is still guaranteed because M_j (or M_k) includes the Yellow + All-Red of the next phase (or the next phase after the track clearance phase). Then the problems mentioned above will be eliminated automatically by changing the terminating time of the phase before the track clearance phase at $X = Y_i + R_i$.

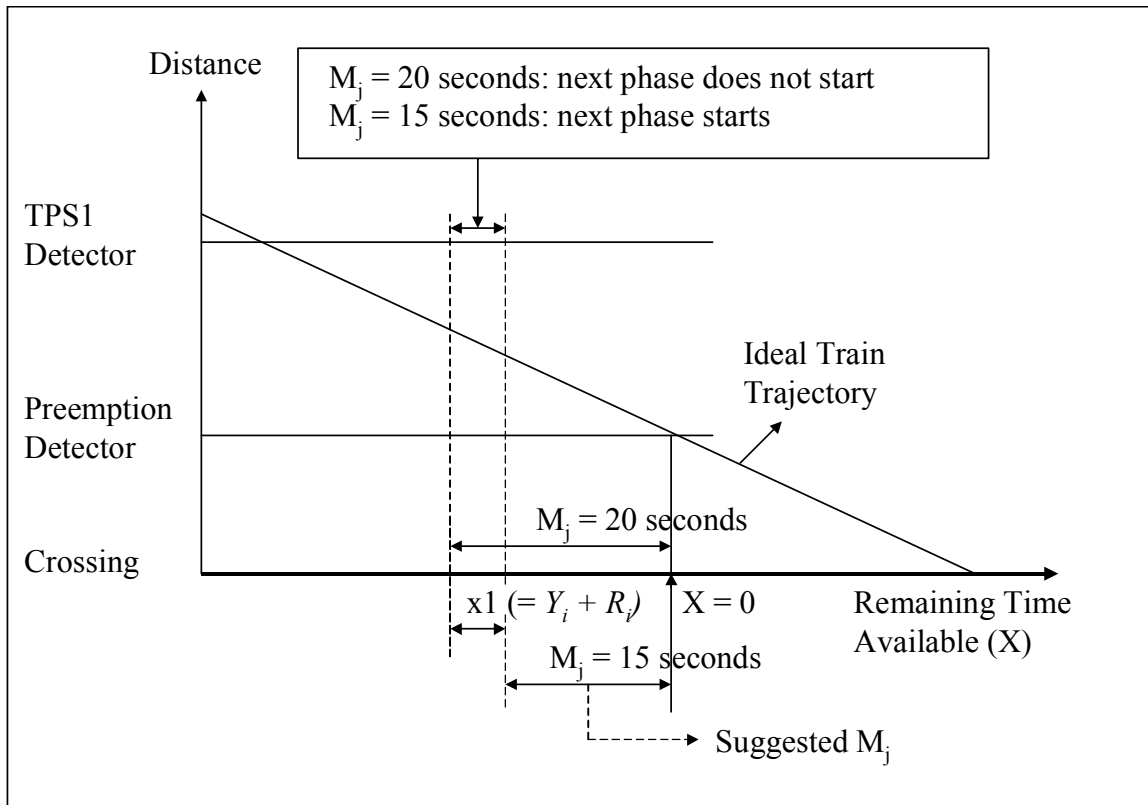


FIGURE 5-4 Time Frame with No Vehicle Call for the Current Phase

5.1.2 Issue 2: Longer Service Times of the Dwell Phases

The current TPS logic may provide an excessively long dwell phase time. Figure 5-5 shows the conditions that may provide an excessively long dwell phase. Basically, these conditions occur when the current phase is the dwell phase and 1) there is a call for the phase ($\Lambda_i = 1$) and X is greater than $M_k + B_i$, or 2) there is no call for the phase ($\Lambda_i = 0$) and X is less than M_k .

Because the dwell phases are served an adequate length of time, as compared to the other phases during the preemption, those phases do not need to be served just before the preemption. Therefore, if there is a call for the blocked phases, which are not provided during the preemption mode, the dwell phases should be terminated and the next phases

should be served even if there is still a call. Once the preemption starts, these vehicles on the roadway will be served from the parallel roadway. It is hypothesized that making this change will reduce overall delay for the vehicles in the IHRGC.

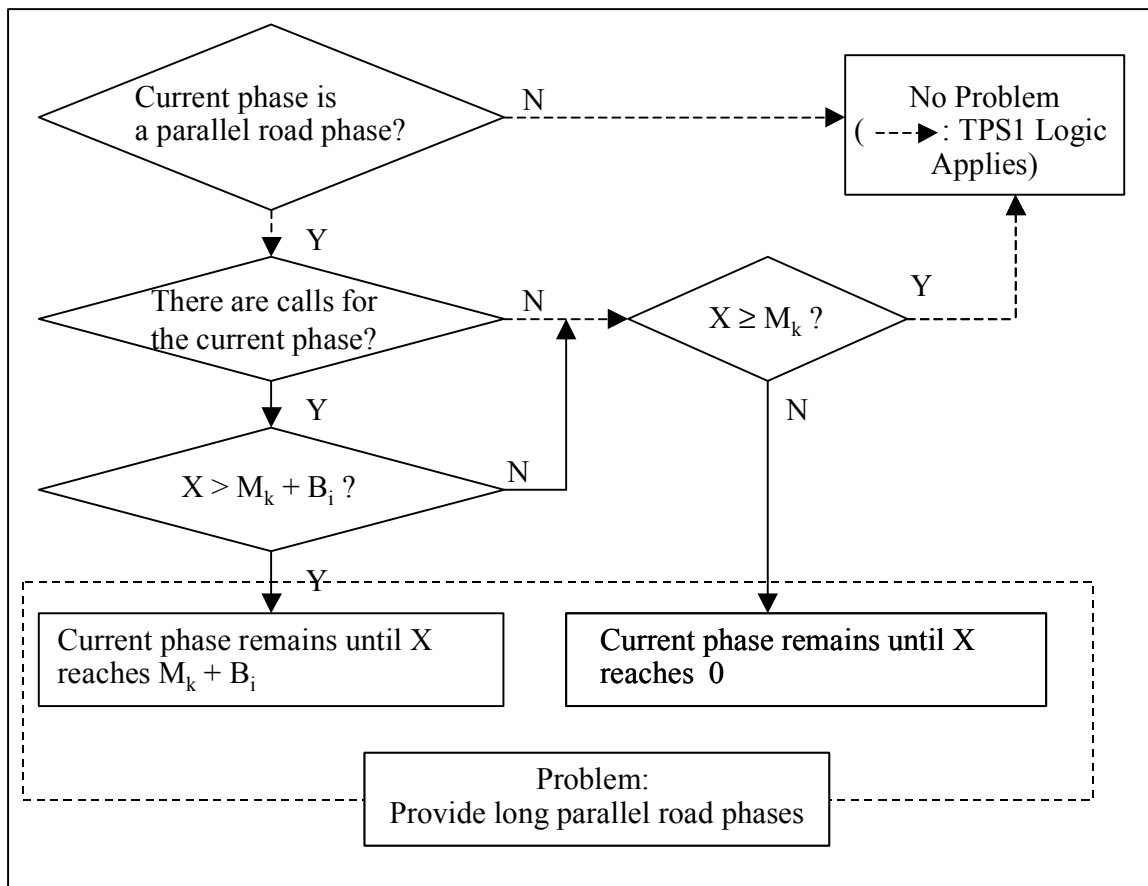


FIGURE 5-5 Conditions to Provide Longer Service Times of the Dwell Phase

The phase and the ring structure of the test bed are shown in Figure 5-6 to illustrate the problem and develop the new TPS algorithm. Although the new TPS algorithm is developed based on this specific ring structure and phase sequence, it can be applied to any IHRGC having different signal timing. As discussed in Chapter III, phases 2 and 6

are for the through (and right-turn) movements of Wellborn Road and phases 1 and 5 are the left-turn movements of George Bush Drive. Phase 3 is the track clearance phase.

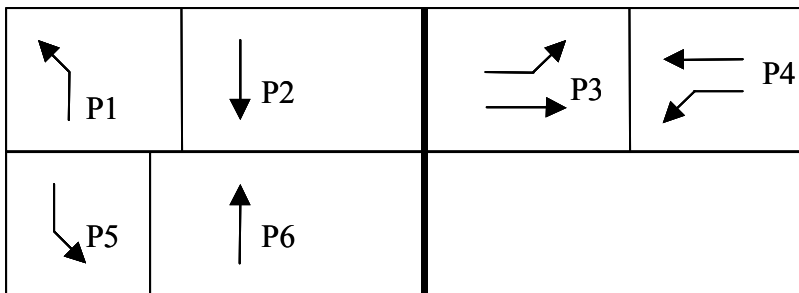


FIGURE 5-6 Ring Structure

The objective is to reduce the phase lengths for dwell phases. In the Wellborn Road situation, this would be phases 2 and 6. To remove the problems of an ineffectively long phase 2 or phase 6 just before the preemption, the TPS algorithm will be modified based on the methods discussed below. The problems and solutions are explained in two cases: 1) when there is still a call for the current phase (phase 2 or 6, and $\Lambda_i = 1$), and 2) when there is no call for the current phase (phase 2 or 6, and $\Lambda_i = 0$).

5.1.2.1 Case 1: When There Is Still a Call for the Current Phase (Phase 2 or 6)

Figure 5-7 shows a schematic time diagram for the current TPS algorithm to illustrate the problem when there is a call for the current phases (Phase 2 or 6, and $\Lambda_i = 1$). The current phase is changed to the next phase regardless of a call for next phases only when X is greater than M_k and less than M_k plus the extended time of phase i . This condition is shown by Equation 5-5.

$$M_k + B_i \geq X \geq M_k \quad (5-5)$$

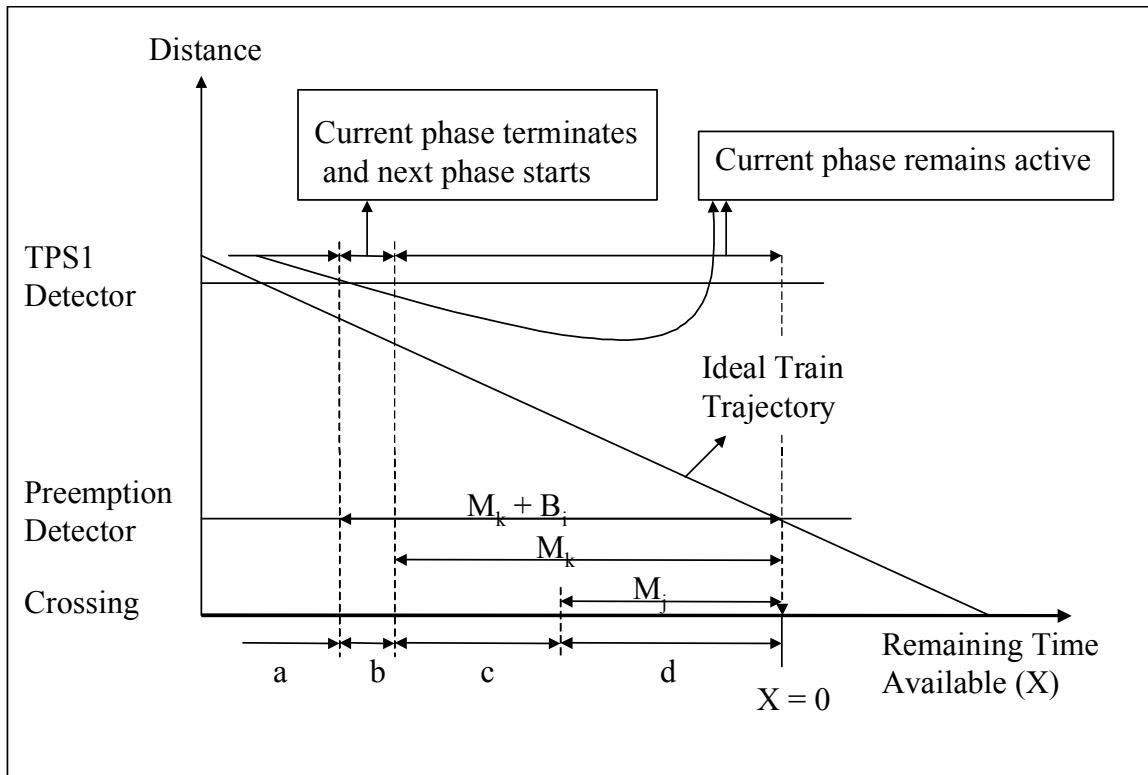


FIGURE 5-7 Time Frame with a Vehicle Call for the Current Phases (Phase 2 or 6)

When X is in the time period “a,” the current phase is served until X reaches the $M_k + B_i$ regardless of whether there is a call for either of the next two phases (phase 3 or 4). The amount of time that phases 2 and 6 are operated ineffectively (i.e., provides these phases excessively long before the preemption) can be calculated using Equation 5-6.

$$t = X - (M_k + B_i) \quad (5-6)$$

where;

t = Amount of time that is operated ineffectively (s);

The length of the dwell phase is a function of the time when the TPS1 algorithm starts (the advance preemption warning time) and $M_k + B_i$. The maximum occurs when the

last second of the dwell phase is provided at the onset of the TPS1 algorithm. The minimum occurs when the first second of the dwell phase is provided at the onset of the TPS1 algorithm. These values are shown in Equations 5-7 and 5-8.

$$\tau_{MAX} = APWT - (M_k + B_i) \quad (5-7)$$

$$\tau_{MIN} = APWT - G_i - (M_k + B_i) \quad (5-8)$$

where;

$APWT$ = Advance preemption warning time (s);

τ_{MAX} = Maximum amount of time that is operated ineffectively (s); and

τ_{MIN} = Minimum amount of time that is operated ineffectively (s).

In addition, based on the current TPS logic, after the current phase is terminated at time $M_k + B_i$, the track clearance phase is served even if there is no call for the phase ($\Lambda_j = 0$). In this case, the amount of time that is operated ineffectively (i.e., operates this phase without a call) is $M_k + B_i$.

If no call exists for the next phase ($\Lambda_j = 0$), the current phase should be provided until there is a call for the next phase as long as there is still a call for the current phase. The current TPS algorithm will be modified such that the current phase is terminated once the minimum green time of the current phase is served and the next phase (phase 3 or 4) with a call is served if there is a call for either of the next two phases (phase 3 or 4). These conditions are shown by Equations 5-9 and 5-10 depending on whether there is a call for the current phase. The condition to change to phase 4 is shown in Equation 5-11.

$$\text{If } \Lambda_i = 1 \ \& \ X \geq M_k \ \& \ (\Lambda_j = 1 \ \text{or} \ \Lambda_k = 1) \tag{5-9}$$

OR

$$\Lambda_i = 1 \ \& \ X < M_k \ \& \ X < M_j \ \& \ \Lambda_j = 1$$

OR

$$\Lambda_i = 1 \ \& \ X < M_k \ \& \ X \geq M_j \ \& \ \Lambda_k = 0 \ \& \ \Lambda_j = 1$$

then, change to phase 3

$$\text{If } \Lambda_i = 0 \ \& \ X \geq M_k \tag{5-10}$$

OR

$$\Lambda_i = 0 \ \& \ X < M_k \ \& \ X < M_j$$

OR

$$\Lambda_i = 0 \ \& \ X < M_k \ \& \ X \geq M_j \ \& \ \Lambda_k = 0$$

then, change to phase 3

$$\text{If } \Lambda_i = 1 \ \& \ X < M_k \ \& \ X \geq M_j \ \& \ \Lambda_k = 1 \tag{5-11}$$

OR

$$\Lambda_i = 1 \ \& \ X < M_k \ \& \ X \geq M_j \ \& \ \Lambda_k = 1$$

then, change to phase 4

When X is equal to or greater than M_j and equal to or less than M_k ($M_k \geq X \geq M_j$), even if there is a call for both of the next two phases (phases 3 and 4, and $\Lambda_j = 1$ and $\Lambda_k = 1$), the current phase remains until X reaches zero. It will be modified to terminate the current phase and serve phase 3 if there is a call for phase 3 ($\Lambda_j = 1$) and there is no call for phase 4 ($\Lambda_k = 0$). If there is a call for phase 4 ($\Lambda_k = 1$) regardless of a call for phase 3, the current phase will be terminated and phase 4 will be served. Note that the phase 2 or 6 followed by phase 4 could violate driver expectancy, because the sequence is out of order compared to the normal operation. However, because phase 3 is provided at the

onset of preemption, it is proper to serve phase 4 before the preemption from an efficiency standpoint.

When X is in the time interval “d,” even if there is a call for the next phase (phase 3 and $\Lambda_j = 1$), the current phase remains. It will be modified to terminate the current phase and serve phase 3 if there is a call for phase 3 ($\Lambda_j = 1$). In this case, because phase 3 is the track clearance phase and the phase will be started to serve when X reaches zero, minimum green time does not need to be guaranteed.

5.1.2.2 Case 2: *When There Is No Call for the Current Phase (Phase 2 or 6)*

Figure 5-8 shows the time frame during the current TPS algorithm to illustrate the problem when there is no call for the current phase ($\Lambda_i = 0$). The current phase is changed to the next phase regardless of a call for next phases when X is greater than M_k . Therefore, if X is in the period of “a,” there is no problem with an ineffectively long phase 2 or phase 6 because the signal phase changes to the next phase once the minimum length of the phase is provided.

However, when X is in the time interval “b,” even if there is a call for the next phase (phase 3 and $\Lambda_j = 1$), the current phase remains until X reaches zero. It will be modified to terminate the current phase and serve phase 3 if there is no call for phase 4 ($\Lambda_k = 0$), regardless of a call for the next phase (phase 3) because there is enough time to serve the next phase. If there is a call for phase 4 ($\Lambda_k = 1$) regardless of a call for phase 3, the current phase is terminated and phase 4 will be served. Note that phase 2 or 6 followed by phase 4 could violate driver expectancy, because the sequence is out of order compared to the normal operation. However, because phase 3 is provided at the onset of preemption, it is proper to serve phase 4 before the preemption from an efficiency standpoint.

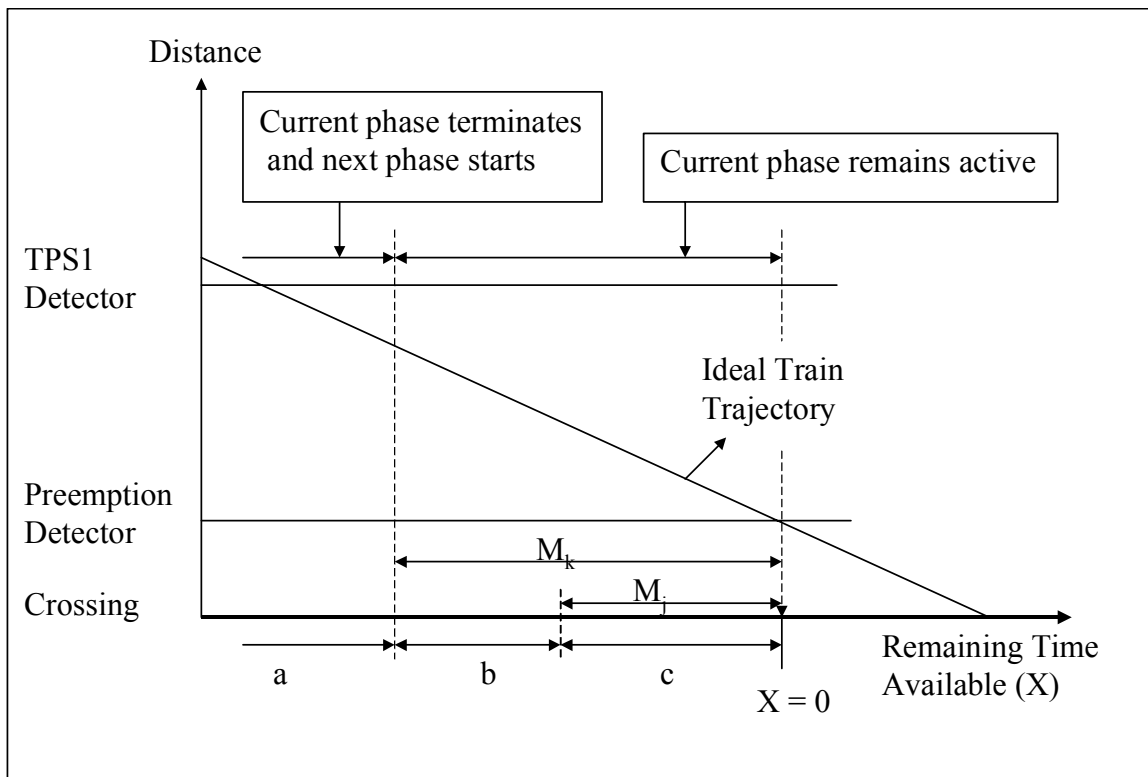


FIGURE 5-8 Time Frame with No Vehicle Call for the Current Phase (Phase 2 or 6)

When X is in the time interval “c,” even if there is a call for the next phase (phase 3 and $\Lambda_j = 1$), the current phase remains. It will be modified to terminate the current phase and serve phase 3 if there is a call for phase 3 ($\Lambda_j = 1$). In this case, because phase 3 is the track clearance phase and the phase will be served when X reaches zero, minimum green time does not need to be guaranteed.

5.2 DEVELOPING THE NEW TPS ALGORITHM (TPS2)

While the TPS1 algorithm is designed to increase vehicle and pedestrian safety, it does not consider the intersection performance. Therefore, there is a need to develop a new transition preemption algorithm that considers intersection performance while maintaining, and preferably improving, pedestrian safety. The basic idea of the new

transition preemption algorithm is to provide non-dwell phases, which are the phases blocked during the preemption, more time before the preemption mode starts. Based on the analysis of the TPS1 algorithm, a new algorithm, TPS2, was developed. The variables used in the TPS1 algorithm were also used for the TPS2 algorithm.

Note that a four-leg intersection setup was assumed to develop the TPS2 algorithm. The phase number of each movement and phase sequence also were assumed as shown in Figure 5-9. That is, the number of phases of the parallel road is four and the number of phases of the perpendicular road is two as shown in Equation 5-12. These values and phase numbers can be modified for the different locations. However, the principles can be applied to any signal by using the appropriate phases for the parallel and perpendicular roadways.

$$N_i = 4 \quad (5-12)$$

$$N_j = 2$$

where;

N_i = Number of phases of parallel road (phases 1,2,5,and 6); and

N_j = Number of phases of perpendicular road (phases 3 and 4).

In the TPS2 algorithm, phase 4 indicates the opposite phase of the track clearance phase for four-leg intersections and the blocked phase during the preemption phase for three-leg intersections. However, the new TPS algorithm can be applied to any IHRGC.

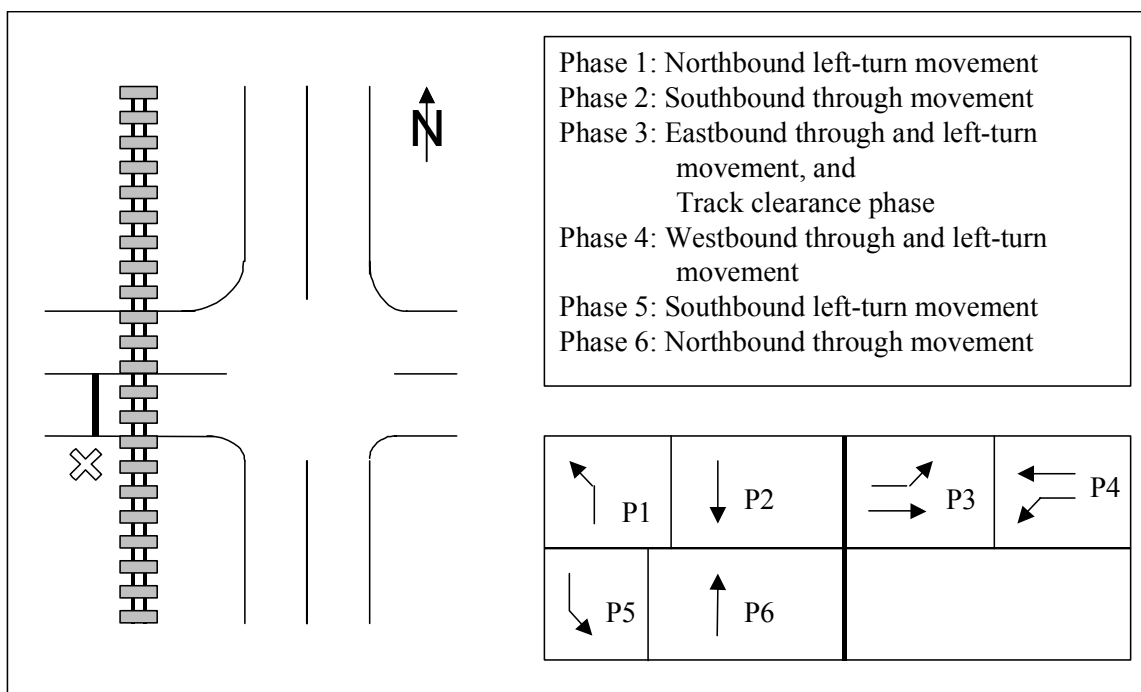


FIGURE 5-9 Phase Number of Each Movement and Phase Sequence for Developing the TPS2 Algorithm

The process begins once a train has been detected. The predicted arrival times are estimated every second. Once the predicted train arrival time is less than the advance preemption warning time, the TPS2 algorithm is started as listed in the steps described below. The logic is also presented graphically in the flow chart shown in Figure B-2 in Appendix B.

Step 1:

The status of the current phase is checked to determine if both the minimum vehicle green time and minimum pedestrian green/clearance time have been served. If the minimum green time has not been completely served, the current phase remains active. This condition is shown by Equation 5-13. Otherwise, the logic proceeds to step 2.

If $t_i \geq M_i$, (5-13)
then, the logic proceeds to step 2
otherwise, keep the current phase active

where;

t_i = Length of the current phase.

Note that the process is updated every t seconds. This is set in the controller logic. Typically in North America t is equal to 1 second and this was the value used at the test bed.

Step 2:

If the remaining time available (X) is equal to or less than the Yellow+All-Red interval of the current (Y_i+R_i) phase, the current phase is terminated and the track clearance phase is started (End the TPS2 algorithm). This condition is shown by Equation 5-14.

If $X \leq Y_i+R_i$, (5-14)
then, terminate the current phase, start the track clearance
phase, and leave the TPS2 logic
otherwise, the logic proceeds to step 3

Step 3:

The current phase is checked. If the current phase is the track clearance phase, then the logic proceeds to step 5B-3. This condition is shown by Equation 5-15.

If current phase = track clearance phase, (5-15)
then, the logic proceeds to step 5B-3
otherwise, the logic proceeds to step 4

Step 4:

The next phase is checked. If the next phase is not the track clearance phase, the logic proceeds to step 5B-1. This condition is shown by Equation 5-16.

$$\begin{aligned} & \textit{If next phase} \neq \textit{ track clearance phase,} & (5-16) \\ & \quad \textit{then, the logic proceeds to step 5B-1} \\ & \quad \textit{otherwise, the logic proceeds to step 5A-1} \end{aligned}$$

Step 5A-1: Next phase is the track clearance phase

The vehicle call status for the current phase is checked. If there is no vehicle call for the current phase ($\Lambda_i = 0$), the logic proceeds to step 5A-3. This condition is shown by Equation 5-17.

$$\begin{aligned} & \textit{If } \Lambda_i = 0, & (5-17) \\ & \quad \textit{then, the logic proceeds to step 5A-3} \\ & \quad \textit{otherwise, the logic proceeds to step 5A-2} \end{aligned}$$

Note that in the logic of the following steps, the (B), (C), and (D) indicate the logic flow as shown in the flow chart form in Figure B-2 in Appendix B.

Step 5A-2: Vehicle call for the current phase

If $X \geq M_k$,

- If there is no call for both of the next two phases ($\Lambda_j = 0$ and $\Lambda_k = 0$), the current phase remains. The logic proceeds to step 6. (D)
- If there is a call for either of the next two phases ($\Lambda_j = 1$ or $\Lambda_k = 1$), the current phase is terminated and the next phase is started. The logic proceeds to step 6. (B)

These conditions are shown by Equation 5-18.

If $X \geq M_k$, (5-18)

If $\Lambda_j = 0$ & $\Lambda_k = 0$,

then, keep the current phase active and the logic proceeds to step

6

else if $\Lambda_j = 1$ or $\Lambda_k = 1$,

then, terminate the current phase, start the next phase, and the

logic proceeds to step 6

If $M_k \geq X \geq M_j$

- If there is no call for both of the next two phases ($\Lambda_j = 0$ and $\Lambda_k = 0$), the current phase remains active. The logic proceeds to step 6. (D)
- If there is a call for the next phase and there is no call for the next phase of the track clearance phase ($\Lambda_j = 1$ and $\Lambda_k = 0$), the current phase is terminated and track clearance phase will start. The logic proceeds to step 6. (B)
- If there is a call for the next phase of the track clearance phase ($\Lambda_k = 1$) regardless of a call for the next phase, the current phase is terminated and the next phase of the track clearance phase is started. The logic proceeds to step 6. (C)

These conditions are shown by Equation 5-19.

If $M_k \geq X \geq M_j$, (5-19)

If $\Lambda_j = 0$ & $\Lambda_k = 0$,

then, keep the current phase active and the logic proceeds to step

6

else if $\Lambda_j = 1$ & $\Lambda_k = 0$,

then, terminate the current phase, start the track clearance

phase, and the logic proceeds to step 6

else if $\Lambda_k = 1$,

then, terminate the current phase, start the next phase of the

track clearance phase, and the logic proceeds to step 6

If $X \leq M_j$,

- If there is no call for the next phase ($\Lambda_j = 0$), the current phase remains active. The logic proceeds to step 6. (D)

- If there is a call for the next phase ($\Lambda_j = 1$), the current phase is terminated and the next phase is started. Note that because the next phase is the track clearance phase the minimum green time does not need to be guaranteed. The logic proceeds to step 6. (B).

These conditions are shown by Equation 5-20.

If $X \leq M_j$, (5-20)

If $\Lambda_j = 0$,

then, keep the current phase active and the logic proceeds to step

6

else if $\Lambda_j = 1$,

then, terminate the current phase, start the next phase, and

the logic proceeds to step 6

Step 5A-3:

If $X \geq M_k$,

The current phase is terminated and the next phase will begin timing regardless of a call for the next phase. The logic proceeds to step 6. (B)

This condition is shown by Equation 5-21.

$$\text{If } X \geq M_k, \quad (5-21)$$

then, terminate the current phase, start the next phase, and the logic proceeds to step 6

If $M_k \geq X \geq M_j$,

- If there is no call for the next phase of the track clearance phase ($\Lambda_k = 0$) regardless of a call for the next phase, the current phase is terminated and the next phase is started. The logic proceeds to step 6. (B)

- If there is a call for the next phase of the track clearance phase ($\Lambda_k = 1$) regardless of a call for the next phase, the current phase is terminated and the next phase of the track clearance phase is started. The logic proceeds to step 6. (C)

These conditions are shown by Equation 5-22.

$$\text{If } M_k \geq X \geq M_j, \quad (5-22)$$

If $\Lambda_k = 0$,

then, terminate the current phase, start the next phase, and the logic proceeds to step 6

else if $\Lambda_k = 1$,

then, terminate the current phase, start the next phase of the track clearance phase and the logic proceeds to step 6

If $X \leq M_j$,

- The current phase is terminated and the next phase is started regardless of a call for the next phase. The logic proceeds to step 6. (B)

This condition is shown by Equation 5-23.

$$\begin{aligned} & \text{If } X \leq M_j, & (5-23) \\ & \text{then, terminate the current phase, start the next phase, and the} \\ & \text{logic proceeds go to step 6} \end{aligned}$$

Step 5B-1:

Vehicle call for the current phase is checked. If there is still a vehicle call for the current phase ($\Lambda_i = 1$), then the logic proceeds to step 5B-2. Otherwise, the logic proceeds to step 5B-3. This condition is shown by Equation 5-24.

$$\begin{aligned} & \text{If } \Lambda_i = 1, & (5-24) \\ & \text{then, the logic proceeds to step 5B-2.} \\ & \text{otherwise, the logic proceeds to step 5B-3} \end{aligned}$$

Step 5B-2:

- If $M_j + B_i < X$ or $X < M_j$, the current phase remains active. The logic proceeds to step 6.
- If $M_j + B_i \geq X \geq M_j$, the current phase will be terminated and the next phase will begin timing. The logic proceeds to step 6.

These conditions are shown by Equation 5-25.

If $(M_j + B_i < X)$ or $(X < M_j)$, (5-25)
then, keep the current phase active and the logic proceeds to step 6
else if $(M_j + B_i \geq X \geq M_j)$,
then, terminate the current phase, start the next phase, and the
logic proceeds to step 6

Step 5B-3:

- If $X < M_j$, the current phase remains active. The logic proceeds to step 6.
- If $X \geq M_j$, the current phase will be terminated and the next phase will begin timing.

The logic proceeds to step 6.

These conditions are shown by Equation 5-26.

If $X < M_j$, (5-26)
then, keep the current phase active and the logic proceeds to step 6
else if $(X \geq M_j)$,
then, terminate the current phase, start the next phase, and the
logic proceeds to step 6

Step 6:

Decrement T ($T = T - 1$). Return to Step 1 to ensure that the minimum times of the current phase have been satisfied.

The above steps will be performed every time the train's predicted arrival time at the crossing is updated and each time a new signal phase becomes active.

The time period that the TPS2 algorithm is operated also affects intersection performance and safety. The TPS2 algorithm is designed to start at the advance preemption warning time, which is an estimated time of arrival of the train at the

crossing. This time is estimated using the Doppler detector data. In contrast, the preemption is initiated at the preemption warning time, which is also an estimated time of arrival of the train at the crossing. This time is estimated using the CWT detector data. Therefore the TPS2 algorithm is operated in the time period between these two timings. This time period is decided by the two predicted arrival times. However, because the variability in the predicted arrival time was not considered in the TPS2 algorithm, the pedestrian phase truncation may still occur and the intersection performance may not be improved. In the following section, the TPS3 algorithm will be developed, which incorporates the prediction error.

5.3 MODIFYING THE NEW TPS ALGORITHM ASSOCIATED WITH THE PREDICTION ERROR BOUND (TPS3)

Because both predicted arrival times for the TPS2 (or TPS1) algorithms and the standard preemption have variability, the preemption can be started before (or after) the TPS2 (or TPS1) algorithm is complete. Both the TPS2 and the TPS1 algorithms are designed to provide the track clearance phase just before preemption is initiated in order to eliminate the possibility that any pedestrian phase is active at the onset of preemption. However, if the predicted arrival time is longer than the actual arrival time (that is, a train arrives earlier at the position that the CWT detector activates a preemption than the predicted arrival time), the TPS2 algorithm will be terminated immediately meaning that some of its steps will not be completed. As shown in Figure 5-10, the preemption mode will be started immediately following this termination. In this case, the IHRGC has not been adequately prepared for the traffic signal preemption because the TPS2 algorithm is operated based on the predicted arrival time. Therefore, most of the benefit of an advance warning of a train arrival is lost. As was discussed in Chapter IV, errors associated with any given train arrival estimate exist. Therefore, the probability that a given train arrives x percent earlier than predicted can be readily calculated. A train could arrive earlier than predicted time. As long as train arrives early, the safety problem cannot be eliminated at the onset of preemption.

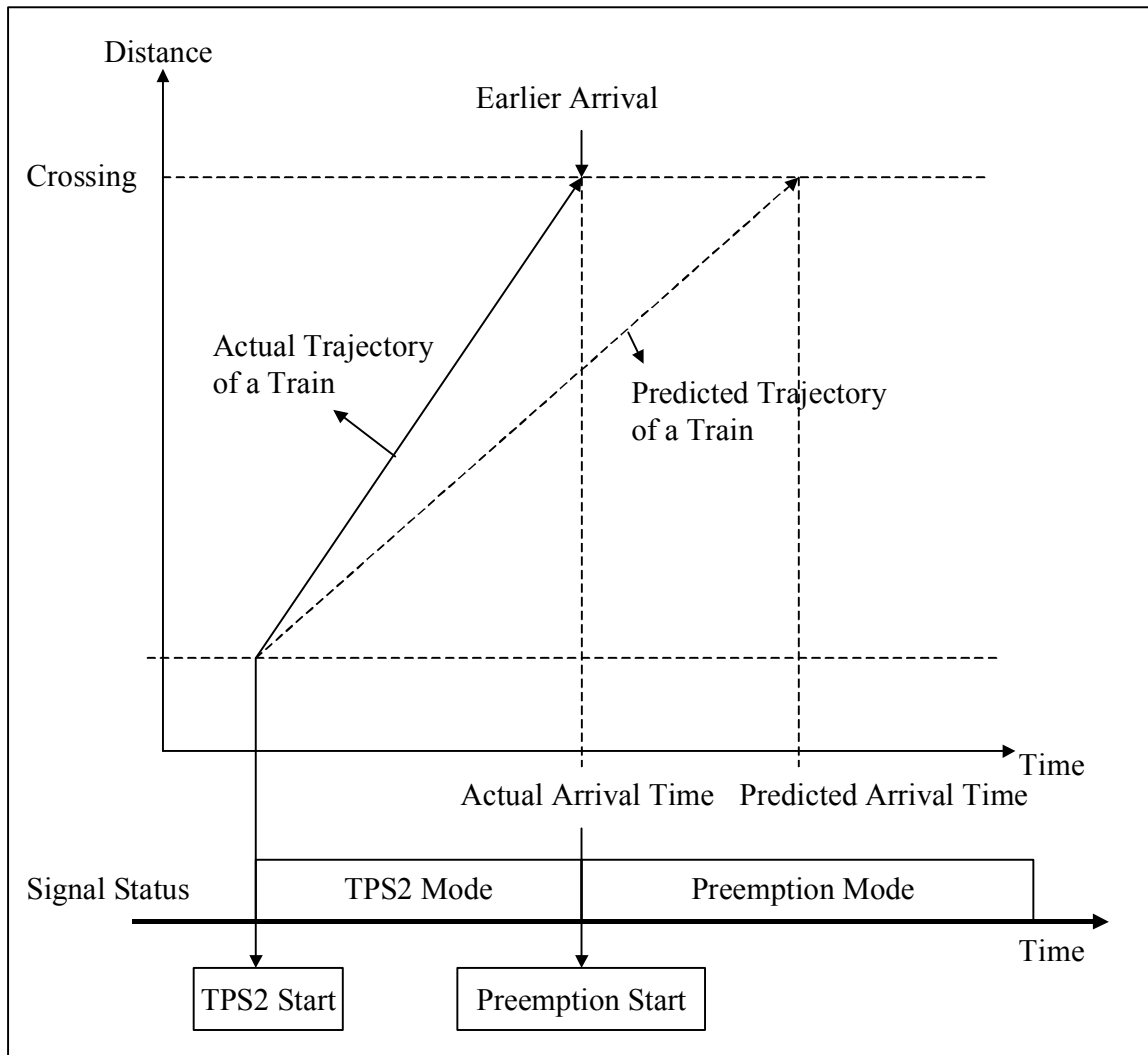


FIGURE 5-10 Time Frame of Earlier Arrival Case

To minimize the truncations of the pedestrian clearance phase, pedestrian phases will not be provided once the TPS2 algorithm starts and the minimum advance preemption warning time will be provided. This value will be identified in the sensitivity analysis. With this strategy, safety problems caused by the earlier arrival can be reduced. Note that even if pedestrian phases will not be provided once the TPS2 algorithm starts and a minimum advance preemption warning time is provided, the pedestrian phase truncation may occur in some extreme cases when a preemption occurs before the pedestrian clearance phase at the onset of the TPS2 is completed. Therefore, a way does not exist

to eliminate the truncations completely as long as variability in the predicted arrival time occurs. This study was performed based on the data observed from the test bed, in which the extreme cases did not occur.

The extreme cases indicate when the time difference between the APWT and the preemption warning time is less than the length of the pedestrian clearance phase. This circumstance can be caused by either the prediction error or the train speed. The following two examples show the cases assuming 100 percent accuracy of the preemption warning time, and 15 seconds of the pedestrian clearance phase.

Example 1: When the predicted APWT is 120 seconds and the error in the APWT is greater than 70 seconds, the train arrives at the crossing within 50 seconds after predicting 120 seconds of APWT. Therefore, the pedestrian phase truncation can occur. Equation 5-27 shows the condition where the pedestrian phase truncation occurs due to the prediction error.

$$\begin{aligned} APWT(t) - A(t) &> APWT(t) - (P_{WT} + F) \\ A(t) &< (P_{WT} + F) \end{aligned} \quad (5-27)$$

where;

- $APWT(t)$ = t seconds of APWT;
- $A(t)$ = When APWT is t, the actual arrival time (s);
- P_{WT} = Preemption warning time (s); and
- F = Length of pedestrian clearance phase (s).

Example 2: The distance between the Doppler detector and the crossing is about 2.2 km. When the train speed is greater than 160 km/h, the train arrives at the crossing within 50 seconds after detection. Therefore, the pedestrian phase truncation can occur. Equation 5-28 shows the condition where the pedestrian phase truncation occurs due to the train speed.

$$\frac{D}{V} < P_{WT} + F \quad (5-28)$$

where;

D = Distance from the detector at FM 2818 to the detector at George Bush (m);

V = Train speed (m/s);

P_{WT} = Preemption warning time (s); and

F = Length of pedestrian clearance phase (s).

A potential solution to the above problem is to input the minimum pedestrian clearance time into the preemption mode of the controller to guarantee the minimum pedestrian clearance time in that case. However, because the extension of the preemption warning time is required to provide minimum pedestrian clearance time, dwell time may increase and the intersection performance will deteriorate. Consequently, the benefit of the TPS2 algorithm will be reduced. Therefore, the extension of the preemption warning time is not a good solution.

If the predicted arrival time is shorter than the actual arrival time (that is, a train arrives later at the position that the preemption warning time detector activates a preemption than the predicted arrival time), the TPS2 algorithm will provide the track clearance phase before a preemption is initiated. As the predicted arrival time is earlier than the preemption start time, the duration of the track clearance phase before the preemption will be longer as compared to the desired time. Because enough track clearance time is usually provided to serve the demand volume as calculated in Chapter II, the extra track clearance time (x in Figure 5-11) is not necessary. Therefore, the late arrival leads to ineffective signal operation and negatively affects intersection performance even if there is no truncation in this case. If the probability of the late arrival is reduced, intersection performance will be improved. This can be achieved by applying the prediction error interval into the predicted arrival time.

The goal of obtaining prediction interval is to provide the amount of the increase required for the predicted value. Under the assumption that the fitted model is close to the true model, the prediction error can be explained only by the residuals. In this dissertation, the predicted arrival time was lengthened by the absolute value of the lower limit of the prediction error interval. It is not necessary to consider the problem of the earlier arrival because the problem is already solved by eliminating the pedestrian phase once the TPS2 algorithm starts.

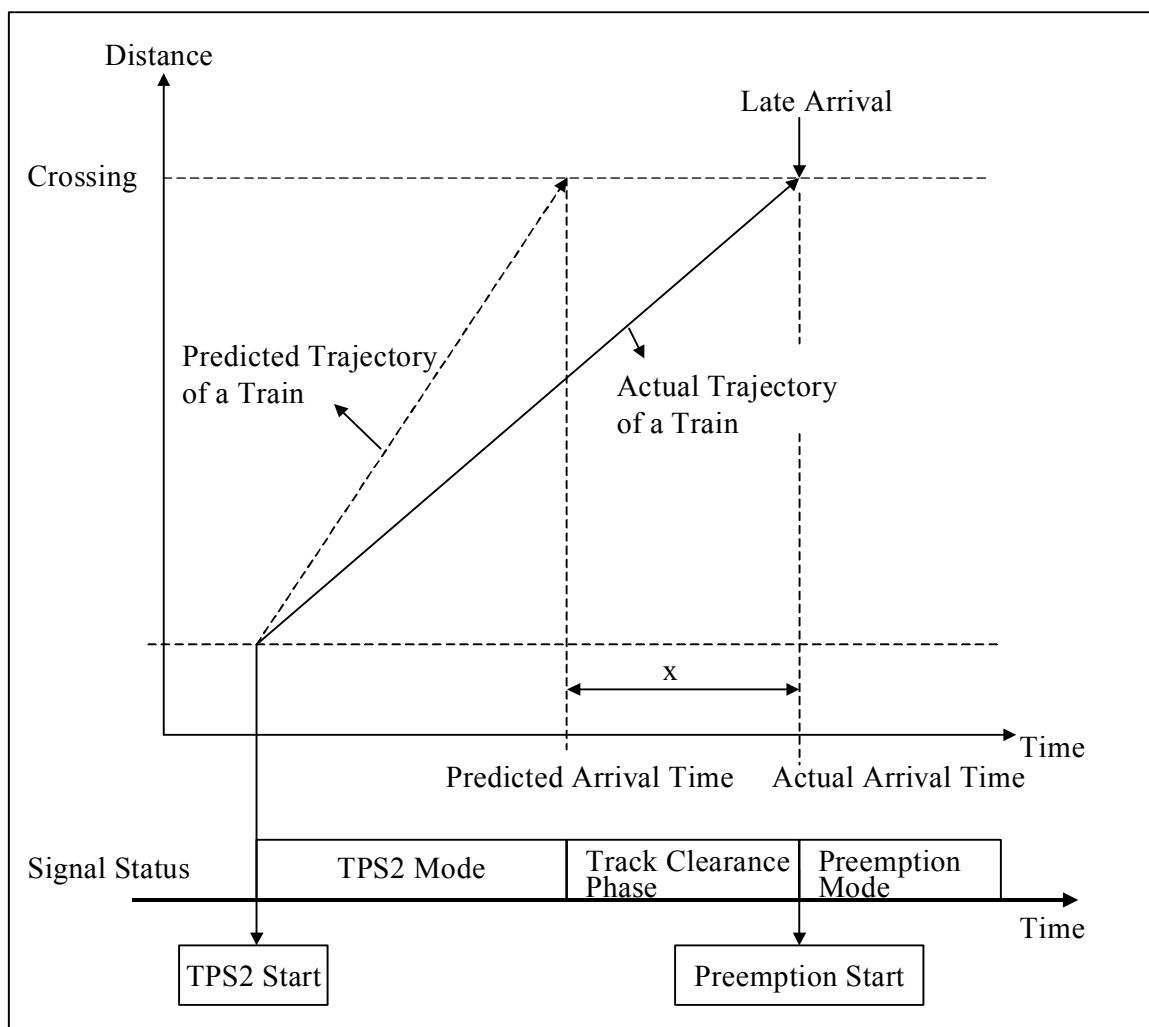


FIGURE 5-11 Time Frame of the Late Arrival Case

Prediction error intervals of the mean error were obtained using bootstrap method for 24 MANN models. The bootstrap procedure for calculating the mean error over the trains is described as follows:

- Step 1: Generate a bootstrap sample from the training set and the testing set. The size of the bootstrap sample is equal to the size of the observed data set for the model under consideration. The sampling is random and with replacement.
- Step 2: MANN model is re-fitted and the mean of prediction error is calculated based on the bootstrap sample.
- Step 3: Repeat Steps 1 and 2 R times.
- Step 4: Sort the mean calculated in step 2 in ascending order. Extract the αR^{th} and $(1-\alpha)R^{\text{th}}$ mean error from the ordered R mean values. These represent the lower bound and upper bound of the $1 - 2\alpha$ percentile interval for the mean error. In this dissertation, R was set to 10,000.

As an example consider Model 1. R sample data sets, of size 184, were created and the mean error for each sample was calculated. Figure 5-12 shows a histogram of these sample means. These values are normal in shape. The $(1-0.05)$ percentile lower and upper bounds are shown on the diagram and these represent the prediction error for this model.

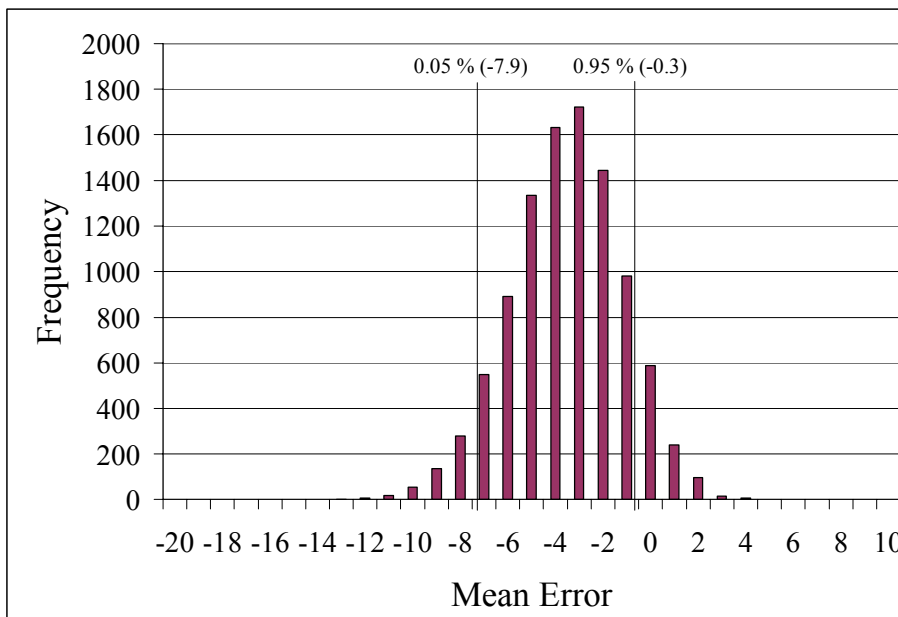


FIGURE 5-12 Example of Histogram of Sample Means and (1–0.05) Percentile Lower and Upper Bound

Table 5-1 shows the prediction intervals of each time period with the 90 percent and 95 percent levels of significance. As the time in duration increases, the prediction interval for a particular train tends to decrease.

TABLE 5-1 Prediction Interval Depending on Significant Level and Input Data Duration without Model Refitting

Model	Time in Detection ¹	Error Mean	90% Bound		95% Bound	
			Lower	Upper	Lower	Upper
1	10	-4.1	-7.9	-0.3	-8.8	0.3
2	20	-1.8	-5.6	1.9	-6.4	2.5
3	30	-3.6	-7.6	0.0	-8.5	0.6
4	40	-3.6	-7.6	0.0	-8.4	0.6
5	50	-5.1	-9.1	-1.4	-9.9	-0.8
6	60	-4.6	-8.7	-0.9	-9.8	-0.3
7	70	-5.0	-9.3	-1.2	-10.3	-0.5
8	80	-5.9	-10.5	-1.9	-11.6	-1.2
9	90	-3.9	-8.3	-0.1	-9.2	0.5
10	100	-5.9	-10.5	-2.1	-11.4	-1.6
11	110	-2.4	-5.2	0.2	-5.8	0.8
12	120	-2.6	-5.7	0.4	-6.3	0.8
13	130	2.1	-1.1	5.3	-1.8	5.8
14	140	-1.6	-5.8	2.4	-6.7	3.0
15	150	-2.3	-6.1	1.2	-7.0	1.9
16	160	-5.7	-10.6	-1.4	-11.7	-0.7
17	170	2.5	-1.7	8.2	-2.3	9.4
18	180	1.8	-2.4	6.1	-3.1	7.0
19	190	-1.4	-4.3	1.5	-4.9	2.0
20	200	-2.3	-6.4	1.5	-7.2	2.2
21	210	-2.2	-4.7	0.2	-5.3	0.6
22	220	1.3	-1.1	4.2	-1.4	4.9
23	230	-1.0	-3.3	0.4	-3.4	0.5
24	240	2.6	-2.1	8.9	-2.6	10.1

¹: Time since train was first detected

Therefore, the modified prediction error and modified predicted arrival time will be obtained using Equations 5-29 and 5-30.

$$\begin{aligned}
\Pi &= (P + ABS(L)) - A \\
\Pi - ABS(L) &= P - A \\
L &< \Pi - ABS(L) < U \\
L + ABS(L) &< \Pi < U + ABS(L)
\end{aligned}
\tag{5-29}$$

where;

- Π = Modified prediction error (s);
- P = Predicted arrival time from prediction algorithm (s); and
- A = Actual arrival time (s); and
- $[L, U]_{(1-2\alpha)}$ = $(1-2\alpha)$ percentile interval for prediction error (Predicted Arrival Time – Actual Time), where L is the low bound and U is the upper bound of the prediction error interval.

$$\begin{aligned}
L + ABS(L) &< P + ABS(L) - A < U + ABS(L) \\
L + ABS(L) + A &< P + ABS(L) = \pi < U + ABS(L) + A
\end{aligned}
\tag{5-30}$$

where;

- π = Modified predicted arrival time (s).

Therefore, the predicted arrival time of $(1-\alpha) \times 100$ ($= (1-2\alpha) + \alpha$) percent of trains is greater than the actual arrival time. This relationship can be shown in Figures 5-13 and 5-14 for the negative upper bound and the positive upper bound, respectively. Based on the results of the bootstrap method, while the lower bounds of the prediction error are less than zero for all 24 prediction models, the upper bounds of the prediction error are greater than zero for some models shown in Table 5-1. Therefore, these two cases were considered: 1) when the upper bound is negative with a negative lower bound, and 2) when the upper bound is positive with a negative lower bound. In this dissertation, the predicted arrival time will be obtained using 90 percent prediction intervals.

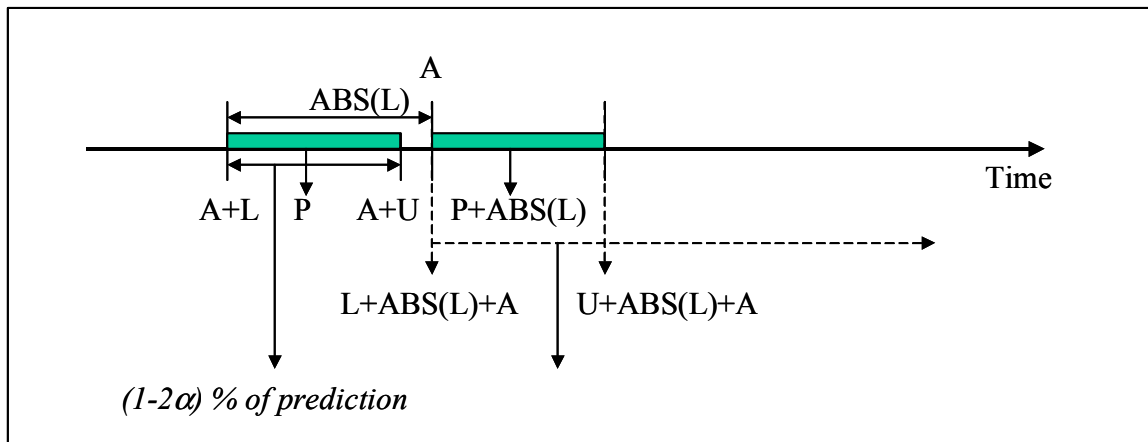


FIGURE 5-13 Application of Prediction Error to Predicted Arrival Time in Case of $U < 0$

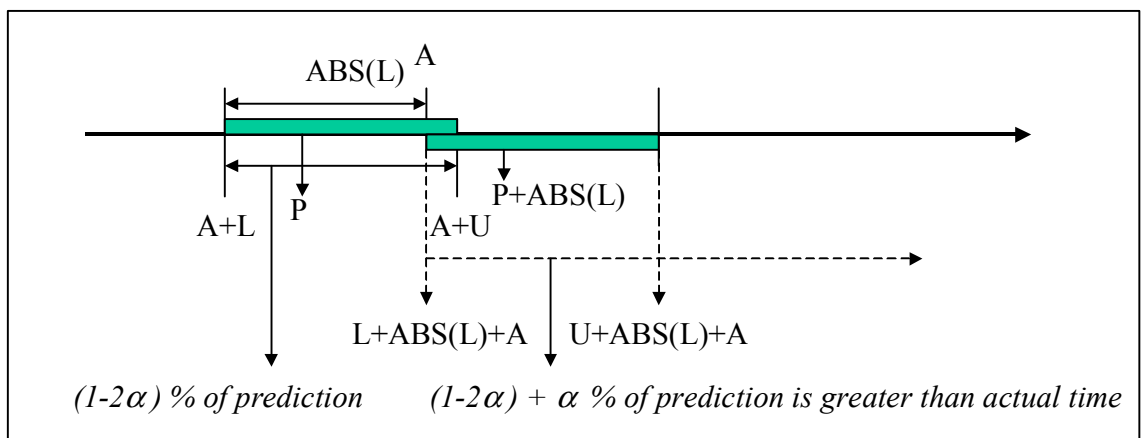


FIGURE 5-14 Application of Prediction Error to Predicted Arrival Time in Case of $U > 0$

If the predicted arrival time is longer than the actual arrival time, the TPS2 algorithm does not complete its process and the preemption will start. In this case, there still exists a safety problem that can be reduced by omitting the pedestrian phases once the TPS2 algorithm is initiated. If the predicted arrival time is shorter than the actual arrival time, the TPS2 algorithm will complete its process and hold the track clearance phase until the

preemption starts. In this case, the intersection is operated inefficiently. This problem can be reduced by increasing the predicted arrival time with the prediction interval. The new TPS algorithm (TPS3) is presented graphically in the flow chart shown in Figure B-3 in Appendix B.

It should be noted that a preemption may not occur after TPS3 starts in situation where the train stops upstream of the crossing. In this case, the traffic signal is operated in the TPS3 mode continuously. Therefore, this case should be addressed in the TPS3 algorithm so that the signal mode will be returned back to the normal signal mode. This can be done simply by adding a delay function into the TPS3 algorithm. That is, when the TPS3 algorithm starts, the delay begins its timing with the user-defined value. If a preemption does not start at the completion of delay, the signal mode will return to the normal mode. Under these circumstances the “safety” metrics at the intersection will be the same as that of the current technology.

Once the TPS2 (or TPS1) algorithm is initiated, the predicted arrival time is automatically updated (i.e., countdown) as the train approaches the crossing. Because the train speed is obtained continuously by the Doppler detector, the predicted train arrival time can be performed continuously. In this dissertation this update occurred every 10 seconds. However, once the train is completely past the Doppler detector, the predicted arrival time cannot be updated using observed speed data. Rather the predicted travel time is simply the last predicted arrival time minus the time that has elapsed since it was calculated as shown in Equation 5-31.

$$P = Z - z \quad (5-31)$$

where;

- P = Predicted train arrival time (s);
- z = Time since last prediction (s); and
- Z = Last predicted train arrival time (s).

Intuitively, the APWT that the TPS3 algorithm uses will affect the intersection performance in terms of both safety and delay. However, it was not considered in the stage of development of the TPS3 algorithm because it is difficult to calculate the optimum period theoretically. The optimal value for AWPT will be found using sensitivity analyses as will be in the next chapter.

The TPS3 algorithm was motivated using the four-leg IHRGC and six phases of signal structure. However, the TPS3 algorithm can still work for other geometric condition and other traffic signal phase plans. The TPS3 algorithm also was developed based on the vehicle detector information at each movement. However, even if no vehicle detectors are installed at the IHRGC, the TPS3 algorithm still can work because it may assume there is a vehicle call during every time in the period of time that the TPS3 algorithm is operated.

5.4 CONCLUDING REMARKS

The current transition preemption strategy has a number of advantages and disadvantages. The main advantage is that it can reduce the possibility of pedestrian phase truncations at the onset of preemption. There are two main disadvantages. The first is that it may provide exceedingly long service of the parallel road of the track before a preemption resulting in poor intersection performance. The second, and more important, is that the pedestrian phase truncations can still occur at the onset of preemption.

In this chapter a new transition preemption strategy was developed to improve the intersection performance and considerably reduce truncations of the pedestrian clearance phase at the onset of preemption. The new prediction algorithm and its prediction error bound developed in Chapter IV were used as input to the approach. The basic idea of the new transition preemption method is to provide more time to the blocked phases during the preemption mode than phases that are served during the preemption mode.

However, it is still possible that the pedestrian phase truncation can still occur when the advance preemption warning time is less than a critical value. The new transition preemption methodology will be evaluated and a sensitivity analysis of the major parameter will be conducted in Chapter VI.

CHAPTER VI

SENSITIVITY ANALYSIS

A new prediction algorithm for train arrival time and a new transition preemption algorithm were developed in the previous two chapters. The predicted time and prediction interval were incorporated into a new transition preemption algorithm as discussed in Chapter V. In this chapter the proposed method will be tested and compared to existing systems using a simulation study of the Wellborn Road test bed.

6.1 SIMULATION DESIGN

6.1.1 Simulation Duration

Two key components of any simulation analysis are the simulation duration and the analysis time. In this dissertation, it was assumed that initially the network is operating under steady state conditions. At some point a train passes through the network disrupting traffic, and then the system eventually returns to the original conditions. There were two questions that need to be answered: 1) how long should the simulation last, and 2) how long should the analysis phase last?

To answer the first question, a test simulation run was performed to identify when the network reaches a steady state condition. The traffic volume was measured 100 m downstream for each approach at an interval of 120 seconds (i.e., the cycle length). The relationship between volume and time for a train preemption event is shown in Figure 6-1. The network reaches a steady state condition approximately 300 seconds after the simulation is started. Consequently, all of the analyses were begun 300 seconds after the simulation began.

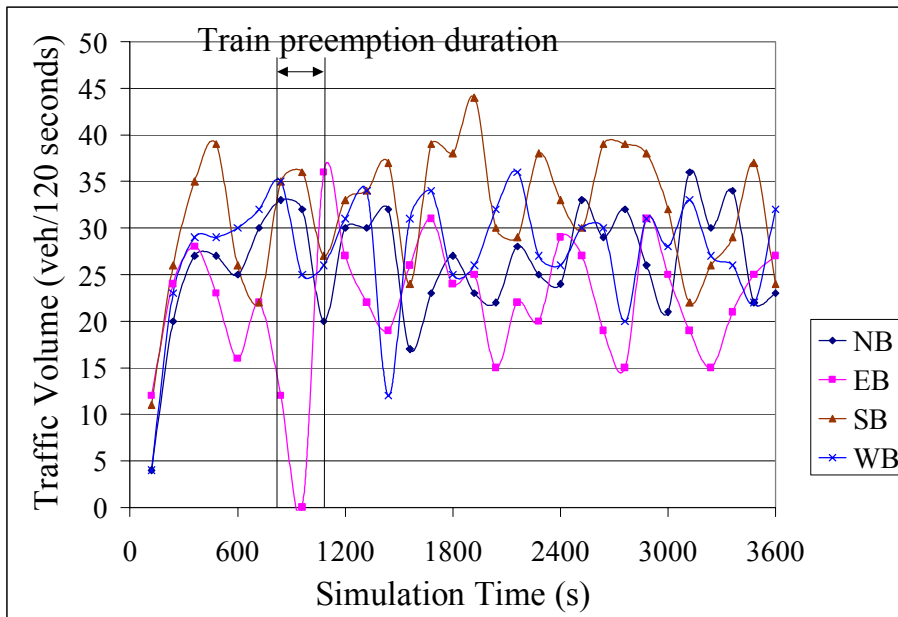


FIGURE 6-1 Change of Volume during Simulation

Simulation time is dependent on the analysis time. The analysis time should be long enough to ensure that the network returns to a steady state condition after a train passes through the network. The analysis time also depends on the train arrival time at the crossing. Therefore, train arrival time is also a key component for identifying the simulation duration and the analysis duration.

Two issues should be considered simultaneously to decide the train arrival time. The first consideration is to ensure that a pedestrian phase will be active at the onset of preemption. In this dissertation, trains are designed to arrive at the George Bush Drive crossing between 835 and 855 seconds after the simulation starts. This ensures that Phase 4 (westbound through and left turn) and its corresponding pedestrian phase are active.

After the train departs, it takes a certain amount of time for the system to return to steady state conditions. In this dissertation, it was decided to allow for a total of 60 minutes of

simulation time to ensure that this happens. The simulation period, the analysis period, and the train arrival time range at the crossing during simulation are shown in Figure 6-2.

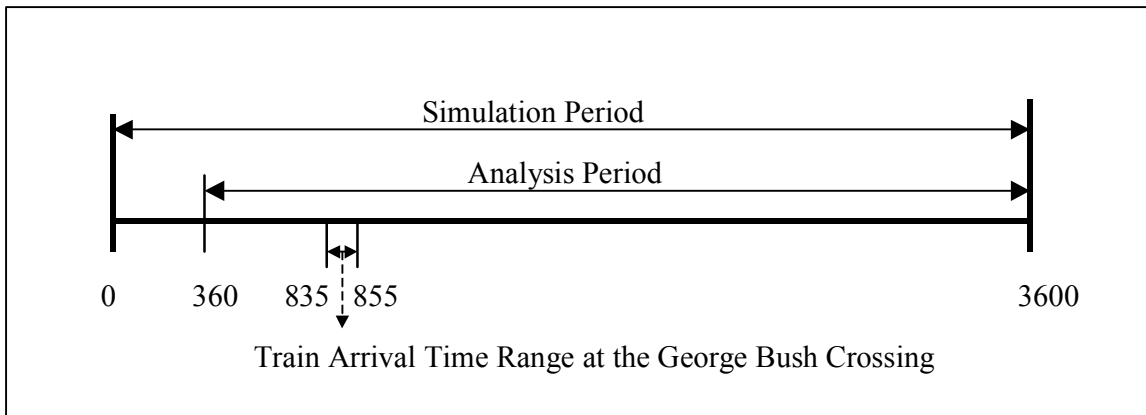


FIGURE 6-2 Time Frame for Analysis Period and Train Arrival Time Range at the Crossing during Simulation for Fixed Train Arrival Time

6.1.2 Estimating the Difference between CWT and Actual Arrival Time

The TPS0 algorithm is initiated in the controller when the CWT detector predicts the train arrival time to be 35 seconds. As discussed in Chapter IV, a difference between the predicted time and the actual arrival time exists because of the variation in the predicted time. Therefore, the difference between the actual train arrival time and the predicted time (i.e., 35 seconds) is required if the system is to be simulated accurately. However, this difference was not measured in the data set that was used to develop the prediction model. Therefore, a study was conducted to identify the relationship between the actual arrival time and the predicted time using new train data.

Data from 204 trains were collected for this study and will be referred to as Train Data Set2. These data are different from the data on 683 trains that were used in forecasting train arrival time, which will be referred to as Train Data Set1.

Figures 6-3, 6-4, 6-5, and 6-6 show the relationship between the actual warning time and the first measured speed, the last measured speed, the average speed, and the difference between the first and last speed, respectively. Two things can be noted from the graphs. The first is that the actual time is always greater than the predicted time of 35 seconds. This is expected because the system is set up to provide a minimum of 35 seconds warning time. In addition, the train speed at FM 2818 can be considerably different than the speed at George Bush Drive, and this accounts for the variation in warning time. The second is that there does not appear to be any relationship between warning time and any of the speed metrics. This would be expected because the warning time algorithm at George Bush Drive is designed to give a constant warning time of 35 seconds irrespective of the train speed.

Table 6-1 shows the correlation coefficient between warning time and the different speed metrics including the first train speed, the last train speed, the average speed, and the speed change during detection. The low values are consistent with a visual inspection of the data.

TABLE 6-1 Correlation between the Variables

Variables	Correlation Coefficient
First Speed ¹ and Preemption Warning Time	0.1716
Last Speed ¹ and Preemption Warning Time	0.0346
Average Speed and Preemption Warning Time	0.1333
Speed Change (Last – First) and Preemption Warning Time	-0.1606

¹: FM 2818

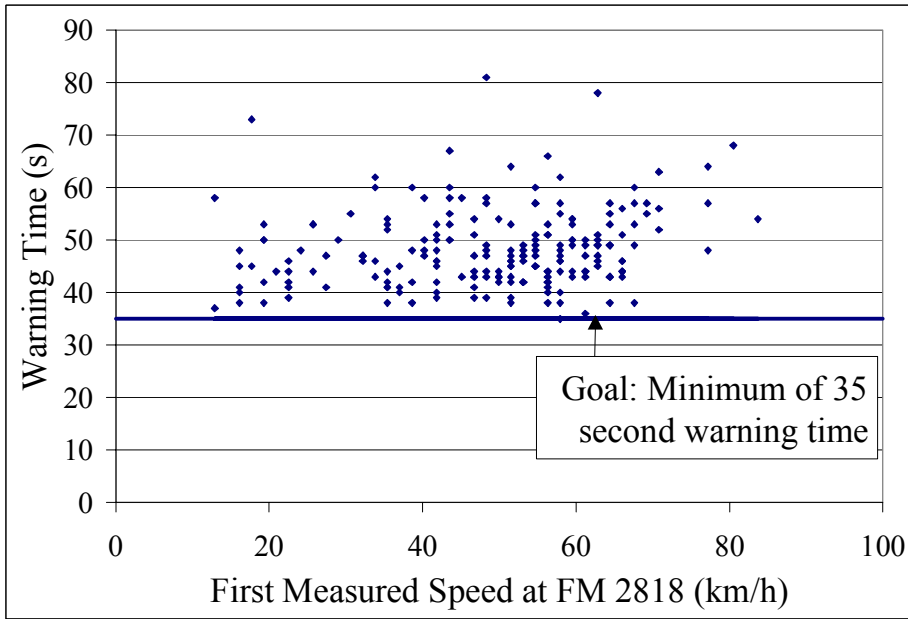


FIGURE 6-3 Preemption Warning Time versus First Train Speed

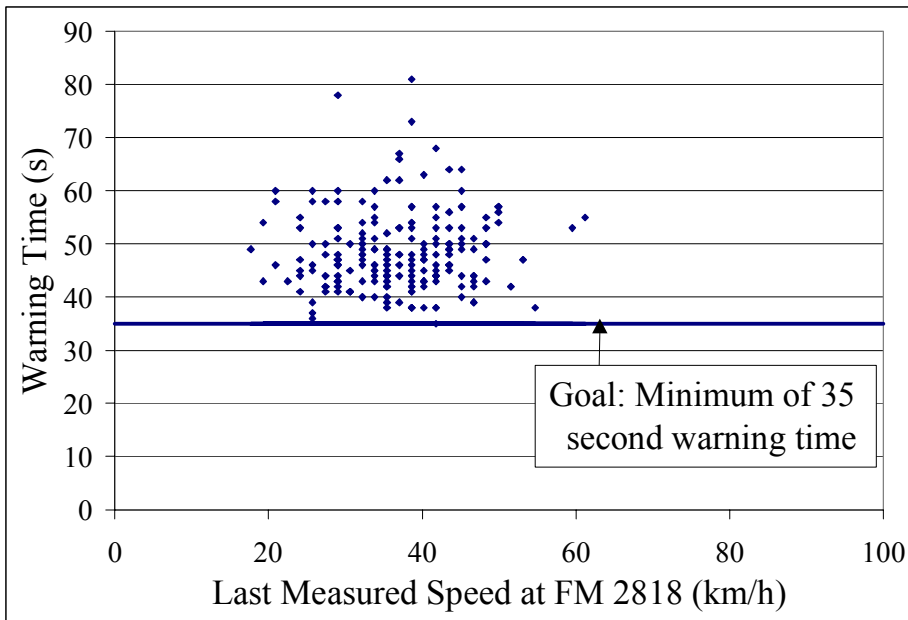


FIGURE 6-4 Preemption Warning Time versus Last Train Speed

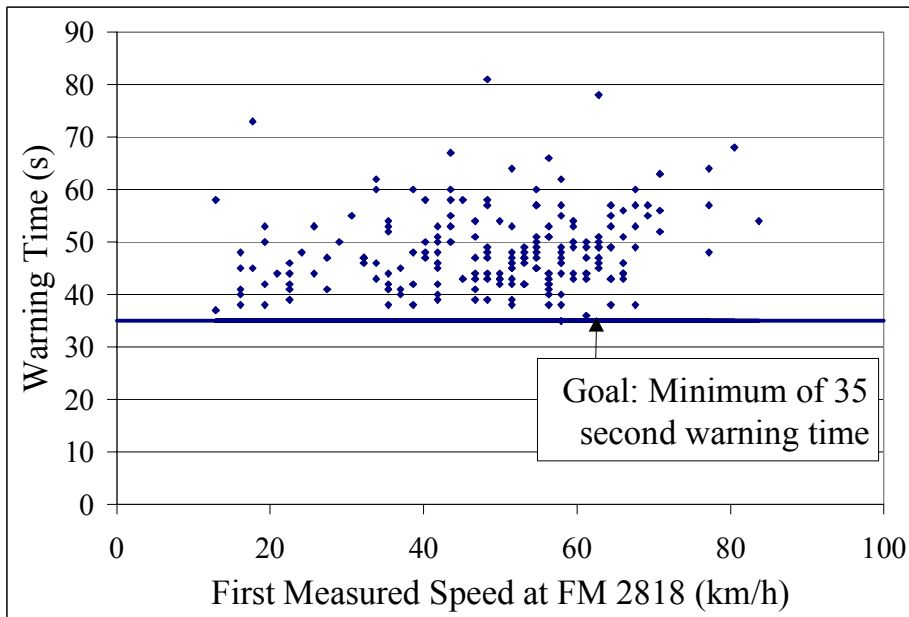


FIGURE 6-5 Preemption Warning Time versus Average Train Speed

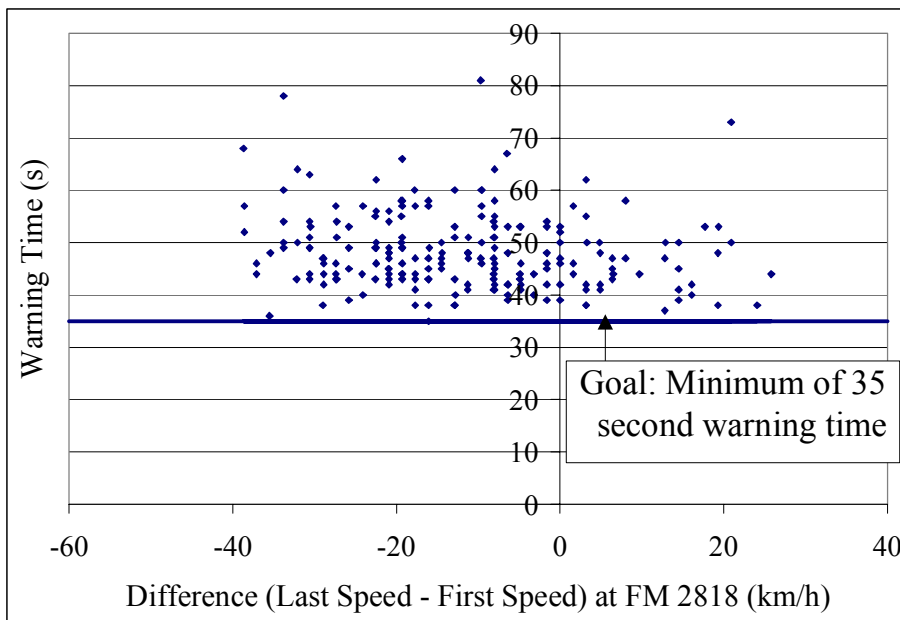


FIGURE 6-6 Preemption Warning Time versus Difference in Train Speed

To test if there was any statistical relationship between the variables, a simple linear regression of the form shown in Equation 6-1 was performed. All four speed measures (First speed, Last speed, Average speed, and Speed change) were tested as the independent variable, and the preemption warning time was used as the dependent variable.

$$\begin{aligned}
 \text{Model 1 : } Y &= b_0 + b_1x_1 \\
 \text{Model 2 : } Y &= b_0 + b_1x_2 \\
 \text{Model 3 : } Y &= b_0 + b_1x_3 \\
 \text{Model 4 : } Y &= b_0 + b_1x_4
 \end{aligned}
 \tag{6-1}$$

where;

- Y = Estimated preemption warning time;
- b_0 = Coefficients of the intercept;
- b_1 = Coefficients of slope;
- x_1 = First speed at FM 2818;
- x_2 = Last speed at FM 2818;
- x_3 = Average speed at FM 2818; and
- x_4 = Speed change (Last speed – First speed) at FM 2818.

The parameters, p-value, and average absolute error of each model are shown in Table 6-2.

TABLE 6-2 Results of the Simple Regression Models

	Coefficients		P-value		AAE
	b_0	b_1	b_0	b_1	
Model 1	44.18	0.08	0.000*	0.014*	5.55
Model 2	47.12	0.03	0.000*	0.623	5.67
Model 3	43.69	0.11	0.000*	0.057	5.56
Model 4	47.33	-0.08	0.000*	0.022*	5.60

*: Statistically significant at 0.05 significance level

Models 1 and 4 have coefficients statistically significant at the 0.05 significance level. Because 1) the AAE of Model 1 was smaller than the AAE of Model 4, and 2) it was a simpler model, Model 1 was chosen as the best linear regression model.

A further study was conducted to identify whether multiple independent variables could improve the results. The models considered are shown in Equation 6-2.

$$\begin{aligned}
 \text{Model 5 : } Y &= b_0 + b_1x_1 + b_2x_2 \\
 \text{Model 6 : } Y &= b_0 + b_1x_1 + b_2x_3 \\
 \text{Model 7 : } Y &= b_0 + b_1x_1 + b_2x_4 \\
 \text{Model 8 : } Y &= b_0 + b_1x_2 + b_2x_3 \\
 \text{Model 9 : } Y &= b_0 + b_1x_2 + b_2x_4 \\
 \text{Model 10 : } Y &= b_0 + b_1x_3 + b_2x_4
 \end{aligned}
 \tag{6-2}$$

where;

- Y = Estimated preemption warning time;
- b_0 = Coefficients of the intercept;
- b_1 = Coefficients of slope;
- x_1 = First speed at FM 2818;
- x_2 = Last speed at FM 2818;
- x_3 = Average speed at FM 2818; and
- x_4 = Speed change (Last speed – First speed) at FM 2818.

The correlations between the independent variables in each model are shown in Table 6-3.

TABLE 6-3 Correlation between the Independent Variables in Each of the Multiple Linear Regression Models

	Variables	Correlation Coefficient
Model 5	First Speed ¹ and Last Speed ¹	0.347
Model 6	First Speed ¹ and Average Speed	0.816
Model 7	First Speed ¹ and Speed Change (Last – First)	-0.857
Model 8	Last Speed ¹ and Average Speed	0.755
Model 9	Last Speed ¹ and Speed Change (Last – First)	0.187
Model 10	Average Speed and Speed Change (Last – First)	-0.439

¹: FM 2818

It was decided to eliminate the models that had variables where the absolute value of the correlation coefficient was greater than 0.5. The two independent variables in Model 6, 7, and 8 are strongly correlated and therefore, these models were not calibrated. The coefficients, p-value, and AAE of the remaining models are shown in Table 6-4.

TABLE 6-4 Results of the Multiple Regression Models

	Coefficients			P-value			AAE
	b ₀	b ₁	b ₂	b ₀	b ₁	b ₂	
Model 5	44.93	0.090	-0.027	0.000*	0.015*	0.703	5.56
Model 9	44.93	0.063	-0.090	0.000*	0.345	0.015*	5.56
Model 10	44.84	0.065	-0.066	0.000*	0.316	0.103	5.56

*: Statistically significant at 0.05 significance level

None of the three models had coefficients that were statistically significant at the 0.05 significance level. Therefore, all of these models were rejected for use and Model 1 was chosen for all analyses.

An alternative approach assumed that the preemption warning time was not influenced by train speed. In this situation, the preemption warning time for the old data was

generated randomly based on the preemption warning time distribution from the new data. The normal distribution was assumed for the preemption warning time distribution where the mean was 48.3 seconds and the standard deviation was 7.48 seconds. This assumption was tested using the K-S test and passed at the 0.05 level of significance. Based on the results of 100 simulations, the average AAE was 8.2, which was 49.1 percent larger than the results of the best regression model. Therefore, Model 1 was used to estimate the preemption warning time for the trains in Data Set 1.

6.1.3 Simulation Scenarios

The four transition preemption methods discussed in Chapter V were tested: standard preemption (TPS0), current TPS (TPS1), modified TPS (TPS2), and modified TPS using updated predicted arrival time and prediction intervals (TPS3). The traffic volume of the base case (evening peak period) was used for all the simulations conducted.

Two objectives were considered in this analysis. The primary objective was safety, and the measures of effectiveness (MOEs) used were the number of truncated pedestrian clearance phases and the total amount of time truncated from these pedestrian clearance phases. The secondary objective was the intersection performance, and the MOE used was average control delay.

Because the intersection performance, in terms of both safety and efficiency, depends on the advance preemption warning time, the optimal starting time of the transition preemption strategy needs to be identified for TPS1, TPS2, and TPS3. The optimization strategy employed in this dissertation was to test each TPS method with different APWTs at fixed intervals. Because the APWT should be greater than the standard preemption warning time (35 seconds), the minimum advance preemption warning time tested was 40 seconds. The maximum APWT tested was 120 seconds, and the increment size was 10 seconds.

Algorithm performance was evaluated under two conditions: 1) no pedestrians (pedestrian phase inactive), and 2) pedestrians present (pedestrian phase active). The former scenario is straightforward to model because the number of pedestrians per hour is set to zero. The pedestrian phase inactive scenario would be analogous to having a single MOE of average intersection delay.

The second condition required a mathematical analysis. The probability that a pedestrian phase is active in every cycle is a function of the pedestrian volume, pedestrian arrival pattern, and the length of the time period in which the pedestrian can affect the next pedestrian phase. This latter time period is based on the pedestrian green phase of each phase and the cycle length. Because the pedestrian green phase is 4 seconds for each movement and the cycle length is 120 seconds for this study, the length of the time period that the pedestrian can affect the next pedestrian phase is 116 seconds. That is, if pedestrians arrive at the intersection during this 116-second time interval, the next pedestrian phase will be active. It was assumed that pedestrians arrive at the crosswalk randomly and, therefore, a negative exponential distribution was used in this dissertation. The probability of the pedestrian phase being active during every cycle is equal to the probability of more than one pedestrian arriving during a given time period. This value can be calculated using Equation 6-3.

$$P_r = 1 - P_r(0) = 1 - e^{(-\lambda \times t)} \quad (6-3)$$

where;

- P_r = Probability of one or more than one pedestrian arriving during the time period at every cycle;
- $P_r(0)$ = Probability of no pedestrians arriving in a time interval (the probability that the next pedestrian phase will not be active);
- λ = Pedestrian arrival rate (= 400 ped/h);
- t = Length of the time period that a given pedestrian can affect the next pedestrian phase (= 116 seconds); and

e = Constant, Napierian base of logarithms ($e = 2.71828\dots$).

If the pedestrian volume is 400 ped/h, the probability that the pedestrian phase will be active when the preemption starts is 99.99 percent. Consequently, this pedestrian volume was used in the analysis.

As shown in Chapter IV, the train arrival prediction accuracy is a function of the train speed profile. Therefore, the simulation study was performed for different speed profiles. Based on the analysis conducted in Chapter IV, it was decided to use three categories (increasing speed (Group 1), constant speed (Group 2), and decreasing speed (Group 3)). To provide results that could be tested statistically, 30 trains from each category were used. The 30 trains in each group were selected randomly. The speed profiles of each group are shown in Figure 6-7. The average speed of the trains in Group 1 is 30 km/h and the AAE was 10.9 seconds. The train speed tends to increase slightly with detection time. The average speed of the Group 2 trains is 41 km/h and the AAE was 7.9 seconds. The train speed tends to decrease slightly as time in detection increases. The average speed of the Group 3 trains is 51 km/h and the AAE was 6.1 seconds. The train speed tends to decrease drastically with detection time. For each of the 90 scenarios a different random seed was chosen in order to represent the stochastic nature of the traffic.

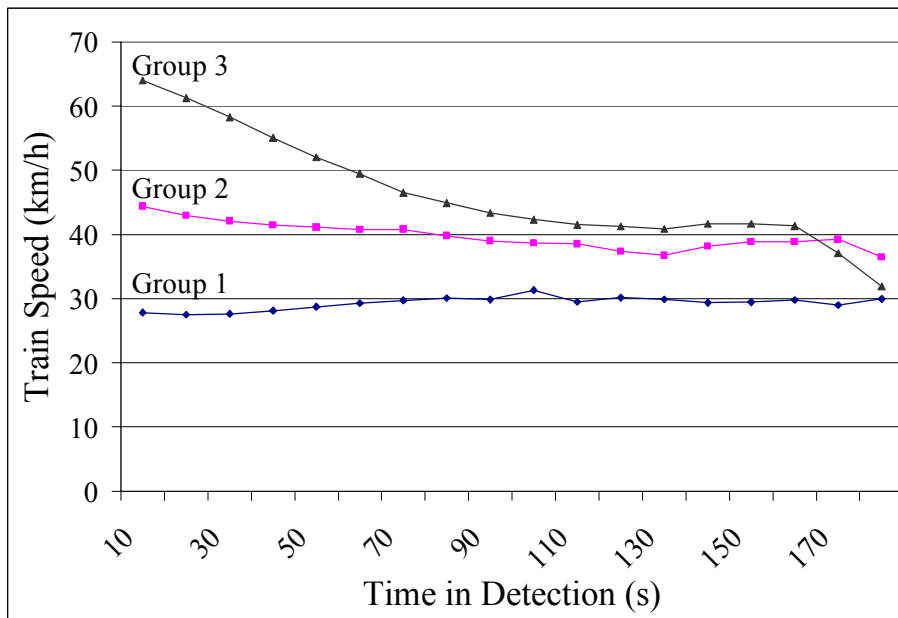


FIGURE 6-7 Speed Profile of the 30 Trains in Each Subgroup

Table 6-5 shows the number of trains for each group and the time in detection. As the time in detection increases, the number of trains per group decreases. In general, Group 3 trains spent less time in detection than the Group 2 trains, which, in turn, spent less time in detection than Group 1 trains. It would be expected that the faster trains would spend less time in detection, all else being equal, and this is shown in Table 6-5.

TABLE 6-5 Number of Train Speed Observations in Each Group Depending on Time in Detection

Time in Detection	Group 1	Group 2	Group 3
10	30	30	30
20	30	30	30
30	30	30	30
40	30	30	30
50	30	30	30
60	30	30	30
70	30	30	30
80	29	26	28
90	27	25	24
100	25	23	19
110	22	21	18
120	22	19	16
130	20	18	13
140	18	15	8
150	17	12	7
160	16	12	5
170	14	9	3
180	12	7	1
190	10	4	0
200	9	3	0
210	6	3	0
220	5	1	0
230	5	1	0
240	5	0	0

6.2 SIMULATION RESULTS (FIXED TRAIN ARRIVAL TIMES)

6.2.1 Metric 1: Truncation of Pedestrian Clearance Interval Results

As discussed in Chapter V a new transition preemption strategy was developed to improve the safety of the intersection at the onset of preemption. This new strategy implicitly accounts for the variability of train arrival time prediction. It should be remembered that all the TPS algorithms were designed with the goal of eliminating the possibility of the truncation of the pedestrian clearance interval. However, if the

duration that the TPS is operated is short or the predicted time is not accurate, the possibility that the pedestrian phase will be truncated in an unsafe manner exists. As discussed in Section 6.1.3 the safety MOEs were the number of pedestrian phases that were truncated (out of 90) and the average abbreviation time for each truncated phase (range 0 to 15 seconds).

The truncation number and abbreviation time of the pedestrian clearance interval for the pedestrian phase active scenario as a function of the APWT is shown in Table 6-6.

TABLE 6-6 Number of Pedestrian Phase Truncations and Average Phase Abbreviation Time at the Onset of Preemption for Pedestrian Phase Active Scenario and Fixed Train Arrival Time

APWT*	TPS0 ¹	TPS1 ²	TPS2 ³	TPS3 ⁴
	90(6)			
40		90(6)	90(6)	90(6)
50		77(6)	77(6)	84(6)
60		59(6)	59(6)	76(6)
70		18(6)	18(6)	45(6)
80		5(6)	5(6)	14(6)
90		4(4)	4(4)	1(6)
100		4(4)	4(4)	0(0)
110		1(3)	5(4)	0(0)
120		1(3)	5(3)	0(0)

*: Advance preemption warning time

¹: Normal preemption without TPS

²: Current TPS

³: Modified TPS

⁴: Modified TPS using updated predicted arrival time and prediction intervals

(): Seconds of phase abbreviation

Because the analyses were designed such that a pedestrian phase is always active at the onset of preemption, a pedestrian phase truncation occurred in every TPS0 scenario. Note that this constraint will be relaxed in Section 6.3. The average abbreviation time of

the pedestrian clearance was 6 seconds. Therefore, the normal preemption operation is considered unsafe when the pedestrian phase of phase 4 is active when a train arrives. In this situation, the pedestrian phase is immediately truncated with the possibility of stranding a pedestrian in the intersection.

There are two necessary conditions for a pedestrian phase truncation to occur for the TPS1, TPS2, and TPS3 algorithms. If the predicted arrival time is equal to or less than the actual arrival time, then the track clearance phase will be initiated before the preemption is started and pedestrian phase truncations will not occur. Therefore, the first necessary condition for a pedestrian phase truncation to occur during the TPS1, TPS2, and TPS3 algorithms is that the predicted arrival time is greater than the actual arrival time. However, even if the predicted arrival time is greater than the actual arrival time, if the pedestrian phase is not active at the onset of preemption, a pedestrian phase truncation will not occur. Therefore, the second necessary condition for a pedestrian phase truncation is that the pedestrian phase is active at the onset of preemption under the first necessary condition. That is, no matter how large the APWT is, a pedestrian phase can be truncated if the two necessary conditions are satisfied.

Two examples are used to demonstrate how a pedestrian phase can be truncated in the TPS1 algorithm for the test bed. The first example (train 3 in Group 1) has an APWT value of 80 seconds and the second (train 89 in Group 3) has an APWT value of 110 seconds. The traffic signal is operated based on current traffic and pedestrian conditions and the predicted arrival time during the TPS algorithms. Therefore, the situation that a pedestrian phase is active at the onset of preemption is a function of traffic and pedestrian condition and the predicted arrival time.

A pedestrian phase truncation occurred in the TPS1 algorithm for train 3 (out of 90) when the APWT was 80 seconds. Figure 6-8 shows the process by which the pedestrian phase was truncated for this case. The TPS1 algorithm is initiated 23 seconds after

phase 3 is started (i.e., 784 seconds into the simulation). Because the pedestrian clearance phase was completed at time 780 seconds, phase 3 is terminated at this point and the TPS1 algorithm begins. When the TPS1 algorithm was started, the predicted arrival time was 75 seconds, which is enough time to serve the minimum length of the next phase before preemption starts. Therefore, 5 seconds of Yellow + All-red clearance time was provided and phase 4 was started at time 789 seconds. Note that the train arrived at the preemption detector at time 794 seconds, which is 30 seconds earlier than expected and 5 seconds after phase 4 began. Therefore, the pedestrian clearance phase is truncated at 794 seconds in order to serve the track clearance phase (phase 3).

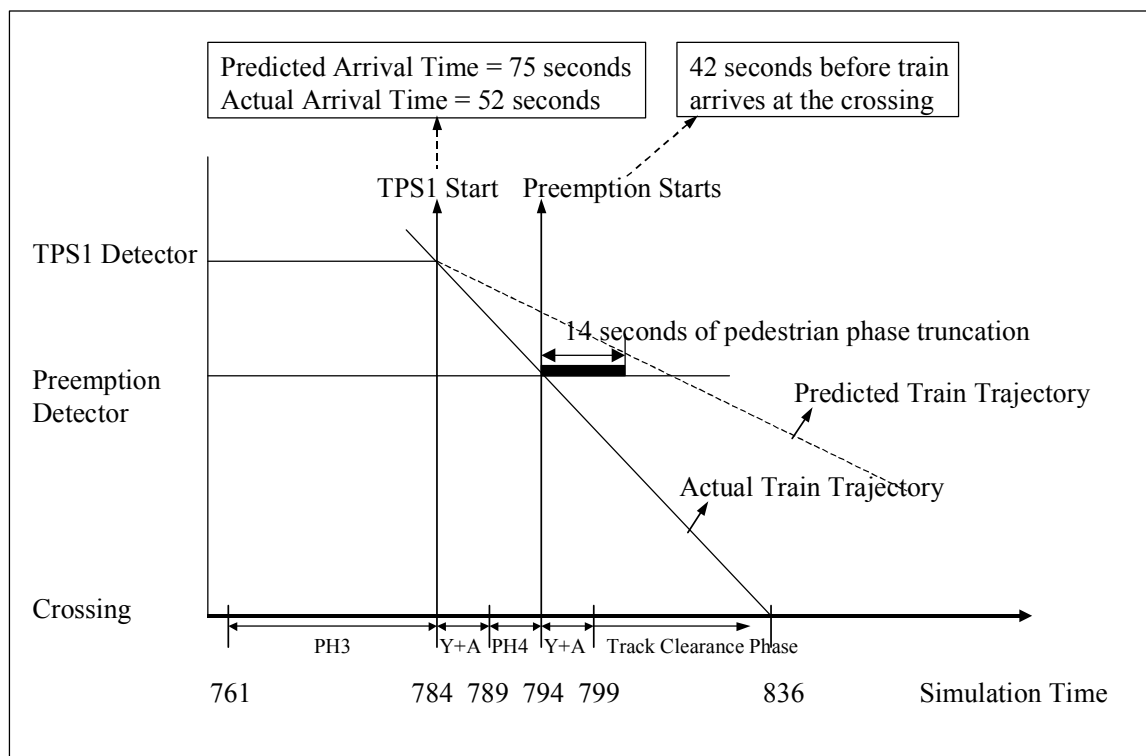


FIGURE 6-8 Example of a Pedestrian Phase Truncation for the TPS1 (Train 3, APWT = 80 seconds)

As another example consider train 89 when the APWT is 110 seconds as shown in Figure 6-9. The TPS1 algorithm is initiated 3 seconds after phases 2 and 6 are ended. Because the Yellow + All-red clearance must be completed, the TPS1 algorithm begins at time 761 seconds. When the TPS1 algorithm was started, the predicted arrival time was 108 seconds, which is enough time to serve the minimum length of phase 3 before the preemption starts. Therefore, phase 3 is started at 761 seconds and is served for 19 seconds, which is the minimum required for the pedestrian green phase and the pedestrian clearance interval. After the end of phase 3, the TPS1 algorithm evaluates the traffic and pedestrian condition and the predicted arrival time. The predicted arrival time is now 82 seconds, which is large enough to serve the minimum length of phase 4 before preemption starts. Therefore phase 4 is started at time 785 seconds. Note that the

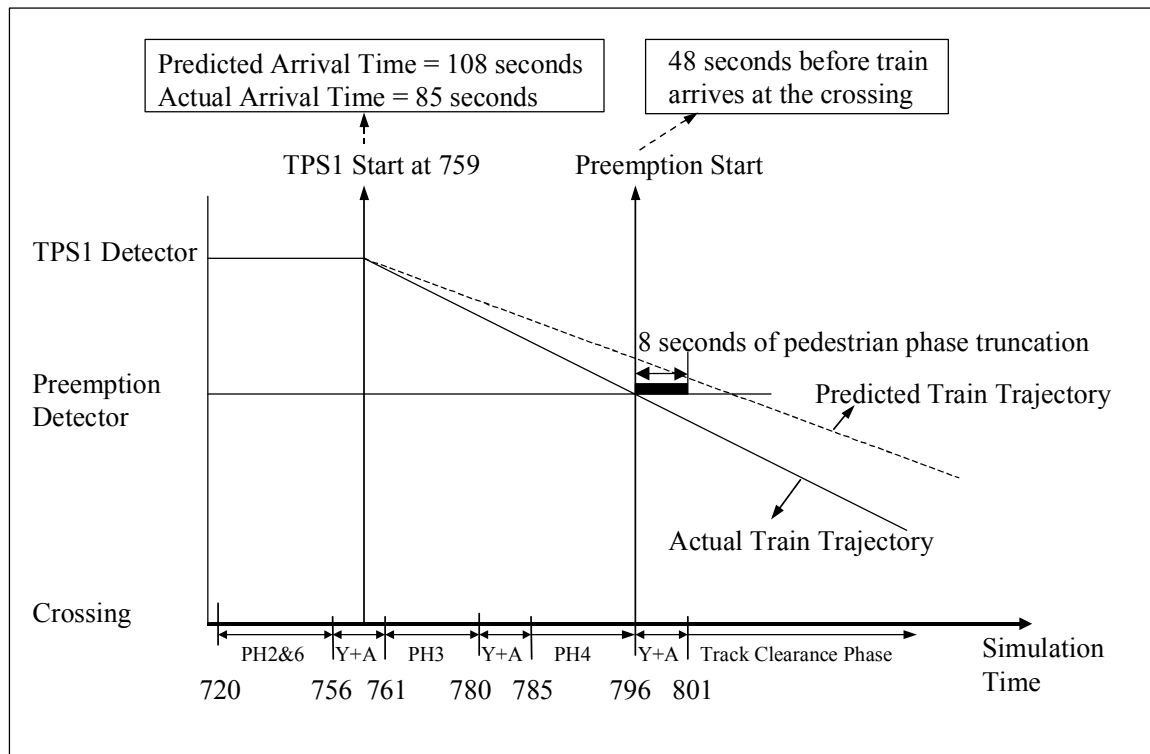


FIGURE 6-9 Example of a Pedestrian Phase Truncation for the TPS1 (Train 89, APWT = 110 seconds)

train arrived at the preemption detector at time 796 seconds, which is 36 seconds earlier than expected. This is only 11 seconds after phase 4 is started. Consequently, phase 4 is truncated and pedestrians could be stranded in the crosswalk.

For the TPS1 algorithm as the APWT increases, the number of pedestrian phase truncations decreases. The truncation number is reduced to 5, 4, and 1 for the APWT values of 80, 90, and 110 seconds, respectively. In the original TPS1 algorithm study, the evaluation was conducted at an APWT value of 70 seconds. It was found that 11 truncations occurred out of 51 simulations, which is approximately 22 percent (5). When an APWT value of 70 was used in this dissertation, 18 truncations occurred out of 90 simulations, which is approximately 20 percent. Based on the results of this analysis, a longer APWT will result in better metrics for the TPS1 algorithm. It should be noted that a truncation occurred once out of 90 preemption cases when the APWT was set to 110 and 120 seconds, and that this situation is still unsafe.

With respect to the TPS2 algorithm it can be seen in Table 6-6 that as the APWT increases, the number of phases that are truncated decreases. Once the APWT was equal to or greater than 80 seconds, the truncation number varied from 4 to 5. Interestingly, only when the APWT was 110 and 120 seconds, the results of the TPS2 algorithm were different from that of the TPS1 algorithm. This result occurs because the TPS1 algorithm provides excessively long dwell phases for large APWT values. In contrast, the TPS2 algorithm terminates the dwell phases and provides the non-dwell phase with the corresponding pedestrian phase at the onset of preemption. Therefore, a pedestrian phase truncation occurred in the TPS2 algorithm and this led to the difference in results.

Table 6-6 shows that for the TPS3 algorithm as the APWT increases, the number of pedestrian phase truncations decreases. This result is similar to the other TPS algorithms. Interestingly, the number of truncations for the TPS3 algorithm is greater than that for the TPS1 and TPS2 algorithms when the APWT is equal to or less than 80

seconds. However, once the APWT was equal to or greater than 100 seconds, pedestrian truncation did not occur at all. Therefore, the best algorithm in terms of the safety MOE was the TPS3 algorithm. For this test bed the TPS3 algorithm should be used with a minimum APWT value of 100 seconds. This will reduce the possibility of the truncation of the pedestrian clearance time, which is the primary goal of TPS.

There were more pedestrian phase truncations at the low APWT values because the probability will be higher that a pedestrian phase will be active when the preemption starts. Table 6-7 shows the average length of time each of the TPS algorithms are active as a function of the design length of time. As the APWT increases, the amount of time that the TPS algorithms are active increases. Particularly for small APWT, some cases exist where the TPS was not even initiated due to the variability of the predicted arrival time. For example, when the APWT is 40 seconds every TPS algorithm should operate for 5 seconds if there is no error in the predicted arrival time. However, it can be seen that for an APWT value of 40 seconds none of the preemption algorithms were active. The reason for the difference between the design and actual TPS operation time is the variability of predicted arrival times.

TABLE 6-7 Average TPS Duration as Function of Advance Preemption Warning Time for Pedestrian Phase Active Scenario and Fixed Train Arrival Time

APWT*	Designed TPS Duration (seconds)	TPS1 & TPS2 (seconds)	TPS3 (seconds)
40	5	0 (0)	0 (0)
50	15	5 (34)	2 (14)
60	25	11 (74)	6 (52)
70	35	21 (87)	13 (80)
80	45	29 (90)	23 (89)
90	55	39 (90)	32 (90)
100	65	48 (90)	41 (90)
110	75	60 (90)	51 (90)
120	85	69 (90)	61 (90)

*: Advance preemption warning time

(): Number of simulation runs that TPS algorithm is operated (out of 90)

6.2.2 Metric 2: Phase Length Results

One objective of the TPS2 and TPS3 algorithms is to provide more green time to the road that runs perpendicular to the railroad tracks, which will be blocked during the preemption, before the preemption is started. The phase lengths of each phase before the preemption began were obtained from the simulation output files to evaluate the extent to which this objective was met. Intuitively, it would be hard to measure a difference in average phase length among the TPS scenarios over the entire simulation time because the signal plan is impacted for a maximum of 85 seconds during the 1 hour simulation time. Therefore, the phase length just before the preemption was used as a measure of effectiveness.

The time period between the TPS algorithm start time and the preemption start time is the appropriate period for obtaining values for the phase length metric comparison because the duration of the phase length in this period is a function of the TPS algorithm. However, because this period may be different for each simulation run based on the train attributes and TPS scenarios, an absolute reference time is required to serve as a basis. In all simulations, the TPS is initiated between 694 seconds and 763 seconds and the train arrival time ranges between 835 seconds and 855 seconds. Because the traffic signal at George Bush Drive and Wellborn Road is operated with the coordinated actuated signal mode, it has a constant cycle length. As discussed in Chapter III, this cycle length was measured directly from the signal controller and the value was used in the simulation. Therefore, the cycle start time before the TPS algorithm begins is constant for all simulations. The cycle start time before the start of the TPS algorithm was chosen as the starting time for calculating the phase length metrics and corresponds to the 600-second mark of the simulation.

The time period for calculating the phase length metric should include the track clearance time in preemption mode to check the effect of a given TPS algorithm. Because the end of track clearance time is different for each scenario, an absolute

reference time after the end of track clearance time is required. The maximum crossing time for all 90 trains was chosen as the end reference time and this corresponds to the 855-second mark of the simulation. Consequently, the total analysis period is 255 seconds and this period also is long enough to guarantee the inclusion of all phases at least once. Table 6-8 gives the total phase length for each TPS algorithm and each APWT studied during the comparison period. The phase length results during the analysis period are also presented in Table C-1 in Appendix C. Similar results were found, although because the analysis time was longer (225 seconds versus 3240 seconds) the difference in the phase length between the scenarios was not as significant.

Table 6-8 shows that for the TPS3 algorithm as the APWT increases, the total length of phases 1 and 5 increases during the comparison period for signal timing. It should be noted that phase 1 is blocked during the preemption but phase 5 is served. Moreover, when the APWT is small, the difference in the phase length of phase 1 is relatively small or non-existent. This can be attributed to the fact that when the APWT is small (i.e., <80 seconds), the TPS may not even be active. If it is active then its duration is small as was shown in Table 6-7 for the APWT values less than 80 seconds. When the APWT is greater than 80 seconds, the difference in the phase length of phase 1 can be seen. For example, when the APWT is 120 seconds, the TPS3 algorithm provided 28 seconds to phase 1, which is 46 percent more than the TPS0 algorithm, 52 percent more than the TPS1 algorithm, and 34 percent more than the TPS2 algorithm. Therefore, the TPS3 algorithm provided more time to phase 1 before preemption as compared to the other TPS algorithms for the APWT values greater than 80 seconds.

TABLE 6-8 Total Phase Length for APWT and TPS Algorithms (Comparison Period for Signal Timing¹; Pedestrian Phase Active Scenario; and Fixed Train Arrival Time)

APWT ²	TPS Algorithm	Phase 1 (second)	Phase 2 (second)	Phase 3 (second)	Phase 4 (second)	Phase 5 (second)	Phase 6 (second)
	TPS0	19	96	72	28	36	42
40	TPS1	19	96	72	28	36	42
	TPS2	19	96	72	28	36	42
	TPS3	19	96	72	28	36	42
50	TPS1	19	97	74	27	37	42
	TPS2	19	97	74	27	37	42
	TPS3	19	96	73	27	37	42
60	TPS1	19	98	74	27	37	43
	TPS2	19	97	74	27	37	42
	TPS3	19	97	73	27	37	42
70	TPS1	19	98	71	29	37	44
	TPS2	19	97	72	29	37	43
	TPS3	19	97	71	29	37	42
80	TPS1	19	99	69	30	37	44
	TPS2	19	98	70	30	37	43
	TPS3	19	97	69	30	37	42
90	TPS1	19	101	71	28	37	46
	TPS2	19	97	69	31	37	42
	TPS3	20	97	66	32	37	42
100	TPS1	19	104	73	25	37	49
	TPS2	19	95	69	32	37	41
	TPS3	21	96	63	33	38	42
110	TPS1	19	111	73	21	37	54
	TPS2	19	92	69	34	38	37
	TPS3	24	95	60	32	39	42
120	TPS1	18	112	72	22	37	54
	TPS2	21	89	68	36	38	34
	TPS3	28	92	58	31	41	40

¹: 600 to 855 seconds

²: Advance preemption warning time

While the TPS3 algorithm provided more time to phase 1, as was discussed in Chapter V, it provided less time to phases 2 and 6 compared to TPS1. For the TPS3 algorithm as the APWT increases, the total length of phases 2 and 6 decreases. For example, when the APWT is 120 seconds, the total length of phases 2 and 6 for the TPS3 algorithm decreased 5 and 6 percent, respectively, as compared to the TPS0 algorithm. In effect, this time was allocated to the blocked phases (i.e., phases 1 and 4). In contrast the TPS1 algorithm increased the total length of phases 2 and 6 compared to the TPS0 algorithm.

The TPS3 algorithm was designed to serve phase 3 more than the TPS0 and TPS1 algorithms. However, Table 6-8 shows that the length of phase 3 was smaller in TPS3 than in the TPS0, TPS1, and TPS2 algorithms. The reason that phase 3 was allocated less time was related to the variability in prediction. That is, the TPS3 algorithm does not serve phase 3 more than a necessary length for the given traffic condition. Moreover, because the TPS3 algorithm was designed to reduce the possibility of excessively long track clearance time by increasing the APWT, the length of phase 3 can be shorter in the TPS3 algorithm than in the TPS0, TPS1, and TPS2 algorithms. That is, if the predicted train arrival time is shorter than the actual train arrival time, the TPS0, TPS1, and TPS2 algorithms are terminated and the track clearance phase is started earlier than expected. In this case, the track clearance phase will be served longer than necessary, which means that the vehicles are not served by the track clearance phase. The TPS3 algorithm serves phase 3 more than the TPS0, TPS1, and TPS2 algorithms only if all conditions are identical, including TPS duration and traffic/pedestrian volume. Therefore, even if the length of phase 3 during the TPS3 algorithm is reduced, it is hypothesized that the available time was used more efficiently. The delay metric will be used to test this hypothesis.

As discussed in Chapter V phase 4 should have longer time in the TPS2 and TPS3 algorithms as compared to the TPS0 and TPS1 algorithms. Similar to the previous analysis, this only occurred when the APWT was over 90 seconds. For example, when

the APWT is 120 seconds, the TPS3 algorithm provided 31 seconds to phase 4, which is 13 percent more than the TPS0 algorithm and 45 percent more than the TPS1 algorithm. When the APWT is less than 90 seconds, the length of phase 4 is the same regardless of the TPS algorithms. The reason this occurred for the lower APWT values is that there was not enough time for the TPS3 algorithm to achieve its goal.

Based on the above analysis of the phase lengths (calculated prior to the train arriving at the crossing) shown in Table 6-8, it was concluded that the TPS3 algorithm operated as designed.

A similar analysis was conducted for the pedestrian phase inactive scenario. The phase length data are shown in Table 6-9. There is less difference in the length of phases 3 and 4 in the TPS3 algorithm as compared to both the TPS1 and TPS2 algorithms. The reason for this is that in the pedestrian phase active scenarios the pedestrian phases for phases 3 and 4 are always active and therefore are served in the TPS1 and TPS2 algorithms. Once the pedestrian phase is active, 15 seconds of clearance time is provided and, therefore, the length of phases 3 and 4 should also be extended to the minimum value of 19 seconds. However, because the TPS3 algorithm was designed to cancel the pedestrian phases, when a train is approaching, the minimum time for phases 3 and 4 is only 10 seconds. Therefore, while there is a maximum 32 percent difference between pedestrian phase active scenarios and pedestrian phase inactive scenarios in the TPS1 and TPS2 algorithms, the difference is reduced by 3 percent in the TPS3 algorithm. However, the same general pattern as the pedestrian phase active scenario was found. It was concluded that the TPS3 algorithm performed as designed.

The phase length of each phase for the analysis period in the pedestrian phase inactive scenario is also shown in Table C-2 in Appendix C. Similar results were found, although because the analysis time was longer (225 seconds versus 3240 seconds) the difference in the phase length between the scenarios was not as significant.

TABLE 6-9 Total Phase Length for APWT and TPS Algorithms (Comparison Period for Signal Timing¹; Pedestrian Phase Inactive Scenario; and Fixed Train Arrival Time)

APWT ²	TPS Algorithm	Phase 1 (second)	Phase 2 (second)	Phase 3 (second)	Phase 4 (second)	Phase 5 (second)	Phase 6 (second)
	TPS0	19	96	72	28	35	42
40	TPS1	19	96	72	28	35	42
	TPS2	19	96	72	28	35	42
	TPS3	19	96	72	28	35	42
50	TPS1	19	97	74	27	36	43
	TPS2	19	97	74	27	36	43
	TPS3	19	96	73	27	36	43
60	TPS1	19	98	72	27	36	43
	TPS2	19	97	73	27	36	43
	TPS3	19	97	73	27	36	43
70	TPS1	19	98	67	32	36	44
	TPS2	19	97	68	32	36	43
	TPS3	19	97	70	29	36	43
80	TPS1	22	99	61	32	37	45
	TPS2	22	98	62	32	37	44
	TPS3	21	97	65	31	36	44
90	TPS1	23	99	59	32	37	46
	TPS2	23	97	59	33	37	44
	TPS3	23	97	60	32	37	44
100	TPS1	22	102	59	31	37	49
	TPS2	24	95	59	34	38	43
	TPS3	24	96	58	33	37	44
110	TPS1	20	107	59	30	36	52
	TPS2	28	92	59	31	39	41
	TPS3	26	95	58	32	38	43
120	TPS1	20	108	59	29	36	53
	TPS2	30	89	59	31	41	38
	TPS3	28	92	58	32	39	41

¹: 600 to 855 seconds

²: Advance preemption warning time

6.2.3 Metric 3: Delay Results

For a given TPS algorithm, three factors influence vehicle delay: the advance preemption warning time, the pedestrian volume, and the train speed. These three factors were analyzed individually, as there is not any correlation between the factors. First, the effect of the TPS algorithm on intersection delay will be evaluated as a function of the APWT. Then, the effect of pedestrian volume on delay will be tested. Last, the effect of train speed on delay will be evaluated as a function of train classification.

6.2.3.1 Effect of TPS Algorithm

Similar to the preceding phase length analysis, it would be difficult to measure a statistically significant difference in vehicle delay between the different TPS algorithms over the 54-minute analysis period. This is because the TPS algorithms only impact the signal plan for a maximum of 85 seconds in the 54-minute analysis period. Therefore, the delay for a set time before and a set time after the preemption was used to analyze the effectiveness of the TPS algorithms. The TPS algorithms are initiated between 694 seconds and 763 seconds, and the preemption is terminated between 911 seconds and 1142 seconds. Consequently the delay comparison period selected began at 600 seconds and ended at 1320 seconds. This period included six cycles where at least one of these cycles occurs after the preemption ends.

Pedestrian Phase Active Scenario

The average delay and the graph of delay versus APWT during the delay comparison period (12 minutes) for the pedestrian phase active scenario are shown in Table 6-10 and Figure C-1 in Appendix C, respectively.

TABLE 6-10 Average Delay (Delay Comparison Period¹; Pedestrian Phase Active Scenario; and Fixed Train Arrival Time)

APWT ²	TPS0 (sec/veh)	TPS1 (sec/veh)	TPS2 (sec/veh)	TPS3 (sec/veh)
	54.7			
40		54.7	54.7	54.7
50		56.5	56.5	55.5
60		56.4	56.5	55.8
70		55.2	55.4	54.8
80		54.7	54.8	53.9
90		56.5	54.4	52.9
100		59.5	53.4	52.2*
110		61.7	53.2	52.0*
120		61.2	52.7	51.8*
Mean	54.7	57.4	54.6	53.7

¹: 600 to 1320 seconds

²: Advance Preemption Warning Time

*: Recommended APWT based on safety analyses

Bold: Minimum delay for each TPS algorithm

From Table 6-10, It can be seen that the average delay for the base case (TPS0) was 54.7 sec/veh. The average delay for the TPS1 algorithm across all the APWT scenarios was 57.4 sec/veh. The smallest average delay was 54.7 sec/veh and occurred at the APWT values of 40 and 80 seconds. However, for these APWT values, pedestrian phase truncations occurred in 90 and 5 out of the 90 preemption cases, respectively. When the TPS2 algorithm is used, the lowest average delay was 52.7 sec/veh and occurred at an APWT value of 120 seconds. However, pedestrian phase truncations occurred in 5 out of the 90 preemption cases. Table 6-10 also shows that once the APWT is longer than 80 seconds, the delay in the TPS3 algorithm decreases with an increase in APWT. The minimum delay for the TPS3 algorithm was 51.8 sec/veh at an APWT value of 120 seconds. The best TPS3 algorithm delay was 2.9, 2.9, and 0.9 seconds lower than the best delay identified for the TPS0, TPS1, and TPS2 algorithms, respectively.

It was hypothesized in Section 6.2.2 that the TPS3 algorithm provides the signal time more efficiently. Therefore, for this test bed, it can be concluded that the hypothesis is correct.

The above analyses also were conducted for the analysis period. The data can be found in Table C-3 and Figure C-2 in Appendix C, respectively. Similar results were found in that the delay decreased overall and the difference in delay between each scenario also decreased compared to the comparison period analysis. Therefore, it was relatively hard to evaluate the effect of each TPS algorithm and the APWT. These results are attributable to the relatively long analysis period compared to the duration of the TPS algorithms.

A pairwise comparison method was used to compare each pair among the four TPS algorithms for each APWT. In this dissertation, Duncan's multiple range test was performed and is conducted as follows (42):

- Step 1: Linearly order the k sample means.
 $k = 3$; For the comparison of the APWT value and the train group and
 $k = 4$; For the comparison of the TPS algorithms
- Step 2: Find the value of the least significant "studentized range," r_p , for each $p = 2, 3, \dots, k$. This value is given in the table developed by Duncan (42). In this table r denotes the number of degrees of freedom associated with MS_E , the error mean square in the original analysis of variance.
- Step 3: For each $p = 2, 3, \dots, k$ find the shortest or least significant range, SSR_p . This value is given by Equation 6-4.

$$SSR_p = r_p \sqrt{\frac{MS_E}{n}} \quad (6-4)$$

where;

MS_E = Error mean square in the original analysis of variance; and

n = Sample size (90 in this dissertation).

Step 4: Consider any subset of p adjacent sample means. Let $|\bar{Y}_i - \bar{Y}_j|$ denote the range of the means in this subgroup. The population means, of span p , μ_i and μ_j are considered to be different if

$$|\bar{Y}_i - \bar{Y}_j| > SSR_p$$

The experimentwise error rate was set to 0.06, which means that the common level of significance per test is 0.01. The results of the delay comparison period for the pedestrian phase active scenarios are shown in Table 6-11. The table only shows the test results having a statistical difference between the TPS algorithms. That is, only 12 out of a possible 54 pairings were found to have statistically significant differences in mean delay.

It was found that the delay in the TPS3 algorithm is smaller than the delay in the TPS1 for the APWT values of 90, 100, 110, and 120 seconds. For the APWT values of 110 and 120 seconds, the delay in the TPS3 algorithm is smaller than the delay in the TPS0 algorithm. Once the APWT is equal to or greater than 90 seconds, the TPS3 algorithm has a positive impact on the intersection delay. Therefore, it can be concluded that for the pedestrian phase active scenarios the TPS3 algorithm with an APWT value of 90, 100, 110, or 120 seconds is the best operational strategy in terms of efficiency.

TABLE 6-11 Results of Duncan Test between TPS Algorithms (Delay Comparison Period¹; Pedestrian Phase Active Scenario; Fixed Train Arrival Time; and Pooled Test)

APWT ²	Algorithm Comparison		Mean (sec/veh)		Test Statistic	Critical Value	Result
	Algo.1	Algo.2	Algo.1	Algo.2			
90	TPS3	TPS1	52.9	56.5	3.66	2.81	Reject H ₀ ³
100	TPS3	TPS1	52.2	59.5	7.24	2.84	Reject H ₀
	TPS2	TPS1	53.4	59.5	6.04	2.76	Reject H ₀
	TPS0	TPS1	54.7	59.5	4.73	2.65	Reject H ₀
110	TPS3	TPS1	52.0	61.7	9.75	2.77	Reject H ₀
	TPS3	TPS0	52.0	54.7	2.79	2.69	Reject H ₀
	TPS2	TPS1	53.2	61.7	8.53	2.69	Reject H ₀
	TPS0	TPS1	54.7	61.7	6.96	2.58	Reject H ₀
120	TPS3	TPS1	51.8	61.2	9.46	2.77	Reject H ₀
	TPS3	TPS0	51.8	54.7	2.98	2.69	Reject H ₀
	TPS2	TPS1	52.7	61.2	8.55	2.69	Reject H ₀
	TPS0	TPS1	54.7	61.2	6.49	2.58	Reject H ₀

¹: 600 to 1320 seconds

²: Advance preemption warning time

³: Statistically different between two means at 0.01 level of significance

Pedestrian Phase Inactive Scenario

For the pedestrian phase inactive scenario, the safety problem caused by the truncation of the pedestrian clearance phase will not occur. However, the TPS3 algorithm may have a benefit in terms of delay. The average delay and the graphs of delay versus the APWT during the delay comparison period for the pedestrian phase inactive scenario are shown in Table 6-12 and Figure C-3 in Appendix C, respectively.

TABLE 6-12 Average Delay (Delay Comparison Period¹; Pedestrian Phase Inactive Scenario; and Fixed Train Arrival Time)

APWT ²	TPS0 (sec/veh)	TPS1 (sec/veh)	TPS2 (sec/veh)	TPS3 (sec/veh)
	49.7			
40		49.7	49.7	49.7
50		51.2	51.2	50.6
60		50.5	50.6	50.6
70		48.9	49.0	49.4
80		48.2	48.4	48.4
90		47.7	47.7	47.3
100		48.2	47.5	46.8
110		49.8	47.8	46.9
120		50.2	47.6	47.1
Mean	49.7	49.4	48.8	48.5

¹: 600 to 1320 seconds

²: Advance preemption warning time

Bold: Minimum delay for each TPS algorithm

When the preemption is operated for the base case (TPS0), the average delay was 49.7 sec/veh. When the preemption was operated with the TPS1 algorithm, the minimum average delay was 47.7 sec/veh, which occurred at an APWT value of 90 seconds. When the preemption was operated with the TPS2 algorithm, the minimum average delay was 47.5 sec/veh, which occurred at an APWT value of 100 seconds. When the TPS3 algorithm was applied with an APWT value of 100 seconds, the average delay was 46.8 sec/veh. This was the lowest value of the nine APWT values tested. Therefore, the best TPS3 algorithm delay was 2.9, 0.9, and 0.7 seconds lower than the best delay identified for the TPS0, TPS1, and TPS2 algorithms, respectively.

The above analyses also were conducted for the analysis period. The data can be found in Table C-5 and Figure C-4 in Appendix C, respectively. Similar results were found in that the delay decreased overall and the difference in delay between each scenario also decreased compared to the comparison period analysis. Therefore, it was relatively hard

to evaluate the effect of each TPS algorithm and the APWT. These results are attributed to relatively long analysis periods compared to the duration of the TPS algorithms.

Similar to before, Duncan's multiple range test was used to compare the four TPS algorithms for each APWT value. The experimentwise error rate was set to 0.06, which means that the common level of significance per test is 0.01. The results of the delay comparison period for the pedestrian phase inactive scenario are shown in Table 6-13. The table only shows the test results that had a statistically significant difference between the TPS algorithms. Only four comparisons, out of a possible 54, were found to have statistically significant differences in means.

TABLE 6-13 Results of Duncan Test between TPS Algorithms (Delay Comparison Period¹; Pedestrian Phase Inactive Scenario; Fixed Train Arrival Time; and Pooled Test)

APWT ²	Algorithm Comparison		Mean (sec/veh)		Test Statistic	Critical Value	Result
	Algo.1	Algo.2	Algo.1	Algo.2			
100	TPS3	TPS0	46.8	49.7	2.89	2.84	Reject H ₀ ³
110	TPS3	TPS1	46.9	49.8	2.86	2.77	Reject H ₀
	TPS3	TPS0	46.9	49.7	2.81	2.69	Reject H ₀
120	TPS3	TPS1	47.1	50.2	3.05	2.77	Reject H ₀

¹: 600 to 1320 seconds

²: Advance preemption warning time

³: Statistically different between two means at 0.01 level of significance

It was found that the TPS3 algorithm delay was smaller than the TPS0 algorithm delay for the APWT values of 100 and 110 seconds. In addition, for the APWT values of 110 and 120 seconds, the TPS3 algorithm delay was smaller than the TPS1 algorithm delay. Therefore, under certain circumstances the TPS3 algorithm does provide statistically better delay values than the state-of-the-practice approaches. However, for the no-pedestrian case this only occurred for four out of the 54 scenarios examined.

Paired Test

The above analyses showed some statistical difference between the TPS algorithms at an aggregate level. To test the relationship further, a paired t-test was used for the results of each train. To illustrate the rationale behind this approach, 10 trains were chosen. Table 6-14 shows the delay for 10 trains for the pedestrian phase active scenario with an APWT value of 120 seconds.

TABLE 6-14 Delays during the Comparison Period (APWT of 120 Seconds; Pedestrian Phase Active Scenario; and Fixed Train Arrival Time)

Train	TPS0 (sec/veh)	TPS1 (sec/veh)	TPS2 (sec/veh)	TPS3 (sec/veh)
1	56.8	65.9	65.9	61.4
2	47.8	57.3	48.2	47.3
3	75.6	83.6	72.2	70.3
4	100	106	88	92.4
5	54.6	66.6	51.8	51.4
6	50.9	65.5	51.4	49.6
7	81.1	80.1	67.7	70.5
8	67.4	79.4	62.3	60.5
9	80.7	87.7	80.1	78.6
10	59.9	58.4	61.2	55.9

For example, while the intersection delay for Train 4 is 100, 106, 88, and 92.4 sec/veh for the TPS0, TPS1, TPS2, and TPS3 algorithms, respectively, the intersection delay for Train 5 is 54.6, 66.6, 51.8, and 51.4 sec/veh for the TPS0, TPS1, TPS2, and TPS3 algorithms, respectively. That is, the difference in delay between TPS algorithms for a given train is much less than the difference between Train 4 and Train 5. In this case, when the delay between two TPS algorithms is compared, the difference between Train 4 and Train 5 significantly affected the comparison results under the pooled test. However, in this analysis the difference between paired observations rather than the variance within each sample is more interesting. Pairing typically reduces variability

that might obscure significant difference (43). Therefore, a paired t-test is appropriate for this simulation design.

Because there are four treatments, which are four different TPS algorithms, in this simulation study, the block design, which is an extension of the paired t-test, was employed such that each train is considered as a block. Duncan's multiple range test also was applied to compare each pair combination of the four TPS algorithms for each value of the APWT. Note that all further statistical comparisons in the following sections were performed using a block design.

Pedestrian Phase Active Scenario

The experimentwise error rate was set to 0.06, which means that the common level of significance per test is 0.01. The result of the delay comparison period for the pedestrian phase active scenario is shown in Table 6-15. The table only shows the test results that have a statistically significant difference between the TPS algorithms. It can be seen that 27 out of the 54 combinations were found to be statistically significant. Because the paired test is a stronger test, more differences between the TPS algorithms were detected compared to the pooled test as expected. The average percent difference between the algorithms was 3.6 percent and this corresponded to an average absolute difference in delay of 2.1 seconds for all pairs. For the pairs having a statistically significant difference, the average percent difference between the algorithms was 6.4 percent and this corresponded to an average absolute difference in delay of 3.8 seconds.

TABLE 6-15 Results of Duncan Test between TPS Algorithms (Delay Comparison Period¹; Pedestrian Phase Active Scenario; and Fixed Train Arrival Time)

APWT ²	Algorithm Comparison		Mean (sec/veh)		Test Statistic	Critical Value	Result
	Algo.1	Algo.2	Algo.1	Algo.2			
50	TPS0	TPS1	54.7	56.5	1.71	0.86	Reject H ₀ ³
	TPS0	TPS2	54.7	56.5	1.71	0.84	Reject H ₀
	TPS3	TPS1	55.5	56.5	0.93	0.84	Reject H ₀
	TPS3	TPS2	55.5	56.5	0.93	0.81	Reject H ₀
60	TPS0	TPS2	54.7	56.5	1.72	1.06	Reject H ₀
	TPS0	TPS1	54.7	56.4	1.67	1.03	Reject H ₀
	TPS0	TPS3	54.7	55.8	1.09	0.99	Reject H ₀
90	TPS3	TPS1	52.9	56.5	3.66	1.48	Reject H ₀
	TPS3	TPS0	52.9	54.7	1.87	1.45	Reject H ₀
	TPS3	TPS2	52.9	54.4	1.54	1.39	Reject H ₀
	TPS2	TPS1	54.4	56.5	2.12	1.45	Reject H ₀
	TPS0	TPS1	54.7	56.5	1.79	1.39	Reject H ₀
100	TPS3	TPS1	52.2	59.5	7.24	1.44	Reject H ₀
	TPS3	TPS0	52.2	54.7	2.51	1.41	Reject H ₀
	TPS2	TPS1	53.4	59.5	6.04	1.41	Reject H ₀
	TPS0	TPS1	54.7	59.5	4.73	1.35	Reject H ₀
110	TPS3	TPS1	52.0	61.7	9.75	1.19	Reject H ₀
	TPS3	TPS0	52.0	54.7	2.79	1.16	Reject H ₀
	TPS3	TPS2	52.0	53.2	1.21	1.11	Reject H ₀
	TPS2	TPS1	53.2	61.7	8.53	1.16	Reject H ₀
	TPS2	TPS0	53.2	54.7	1.57	1.11	Reject H ₀
	TPS0	TPS1	54.7	61.7	6.96	1.11	Reject H ₀
120	TPS3	TPS1	51.8	61.2	9.46	1.17	Reject H ₀
	TPS3	TPS0	51.8	54.7	2.98	1.14	Reject H ₀
	TPS2	TPS1	52.7	61.2	8.55	1.14	Reject H ₀
	TPS2	TPS0	52.7	54.7	2.07	1.09	Reject H ₀
	TPS0	TPS1	54.7	61.2	6.49	1.09	Reject H ₀

¹: 600 to 1320 seconds

²: Advance preemption warning time

³: Statistically different between two means at 0.01 level of significance

It was found that the delay in the TPS3 algorithm was statistically smaller than the delay in the TPS0 and TPS1 algorithms for the APWT values of 90, 100, 110, and 120

seconds. At the APWT values of 50, 90, and 110 seconds, the delay in the TPS3 algorithm was statistically smaller than the delay in the TPS2 algorithm.

As discussed in Section 6.2.1, the best values of the APWT from a safety perspective were 100, 110, and 120 seconds. It was found that there is no difference statistically at the 0.03 level of significance in delay among these values. Therefore, it can be concluded that the TPS3 algorithm with APWT values of among 100, 110, and 120 seconds provide the same level of safety and delay.

A comparison among the best delays identified for each of the TPS algorithms also was performed. It was found that the best delay in the TPS3 algorithm was statistically smaller than both the delay in the TPS0 algorithm and the best delay identified for the TPS1 algorithm at the 0.06 level of significance.

It was found that for the delay comparison period, the delay for the TPS3 algorithm with the APWT values of 100, 110, or 120 seconds was less than the delay for the TPS0 algorithm and the best delay identified for the TPS1 algorithm. That is, when the TPS3 algorithm is applied with an APWT value of 120 seconds, there was an improvement of 2.9 sec/veh (or 5.4 percent reduction) compared to the TPS0 and TPS1 algorithms. Therefore, it can be concluded that for the pedestrian phase active scenario the TPS3 algorithm with the APWT value of 100, 110, or 120 seconds is the best operation strategy in terms of both safety and efficiency.

The above analyses also were conducted for the analysis period. The results can be found in Table C-4 in Appendix C. As expected, it was found that while similar results were found, there are fewer statistically significant differences between the TPS algorithms.

Pedestrian Phase Inactive Scenario

The results of the delay comparison period for the pedestrian phase inactive scenario are shown in Table 6-16. The table shows only the test results that have a statistically significant difference between TPS algorithms. That is, only 21 pairs out of a possible 54 were found to be statistically significant.

TABLE 6-16 Results of Duncan Test between TPS Algorithms (Delay Comparison Period; Pedestrian Phase Inactive Scenario; and Fixed Train Arrival Time)

APWT ²	Algorithm Comparison		Mean (sec/veh)		Test Statistic	Critical Value	Result
	Algo.1	Algo.2	Algo.1	Algo.2			
50	TPS0	TPS1	49.7	51.2	1.47	0.81	Reject H ₀ ³
	TPS0	TPS2	49.7	51.2	1.47	0.79	Reject H ₀
	TPS0	TPS3	49.7	50.6	0.82	0.76	Reject H ₀
80	TPS1	TPS0	48.2	49.7	1.50	0.96	Reject H ₀
	TPS2	TPS0	48.4	49.7	1.33	0.94	Reject H ₀
	TPS3	TPS0	48.4	49.7	1.32	0.90	Reject H ₀
90	TPS3	TPS0	47.3	49.7	2.48	0.84	Reject H ₀
	TPS2	TPS0	47.7	49.7	2.06	0.82	Reject H ₀
	TPS1	TPS0	47.7	49.7	2.01	0.78	Reject H ₀
100	TPS3	TPS0	46.8	49.7	2.89	0.81	Reject H ₀
	TPS3	TPS1	46.8	48.2	1.41	0.79	Reject H ₀
	TPS2	TPS0	47.5	49.7	2.23	0.79	Reject H ₀
	TPS1	TPS0	48.2	49.7	1.48	0.76	Reject H ₀
110	TPS3	TPS1	46.9	49.8	2.86	1.07	Reject H ₀
	TPS3	TPS0	46.9	49.7	2.81	1.04	Reject H ₀
	TPS2	TPS1	47.8	49.8	2.00	1.04	Reject H ₀
	TPS2	TPS0	47.8	49.7	1.95	1.00	Reject H ₀
120	TPS3	TPS1	47.1	50.2	3.05	1.06	Reject H ₀
	TPS3	TPS0	47.1	49.7	2.60	1.03	Reject H ₀
	TPS2	TPS1	47.6	50.2	2.58	1.03	Reject H ₀
	TPS2	TPS0	47.6	49.7	2.13	0.99	Reject H ₀

¹: 600 to 1320 seconds

²: Advance preemption warning time

³: Statistically different between two means at 0.01 level of significance

It was found that the delay in the TPS3 algorithm is 1) smaller than the delay in the TPS0 algorithm at the APWT values of 80, 90, 100, 110, and 120 seconds and 2) smaller than the delay in the TPS1 algorithm at the APWT values of 100, 110, and 120 seconds.

A comparison among the best delays identified for each of TPS algorithms also was performed. It was found that the best delay in the TPS3 algorithm was statistically smaller than both the delay for the TPS0 algorithm and the best delay identified for the TPS1 algorithm at the 0.06 level of significance.

During the delay comparison period the delay in the TPS3 algorithm with an APWT value of 100 seconds decreased compared to the delay for the TPS0 and the best delay identified for the TPS1 algorithm. Therefore, it can be concluded that for the pedestrian phase inactive scenario the TPS3 algorithm with an APWT value of 100 seconds is the best operation strategy for efficiency. Therefore, the conclusion mentioned previously that the TPS3 algorithm has a benefit compared to the other TPS algorithms even at the condition where there is no safety problem originally was confirmed again.

The above analyses also were conducted for the analysis period. The results can be found in Table C-6 in Appendix C. As expected, it was found that while similar results were found, fewer statistically significant differences between the TPS algorithms were detected.

6.2.3.2 Effect of Pedestrians

During the delay comparison period, the average delays were 54.7, 57.4, 54.6, and 53.7 sec/veh for the TPS0, TPS1, TPS2, and TPS3 algorithms in the pedestrian phase active scenario, respectively, as shown in Table 6-10. However, in the pedestrian phase inactive scenario delay decreased to 49.7, 49.4, 48.8, and 48.5 sec/veh for the TPS0, TPS1, TPS2, and TPS3 algorithms, respectively, as shown in Table 6-12.

During the analysis period, the average delays were 50.9, 51.9, 50.9, and 50.8 sec/veh for the TPS0, TPS1, TPS2, and TPS3 algorithms in the pedestrian phase active scenario, respectively, as shown in Table C-3 in Appendix C. However, in the pedestrian phase inactive scenario delay decreased to 42.5, 42.5, 42.3, and 42.3 sec/veh for the TPS0, TPS1, TPS2, and TPS3 algorithms, respectively, as shown in Table C-5 in Appendix C. These results show that the delay decreases by approximately 5 to 15 percent compared to the delay comparison period.

To check statistically the difference between the pedestrian volume levels, a paired t-test was performed at the 0.05 level of significance. The null hypotheses and alternative hypotheses were set as $H_0: \text{Delay}_{400\text{ped/h}} = \text{Delay}_{0\text{ped/h}}$ and $H_1: \text{Delay}_{400\text{ped/h}} > \text{Delay}_{0\text{ped/h}}$, respectively, for both the delay comparison period and the analysis period. The results for both the analysis period and the delay comparison period are shown in Table 6-17.

TABLE 6-17 Results of Paired t-Test between Two Pedestrian Scenarios (Pedestrian Phase Active Scenario vs. Pedestrian Phase Inactive Scenario) for Fixed Train Arrival

	Pedestrian Scenario Comparison		Mean (sec/veh)		Test Statistic	Critical Value	Result
			400 ped/h	0 ped/h			
Comparison Period ¹	400 ped/h	0 ped/h	55.2	48.9	70.97	1.96	Reject H_0 ³
Analysis Period ²	400 ped/h	0 ped/h	51.2	42.4	92.53	1.96	Reject H_0

¹: 600 to 1320 seconds

²: 6 to 60 minutes

³: Statistically different between two means at 0.05 level of significance

It is concluded that the delay in the simulation with the pedestrian phase active scenario is greater than the delay in the simulation with the pedestrian phase inactive scenario for both the delay comparison period and analysis period. These results confirm the fact

that pedestrians can increase the average delay experienced by vehicles at the intersection.

The difference in results for the two pedestrian scenarios is mainly caused by the right-turning vehicles, as shown in Tables 6-18 and 6-19, because the right-turning vehicles must yield to pedestrians. Through vehicles using the shared lane who are behind the right-turning vehicles also are affected by the right-turning vehicles. The detailed delay results depending on the APWT also are shown in Tables C-7 and C-8 in Appendix C.

TABLE 6-18 Average Delay of Each Movement During Analysis Period¹ for Pedestrian Phase Active Scenario and Fixed Train Arrival Time

T P S	Southbound (sec/veh)				Eastbound (sec/veh)				Northbound (sec/veh)				Westbound (sec/veh)				TOT AL
	LT	T H	R T	S U M	L T	T H	R T	S U M	L T	T H	R T	S U M	L T	T H	R T	S U M	
0	115	34	41	59	49	60	66	60	50	31	34	35	59	58	15	48	50.9
1	113	34	41	58	51	63	69	63	50	31	34	34	61	61	15	51	51.9
2	112	34	41	58	50	61	67	61	50	31	34	34	59	58	15	49	50.9
3	113	34	41	58	50	61	67	61	49	31	34	34	58	58	15	48	50.8

¹: 6 to 60 minutes

TABLE 6-19 Average Delay of Each Movement During Analysis Period¹ for Pedestrian Phase Inactive Scenario and Fixed Train Arrival Time

T P S	Southbound (sec/veh)				Eastbound (sec/veh)				Northbound (sec/veh)				Westbound (sec/veh)				TOT AL
	LT	T H	R T	S U M	L T	T H	R T	S U M	L T	T H	R T	S U M	L T	T H	R T	S U M	
0	68	33	33	44	44	49	43	47	47	30	26	32	58	57	10	46	42.5
1	68	33	32	43	45	49	43	48	46	30	26	32	58	57	10	46	42.5
2	68	33	33	44	44	49	43	47	45	30	26	32	57	56	10	46	42.3
3	68	33	33	43	44	49	43	47	45	30	26	32	57	56	10	46	42.3

¹: 6 to 60 minutes

In the southbound left-turn movement, the delay is considerably different for the two pedestrian scenarios. This result is not a direct effect of pedestrians in contrast to the right-turning movement situation. A difference in signal timing occurs during transition back to the normal mode. Because the first cycle after preemption is operated as fully actuated, the signal timing is very sensitive to the traffic volume and distribution. Intuitively, the difference in signal timing during this time period affects all following time periods. Moreover, the demand volume of the southbound left-turn movement was 308 veh/h and the capacity is about 250 veh/h during the coordinated mode. Therefore, this over-saturation condition increases the delay for the left-turning movement by approximately 9 sec/veh.

6.2.3.3 *Effect of Train Speed Profile*

Pedestrian Phase Active Scenario

The average delay by train speed groups is shown in Table 6-20 during the delay comparison period for the pedestrian phase active scenario. Detailed results of the average delay as a function of the APWT also are shown in Table C-9 in Appendix C.

TABLE 6-20 Average Delay by Train Group (Delay Comparison Period¹; Pedestrian Phase Active Scenario; and Fixed Train Arrival Time)

	Train Group	TPS0 (sec/veh)	TPS1 (sec/veh)	TPS2 (sec/veh)	TPS3 (sec/veh)	Average
Average By Group	Group 1	60.4	64.6	61.5	60.0	61.6
	Group 2	53.9	56.2	53.0	52.4	53.9
	Group 3	49.9	51.4	49.3	48.9	49.9
Average		54.7	57.4	54.6	53.7	55.1

¹: 600 to 1320 seconds

In all of the TPS algorithms, Group 3 has the smallest average delay at 49.9 sec/veh and Group 1 has the largest average delay of 61.6 sec/veh. The difference in delay between Group 1 and Group 3 was 10.5 sec/veh for the TPS0 algorithm, 13.2 sec/veh in the TPS1 algorithm, 12.2 sec/veh in the TPS2 algorithm, and 11.1 sec/veh in the TPS3 algorithm for the pedestrian phase active scenario. For the delay comparison period, the delay of Group 2 is much smaller than that of Group 1, unlike the analysis period.

To check statistically the difference among the train speed groups, Duncan's multiple range test was performed. The experimentwise error rate was set to 0.03, which means that the common level of significance per test is 0.01. The results are shown in Table 6-21.

TABLE 6-21 Results of Duncan Test between Train Speed Groups (Delay Comparison Period¹; Pedestrian Phase Active Scenario; and Fixed Train Arrival Time)

Group Comparison		Mean (sec/veh)		Test Statistic	Critical Value	Result
		1 st Group	2 nd Group			
Group3	Group1	49.9	62.0	12.09	1.14	Reject H ₀ ²
Group3	Group2	49.9	53.9	3.98	1.09	Reject H ₀
Group2	Group1	53.9	62.0	8.12	1.09	Reject H ₀

¹: 600 to 1320 seconds

²: Statistical different between two means at 0.01 level of significance

H₀: Delay_{group i} = Delay_{group j} (i≠j, where, i=1,2 and j=2,3)

It was found that the delay in Group 3 is statistically smaller than the delay in Groups 1 and 2 at the 0.01 level of significance, and that the delay in Group 2 is statistically smaller than the delay in Group 1 at the 0.01 level of significance.

Safety also was evaluated for the train speed. The number of pedestrian phase truncations and average abbreviation time at the onset of preemption by each train speed group also were evaluated as shown in Table 6-22.

TABLE 6-22 Number of Pedestrian Phase Truncations and Average Phase Abbreviation Time at the Onset of Preemption by Train Speed Group for Pedestrian Phase Active Scenario and Fixed Train Arrival Time

AP WT ¹	TPS0 (sec/veh)			TPS1 (sec/veh)			TPS2 (sec/veh)			TPS3 (sec/veh)		
	G1 ²	G2 ³	G3 ⁴	G1	G2	G3	G1	G2	G3	G1	G2	G3
	30 (6)	30 (7)	30 (6)									
40				30 (6)	30 (7)	30 (6)	30 (6)	30 (7)	30 (6)	30 (6)	30 (7)	30 (6)
50				21 (6)	27 (7)	29 (6)	21 (6)	27 (7)	29 (6)	25 (6)	29 (7)	30 (6)
60				15 (5)	20 (7)	24 (6)	15 (5)	20 (7)	24 (6)	21 (6)	27 (7)	28 (6)
70				4 (6)	5 (8)	9 (6)	4 (6)	5 (8)	9 (6)	11 (5)	14 (7)	20 (5)
80				1 (10)	2 (8)	2 (4)	1 (10)	2 (8)	2 (4)	2 (2)	4 (8)	8 (6)
90				1(6)	3(3)	0(0)	1(6)	3(3)	0(0)	0(0)	0(0)	1(6)
100				1(6)	3(3)	0(0)	1(6)	3(3)	0(0)	0(0)	0(0)	0(0)
110				0(0)	0(0)	1(3)	1(6)	3(3)	1(3)	0(0)	0(0)	0(0)
120				0(0)	0(0)	1(3)	1(6)	2(2)	2(2)	0(0)	0(0)	0(0)

¹: Advance preemption warning time

²: Train group 1

³: Train group 2

⁴: Train group 3

For the TPS0 algorithm, a truncation occurred in every train group and the average abbreviation time of the pedestrian clearance phase was approximately 6 seconds. Therefore, it can be concluded that unlike the effect of the train speed groups on delay, safety was not affected by train speed at FM 2818 under the normal preemption operation.

The number of truncations is the highest in Group 3 for the TPS1, TPS2, and TPS3 algorithms when the APWT is less than 90 seconds. Therefore, it can be concluded that the probability of truncations increases as train speed increases in the low region of the APWT. However, as the APWT increases, the effect of train speed on truncation

decreases for all TPS algorithms. That is, truncations occurred regardless of the train speed groups for the TPS1 and TPS2 algorithms. Therefore, it can be concluded that the safety of the intersection is not affected by the train speed once an APWT is equal to or greater than 90 seconds.

The above analyses also were conducted for the analysis period. It was found that even though the delay of each group was not as great compared to the delay comparison period, the results of the comparison were similar. But it was found that there was no statistically significant difference between Group 1 and Group 2. Detailed results can be found in Tables C-10, C-11, and C-12 in Appendix C.

Pedestrian Phase Inactive Scenario

The effect of train speed also was evaluated when there is no pedestrian in the intersection. The average delay by train speed groups during the delay comparison period for the pedestrian phase inactive scenario is shown in Table 6-23. The detailed result of the average delay depending on the APWT also is shown in Table C-13 in Appendix C.

TABLE 6-23 Average Delay by Group (Delay Comparison Period¹; Pedestrian Phase Inactive Scenario; and Fixed Train Arrival Time)

	Train Group	TPS0 (sec/veh)	TPS1 (sec/veh)	TPS2 (sec/veh)	TPS3 (sec/veh)	Average (sec/veh)
Average By Group	Group 1	55.6	55.5	55.4	54.8	55.2
	Group 2	49.1	48.2	47.3	47.4	47.7
	Group 3	44.6	44.4	43.8	43.5	43.9
Average		49.7	49.4	48.8	48.5	49.1

¹: 600 to 1320 seconds

It can be seen that for all the TPS algorithms, Group 3 has the smallest delay with an average 43.9 sec/veh and Group 1 has the largest delay with an average delay of 55.2 sec/veh. The difference in delay between Group 1 and Group 3 was 11.0 sec/veh in the TPS0 algorithm, 11.1 sec/veh in the TPS1 algorithm, 11.6 sec/veh in the TPS2 algorithm, and 11.3 sec/veh in the TPS3 algorithm for the pedestrian phase active scenario. For the delay comparison period, the delay of Group 2 is much smaller than that of Group 1, unlike the analysis period. Therefore, it can be concluded that the effect of train speed decreases as time increase.

To check statistically the difference among the train speed groups, Duncan's multiple range test also was performed. Experimentwise error rate was set to 0.03, which means that the common level of significance per test is 0.01. The result is shown in Table 6-24.

TABLE 6-24 Results of Duncan Test between Train Speed Groups (Delay Comparison Period¹; Pedestrian Phase Inactive Scenario; and Fixed Train Arrival Time)

Group Comparison		Mean (sec/veh)		Test Statistic	Critical Value	Result
		1st Group	2 nd Group			
Group3	Group1	43.9	55.2	11.31	1.04	Reject H ₀ ²
Group3	Group2	43.9	47.7	3.78	1.00	Reject H ₀
Group2	Group1	47.7	55.2	7.53	1.00	Reject H ₀

¹: 600 to 1320 seconds

²: Statistically different between two means at 0.01 level of significance

It was found that the delay in Group 3 is statistically smaller than the delay in Groups 1 and 2 at the 0.01 level of significance, and that the delay in Group 2 is statistically smaller than the delay in Group 1 at the 0.01 level of significance.

Intuitively, delay is affected by the time the train is blocking the crossing, and the blocking time is affected by the train speed. That is, as train speed decreases the blocking time increases and then the delay will increase. To evaluate the relationship between the delay and the blocking time, the blocking time was measured using train speed and train length. Average train speed, average train length, and average blocking time by each group are shown in Table 6-25.

TABLE 6-25 Average Train Speed, Average Train Length, and Average Blocking Time by Each Train Group

Train Group	Train Speed (km/h)	Train Length (m)	Blocking Time (s)
Group 1	30	1284	161
Group 2	41	1523	136
Group 3	51	1625	116
Average	41	1477	138

It was found that the blocking time was the smallest in Group 3. Therefore, it is reasonable that the delay of Group 3 was the smallest. Therefore, it can be concluded that the delay is affected more by blocking time than the TPS algorithms.

The above analyses also were conducted for the analysis period. It was found that even though the delay of each group was not as great compared to the delay comparison period, the results of the comparison were same. Detailed results can be found in Tables C-14, C-15, and C-16 in Appendix C.

6.2.3.4 Preemption Trap

In terms of the crossing safety, the preempt trap should not occur. That is, the track clearance green should end after the warning lights start to flash. For this safety metric, the end times of the track clearance green were collected from the simulations. The warning lights start to flash 25 seconds before a train arrives at the crossing. The gate

starts to descend after 4 seconds of the gate delay time. In the simulation the yield sign was used to emulate both the warning lights and the gate. Therefore, it was assumed that the warning lights start to flash 25 seconds before a train arrives at the crossing. The train arrival times were collected from the simulations. Twenty-five seconds were extracted from the train arrival times to obtain the start time of the warning lights. The preempt trap was calculated as the start time of the warning lights minus the end times of the track clearance green as shown in Equation 6-5.

$$\Sigma = \Psi - \Xi \quad (6-5)$$

where;

- Σ = Preempt trap interval;
- Ψ = Start time of warning lights; and
- Ξ = End times of the track clearance green.

If the preempt trap interval is positive, the preempt trap occurs. For the TPS0, TPS1, TPS2, and TPS3 algorithms under both the fixed train arrival time scenario and random train arrival time scenario, there was no preemption trap. Therefore, it can be concluded that the TPS3 algorithm does not affect the preemption trap.

6.3 SIMULATION RESULTS AND FINDINGS WITH RANDOM TRAIN ARRIVAL

6.3.1 Truncation of Pedestrian Clearance Interval

In Section 6.2, all simulations were designed so that the traffic signal controller is preempted by a train during a specific pedestrian clearance interval under the TPS0 algorithm. In other words, the study was designed to examine the worst case scenario. However, a preemption can be initiated at any time in the cycle. When a preemption is initiated at the period of the cycle that does not provide a pedestrian green/clearance phase, the truncation problem will never occur. Therefore, the signal can be operated safely without the need for the TPS algorithm in these situations.

In this section, simulations were performed under the same conditions as the previous section except that the trains arrive at the crossing randomly. A detailed description of this case is illustrated in Appendix D.

6.3.2 Results

All evaluations follow the process described in Section 6.2. It was found that the effect of the TPS3 algorithm on delay was almost the same. That is, at the best APWT values for each TPS algorithm, the difference in delay decreases only by 0.2 to 0.7 seconds compared to the fixed arrival time scenario. Therefore, in both situations the TPS3 algorithm produced a minimum delay. Therefore, no matter when a preemption is initiated during a cycle, the TPS3 algorithm can operate the intersection without safety problems and at the same time decrease the intersection delay. Detailed results for this case are illustrated in Appendix D.

6.4 BENEFIT/COST ANALYSIS

To evaluate the viability of the TPS3 algorithm, a benefit/cost analysis was performed. The equivalent annual cost, the net present worth of benefits, and the benefit/cost (B/C) ratio were calculated.

Capital cost elements included the Doppler radar detectors, the field hardened computer, the interface equipment, the communications processor, and software. The ongoing operation and maintenance costs also were considered. Both the equivalent annual cost and the net present worth for each element are shown in Table 6-26. It was assumed that the lifetime of all elements is 6 years, the salvage value is zero, and the interest rate is 6 percent.

TABLE 6-26 Elements of the TPS3 System and Its Cost

Items	EAC ¹	NPW ²
2x Doppler radar stations with communication: \$1,500 each	\$610	\$3,000
1x Central communication processor: \$1,000	\$203	\$1,000
1x Field hardened computer: \$1,500	\$305	\$1,500
Cabinet interface equipment: \$2,000	\$407	\$2,000
Operational and maintenance cost: \$50/mo	\$600	\$2,950
2x Software: \$2,000 each	\$813	\$4,000
Sum	\$2,939	\$14,450

¹: Equivalent annual cost

²: Net present worth

Net present worth of all elements except the operational and maintenance cost was converted to the equivalent annual costs using an interest rate of 6 percent per year because these elements have only the initial cost. The operational and maintenance cost, \$600, was used as the equivalent annual cost because the operational and maintenance cost occurs every year.

The equivalent annual costs of each element depending on interest rate are shown in Figure 6-10.

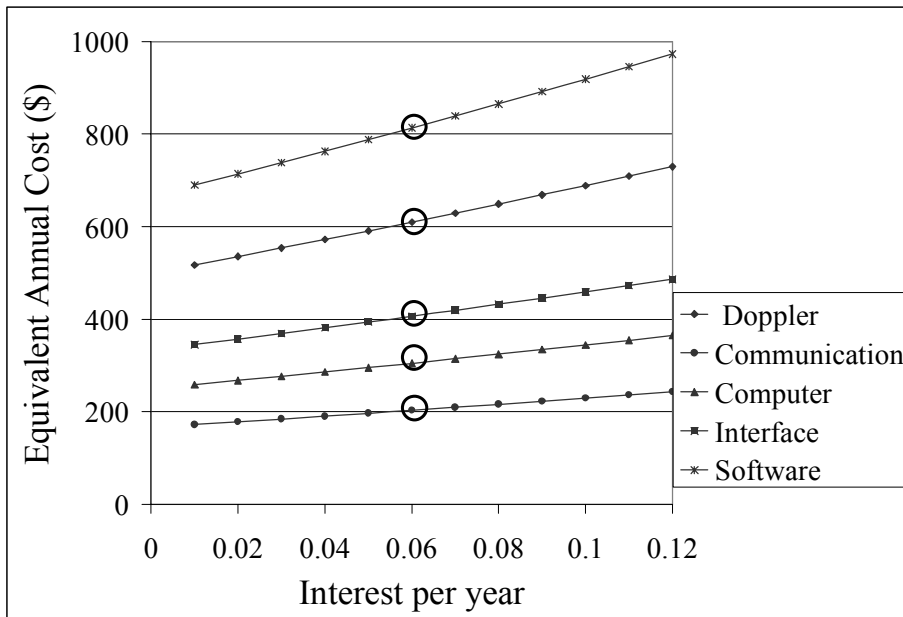


FIGURE 6-10 Equivalent Annual Cost of Each Element versus Interest Rate

It was found that as the interest rate increases the equivalent annual cost of each element increases. Therefore, assuming an interest rate of 6 percent per year, the equivalent annual cost of the system is \$2,939.

There are two types of benefit of the TPS3 system: 1) safety and 2) delay. First, the cost per accident was used to determine the annual safety benefit. To estimate the number of accidents, first the number of pedestrian phase truncations was estimated from the observed data at the test bed. The number of pedestrian phase truncations was estimated using the simulation study assuming random train arrival. While there is no pedestrian phase truncation under the TPS3 algorithm, 36 pedestrian phase truncations out of 90 trains (40 percent) occurred in the normal preemption condition as shown in Table D-1. When a pedestrian volume of 400 ped/h was used for simulation study, the pedestrian phase was active with 99.99 percent probability during the simulations. If the pedestrian volume decreases, the pedestrian phase may not be active at every cycle. Therefore, the pedestrian phase truncation may not occur in some cases. The probability that the

pedestrian phase is active at the onset of preemption was calculated assuming random arrival of pedestrians. The observed pedestrian volume at the test bed was 10 ped/h, and the train volume was approximately 50 trains/day. Therefore, the probability that the pedestrian phase is active was 0.28 and a total of 2044 ($= 50 \times 0.4 \times 0.28 \times 365$) pedestrian phase truncations will occur every year. The results are shown in Table 6-27.

TABLE 6-27 Calculation of Number of Pedestrian Phase Truncations

Trains /day	20
Probability that pedestrian phase truncation occurs	0.4
Probability that pedestrian phase is active at the onset of preemption	0.28
Truncations/day	2.2
Truncations/year	818

The comprehensive costs recommended for use by state and local highway and safety agencies was used as the accident cost for this analysis. The relationship between cost per injury and injury severity by K-A-B-C Scale are shown in Table 6-28 (44,45).

TABLE 6-28 Comprehensive Costs in Police-Reported Crashes by K-A-B-C Scale Severity (1994)

Severity	Descriptor	Cost Per Injury
K	Fatal	\$2,600,000
A	Incapacitating	\$180,000
B	Evident	\$36,000
C	Possible	\$19,000
PDO	Property Only Damage	\$2,000

Although as truncations increase the accidents increase, occurrence of pedestrian phase truncation does not necessarily mean accidents. Because the probability of an accident

occurring given a pedestrian phase truncation is unknown, a sensitivity analysis was performed. The probability ranged from 0.0001 to 0.1. The accident cost (benefit) was estimated as a function of the probability that accidents occur and the accident severity and the results values are shown in Table 6-29.

TABLE 6-29 Accident Cost Depending on the Probability of Accident and the Accident Severity

Pro. ¹	Num ²	Fatal (\$)	Incap. ³ (\$)	Evident (\$)	Possible (\$)	Property Only Damage (\$)	Cost (\$)
0.001	0.82	2,125,760 (723)	147,168 (50)	29,434 (10)	15,534 (5)	1,635 (0.56)	\$2,939
0.002	1.64	4,251,520 (1,447)	294,336 (100)	58,867 (20)	31,069 (11)	3,270 (1.11)	\$2,939
0.003	2.45	6,377,280 (2,170)	441,504 (150)	88,301 (30)	46,603 (16)	4,906 (1.67)	\$2,939
0.004	3.27	8,503,040 (2,893)	588,672 (200)	117,734 (40)	62,138 (21)	6,541 (2.23)	\$2,939
0.005	4.09	10,628,800 (3,617)	735,840 (250)	147,168 (50)	77,672 (26)	8,176 (2.78)	\$2,939
0.006	4.91	12,754,560 (4,340)	883,008 (300)	176,602 (60)	93,206 (32)	9,811 (3.34)	\$2,939
0.007	5.72	14,880,320 (5,064)	1,030,176 (351)	206,035 (70)	108,741 (37)	11,446 (3.89)	\$2,939
0.008	6.54	17,006,080 (5,787)	1,177,344 (401)	235,469 (80)	124,275 (42)	13,082 (4.45)	\$2,939
0.009	7.36	19,131,840 (6,510)	1,324,512 (451)	264,902 (90)	139,810 (48)	14,717 (5.01)	\$2,939
0.01	8.18	21,257,600 (7,234)	1,471,680 (501)	294,336 (100)	155,344 (53)	16,352 (5.56)	\$2,939

¹: Probability of accident when pedestrian phase truncation occurs

²: Number of accident/ year

³: Incapacitating

(): B/C ratio

The analysis resulted in a B/C ratio of 0.56 with a net benefit of \$1,635 under the most conservative scenario, that is, assuming a 0.1 percent probability of accident and property only damage. The B/C ratio increases as the accident probability and accident severity level increases. As an example, Figure 6-11 shows the change of B/C ratio depending on the probability of accident considering property only damage as the benefit.

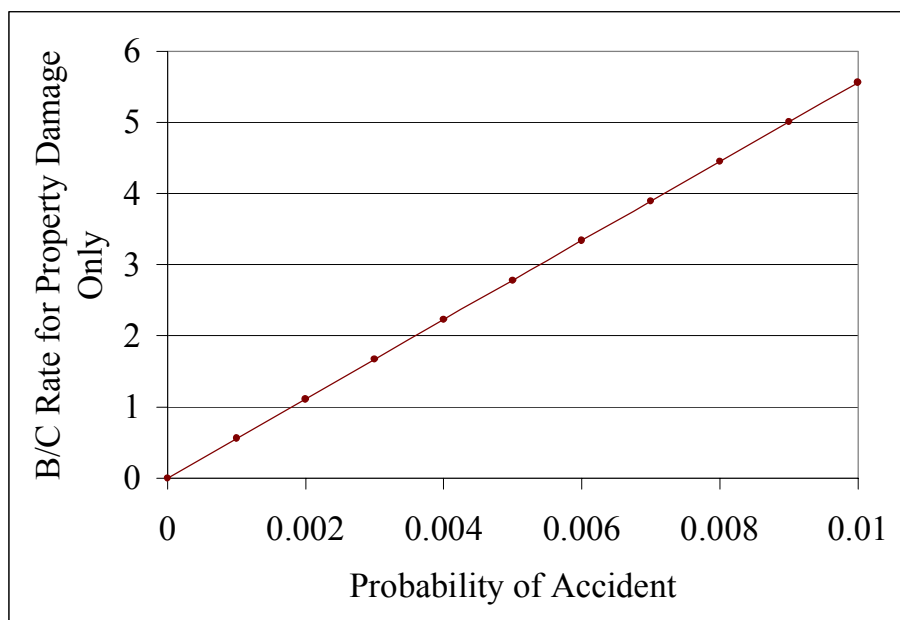


FIGURE 6-11 B/C Ratio Depending on the Probability of Accident Considering Property Only Damage as the Benefit

It was found that as the probability of accident increases, B/C ratio increases. The B/C ratio becomes 1 at a probability of accident of 0.0018. Therefore, when the probability of accident is more than 0.18 percent and property only damage is considered, the viability of the proposed system is validated.

From the simulation results, the intersection delay was reduced in the TPS3 algorithm as compared to the TPS0 algorithm (normal preemption method) for both the pedestrian phase active scenario and the pedestrian phase inactive scenario as shown in Tables C-7 and C-9. Thus, in addition to safety benefit from accident reductions, it can be expected that there is also intersection delay benefit with 10 ped/h. Rather than rerun the simulation for 10 ped/h, the delay was calculated using the 0 ped/h results. While this approach is conservative, it does not appreciably affect the final results.

The delay reduction of the simulation results with 0 ped/h (0.6 sec/veh) also was used to determine the annual delay benefit. When the average traffic volume of 50 observations at the test bed (2496 veh/h) is used for this analysis, the total delay savings is 3644 hours per year as shown in Table 6-30.

TABLE 6-30 Calculation of Annual Delay Reduced

Delay Reduced	0.6 sec/veh
Average Traffic Volume	2496 veh/h
Total Reduced Delay	1498 sec/hr
	0.42 hr/hr
	3644 hr/year

\$11.97 of the value of time recommended by the State of Texas TxDOT was used as the benefit of delay reduced for this analysis (46). The value of time was estimated by Speed Choice Model developed by Chui and McFarland of Texas Transportation Institute (47).

The benefit and B/C ratio is based on the value of time applied to analysis. The change of B/C ratio depending on the value of time is shown in Figure 6-12.

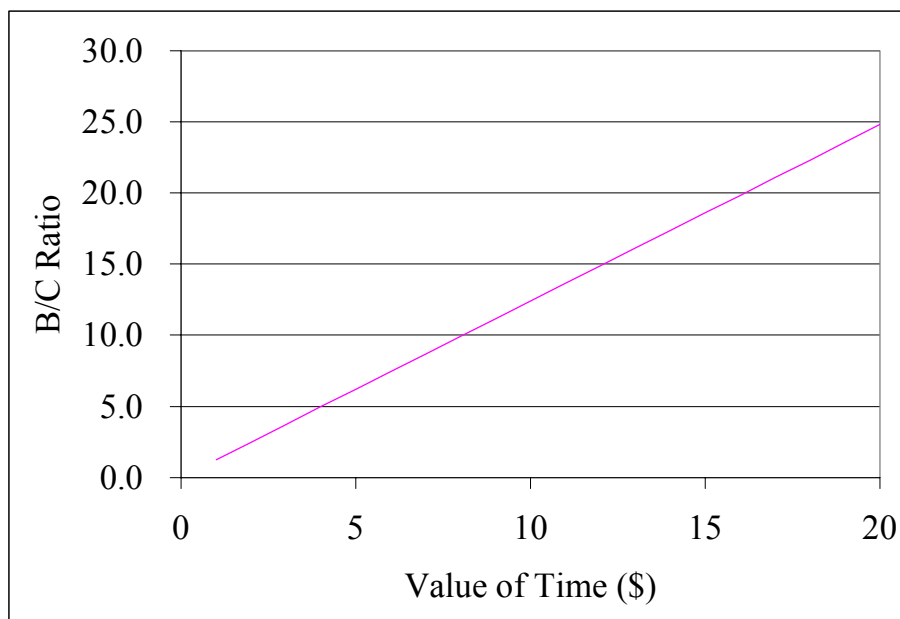


FIGURE 6-12 B/C Ratio versus Value of Time

It can be seen that the B/C ratio increases as the value of time increases. When \$11.97 of the value of time was used for this analysis, the annual delay benefit was \$43,623 (= 3644×11.97) per year. B/C ratio was 14.84 (= $43,623/2,939$) concerning only the benefit from delay savings. When the delay benefit is combined into the safety benefit, the B/C ratio increases by 14.84. Therefore, it can be concluded that it is appropriate to install the TPS3 system at this IHRGC. It is hypothesized that similar results will be found at any IHRGC where there are pedestrians present.

6.5 CONCLUDING REMARKS

6.5.1 TPS Algorithm

It was found that safety problems did not occur when the TPS3 algorithm was used with the APWT values of 100, 110, and 120 seconds. Therefore, it can be concluded that for this test bed, safety problems can be solved with the TPS3 algorithm. These results only apply to the test bed but the analysis methodology can be applied anywhere.

When the delay comparison period was analyzed, the delay increased overall and the difference in delay between each scenario also increased compared to the analysis period. Therefore, it was relatively easy to evaluate the effect of each TPS algorithm and the APWT. During the delay comparison period the delay in the TPS3 algorithm with an APWT value of 120 seconds was 5.4 percent lower than the delay for both the TPS0 and TPS1 algorithms. In addition, the TPS3 algorithm had zero truncation for the APWT values of 100, 110, and 120 seconds as compared to 90 and 1 truncations for the TPS0 and TPS1 algorithms. Therefore, it can be concluded for the pedestrian phase active scenario that the TPS3 algorithm with an APWT value of 100, 110, or 120 seconds is the best operation strategy for both safety and efficiency for the test bed.

For the pedestrian phase inactive scenario, it was concluded that the TPS3 algorithm with an APWT value of 100 or 110 seconds results in a lower delay compared to the TPS0 algorithm even when there are no pedestrian present.

6.5.2 Effect of Pedestrians

When the pedestrian volume was 400 ped/h, the average delays were 54.7, 57.4, 54.6, and, 53.7 sec/veh for the TPS0, TPS1, TPS2, and TPS3 algorithms, respectively. However, for the pedestrian phase inactive scenario, the average delay decreased to 49.7, 49.4, 48.8, and 48.5 sec/veh for the TPS0, TPS1, TPS2, and TPS3 algorithms, respectively. It is concluded based on the statistical test that the delay in the simulation with the pedestrian phase active scenario is greater than the delay in the simulation with the pedestrian phase inactive scenario for both the delay comparison and analysis periods. The difference is mainly caused by the right-turning vehicles because the right-turning vehicles must yield the right of way to the crossing pedestrians when the phases are served. Through vehicles using the shared lane with right-turning vehicles also were affected by the right-turning vehicles.

6.5.3 Effect of Train Speed Profile

When the delays were compared for each train speed group, Group 3 (fastest train group) had the smallest delay and Group 1 (slowest train group) had the largest delay for all TPS algorithms and both pedestrian phase active and pedestrian phase inactive scenarios. It was hypothesized that the difference in delay between train speed groups was caused by the difference in blocking time of the crossing for each train speed group. It was found that the blocking time was the smallest in Group 3 while Group 1 had the longest blocking time. It also was found that the difference in delay between train speed groups is much greater than the difference in delay between the TPS algorithms. Therefore, it can be concluded that the delay is affected more by the blocking time than the TPS algorithms. It also was concluded that the safety of the intersection is not affected by the train speed once an APWT is equal to or greater than 90 seconds.

6.5.4 Effect of Random Train Arrival

In the simulation under random train arrival conditions, the effect of the TPS3 algorithm on delay was almost the same. That is, in both situations the TPS3 algorithm produced a minimum delay. Therefore, no matter when a preemption is initiated during a cycle, the TPS3 algorithm can operate the intersection without safety problems while simultaneously decreasing the intersection delay.

6.5.5 Benefit/Cost Analysis

The TPS3 system has a safety benefit of \$1,635 and a delay benefit of \$43,623 per year assuming 0.1 percent probability of accident and property only damage. The estimated cost is \$2,939. Therefore, the B/C ratio is 15.4 ($= (1,635 + 43,623) / 2,939$). This ratio validated the viability of the proposed system. Therefore, it can be concluded that it is appropriate to install the TPS3 system at the IHRGC in the test bed. It is hypothesized that similar results will be found at any IHRGC where there are pedestrians present.

Lastly, if the TPS1 algorithm is used, it was found that the value of the APWT had a profound affect on the results. The optimal value for this test bed was found to be 110 and 120 seconds in terms of safety as compared to the default value of 70 seconds. Therefore, if a decision is made to use the older algorithm it would be best to identify the best APWT rather than assuming the default conditions. The optimization methodology developed in this dissertation can be applied for any location.

CHAPTER VII

CONCLUSIONS

7.1 SUMMARY

7.1.1 Prediction Algorithm

An artificial neural network (ANN) model was developed to predict the train arrival time because there exists a nonlinear relationship between train arrival time and the train speed. Because trains exhibit a wide range of behavior during detection, trains that have markedly different speed profiles may have the same arrival time. Because the modular ANN (MANN) approach first categorizes trains into groups having similar speed profiles, these characteristics of trains can be handled in a MANN. Therefore, the modular approach is appropriate to forecast the train arrival time in the study site. As the speed is updated, the accuracy of forecasting was improved in all methods overall.

Prediction intervals were obtained using a bootstrap method, because the ANN model is a non-parametric model. The prediction intervals were incorporated into a new TPS algorithm.

7.1.2 The Transition Preemption Strategy Algorithm

The current TPS algorithm provides a transition to preemption in a manner that could potentially endanger pedestrians and/or drivers because it does not account for the variability of predicted train arrival times. Therefore, even if the goal of TPS is to eliminate situations where the pedestrian clearance phase is truncated in an unsafe manner, its goal is not achieved successfully. While it is designed to reduce the truncation of minimum vehicle time and pedestrian clearance time before the normal preemption begins, it does not account for overall intersection performance.

In this dissertation, a new transition preemption algorithm that was specifically designed to improve the intersection performance while maintaining or improving the current level of safety was developed using an improved train arrival time prediction model.

7.2 CONCLUSIONS

7.2.1 Predicted Arrival Time

The current forecasting method assumes that the last observed speed will be constant until the train arrives at the crossing. It was found that this method had the highest forecasting error. The MANN approach is promising for train detection in that it provided an average 19.5 percent improvement over a standard ANN model, an average 29.7 percent improvement over a multiple linear regression model, and an average 46 percent improvement over the current method. While the last observed speed is used to predict the train arrival time in the current method and the MLR model, the trend of speed change is used as input to the ANN and MANN model. Therefore, it is concluded that the trend of speed change is a better explanatory variable than the last observed speed when forecasting train arrival time.

7.2.2 The Transition Preemption Strategy Algorithm

When the preemption is operated with TPS0, the truncation occurred 90 times out of 90 preemption cases for the simulation test bed. Therefore, the normal preemption operation is clearly dangerous when the train arrives during the pedestrian phase. When preemption is operated with the TPS1 and TPS2 algorithms, the pedestrian phase truncations still occurred 1 and 5 cases out of 90 preemptions, respectively, even though the advance preemption warning time of 120 seconds was used. For the TPS3 algorithm, the pedestrian phase truncations occurred until the advance preemption warning time reached 90 seconds. Therefore, the advance preemption warning time should be at least 100 seconds to eliminate the possibility of the pedestrian phase truncation.

When the delay comparison period was analyzed, the delay increased overall and the difference in delay between each scenario also increased compared to the analysis period. Therefore, it was relatively easy to evaluate the effect of each TPS algorithm and APWT. During the delay comparison period, that is, during six cycles before and after preemption, the delay in the TPS3 algorithm with an APWT value of 120 seconds was 5.3 percent smaller as compared to the average delay for both the TPS0 and TPS1 algorithms. In addition, the TPS3 algorithm had zero truncation for the APWT value of 100, 110, and 120 seconds as compared to 90 and 1 truncation for the TPS0 and TPS1 algorithms. Therefore, it can be concluded for the pedestrian scenario that the TPS3 algorithm with an APWT value of 100, 110, or 120 seconds is the best operation strategy with respect to both safety and efficiency.

For the pedestrian phase inactive scenario, it was concluded that the TPS3 algorithm with an APWT value of 100 or 110 seconds results in a lower delay compared to the TPS0 algorithm even for the condition where there is no safety problem originally.

When the pedestrian volume was 400 ped/h, the average delays were 54.7, 57.4, 54.6, and 53.7 sec/veh for the TPS0, TPS1, TPS2, and TPS3 algorithms, respectively. However, when no pedestrians were present in the intersection, delay decreases drastically as evidenced by the delay metrics of 49.7, 49.4, 48.8, and 48.5 sec/veh for TPS0, TPS1, TPS2, and TPS3 algorithms, respectively. The difference is mainly caused by the right-turning vehicles because the right-turning vehicles must yield the right of way to the crossing pedestrians when the phases are served. Through vehicles using the shared lane with right-turning vehicles also were affected by the right-turning vehicles.

For all the TPS algorithms, it was found that the trains in Group 3, which had the highest speed, had the smallest delay. In contrast, the train in Group 1, which had the lowest speed, had the largest delay for both pedestrian volume levels. In summary, as train speed increases, the prediction accuracy increases and the intersection is operated better.

Therefore, it is concluded that the new TPS algorithm improves the operation of the intersection near the highway-railroad grade crossing in terms of both safety and efficiency.

7.2.3 Benefit/Cost Analysis

The TPS3 system has a safety benefit of \$1,635 and a delay benefit of \$43,623 per years assuming 0.1 percent probability of accident and property only damage. The estimated cost is \$2,939. Therefore, the B/C ratio is 15.4 ($= (1,635 + 43,623)/2,939$). This ratio validated the viability of the proposed system. Therefore, it can be concluded that it is appropriate to install the TPS3 system at the test bed IHRGC. The methodology developed in this dissertation can be applied at any IHRGC.

7.3 FUTURE RESEARCH

Further sensitivity analyses are required to evaluate how various factors, such as, APWT, the pedestrian volume, etc., affect the new transition preemption strategy. In this dissertation, only nine levels of APWT and two levels of pedestrian volume were tested. A more detailed testing of the algorithm for these factors is required to evaluate the effect of the new transition preemption strategy thoroughly.

The prediction intervals were all calculated at the 90 percent level of significance. A sensitivity analysis on the most appropriate level of significance should be conducted.

All simulations were performed using the traffic volume of the evening peak. The new transition preemption strategy may work differently depending on the traffic volume. Additional simulation studies are needed to evaluate the effect of the new transition preemption strategy as a function of traffic volume. In summary, a more comprehensive sensitivity analysis, including all of the factors mentioned above, is needed to guide usage of the new transition preemption strategy for field implementation.

This dissertation is based on the results of the simulations for evaluating the effect of the new transition preemption strategy. Although the study was designed based on the Eagle EPAC 300 controller, which is currently used in the study site, controlled field studies should be performed to guarantee the safety and efficiency of the new transition preemption strategy before the algorithm is considered for field implementation.

The TPS3 was developed in a simulation environment using VAP. To test TPS3 in the real world, the TPS3 code should be recoded in a general programming language and used to control the traffic signal controller. This would allow the hardware-in-the-loop analysis to be used.

GLOSSARY

Adjustment Time (ϕ):

Time accounted for equipment response, motion sensing and constant warning time detectors, and automatic gate activation time.

Advance Preemption and Advance Preemption Time:

Notification of an approaching train is forwarded to the highway traffic signal controller unit or assembly by railroad equipment for a period of time prior to activating the railroad active warning devices. This period of time is the difference in the maximum preemption time required for highway traffic signal operation and the minimum warning time needed for railroad operations and is called the advance preemption time.

Advance Preemption Warning Time (APWT):

Minimum amount of time the TPS algorithm shall start prior to the arrival of a train at a highway-railroad grade crossing.

Onset of Preemption:

The time at which the traffic signal controller receives the preemption signal from the CWT detector.

Blocking Time:

Time period that a train is blocking the HRGC, that is, from the time when a train arrives at the crossing to the time when the train leaves the crossing.

Buffer Time (β):

Buffer time added for safety purposes into the minimum warning time.

Clear Storage Distance:

The distance available for vehicle storage measured 2 m from the rail nearest the intersection to the intersection STOP BAR or the normal stopping point on the highway.

Comprehensive Cost:

A method of measuring motor vehicle accident costs that includes the effects of injury on people's entire lives. This is the most useful measure of accident cost since it includes all cost components and places a dollar value on each one. Comprehensive life values are estimated by examining risk reduction costs from which the market value of safety is inferred. The 11 components of the comprehensive cost are: property damage, lost earnings, lost household production, medical costs, emergency services, travel delay, vocational rehabilitation, workplace costs, administrative, legal, and pain and lost quality of life.

Delay Comparison Period:

Simulation time period to evaluate the difference in average delay. It begins at 600 seconds and ends at 1320 seconds. This period included six cycles where at least one of these cycles occurs after the preemption ends.

Detector Length 1:

The distance from the HRGC to the preemption warning time detector. It emulates the CWT detector in the real world.

Detector Length 2:

The distance from the HRGC to the Doppler Radar detector in simulation. It emulates the Doppler detector in the real world.

Dwell Phases:

Phases served during the preemption mode.

Extended Time (B_i):

Time period added into the minimum time necessary to service the next phase (M_j) to end a vehicle phase i that has a call. That is, when there is a vehicle call for phase i, phase i is provided until the remaining time available (X) is equal to the minimum time necessary to service the next phase (M_j) plus the extended time (B_i), instead of the minimum time necessary to service the next phase (M_j).

External Start:

An input, which when energized, normally causes the signal controller to revert to its programmed initialization interval.

Flashing Don't Walk (FDW):

Pedestrian clearance interval.

MAPE:

Mean absolute percentage error;

$$MAPE = \frac{\sum_{k=1}^n \frac{|P_i - R_i| \times 100}{R_i}}{n}$$

where;

P_i = Predicted arrival time of *i*th train (s);

R_i = Real arrival time of *i*th train (s); and

n = Number of data sets (trains).

MIN GRN/WLK:

Minimum green time for any vehicle phase and any pedestrian phase at the onset of the preemption. This time must have been displayed prior to its termination for a transition to the preemption.

Minimum Track Clearance Distance (δ):

The length along a highway at one or more railroad tracks, measured either from the railroad stopline, warning device, or 4 m perpendicular to the track centerline, to 2 m beyond the track(s), measured perpendicular to the far rail, along the centerline or right edge line of the highway, as appropriate, to obtain the longest distance.

Minimum Warning Time (W):

The least amount of time active warning devices shall operate prior to the arrival of a train at a highway-railroad grade crossing.

Non-Dwell Phases:

Phases not served during the preemption mode.

Pedestrian Phase:

A traffic phase allocated to pedestrian traffic. The traffic signal may provide a right-of-way pedestrian indication either concurrently with one or more vehicular phases, or to the exclusion of all vehicular phases.

Preemption:

The transfer of normal operation of traffic signal to a special control mode.

Preemption Mode:

The signal mode in the period that the signal controller is preempted.

Preempt Trap (Σ):

Condition where the track clearance green ends before the warning lights start to flash.

Preemption Warning Time (P_{WT}):

The actual amount of time that expires between the initiation of the preemption sequence for the highway traffic signals and the arrival of the train at the highway-rail grade crossing.

Remaining Time Available ($X = T - \tau$):

Effectively, a “countdown” or updating until the track clearance time is initiated.

Return Pedestrian Clearance (Ω):

The time that will be provided to clear a terminating Walk during the transition to normal operation.

Right-of-Way Transfer Time (K):

Required wait time prior to the track clearance phase after the traffic signal controller receives the preempt notification.

Selective Pedestrian Clearance (σ):

The time that will be provided to clear a terminating Walk during the transition to Track Green.

Separation Time (Ω):

The time difference between the time that the minimum track clearance distance is clear of vehicles and the time when the train arrives.

Start-up Flash:

A flashing operation that may be programmed to occur prior to initialization, after electric power is applied to the signal controller.

Time to Train Arrival (T):

The time the train is predicted to arrive at the crossing. It is calculated using input from the train detection equipment. It is “counted down” and/or updated as the train approaches the crossing.

Track Clearance Time (τ):

The time at which the track clearance phase should be initiated.

TPS0:

Normal preemption algorithm.

TPS1:

Current TPS algorithm.

TPS2:

TPS algorithm developed in this dissertation. It uses one time predicted time as input.

TPS3:

TPS2 algorithm developed in this dissertation. It used updated predicted arrival time and prediction intervals as input.

TPS Duration:

The time period that the TPS algorithm is active. It is equal to the difference between the advance preemption warning time and the preemption warning time for all TPS algorithms.

Value of Time:

The dollar value placed on an additional hour spent in traveling (units are dollars per hour).

Yellow + All-Red (Y_i+R_i):

Required yellow change interval time and the required red clearance interval time for phase i.

NOTATIONS

- A = Actual arrival time (s);
 A_{cc} = Acceleration/deceleration rate of train (km/h/s);
 a = Acceleration rate for the design vehicle in first gear (m/s^2);
 AAE_k = Average absolute error in testing set at time index k ($k = 10, 20, \dots, 240$);
 AS_{gi} = Average train speed of g th group and i th speed observation (km/h);
 B_i = Extended Time(s);
 C = Cycle length (s);
 c = Time in the cycle (s);
 D = Distance from the detector at FM 2818 to the detector at George Bush (m);
 E = Total within group error sum of squares;
 E_k = Error sum of squares for group k ;
 F = Length of pedestrian clearance phase (s);
 G_j = Minimum green time of phase $i+1$ (s);
 G_k = Minimum green time of phase k in the preemption mode (s);
 g = Green Split (s);
 H = Time in detection (s);
 K = Right-of-way transfer time (s);
 k_j = Jam density (veh/km);
 L = Lower bound of the prediction error interval;
 M_j = Minimum time necessary to service the next phase (phase $i+1$);
 M_k = Minimum time needed to service the next two phases when the next phase is the track clearance phase;
 m = Average number of arrivals in a given time period (= cycle length) (veh);
 m_k = Number of data sets (speed profile) in k th group ($k = 1, \dots, H$);
 N_i = Number of phases of parallel road (phases 1,2,5, and 6);
 N_j = Number of phases of perpendicular road (phases 3 and 4);
 N_k = Number of trains in testing set i at time index k ($k = 10, 20, \dots, 240$);

- N_G = Number of groups at current iteration of Ward algorithm;
 n_g = Number of data sets (trains) in group g ;
 n = Number of elements in data set (10);
 O_{ki} = Observed arrival time for train i at time index k ($k = 10, 20, \dots, 240$);
 P = Predicted train arrival time (s);
 P_k = Predicted arrival time k seconds after detection (s);
 P_{ki} = Predicted arrival time for train i at time index k ($k = 10, 20, \dots, 240$);
 P_{WT} = Preemption warning time (s);
 P_r = Probability of one or more than one pedestrian arriving during the time period at every cycle;
 Q = Length of queue to be cleared as measured from the intersection stopline to the point where a vehicle needing to be cleared may be stopped (m);
 q_s = Saturation flow rate (veh/h);
 R_i = All-Red interval of current phase i (s);
 R_j = All-Red interval of phase $i+1$ (s);
 R_k = All-Red interval of phase k (s);
 S_i = Start time of phase i in the cycle (s) ($i = 1, \dots, \text{Number of phases in the cycle}$);
 \bar{S}_i = Average train speed at i seconds after the detection (km/h) ($i = 2, 3, \dots, 240$);
 s_{gij} = Speed of i th observation of j th train of group g (km/h);
 T = Time to Train Arrival (s);
 t_0 = Time necessary to discharge vehicles queued in a cycle (s);
 t_l = Time interval until the last vehicle in the blocking queue departs (s);
 t_i = Length of the current phase;
 U = Upper bound of the prediction error interval;
 u_w = Backward shockwave speed (km/h);
 V = Train speed (m/s);
 V_i = Observation train speed at i seconds after the detection (m/s);
 V_k = Train speed k seconds after detection (m/s);
 W = Minimum warning time provided to crossing users (s);

- W^* = Total warning time (s);
 X = Remaining time available ($= T - \tau$) (s);
 x = Expected number of arrivals in a given time period (= cycle length) (veh);
 \bar{x}_{ik} = Sample mean of the m_k observations of element i in the k th group;
 x_{ijk} = Value (speed) of i th element of j th data set (speed profile) in the k th group ($i = 1, \dots, n; j = 1, \dots, m_k; k = 1, \dots, H$);
 Y = Estimated preemption warning time;
 Y_i = Yellow interval of current phase i (s);
 Y_j = Yellow interval of phase $i+1$ (s);
 Y_k = Yellow interval of phase k (s);
 Z = Last predicted train arrival time (s);
 z = Time since last prediction (s);
 β = Buffer time added for safety purposes into the minimum warning time (s);
 Γ = Clearance distance on either side of the tracks (m);
 γ = Minimum green time for any vehicle phase and any pedestrian phase at the onset of the preemption (s);
 Δ = Detector location from the crossing (m);
 δ = Minimum track clearance distance (m);
 ε = Prediction error (s);
 ζ = Length of the design vehicle (m);
 η_k = Estimated distance between crossing and head of train at the crossing k seconds after detection (m);
 Θ = Width of the crossing (m);
 θ = Maximum distance of queue (m);
 ι = Amount of time that is operated ineffectively (s);
 λ = Arrival rate (veh/h);
 μ = Discharge rate (veh/h);
 ν = Maximum speed of the design vehicle in first gear (m/s);
 Ξ = End times of the track clearance green (s);

- ξ = Estimated train length (m);
- Π = Modified prediction error (s);
- π = Modified predicted arrival time (s);
- ρ = Maximum number of queue (veh);
- Σ = Preempt trap interval (s);
- σ = Selective Pedestrian Clearance (s);
- τ = Track clearance time (s);
- Φ = Fastest allowable train speed for the track (m/s);
- ϕ = Adjustment time (s);
- χ = Clearance time for each additional track clearance distance (s);
- Ψ = Start time of warning lights (s);
- ψ = Estimated distance from the head of train to the crossing (m);
- Ω = Separation time (s); and
- ω = Distance traveled while accelerating to maximum speed in first gear (m).

REFERENCES

1. Richards, S.H., K.W. Heathington, and B. Fambro. Evaluation of Constant Warning Times Using Train Predictors at a Grade Crossing with Flashing Light Signals. In *Transportation Research Record 1254*, TRB, National Research Council, Washington, D.C., 1990, pp. 60-71.
2. Jacobson, M. and C.L. Dudek (Editor). *An Investigation of Traffic Signal Preemption at Railroad-Highway Grade Crossings*. Texas Transportation Institute, Texas A&M University, College Station, TX, August 1997.
3. Jacobson, M., S. Venglar, and J. Webb. *Advanced Intersection Controller Response to Railroad Preemption - Stage I Report*. Texas Transportation Institute, Texas A&M University, College Station, TX, May 1999.
4. Engelbrecht R., S. Venglar, and M. Jacobson. *Advanced Intersection Controller Response to Railroad Preemption - Stage II Report*. Texas Transportation Institute, Texas A&M University, College Station, TX, September 1999.
5. Venglar, S., R. Engelbrecht, and S. Sunkari. *Advanced Intersection Controller Response to Railroad Preemption - Stage III Report*. Texas Transportation Institute, Texas A&M University, College Station, TX, January 2000.
6. Venglar, S. *Advanced Intersection Controller Response to Railroad Preemption - Stage IV Report*. Texas Transportation Institute, Texas A&M University, College Station, TX, February 2000.
7. *Manual on Uniform Traffic Control Devices for Streets and Highway*. FHWA, U.S. Department of Transportation, Washington, D.C., 1988.
8. Communication and Signal Section, *Signal Manual of Recommended Practice*. Association of American Railroads, Volume I, Section 3. Washington, D.C., 1995.
9. *Railroad-Highway Grade Crossing Handbook*. Technology Sharing Report No. FHWA-TS-78-214. FHWA, U.S. Department of Transportation, Washington, D.C., August 1978.
10. Traffic Signal Operations Near Highway-Rail Grade Crossing, In *Synthesis of Highway Practice 271*. TRB, National Research Council, Washington, D.C., 1999.
11. Marshall, P.S. and W.D. Berg. Design Guidelines for Railroad Preemption at Signalized Intersections. *ITE Journal*, Vol. 67, No. 2, Washington, D.C., February 1997, pp. 20-25.

12. Oppenlander, J.C. and O. Jane. Storage Requirements for Signalized Intersection Approaches. *ITE Journal*, Vol. 66, No. 2, Washington, D.C., February 1996, pp 27-30.
13. Marshall, P.S. and W.D. Berg. Guideline for Railroad Preemption at Signalized Intersections. *Proceedings of the 1991 Conference on Strategic Highway Research Program and Traffic Safety on Two Continents, Part Three*. Gothenburg, Sweden, 1991/09, pp. 84-96.
14. Marshall, P.S. and W.D. Berg. Evaluation of Railroad Preemption Capability of Traffic Signal Controllers. In *Transportation Research Record 1254*, TRB, National Research Council, Washington, D.C., 1990, pp. 44-49.
15. *Special Report 209: Highway Capacity Manual*. TRB, National Research Council, Washington, D.C., 1994.
16. Homburger, W.S. *Transportation and Traffic Engineering Handbook*. Prentice-Hall, Englewood Cliffs, NJ, 1982.
17. *A Policy on the Geometric Design of Highway and Street*. American Association of State Highway and Transportation Officials, Washington, D.C., 1994.
18. Bremer, W.F. and L.M. Ward. Improving Grade Crossing Safety Near Highway Intersections. *ITE Journal*, Vol. 67, No. 9, Washington, D.C., September 1997, pp. 24-26.
19. Engelbrecht, R., S. Sunkari, T. Urbanik II, S. Venglar, and K. Balke. *The Preempt Trap: How to Make Sure You Do Not Have One*. Report 1752-9. Texas Transportation Institute, Texas A&M University, College Station, TX, March 2002.
20. Venglar, S., M. Jacobson, S. Sunkari, R. Engelbrecht, and T. Urbanik II. *Guide for Traffic Signal Preemption Near Railroad Grade Crossing*. Report 1439-9. Texas Transportation Institute, Texas A&M University, College Station, TX, September 2000.
21. *Manual of Recommended Practices-Signals*. American Railway Engineering and Maintenance-of-Way Association, Landover, MD, 2000.
22. Tustin, B., H.A. Richards, H. McGee, and R. Patterson. *Railroad-Highway Grade Crossing Handbook*, 2nd Edition. Office of Implementation, FHWA, U.S. Department of Transportation, September 1986.

23. *Preemption of Traffic Signals at or Near Railroad Grade Crossings with Active Warning Devices*. Traffic Engineering Council Committee TENC-4M-35. Institute of Transportation Engineers, Washington, D.C., February 1997.
24. Meadow, L. Los Angeles Metro Blue Line Grade Crossing Safety Program. *National Conference on Highway-Rail Safety*, St. Louis, MO, July 1993.
25. Lancaster, T.R. Light Rail Transit Preemption of Actuated Signals. *ITE 1989 Compendium of Technical Papers*, Institute of Transportation Engineers, Washington, D.C., pp. 335-337.
26. Mowatt, M.G. Transit Signal Priority: A Regional Implementation. *ITE 1995 Compendium of Technical Papers*, Institute of Transportation Engineers, Washington, D.C., pp. 85-91.
27. Incremental Train Control System. *Traffic Engineering Council Update*. ITE Traffic Engineering Council Committee 96-04, Institute of Transportation Engineers, Washington, D.C., Spring/Summer 1997, pp. 6-8.
28. Estes, R. M. and L.R. Rilett. Advanced Prediction of Train Arrival and Crossing Times at Highway-Railroad Grade Crossing. In *Transportation Research Record 1708*, TRB, National Research Council, Washington, D.C., 2000, pp 68-76.
29. *VISSIM User's Manual*, Version 3.5. PTV Planning Transport Verkehr AG, Karlsruhe, Germany, December 2000.
30. Engelbrecht, R., C. Poe, and K. Balke. Development of a Distributed Hardware-in-the-Loop Simulation System for Transportation Networks. *Presented at 78th Annual Meeting of the Transportation Research Board*, Washington, D.C., January 2000.
31. ITT Systems & Science Corporation. *CORSIM User's Manual*, Version 1.04. FHWA, U.S. Department of Transportation, Washington, D.C., March 1998.
32. EPAC 300 Actuated Controller Unit, *PIM-177 Product Manual*, Rev C.12. Eagle Traffic Control Systems, A Business Unit of SIEMENS Energy & Automation, Inc., Austin, TX, 1997.
33. Hagan, M.T. and H.B. Demnith. *Neural Network Design*, PWS Publishing Company, Boston, MA, 1996.
34. Dougherty, M.S., H.R. Kirby, and R.D. Boyle. The Use of Neural Networks to Recognize and Predict Traffic Congestion. *Traffic Engineering and Control*, Vol. 34, No. 2, 1993, pp. 311-314.

35. Park, D. and L.R. Rilett. Forecasting Multiple-Period Freeway Link Travel Times Using Modular Neural Networks. In *Transportation Research Record 1617*, TRB, National Research Council, Washington, D.C., 1998, pp.163-170.
36. Park, D. and L.R. Rilett. Forecasting Freeway Link Travel Times with a Multilayer Feedforward Neural Networks. *Computer-Aided Civil Infrastructure Engineering*, Vol. 14, 1999, pp. 357-367
37. Smith, B.L. and M.J. Demetsky. Short-Term Traffic Flow Prediction: Neural Network Approach. In *Transportation Research Record 1453*, TRB, Washington, D.C., 1994, pp. 98-104.
38. Anderberg, M.R. *Cluster Analysis for Applications*, Academic Press, New York, 1973.
39. Sharma, S.C. and A. Werner. Improved Method of Grouping Provincewide Permanent Traffic Counters. In *Transportation Research Record 815*, TRB, Washington, D.C., 1981, pp. 12-18.
40. Lingras, P. Classifying Highways: Hierarchical Grouping versus Kohonen Neural Network. *Journal of Transportation Engineering*, Vol. 121, No. 4, 1995, pp. 364-368.
41. Efron, B. and R.J. Tibshirani. *An Introduction to the Bootstrap*. Chapman & Hall, New York, 1993.
42. Milton, J.S. and J.C. Arnold. *Introduction to Probability and Statistics*, Third Edition. McGraw-Hill International Editions, New York, 1995.
43. Devore, J. and R. Peck. *Statistics, the Exploration and Analysis of Data*, Third Edition. Duxbury Press, Belmont, CA, 1997.
44. The Urban Institute. *The Costs of Highway Crashes*, Research Report No. FHWA-RD-91-055, FHWA, Washington, D.C., October 1991.
45. Motor Vehicle Accident Costs. *Technical Advisory T 7570.2*, FHWA, Washington, D.C., October 1994.
<http://www.fhwa.dot.gov/legsregs/directives/techadv/t75702.htm>
46. Daniels, V. F., D.R. Ellis, W.R. Stockton. *Techniques for Manually Estimating Road User Costs Associated with Construction Projects*. Texas Transportation Institute, Texas A&M University, College Station, Tex., December 1999.

47. Chui, M.K. and W.F. McFarland. *Value of Travel Time: New Estimates Developed Using a Speed-Choice Model*. Report 396-2F. Texas Transportation Institute, Texas A&M University, College Station, Tex., 1985.

APPENDIX A

**AAE AND OPTIMAL NUMBER OF ITERATIONS FOR EACH ANN
STRUCTURE AND EACH GROUP IN 2, 3, AND 4 GROUPINGS**

TABLE A-1 AAE and Optimal Number of Iterations for Each ANN Structure and Each Group in 2 Grouping

Model	Time in Detection*	10-1-1			10-5-1			10-10-1		
		Group 1	Group 2	Average	Group 1	Group 2	Average	Group 1	Group 2	Average
1	10	25.2 (11)	12.3 (3)	20.6	24.3 (13)	12.2 (11)	20	24.6 (14)	12.3 (10)	20.2
2	20	22.7 (9)	11.8 (10)	18.8	22 (8)	11.8 (19)	18.4	22.1 (21)	11.9 (4)	18.4
3	30	22.1 (6)	11.3 (10)	18	21.6 (8)	10.9 (10)	17.5	22.5 (8)	11 (10)	18.1
4	40	21.9 (11)	10.1 (3)	17.5	21.3 (5)	10.1 (9)	17.1	20.5 (9)	10.8 (7)	17
5	50	21.4 (5)	9.7 (10)	17.2	20.8 (10)	9 (8)	16.5	20.7 (14)	10.8 (5)	17.1
6	60	21.9 (9)	7.8 (10)	17	20.8 (13)	7.2 (10)	16.1	21.3 (10)	7 (3)	16.3
7	70	20 (11)	8.5 (13)	16.3	19.8 (13)	8.7 (6)	16.2	20.1 (12)	8.4 (4)	16.3
8	80	22.1 (10)	8.7 (10)	15.7	21.9 (8)	8 (8)	15.3	22.5 (7)	8.1 (9)	15.6
9	90	21.2 (10)	7.6 (9)	14.9	21.4 (8)	6.7 (12)	14.6	21.6 (10)	7 (6)	14.8
10	100	9 (10)	21.5 (9)	13.9	7.2 (65)	22.1 (10)	13.1	8 (10)	24 (15)	14.3
11	110	14.3 (7)	5.9 (10)	10.7	14.3 (14)	5.6 (13)	10.5	14.7 (8)	5.7 (9)	10.8
12	120	15.7 (7)	6.1 (13)	10.7	19 (10)	5.7 (16)	12.1	17.3 (9)	6 (11)	11.5
13	130	5.5 (10)	14.5 (4)	10.7	4.5 (6)	15.6 (11)	10.9	4.3 (40)	15 (15)	10.5
14	140	4.9 (6)	15.5 (7)	11.2	4.4 (10)	16.1 (7)	11.4	4.7 (12)	16.7 (7)	11.9
15	150	4.1 (4)	14.6 (10)	10.6	2.8 (4)	16.2 (10)	11.1	3.7 (9)	16.3 (9)	11.5
16	160	3.9 (11)	14.7 (7)	10.8	3.5 (10)	15.4 (5)	11.1	3.8 (10)	15.4 (11)	11.2
17	170	14.4 (10)	4.4 (10)	11	12.7 (10)	3.3 (6)	9.6	12.5 (5)	3.2 (6)	9.4
18	180	14.7 (10)	3.7 (7)	11.1	12 (13)	3.8 (10)	9.3	11.9 (11)	4.5 (6)	9.4
19	190	8.4 (14)	23.3 (1)	13	4.6 (8)	18.9 (6)	9	5.9 (17)	10.8 (29)	7.4
20	200	11.2 (11)	25.7 (11)	16	4.1 (13)	25.2 (10)	11.1	6.3 (10)	33.1 (4)	15.2
21	210	3.6 (10)	21.2 (11)	9.1	2.6 (9)	15.5 (13)	6.6	3 (12)	17.6 (6)	7.6
22	220	2.5 (10)	43.5 (4)	13.7	2.9 (7)	32.5 (1)	11	2.7 (10)	22.5 (7)	8.1
23	230	8.2 (9)	29.9 (9)	19	5 (11)	26.2 (4)	15.6	7 (3)	26.1 (6)	16.6
24	240	1.1 (10)	36.7 (11)	18.9	10.3 (4)	27.7 (14)	19	4.7 (4)	11.1 (3)	7.9

TABLE A-1 Continued

Model	Time in Detection*	10-20-1			10-30-1		
		Group 1	Group 2	Average	Group 1	Group 2	Average
1	10	24.8 (8)	12.4 (4)	20.3	24.3 (5)	13.4 (2)	20.4
2	20	22 (7)	11.8 (13)	18.4	22 (8)	12.5 (7)	18.6
3	30	22.9 (7)	10.7 (4)	18.2	23.5 (7)	12.8 (4)	19.4
4	40	20.9 (10)	11.4 (11)	17.4	20.9 (6)	12.9 (5)	18
5	50	21.7 (6)	12.1 (2)	18.2	21.4 (8)	14.7 (3)	19
6	60	20.7 (17)	7.5 (4)	16.1	21.4 (6)	10.1 (4)	17.4
7	70	20.4 (13)	10.9 (4)	17.3	20.7 (11)	11.1 (7)	17.6
8	80	22.4 (7)	8.8 (10)	15.9	23.1 (4)	8.9 (6)	16.3
9	90	21.2 (17)	7.3 (7)	14.7	19.9 (17)	7 (4)	13.9
10	100	9.3 (7)	24.5 (8)	15.3	9.9 (7)	26.6 (3)	16.5
11	110	15.4 (7)	6.8 (7)	11.7	16.9 (9)	6.2 (5)	12.3
12	120	20 (4)	5.9 (8)	12.7	20.7 (21)	6.6 (12)	13.4
13	130	4.9 (4)	17.3 (6)	12	4.9 (14)	17.7 (19)	12.3
14	140	4.5 (11)	17 (3)	11.9	4.8 (4)	21.9 (12)	15
15	150	3.6 (10)	17.9 (6)	12.5	4 (4)	17.1 (8)	12.2
16	160	4.1 (6)	16.2 (4)	11.8	4.3 (6)	18.9 (4)	13.7
17	170	14 (5)	4.3 (14)	10.8	16.2 (6)	4.6 (6)	12.4
18	180	13.4 (7)	6.9 (3)	11.2	14.1 (5)	9.1 (3)	12.4
19	190	5.4 (8)	29.3 (4)	12.7	10.2 (10)	61.5 (2)	26
20	200	7.7 (6)	27.6 (3)	14.3	6.6 (5)	83.5 (4)	32.2
21	210	3.5 (9)	34.7 (5)	13.3	5.7 (8)	77.8 (2)	28.2
22	220	2.5 (15)	36.3 (4)	11.7	8.8 (5)	37.9 (5)	16.7
23	230	22.1 (4)	40.7 (3)	31.4	35.1 (5)	64.9 (4)	50
24	240	19.2 (3)	13.8 (4)	16.5	18.8 (2)	29.8 (3)	24.3

(): Optimal number of iterations

*: Time since train was first detected

TABLE A-2 AAE and Optimal Number of Iterations for Each ANN Structure and Each Group in 3 Grouping

Model	Time in Detection*	10-1-1				10-5-1			
		Group 1	Group 2	Group 3	Average	Group 1	Group 2	Group 3	Average
1	10	36.5 (13)	15.4 (10)	12 (11)	20.0	35 (4)	15.1 (5)	11.3 (7)	19.3
2	20	32.8 (6)	14.9 (9)	10.5 (9)	18.7	30.4 (9)	14.1 (20)	9.8 (12)	17.5
3	30	19.8 (13)	31 (8)	10.3 (10)	17.9	18.9 (8)	30.9 (6)	10 (11)	17.3
4	40	29.9 (14)	13 (11)	8.8 (3)	17.2	29.6 (13)	12.4 (11)	9 (10)	16.8
5	50	28.9 (5)	14.7 (8)	8 (5)	16.6	26.8 (10)	14.7 (11)	8.2 (10)	16.1
6	60	28.7 (10)	15 (10)	7.6 (10)	16.6	27.2 (13)	15.2 (8)	6.8 (8)	16.1
7	70	25.1 (7)	15 (10)	8.3 (21)	16.4	24.2 (11)	14.9 (8)	7.8 (4)	15.9
8	80	19.4 (7)	20.3 (7)	8.1 (6)	15.7	20.2 (9)	19.3 (15)	6.9 (10)	15.1
9	90	17.4 (4)	23.6 (8)	7.3 (10)	15.4	17.9 (11)	19.6 (10)	6.6 (10)	14.4
10	100	9.9 (100)	5.5 (10)	23.9 (10)	13.4	8.6 (94)	5.1 (11)	24.9 (6)	13.0
11	110	9.7 (11)	20.7 (7)	5.1 (5)	10.8	9.2 (14)	20.1 (5)	4.8 (5)	10.3
12	120	6.6 (9)	5.2 (10)	16.7 (7)	10.7	6.4 (9)	3.8 (11)	17.7 (11)	10.9
13	130	11.1 (100)	34 (6)	5.1 (7)	11.4	10.9 (11)	29.5 (7)	5 (11)	10.8
14	140	15.5 (100)	30.3 (9)	5.2 (5)	13.4	13.4 (9)	22.2 (13)	5 (10)	11.3
15	150	15.2 (9)	30.7 (3)	4 (4)	13.1	12.5 (26)	27.9 (7)	3.4 (10)	11.2
16	160	11.5 (10)	26.9 (3)	5.1 (5)	11.8	10.3 (10)	32.1 (2)	3.3 (10)	11.4
17	170	11.7 (10)	26.5 (33)	4 (9)	11.4	7.9 (11)	27.2 (9)	2.7 (8)	9.1
18	180	8.6 (13)	34.8 (10)	4 (10)	12.2	4.5 (8)	33.8 (4)	2.9 (9)	9.5
19	190	8.9 (7)	1 (11)	25.3 (4)	12.1	6.9 (10)	1.4 (10)	23.8 (15)	10.6
20	200	12.6 (10)	1.5 (10)	29.1 (8)	15.5	9.1 (13)	1.2 (10)	26.9 (4)	12.6
21	210	2.2 (10)	4 (2)	23.8 (41)	7.7	2.6 (12)	0.4 (3)	28.1 (11)	8.9
22	220	3.8 (13)	0.6 (11)	53.5 (9)	12.5	2.2 (12)	17.3 (2)	19.6 (11)	6.8
23	230	5.3 (10)	10.1 (4)	34 (10)	16.7	1.4 (5)	1.4 (3)	35.1 (17)	14.0
24	240	8 (10)	0.1 (4)	53.5 (16)	21.9	2.6 (4)	12.6 (2)	23.9 (2)	11.4

TABLE A-2 Continued

Model	Time in Detection*	10-10-1				10-20-1			
		Group 1	Group 2	Group 3	Average	Group 1	Group 2	Group 3	Average
1	10	34.4 (8)	16.1 (8)	11.8 (10)	19.7	36.6 (10)	16.1 (41)	11.8 (6)	20.3
2	20	30.6 (7)	14.6 (4)	9.8 (13)	17.8	30.8 (10)	16.1 (5)	9.9 (5)	18.5
3	30	19.2 (9)	28.9 (12)	9.6 (13)	17.1	20.3 (4)	38 (11)	10.1 (4)	18.9
4	40	28.4 (9)	12.5 (9)	9 (8)	16.5	29.2 (8)	12.3 (22)	8.9 (9)	16.6
5	50	25.7 (12)	14.9 (6)	9.5 (10)	16.2	28.9 (9)	16.5 (6)	9.2 (4)	17.7
6	60	25.7 (9)	16.4 (16)	7.2 (13)	16.3	27.4 (10)	16.9 (5)	8.1 (12)	17.3
7	70	23.3 (14)	15.1 (8)	8.1 (4)	15.8	24.9 (5)	15.7 (4)	10 (11)	17.1
8	80	19.9 (13)	20.4 (13)	6.7 (12)	15.3	19.8 (15)	21.2 (5)	7 (16)	15.7
9	90	18 (10)	20.6 (9)	7.1 (7)	14.8	19 (10)	23 (10)	7.6 (9)	16.0
10	100	9.8 (5)	5.9 (7)	23.7 (10)	13.4	10.6 (4)	6.6 (10)	29.2 (9)	15.6
11	110	9.5 (22)	22.2 (9)	4.9 (16)	11.0	10.2 (9)	19.8 (6)	5.6 (12)	10.9
12	120	5.6 (12)	4.2 (7)	18 (12)	10.7	6.4 (6)	4.3 (7)	22.1 (4)	12.9
13	130	11.6 (12)	24.1 (3)	4.8 (9)	10.4	12.8 (11)	42.9 (3)	5 (18)	13.3
14	140	14.9 (4)	41 (9)	4.7 (22)	14.2	14.2 (6)	35 (5)	5 (11)	13.2
15	150	11.1 (12)	47.5 (3)	3 (7)	13.0	13.5 (9)	29.4 (5)	3.6 (9)	11.9
16	160	11.4 (2)	47.8 (4)	3.1 (6)	14.2	12.1 (5)	37.4 (5)	3.6 (9)	13.2
17	170	9.6 (10)	26.8 (5)	3.2 (7)	10.1	10.2 (9)	26.4 (2)	4.3 (12)	10.7
18	180	6.2 (12)	34.1 (3)	3.4 (8)	10.6	8.2 (10)	36.9 (2)	5.5 (7)	12.7
19	190	5.8 (23)	4.1 (3)	27.7 (4)	11.4	5.8 (10)	22.6 (6)	24.7 (5)	13.4
20	200	8.9 (13)	2.7 (2)	18.3 (2)	10.5	10.3 (10)	16.1 (4)	38.9 (4)	17.7
21	210	1.9 (9)	9.7 (2)	30.1 (2)	9.5	3.9 (5)	5 (2)	27.2 (3)	9.8
22	220	3.2 (11)	19.7 (1)	25.8 (2)	8.8	5.3 (5)	0.3 (4)	38.8 (4)	11.0
23	230	6.4 (4)	1.6 (1)	33.6 (6)	16.0	39.2 (5)	16.3 (2)	41.2 (2)	37.1
24	240	13.2 (3)	2.3 (1)	36.4 (1)	19.1	77.6 (2)	16 (3)	20.2 (4)	48.2

TABLE A-2 Continued

Model	Time in Detection*	10-30-1			
		Group 1	Group 2	Group 3	Average
1	10	38.1 (7)	16.4 (6)	11.7 (9)	20.7
2	20	31 (5)	17.3 (5)	10.7 (5)	19.3
3	30	21.4 (7)	46.1 (5)	11.9 (11)	21.1
4	40	30.5 (5)	13.3 (10)	11.3 (4)	18.1
5	50	27.1 (4)	18.2 (7)	11.2 (4)	18.6
6	60	29.1 (4)	18.9 (9)	8.7 (6)	18.8
7	70	26.1 (4)	16 (7)	10.8 (6)	17.7
8	80	22.9 (9)	19.8 (10)	7.2 (9)	16.1
9	90	20 (9)	21.3 (3)	8.2 (8)	16.2
10	100	10.3 (9)	8.6 (4)	32.9 (13)	17.1
11	110	12.2 (5)	21.8 (5)	6.7 (8)	12.6
12	120	7.8 (8)	7.3 (6)	25.7 (7)	15.5
13	130	13.8 (7)	76.3 (5)	5.2 (18)	17.6
14	140	17.3 (7)	47.7 (4)	5.1 (7)	16.4
15	150	13.2 (6)	45.5 (2)	3.6 (22)	14.0
16	160	17.1 (4)	46.4 (2)	4.2 (10)	17.4
17	170	14.5 (4)	34.4 (4)	5.4 (16)	14.5
18	180	12.5 (3)	64.4 (3)	4.5 (3)	20.0
19	190	11.8 (8)	34.7 (5)	34 (2)	21.3
20	200	14.7 (4)	26.4 (4)	47.3 (5)	23.6
21	210	8 (5)	3.6 (4)	57.2 (3)	20.1
22	220	6 (3)	9.2 (1)	18.5 (3)	8.6
23	230	87.9 (2)	52.7 (3)	35.3 (2)	63.8
24	240	100.6 (2)	18.8 (1)	12 (1)	57.4

(): Optimal number of iterations

*: Time since train was first detected

TABLE A-3 AAE and Optimal Number of Iterations for Each ANN Structure and Each Group in 4 Grouping

Model	Time in Detection*	10-1-1					10-5-1				
		Group 1	Group 2	Group 3	Group 4	Ave.	Group 1	Group 2	Group 3	Group 4	Ave.
1	10	29.6 (10)	42.6 (10)	15.6 (12)	11.8 (3)	19.5	27.4 (15)	46.8 (10)	15.1 (10)	11.4 (8)	19
2	20	25.9 (15)	43.1 (7)	15 (9)	10.4 (9)	18.5	25.3 (25)	40.8 (8)	14.4 (10)	9.8 (12)	17.8
3	30	24.8 (9)	14.5 (11)	31.4 (8)	9.1 (10)	17.7	23.7 (8)	13.2 (5)	32.3 (10)	8.8 (10)	16.9
4	40	26.9 (10)	30.1 (7)	13.1 (100)	9.2 (8)	17	26.2 (8)	37 (9)	11.7 (8)	9.4 (10)	16.9
5	50	9.4 (11)	6 (10)	28.6 (4)	15.2 (10)	16.5	10.9 (11)	4.9 (9)	27.5 (41)	14.9 (15)	16.4
6	60	7.5 (8)	5.6 (7)	28.7 (10)	16.7 (10)	16.7	7.5 (4)	6 (10)	27 (8)	16.2 (8)	16.1
7	70	22.7 (10)	29.9 (8)	14.9 (4)	8.8 (11)	16.5	21.2 (5)	27.1 (8)	15.4 (11)	8.4 (5)	16
8	80	9.2 (10)	6.8 (34)	19.2 (7)	23.5 (10)	15.6	8.1 (9)	4.5 (10)	21.9 (9)	22.1 (12)	15.3
9	90	8.4 (10)	4.9 (10)	18.7 (5)	22 (11)	14.6	7.5 (10)	3.5 (4)	18.9 (19)	21.8 (6)	14.2
10	100	20.1 (10)	7.1 (10)	4.7 (9)	20 (9)	14.1	18.8 (7)	5.9 (7)	3.5 (16)	18.4 (11)	12.8
11	110	5.2 (7)	4.7 (10)	10.5 (11)	21.1 (10)	10.8	5.2 (8)	4.1 (8)	11 (10)	19.7 (4)	10.7
12	120	15.7 (68)	26.2 (10)	6.7 (6)	4.9 (11)	11.7	11.8 (13)	22.9 (15)	6.4 (6)	4.2 (7)	9.6
13	130	6.5 (6)	2.6 (5)	11.7 (100)	36.2 (11)	11.8	5.6 (16)	2.4 (5)	11.2 (12)	38.8 (10)	11.6
14	140	5.6 (4)	2.1 (9)	15.6 (10)	31.8 (10)	13.2	5 (14)	1.7 (11)	14.8 (10)	27.4 (3)	12.1
15	150	4.9 (9)	3.8 (10)	11.8 (11)	32.8 (11)	11.9	3.8 (10)	2.6 (13)	9.4 (12)	25.5 (5)	9.4
16	160	5 (7)	3.9 (7)	13.5 (9)	31.7 (7)	13.5	2.9 (15)	2.3 (5)	10.2 (9)	30.6 (11)	11
17	170	5.7 (10)	0 (8)	10.2 (9)	26.5 (85)	11	2.8 (8)	0.2 (9)	7.5 (11)	22.8 (1)	8.2
18	180	9.3 (100)	7.4 (9)	31.9 (27)	3.3 (14)	10.8	6.2 (10)	3.7 (5)	30.4 (10)	3.4 (12)	8.7
19	190	2.4 (5)	11.3 (14)	0.8 (9)	25.3 (14)	11.3	3.1 (5)	10.2 (8)	1.4 (8)	21 (14)	10
20	200	3.3 (8)	16.4 (7)	0.9 (4)	30.1 (3)	15.1	4 (10)	6.8 (10)	1.5 (5)	30.8 (18)	10.3
21	210	2.1 (10)	7.1 (11)	23.2 (14)	29.4 (14)	10.1	1.8 (5)	8.1 (3)	5.2 (4)	23.5 (3)	8.1
22	220	4.2 (12)	6.7 (6)	13.7 (6)	53.5 (10)	14.5	2.2 (9)	1.7 (2)	1.1 (5)	50.9 (4)	10.9
23	230	4.8 (10)	31 (4)	4.2 (9)	6.8 (2)	11.4	0.4 (5)	12.7 (1)	0.3 (12)	10.8 (1)	4.7
24	240	0.4 (10)	26.1 (4)	0.8 (10)	32.1 (2)	14.4	0.1 (7)	60.5 (2)	2.7 (9)	2.8 (2)	21.6

TABLE A-3 Continued

Model	Time in Detection*	10-10-1					10-20-1				
		Group 1	Group 2	Group 3	Group 4	Ave.	Group 1	Group 2	Group 3	Group 4	Ave.
1	10	28.2 (3)	48.6 (25)	15.3 (5)	11.3 (26)	19.3	27.9 (4)	58 (4)	15.4 (5)	10.8 (4)	19.8
2	20	25.4 (3)	37.7 (16)	14.5 (4)	9.8 (10)	17.6	26.1 (7)	50.6 (3)	16.3 (6)	10.1 (6)	19.6
3	30	24.9 (4)	13.3 (5)	31.8 (5)	8.9 (7)	17.3	25.6 (10)	15.1 (10)	39.2 (6)	8.9 (8)	18.7
4	40	25.5 (5)	70.5 (8)	12.6 (8)	9.2 (6)	19.5	25.1 (5)	104 (6)	13 (7)	11 (14)	22.7
5	50	14.9 (3)	6.2 (6)	28.1 (17)	15.3 (8)	17.8	14.3 (6)	7.1 (11)	29.4 (5)	15.4 (7)	18.2
6	60	9.7 (18)	4 (13)	26.4 (9)	16.2 (5)	16.3	10.5 (5)	5.8 (6)	27.9 (9)	18 (7)	17.8
7	70	21.8 (8)	37.5 (7)	15.1 (11)	8.3 (6)	16.8	22.2 (7)	65.6 (4)	15.5 (3)	8.7 (8)	19.4
8	80	8.3 (10)	6 (3)	22 (6)	23 (39)	15.9	7.6 (8)	8 (4)	21 (7)	23.6 (11)	15.8
9	90	7.4 (9)	7.4 (6)	19.1 (10)	20.1 (13)	14.4	8.2 (10)	8.5 (8)	20.6 (6)	27.1 (14)	16.9
10	100	19.6 (9)	6.5 (9)	3.2 (9)	17.9 (6)	13	19.9 (6)	7.7 (8)	4.9 (5)	22.3 (5)	14.8
11	110	5.6 (11)	4.4 (10)	10.5 (10)	20.2 (9)	10.7	5.8 (5)	6.2 (9)	12.4 (12)	24.6 (11)	12.8
12	120	15.3 (9)	30.8 (5)	6.9 (10)	4.1 (6)	11.9	16.7 (7)	39.7 (2)	5.8 (6)	5.4 (12)	13.2
13	130	5 (12)	1.9 (12)	13 (22)	43.7 (2)	12.8	5.6 (17)	2.6 (9)	11.9 (4)	45 (3)	12.7
14	140	4.6 (12)	2.8 (9)	16.2 (9)	32.7 (7)	13.4	4.8 (15)	2.8 (5)	15.8 (15)	35.1 (2)	13.5
15	150	3.6 (9)	2.1 (9)	9.4 (4)	43.1 (9)	11.7	4.9 (7)	2.6 (10)	16.6 (4)	49.2 (3)	16.4
16	160	4 (14)	1.8 (8)	12.1 (12)	29.9 (9)	12.1	5.5 (10)	3.2 (6)	12.2 (4)	28.4 (3)	12.4
17	170	3.9 (8)	6.5 (3)	9.2 (14)	29.9 (5)	10.6	3.9 (12)	0.8 (2)	9.8 (7)	35.4 (2)	11.6
18	180	8.8 (8)	6.5 (4)	37 (2)	3.2 (8)	11.1	10.8 (4)	48 (5)	44.1 (2)	5.2 (6)	21.1
19	190	4.1 (6)	12.7 (10)	2.3 (10)	17.2 (3)	10.5	15.5 (4)	16.6 (20)	20.6 (2)	40.2 (3)	22.3
20	200	3.4 (4)	9.8 (10)	2.8 (9)	24.4 (7)	10.7	34.3 (3)	12.1 (4)	14.6 (2)	20.6 (4)	18.2
21	210	1.8 (11)	25.1 (4)	3.6 (2)	21.9 (3)	13	2.5 (6)	62.2 (4)	9 (2)	34.7 (5)	27.6
22	220	3.3 (9)	28.3 (2)	5.4 (1)	15.4 (2)	10.3	6 (5)	75.3 (1)	3.3 (1)	11 (2)	19.3
23	230	4.6 (3)	4.9 (1)	5.2 (7)	0.8 (4)	4.4	15.2 (2)	121.2 (2)	44.8 (2)	6.7 (3)	51.7
24	240	8.7 (5)	68.3 (1)	9.9 (5)	0.2 (4)	27.5	6.9 (2)	40.5 (2)	39.6 (3)	44.6 (1)	35.3

TABLE A-3 Continued

Model	Time in Detection*	10-30-1				
		Group 1	Group 2	Group 3	Group 4	Average
1	10	30.7 (5)	59.1 (3)	16.4 (4)	12.4 (7)	21.4
2	20	25.9 (3)	79.8 (12)	16.5 (6)	10.6 (5)	22
3	30	25.2 (6)	15.6 (5)	48 (5)	9 (4)	19.6
4	40	25.3 (10)	61.7 (3)	14 (10)	12 (5)	20.1
5	50	18.8 (6)	14.5 (6)	29.6 (5)	16.3 (5)	20.4
6	60	12.3 (6)	8.4 (4)	30 (6)	18.5 (7)	19.2
7	70	26.1 (7)	73.1 (3)	16.1 (8)	8.7 (4)	21.2
8	80	9.1 (7)	13.3 (5)	20.2 (3)	24 (3)	16.8
9	90	7.6 (9)	17.1 (20)	19.6 (15)	29.3 (25)	18.1
10	100	20.1 (18)	6.3 (25)	7.5 (4)	19.8 (4)	14.3
11	110	7.5 (7)	6.5 (4)	10.8 (6)	28.1 (12)	13.5
12	120	16.4 (3)	49.7 (3)	7 (7)	6.7 (7)	14.8
13	130	6.6 (4)	6.7 (5)	13 (3)	76.2 (2)	17.5
14	140	5 (7)	16 (4)	17.4 (5)	78.7 (2)	20.5
15	150	4.7 (6)	4.2 (6)	15 (9)	57.7 (3)	16.9
16	160	6.2 (7)	8.8 (7)	16.3 (5)	52 (2)	18.9
17	170	7 (6)	6.6 (5)	14.6 (16)	49.4 (3)	17.2
18	180	14.2 (6)	80.3 (5)	29.2 (1)	11.7 (6)	27.8
19	190	53.9 (5)	14.8 (3)	27.8 (2)	54 (1)	34.4
20	200	12.2 (2)	29.5 (4)	35.7 (4)	36.1 (2)	28.1
21	210	15.2 (7)	98.2 (3)	7.5 (2)	5.5 (2)	38.8
22	220	23.6 (4)	33.5 (1)	9.2 (3)	20.2 (3)	23.5
23	230	20.3 (4)	111.6 (1)	56.5 (4)	52.4 (1)	60.7
24	240	12.3 (2)	67 (2)	41.2 (1)	28 (3)	42.8

(): Optimal number of iterations

*: Time since train was first detected

APPENDIX B

TPS ALGORITHM FLOW CHARTS

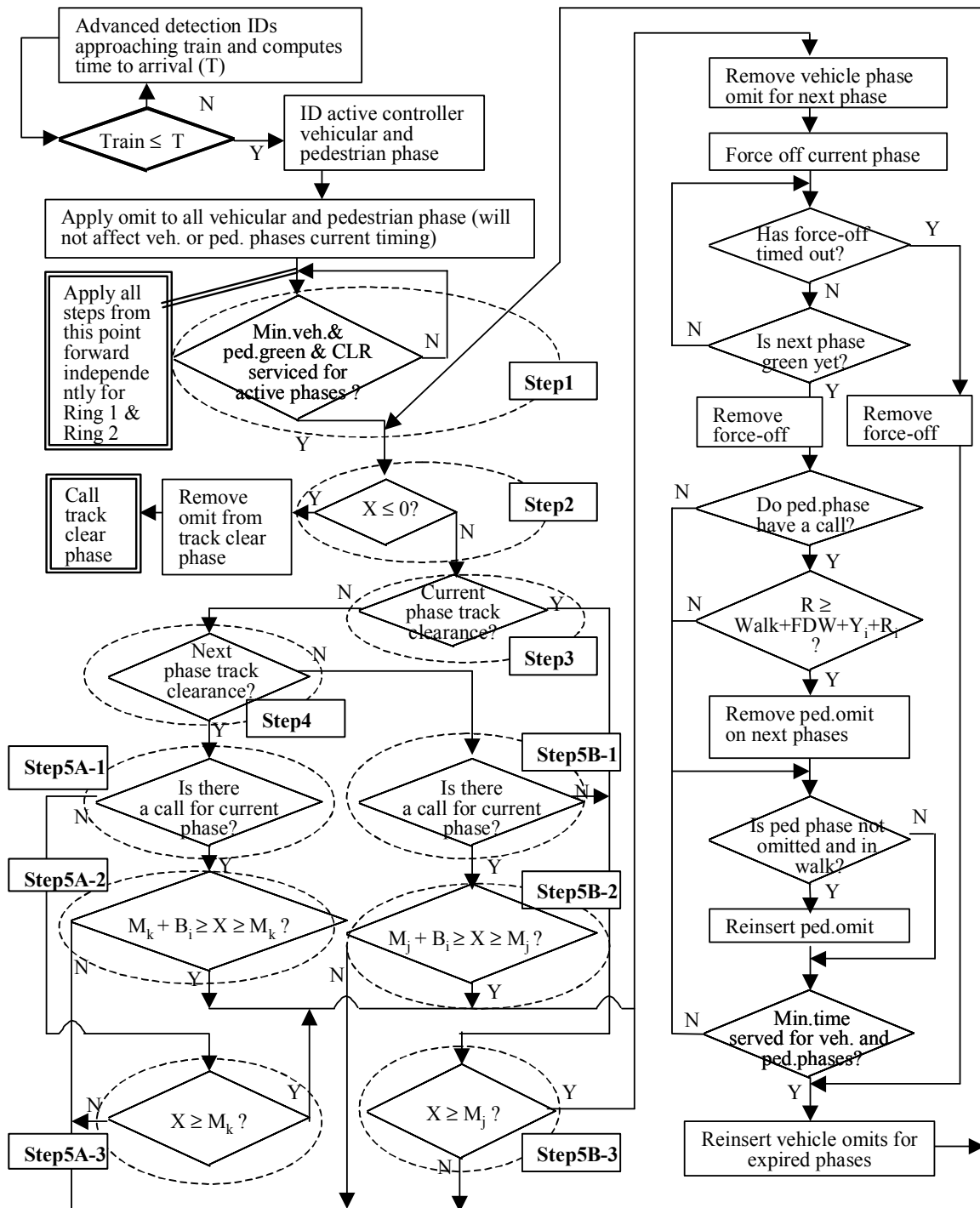


FIGURE B-1 Flow Chart of the Current TPS Algorithm

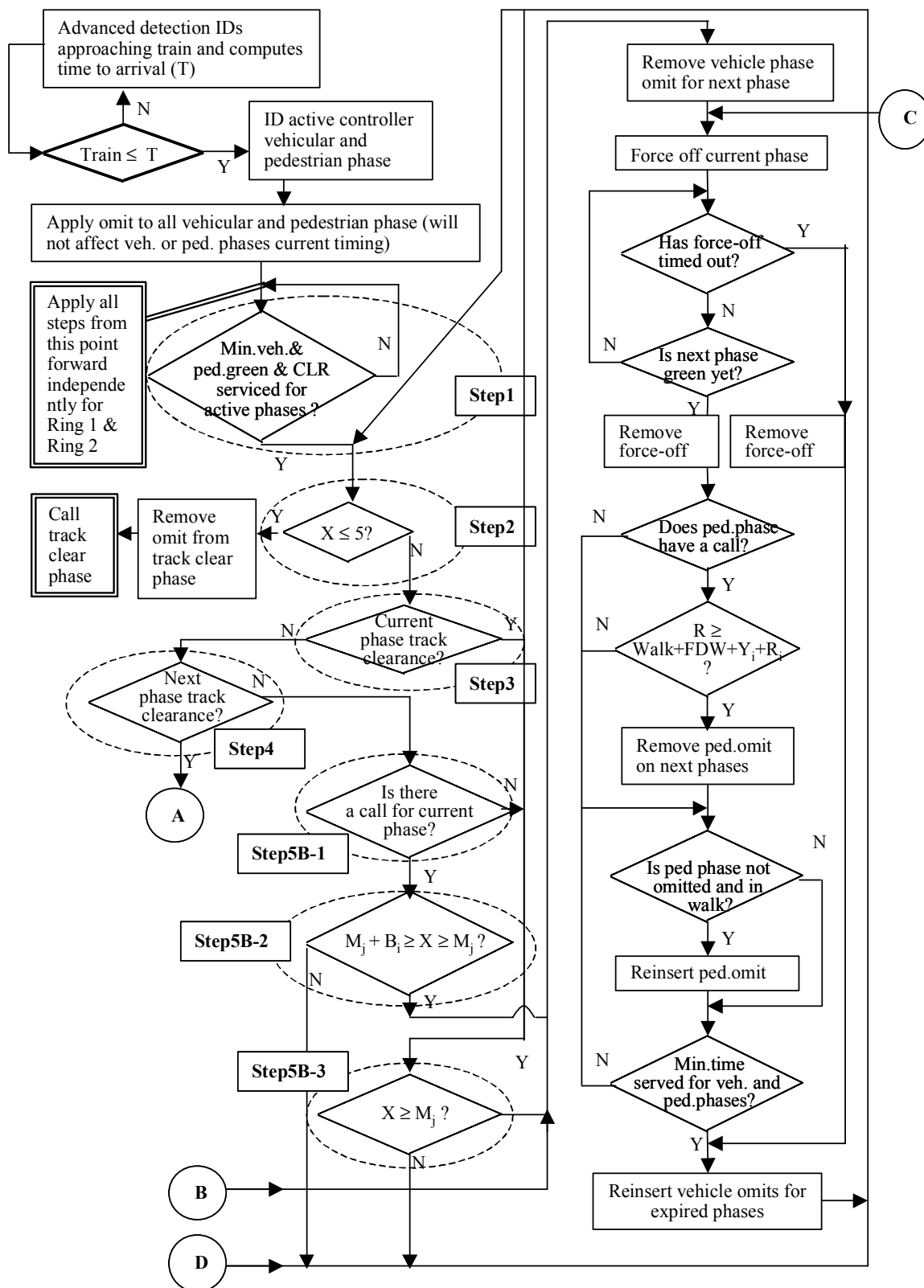
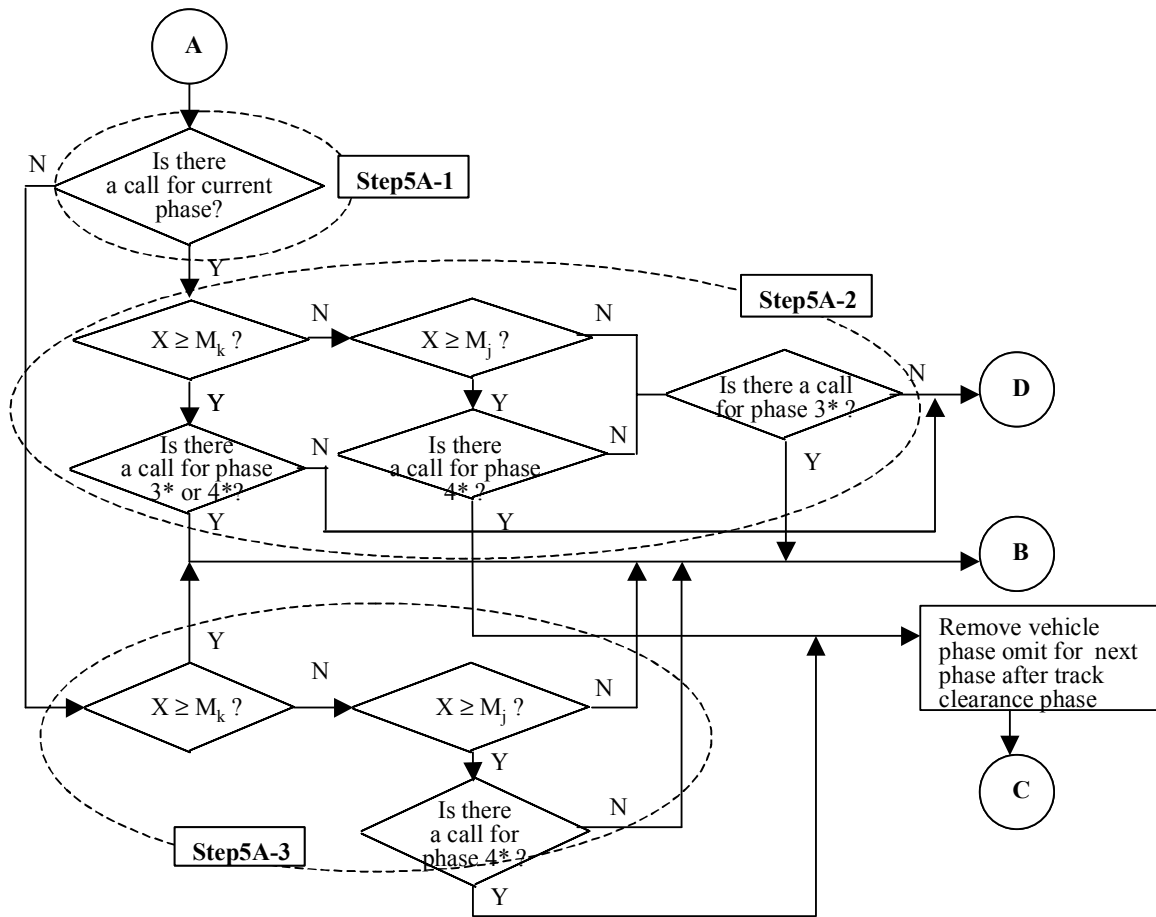


FIGURE B-2 Flow Chart of the TPS2 Algorithm



Phase 3*: Track clearance phase

Phase 4*: Opposite phase of track clearance phase for 4-leg intersection and blocked phase during preemption phase for 3-leg intersection

FIGURE B-2 Continued

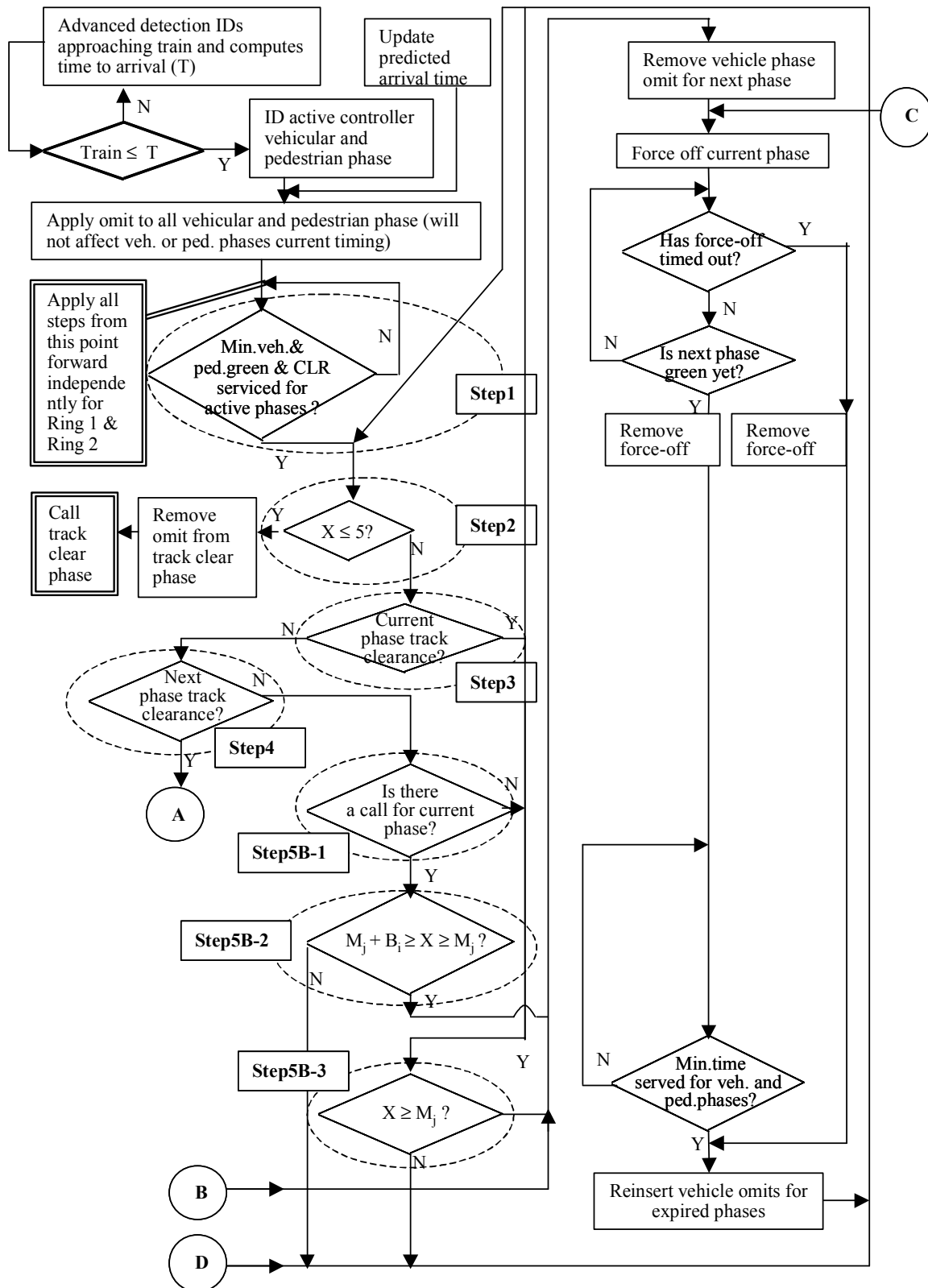
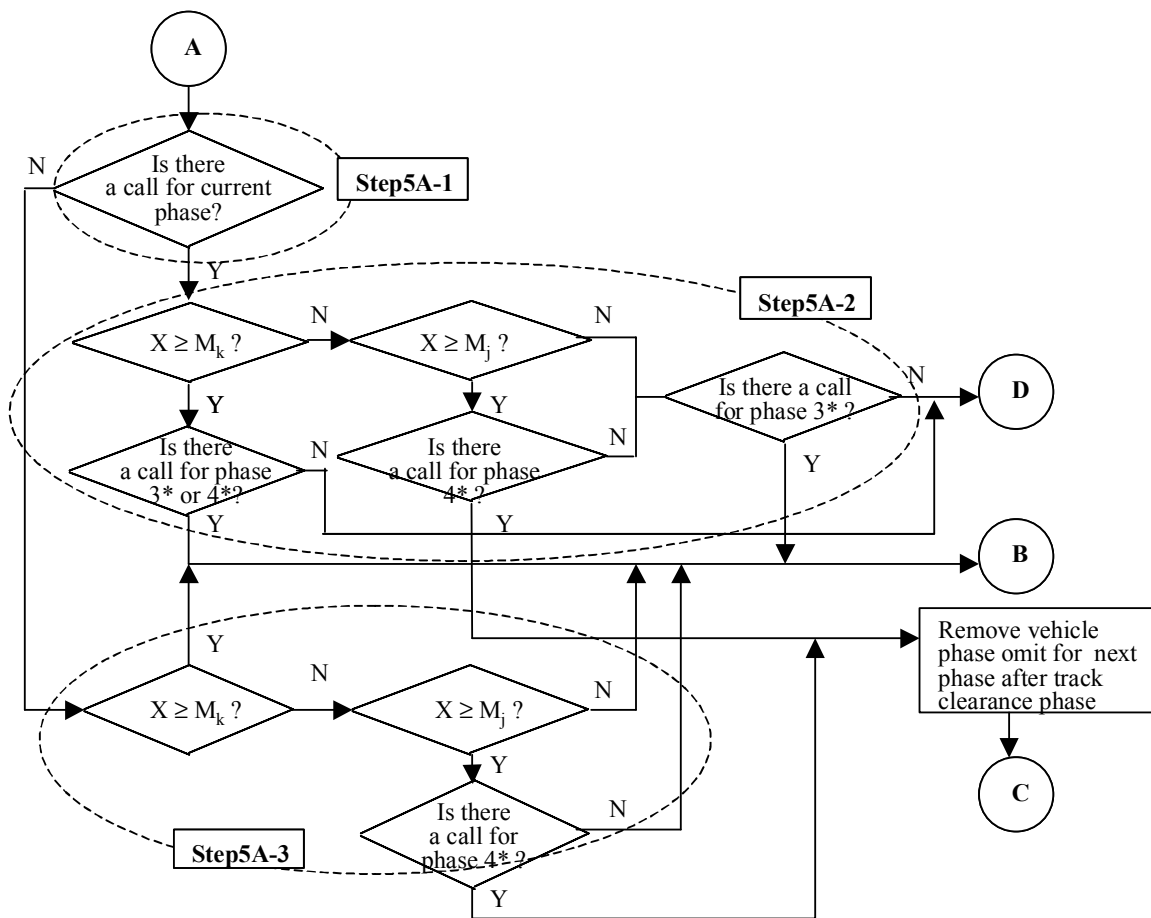


FIGURE B-3 Flow Chart of the TPS3 Algorithm



Phase 3*: Track clearance phase
 Phase 4*: Opposite phase of track clearance phase for 4-leg intersection and blocked phase during preemption phase for 3-leg intersection

FIGURE B-3 Continued

APPENDIX C

FIXED TRAIN ARRIVAL TIME

C.1 PHASE LENGTH RESULTS

TABLE C-1 Total Phase Length versus APWT and TPS Algorithms during Analysis Period¹ for Pedestrian Phase Active Scenario and Fixed Train Arrival Time

APWT ²	TPS Scenario	Phase 1 (second)	Phase 2 (second)	Phase 3 (second)	Phase 4 (second)	Phase 5 (second)	Phase 6 (second)
	TPS0	457	1069	665	522	368	1145
40	TPS1	457	1069	665	522	368	1145
	TPS2	457	1069	665	522	368	1145
	TPS3	457	1069	665	522	368	1145
50	TPS1	457	1071	666	522	368	1146
	TPS2	457	1071	666	522	368	1146
	TPS3	457	1070	666	522	368	1145
60	TPS1	456	1073	665	522	368	1148
	TPS2	456	1073	666	522	368	1147
	TPS3	457	1069	666	522	368	1145
70	TPS1	457	1073	663	523	368	1148
	TPS2	457	1073	664	523	369	1147
	TPS3	457	1070	665	523	369	1145
80	TPS1	457	1073	661	524	369	1148
	TPS2	457	1073	662	524	369	1147
	TPS3	457	1073	661	523	369	1148
90	TPS1	456	1078	662	524	367	1152
	TPS2	457	1073	662	524	368	1147
	TPS3	457	1074	659	524	369	1149
100	TPS1	455	1081	663	524	366	1155
	TPS2	457	1071	662	524	368	1146
	TPS3	459	1072	657	525	368	1149
110	TPS1	454	1085	663	523	366	1158
	TPS2	458	1065	663	527	369	1140
	TPS3	461	1072	653	524	369	1149
120	TPS1	454	1082	662	524	367	1155
	TPS2	459	1063	662	527	370	1138
	TPS3	463	1070	651	524	371	1148

¹: 6 to 60 minutes

²: Advance preemption warning time

TABLE C-2 Total Phase Length versus APWT and TPS Algorithms during Analysis Period¹ for Pedestrian Phase Inactive Scenario and Fixed Train Arrival Time

APWT ²	TPS Scenario	Phase 1 (second)	Phase 2 (second)	Phase 3 (second)	Phase 4 (second)	Phase 5 (second)	Phase 6 (second)
	TPS0	461	1060	666	523	366	1142
40	TPS1	461	1060	666	523	366	1142
	TPS2	461	1060	666	523	366	1142
	TPS3	461	1060	666	523	366	1142
50	TPS1	461	1061	668	523	366	1142
	TPS2	461	1061	668	523	366	1142
	TPS3	461	1060	667	523	366	1141
60	TPS1	461	1060	667	523	366	1142
	TPS2	461	1060	667	523	366	1141
	TPS3	461	1060	667	523	366	1142
70	TPS1	461	1063	661	525	366	1144
	TPS2	461	1062	662	526	366	1143
	TPS3	461	1063	664	523	366	1144
80	TPS1	462	1064	655	526	367	1146
	TPS2	462	1063	657	526	367	1144
	TPS3	462	1063	659	524	366	1145
90	TPS1	463	1065	653	525	367	1147
	TPS2	463	1064	653	526	367	1146
	TPS3	464	1062	655	525	367	1145
100	TPS1	462	1067	653	526	367	1149
	TPS2	464	1061	653	527	368	1143
	TPS3	464	1062	652	525	367	1146
110	TPS1	461	1069	653	526	367	1150
	TPS2	467	1056	654	525	370	1140
	TPS3	466	1060	652	525	367	1144
120	TPS1	459	1074	652	525	365	1155
	TPS2	469	1053	654	526	371	1137
	TPS3	467	1057	653	525	369	1141

¹: 6 to 60 minutes

²: Advance preemption warning time

C.2 DELAY RESULTS

C.2.1 Effect of TPS Algorithm

C.2.1.1 Delay Comparison Period; Pedestrian Phase Active Scenario

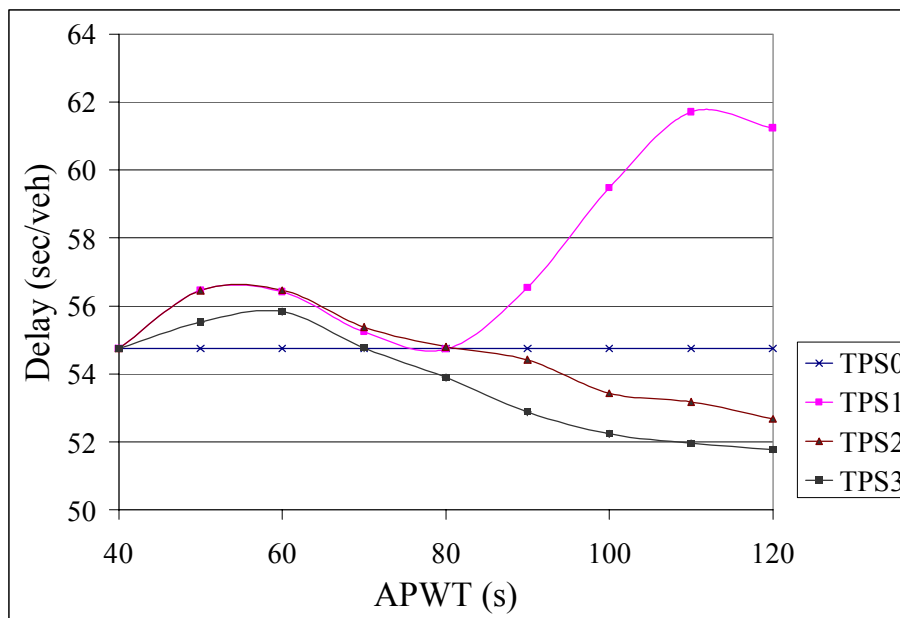


FIGURE C-1 Average Delay versus APWT for each TPS Algorithm (Delay Comparison Period; Pedestrian Phase Active Scenario; and Fixed Train Arrival Time)

C.2.1.2 Analysis Period; Pedestrian Phase Active Scenario

TABLE C-3 Average Delay (Analysis Period¹; Pedestrian Phase Active Scenario; and Fixed Train Arrival Time)

APWT ²	TPS0 (sec/veh)	TPS1 (sec/veh)	TPS2 (sec/veh)	TPS3 (sec/veh)
	50.9			
40		50.9	50.9	50.9
50		51.5	51.5	51.0
60		51.5	51.6	51.1
70		51.1	51.1	50.9
80		50.9	51.0	50.7
90		52.0	51.0	50.5
100		53.1	50.8	50.5*
110		53.4	50.1	50.8*
120		52.5	49.8	50.7*
Mean	50.9	51.9	50.9	50.8

¹: 6 to 60 minutes

²: Advance preemption warning time

*: Recommended APWT based on safety analyses

Bold: Minimum delay for each TPS algorithm

It can be seen that the average delay for the base case (TPS0) was 50.9 sec/veh. As shown in Table 6-6 there was also a safety problem in all 90 simulations. The average delay for the TPS1 algorithm across all the APWT scenarios was 51.9 sec/veh. The smallest average delay was 50.9 sec/veh and occurred at APWT values of 40 and 80 seconds. However, for these APWT values there was a safety problem in 90 and 5 out of the 90 preemption cases, respectively, as shown in Table 6-6. When the TPS2 algorithm is used, the lowest average delay was 49.8 sec/veh and occurred at an APWT value of 120 seconds. This is 0.7 second smaller than the TPS3 algorithm, which had its lowest value at an APWT value of 90 or 100 seconds. However, there was still a safety problem in 5 out of the 90 preemption cases. When the TPS3 algorithm is used, the minimum delay for the analysis period was found for 50.5 sec/veh at APWT values of 90 and 100 seconds. However, because there is one truncation of pedestrian clearance

interval at an APWT value of 90 seconds, it should be excluded as an option. Therefore, when the TPS3 algorithm is applied with an APWT value of 100 seconds, the intersection can be operated safely and efficiently showing improvement of 0.4 sec/veh compared to both the TPS0 and TPS1 algorithms.

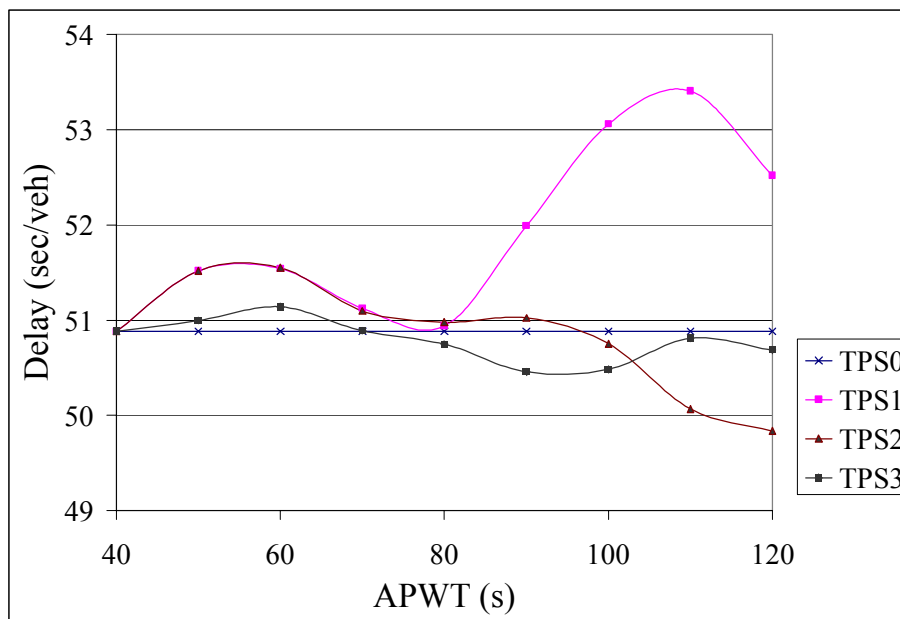


FIGURE C-2 Average Delay versus APWT for each TPS Algorithm (Analysis Period; Pedestrian Phase Active Scenario; and Fixed Train Arrival Time)

TABLE C-4 Results of Duncan Test between TPS Algorithms (Analysis Period¹; Pedestrian Phase Active Scenario; and Fixed Train Arrival Time)

APWT ²	Algorithm Comparison		Mean (sec/veh)		Test Statistic	Critical Value	Result
	Algo.1	Algo.2	Algo.1	Algo.2			
50	TPS0	TPS1	50.9	51.5	0.63	0.45	Reject H ₀ ³
	TPS0	TPS1	50.9	51.5	0.63	0.43	Reject H ₀
	TPS3	TPS1	51.0	51.5	0.52	0.43	Reject H ₀
	TPS3	TPS2	51.0	51.5	0.52	0.42	Reject H ₀
60	TPS0	TPS2	50.9	51.6	0.67	0.61	Reject H ₀
	TPS0	TPS1	50.9	51.5	0.66	0.59	Reject H ₀
90	TPS3	TPS1	50.5	52.0	1.53	1.18	Reject H ₀
100	TPS3	TPS1	50.5	53.1	2.58	1.14	Reject H ₀
	TPS2	TPS1	50.8	53.1	2.31	1.11	Reject H ₀
	TPS0	TPS1	50.9	53.1	2.18	1.07	Reject H ₀
110	TPS2	TPS1	50.1	53.4	3.34	1.00	Reject H ₀
	TPS3	TPS1	50.8	53.4	2.59	0.98	Reject H ₀
	TPS0	TPS1	50.9	53.4	2.52	0.94	Reject H ₀
120	TPS2	TPS1	49.8	52.5	2.68	0.92	Reject H ₀
	TPS2	TPS0	49.8	50.9	1.05	0.89	Reject H ₀
	TPS3	TPS1	50.7	52.5	1.83	0.89	Reject H ₀
	TPS0	TPS1	50.9	52.5	1.64	0.86	Reject H ₀

¹: 6 to 60 minutes

²: Advance preemption warning time

³: Statistically different between two means at 0.01 level of significance

Seventeen out of a possible 54 were found to be significant for the analysis period using a standard paired t-test. It was found that the delay in the TPS3 algorithm is smaller than the delay in the TPS1 algorithm at APWT values of 50, 90, 100, 110, and 120 seconds. Interestingly, there was no evidence statistically that the delay in the TPS3 algorithm is smaller than the delay in the TPS0 algorithm regardless of the APWT. However, the TPS3 algorithm has a benefit in terms of both safety and delay compared to the TPS1 algorithm at APWT values of 50, 90, 100, 110, and 120 seconds.

As discussed in Section 6.2.1, the best values of APWT from a safety perspective were 100, 110, and 120 seconds. It was found that there is no difference statistically at the 0.03 level of significance in delay among these values. Therefore, it can be concluded that the TPS3 algorithm with any APWT among 100, 110, and 120 seconds can provide the same level of safety and delay.

A comparison among the best delays identified for each of the TPS algorithms also was performed. It was found that the best delay in the TPS3 algorithm was not statistically smaller than both the delay in the TPS0 algorithm and the best delay identified for the TPS1 algorithm at the 0.06 level of significance

Therefore, it can be concluded that even if the delay in the TPS3 algorithm with APWT values of 100, 110, or 120 seconds did not decrease compared to the best delay identified for the TPS0, TPS1, and TPS2 algorithms, respectively, safety problems can be solved with the TPS3 algorithm with 100, 110, or 120 seconds during the analysis period, that is, during 54 minutes before and after preemption.

C.2.1.3 Delay Comparison Period; Pedestrian Phase Inactive Scenario

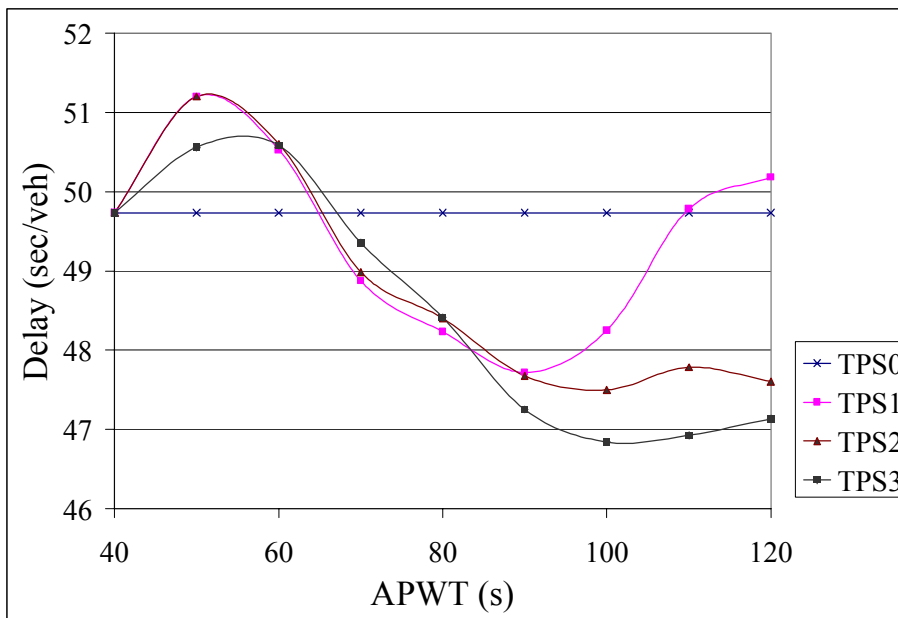


FIGURE C-3 Average Delay versus APWT for each TPS Algorithm (Delay Comparison Period; Pedestrian Phase Inactive Scenario; and Fixed Train Arrival Time)

C.2.1.4 Analysis Period; Pedestrian Phase Inactive Scenario

TABLE C-5 Average Delay (Analysis Period¹; Pedestrian Phase Inactive Scenario; and Fixed Train Arrival Time)

APWT ²	TPS0 (sec/veh)	TPS1 (sec/veh)	TPS2 (sec/veh)	TPS3 (sec/veh)
	42.5			
40		42.5	42.5	42.5
50		42.9	42.9	42.6
60		42.6	42.6	42.7
70		42.3	42.3	42.6
80		42.3	42.3	42.3
90		42.1	42.2	42.0
100		42.2	42.2	41.9
110		42.5	42.2	41.9
120		42.8	42.0	42.0
Mean	42.5	42.5	42.3	42.3

¹: 6 to 60 minutes

²: Advance preemption warning time

Bold: Minimum delay for each TPS algorithm

For the pedestrian phase inactive scenario, the average delay for the base case (TPS0) was 42.5 sec/veh and there was no safety problem at all because there were no pedestrians during the simulations. When the TPS1 algorithm was used, the lowest average delay was 42.1 sec/veh and occurred at an APWT value of 90 seconds. When the TPS2 algorithm was used, the lowest average delay was 42.0 sec/veh and occurred at an APWT value of 120 seconds. When TPS3 was applied with APWT values of 100 or 110 seconds, the average delay was a minimum of 41.9 sec/veh. Difference in delay between APWT scenarios was relatively small in each TPS algorithm compared to the pedestrian phase active scenario. Maximum difference in delay was 0.8 second for the TPS1 algorithm, 0.9 second for the TPS2 algorithm, and 0.8 second for the TPS3 algorithm. The best TPS3 algorithm delay was 0.6, 0.2, and 0.1 second lower than the best delay identified for the TPS0, TPS1, and TPS2 algorithms, respectively. Therefore,

it can be concluded that the effect of the TPS algorithms and the APWT on delay decreases considerably when there is no pedestrian in the intersection.

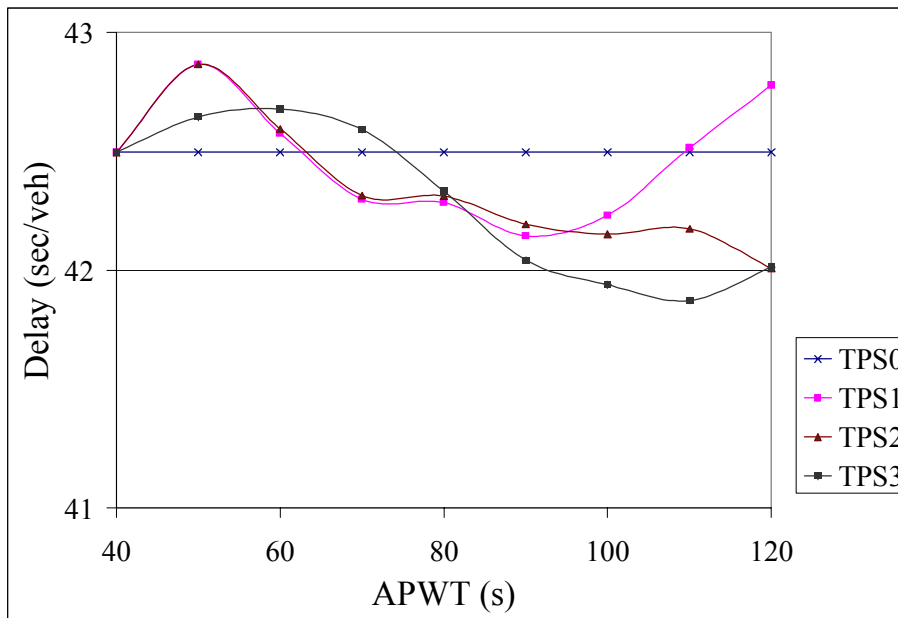


FIGURE C-4 Average Delay versus APWT for each TPS Algorithm (Analysis Period; Pedestrian Phase Inactive Scenario; and Fixed Train Arrival Time)

TABLE C-6 Results of Duncan Test between TPS Algorithms (Analysis Period¹; Pedestrian Phase Inactive Scenario; and Fixed Train Arrival Time)

APWT ²	Algorithm Comparison		Mean (sec/veh)		Test Statistic	Critical Value	Result
	Algo.1	Algo.2	Algo.1	Algo.2			
50	TPS0	TPS1	42.5	42.9	0.37	0.29	Reject H ₀ ³
	TPS0	TPS1	42.5	42.9	0.37	0.29	Reject H ₀
100	TPS3	TPS0	41.9	42.5	0.56	0.44	Reject H ₀
110	TPS3	TPS1	41.9	42.5	0.64	0.51	Reject H ₀
	TPS3	TPS0	41.9	42.5	0.62	0.50	Reject H ₀
120	TPS2	TPS1	42.0	42.8	0.77	0.57	Reject H ₀
	TPS3	TPS1	42.0	42.8	0.77	0.56	Reject H ₀

¹: 6 to 60 minutes

²: Advance preemption warning time

³: Statistically different between two means at 0.01 level of significance

Seven out of a possible 54 were found to be significant for the analysis period using a standard paired t-test. For the pedestrian phase inactive scenario, it was found that the delay in the TPS3 algorithm is smaller than the delay in the TPS0 algorithm at APWT values of 100 and 110 seconds and than the delay in the TPS1 algorithm at APWT values of 110 and 120 seconds.

A comparison among the best delays identified for each of TPS algorithms also was performed. It also was found that the best delay in the TPS3 algorithm is smaller statistically at the 0.06 level of significance than the delay in the TPS0 algorithm; however, it is not different from the delay in the TPS1 algorithm.

Therefore, it can be concluded that even if the effect of the TPS algorithms and the APWT on delay decreases considerably when there is no pedestrian in the intersection, the TPS3 algorithm with APWT value of 100 or 110 seconds can decrease the delay compared to the TPS0 algorithm even at the condition where there is no safety problem originally.

C.2.2 Effect of Pedestrian

TABLE C-7 Average Delay of Each Movement for APWT and TPS Algorithms (Analysis Period¹; Pedestrian Phase Active Scenario; and Fixed Train Arrival Time)

T P S	AP WT ²	SB (sec/veh)				EB (sec/veh)				NB (sec/veh)				WB (sec/veh)				TOT AL
		LT	TH	RT	SUM	LT	TH	RT	SUM	LT	TH	RT	SUM	LT	TH	RT	SUM	
0	40	115	34	41	59	49	60	66	60	50	31	34	35	59	58	15	48	50.9
1	40	115	34	41	59	49	60	66	60	50	31	34	35	59	58	15	48	50.9
	50	115	34	41	59	50	61	68	61	50	31	34	35	60	60	15	50	51.5
	60	115	34	41	59	50	62	68	62	50	31	34	35	60	60	15	50	51.5
	70	111	34	41	58	51	62	68	62	50	31	34	35	60	59	15	49	51.1
	80	110	34	41	57	51	61	68	62	49	31	34	34	59	59	15	49	50.9
	90	112	34	41	58	52	64	71	64	49	31	34	34	61	61	16	51	52.0
	100	114	34	41	58	53	66	74	66	50	31	34	34	63	63	16	52	53.1
	110	114	34	41	58	53	66	74	66	50	31	34	34	65	65	16	54	53.4
120	114	34	41	58	51	63	69	63	50	31	34	34	64	64	16	53	52.5	
2	40	115	34	41	59	49	60	66	60	50	31	34	35	59	58	15	48	50.9
	50	115	34	41	59	50	61	68	61	50	31	34	35	60	60	15	50	51.5
	60	115	34	41	59	50	62	67	62	50	31	34	35	61	60	15	50	51.6
	70	111	34	41	58	51	62	68	62	50	31	34	35	60	59	15	49	51.1
	80	110	34	41	57	51	62	68	62	50	31	34	34	60	59	15	49	51.0
	90	111	34	41	58	51	62	68	62	49	31	33	34	59	59	15	49	51.0
	100	112	34	41	58	51	61	68	62	49	31	34	34	58	57	15	48	50.8
	110	111	34	42	58	49	59	65	59	49	31	34	34	57	56	14	47	50.1
120	111	34	42	58	48	58	64	58	49	31	34	34	57	56	14	47	49.8	
3	40	115	34	41	59	49	60	66	60	50	31	34	35	59	58	15	48	50.9
	50	115	34	41	59	49	60	66	60	50	31	34	35	60	59	15	49	51.0
	60	114	34	41	59	49	60	66	60	50	31	34	35	60	59	15	49	51.1
	70	114	34	41	58	49	61	67	61	50	31	34	34	59	58	15	48	50.9
	80	112	34	41	58	50	61	67	61	50	31	34	34	58	58	15	48	50.7
	90	110	34	41	57	51	61	68	61	49	30	34	34	58	57	15	47	50.5
	100	113	34	41	58	50	61	68	61	48	30	33	34	57	56	14	47	50.5
	110	114	34	41	58	51	62	69	62	46	30	33	34	58	57	14	48	50.8
120	113	34	41	58	50	62	68	62	45	30	33	33	58	58	15	48	50.7	

¹: 6 to 60 minutes

²: Advance preemption warning time

TABLE C-8 Average Delay of Each Movement for APWT and TPS Algorithms (Analysis Period¹; Pedestrian Phase Inactive Scenario; and Fixed Train Arrival Time)

TPS	APWT ²	SB (sec/veh)				EB (sec/veh)				NB (sec/veh)				WB (sec/veh)				TOTAL
		L T	T H	R T	S U M	L T	T H	R T	S U M	L T	T H	R T	S U M	L T	T H	R T	S U M	
0	40	68	33	33	44	44	49	43	47	47	30	26	32	58	57	10	46	42.5
1	40	68	33	33	44	44	49	43	47	47	30	26	32	58	57	10	46	42.5
	50	69	33	33	44	44	49	43	47	48	30	26	32	59	58	10	48	42.9
	60	68	33	33	43	44	49	43	47	47	30	26	32	58	58	10	47	42.6
	70	68	33	33	43	45	49	43	47	47	30	26	32	57	56	10	46	42.3
	80	68	33	32	43	45	50	44	48	45	30	26	32	57	56	10	46	42.3
	90	68	33	32	43	44	49	44	48	44	30	26	32	57	56	10	46	42.1
	100	69	33	32	43	45	50	44	48	45	30	26	32	57	56	10	46	42.2
	110	69	33	32	43	45	50	44	48	46	30	26	32	58	57	10	46	42.5
	120	69	33	32	44	45	50	44	48	46	30	26	32	58	58	10	47	42.8
2	40	68	33	33	44	44	49	43	47	47	30	26	32	58	57	10	46	42.5
	50	69	33	33	44	44	49	43	47	48	30	26	32	59	58	10	48	42.9
	60	68	33	33	43	44	49	43	47	47	30	26	32	58	58	10	47	42.6
	70	68	33	33	43	45	49	43	47	47	30	26	32	57	56	10	46	42.3
	80	68	33	33	43	45	50	43	48	45	30	26	32	57	56	10	46	42.3
	90	68	33	33	43	45	50	44	48	44	30	26	32	56	56	10	45	42.2
	100	69	33	33	44	45	50	44	48	44	30	26	32	56	55	10	45	42.2
	110	69	33	33	44	44	49	43	47	42	30	26	31	56	56	10	46	42.2
	120	68	33	33	43	44	49	43	47	42	30	26	31	56	56	10	45	42.0
3	40	68	33	33	44	44	49	43	47	47	30	26	32	58	57	10	46	42.5
	50	69	33	33	44	44	49	43	47	48	30	26	32	58	57	10	47	42.6
	60	68	33	33	44	44	49	43	47	47	30	26	33	58	58	10	47	42.7
	70	69	33	33	44	45	49	43	47	47	30	26	32	58	57	10	46	42.6
	80	68	33	33	43	44	49	43	48	46	30	26	32	57	56	10	46	42.3
	90	68	33	33	43	44	49	43	47	44	30	26	32	56	55	10	45	42.0
	100	68	33	33	43	45	49	43	48	43	30	26	31	56	55	10	45	41.9
	110	68	33	33	43	45	49	43	48	43	30	26	31	56	55	10	45	41.9
	120	68	33	32	43	45	49	43	48	42	30	25	31	56	56	10	45	42.0

¹: 6 to 60 minutes

²: Advance preemption warning time

C.2.3 Effect of Train Speed Profile

C.2.3.1 Delay Comparison Period; Pedestrian Phase Active Scenario

TABLE C-9 Average Delay by Group and APWT (Delay Comparison Period¹; Pedestrian Phase Active Scenario; and Fixed Train Arrival Time)

APWT ²	Train Group	TPS0 (sec/veh)	TPS1 (sec/veh)	TPS2 (sec/veh)	TPS3 (sec/veh)	Ave. By Group	Ave.
40	Group 1	60.4	60.4	60.4	60.4	60.4	54.7
	Group 2	53.9	53.9	53.9	53.9	53.9	
	Group 3	49.9	49.9	49.9	49.9	49.9	
50	Group 1		63.9	63.9	62.4	63.4	56.1
	Group 2		54.9	54.9	54.2	54.6	
	Group 3		50.6	50.6	50.0	50.4	
60	Group 1		63.7	63.8	63.0	63.5	56.2
	Group 2		54.6	54.6	54.2	54.5	
	Group 3		51.0	51.0	50.3	50.7	
70	Group 1		62.2	62.6	61.1	61.9	55.1
	Group 2		53.2	53.2	53.6	53.3	
	Group 3		50.3	50.3	49.6	50.1	
80	Group 1		61.8	62.0	59.7	61.2	54.5
	Group 2		53.0	53.1	52.7	53.0	
	Group 3		49.3	49.3	49.2	49.3	
90	Group 1		64.5	62.2	58.6	61.8	54.6
	Group 2		55.4	52.4	52.0	53.3	
	Group 3		49.7	48.7	48.0	48.8	
100	Group 1		68.0	60.4	58.3	62.2	55.1
	Group 2		58.1	51.8	50.8	53.5	
	Group 3		52.3	48.2	47.7	49.4	
110	Group 1		68.7	59.7	58.2	62.2	55.6
	Group 2		61.6	51.8	50.2	54.5	
	Group 3		54.8	48.1	47.5	50.1	
120	Group 1		67.9	58.8	58.1	61.6	55.2
	Group 2		61.1	51.4	49.7	54.1	
	Group 3		54.8	47.8	47.5	50.0	
Ave. By Group	Group 1	60.4	64.6	61.5	60.0	61.6	55.1
	Group 2	53.9	56.2	53.0	52.4	53.9	
	Group 3	49.9	51.4	49.3	48.9	49.9	
Average		54.7	57.4	54.6	53.7	55.1	

¹: 600 to 1320 seconds

²: Advance preemption warning time

C.2.3.2 Analysis Period; Pedestrian Phase Active Scenario

TABLE C-10 Average Delay by Group and APWT (Analysis Period¹; Pedestrian Phase Active Scenario; and Fixed Train Arrival Time)

APWT ²	Train Group	TPS0 (sec/veh)	TPS1 (sec/veh)	TPS2 (sec/veh)	TPS3 (sec/veh)	Ave. By Group	Ave.
40	Group 1	52.2	52.2	52.2	52.2	52.2	50.9
	Group 2	52.7	52.7	52.7	52.7	52.7	
	Group 3	47.7	47.7	47.7	47.7	47.7	
50	Group 1		53.3	53.3	52.5	53.1	51.3
	Group 2		53.1	53.1	52.7	53.0	
	Group 3		48.1	48.1	47.7	48.0	
60	Group 1		53.6	53.6	52.9	53.4	51.4
	Group 2		53.1	53.1	52.7	53.0	
	Group 3		47.9	47.9	47.9	47.9	
70	Group 1		52.8	52.8	52.7	52.8	51.0
	Group 2		52.3	52.3	52.3	52.3	
	Group 3		48.3	48.3	47.6	48.1	
80	Group 1		52.5	52.6	52.3	52.4	50.9
	Group 2		52.3	52.3	52.0	52.2	
	Group 3		48.0	48.0	48.0	48.0	
90	Group 1		54.0	53.2	51.9	53.0	51.2
	Group 2		53.2	52.2	51.7	52.3	
	Group 3		48.9	47.7	47.8	48.1	
100	Group 1		55.2	52.7	51.8	53.2	51.4
	Group 2		54.0	52.0	52.1	52.7	
	Group 3		49.9	47.6	47.6	48.4	
110	Group 1		54.8	51.2	52.1	52.7	51.4
	Group 2		54.5	51.2	52.2	52.6	
	Group 3		50.9	47.8	48.2	49.0	
120	Group 1		53.2	50.9	52.2	52.1	51.0
	Group 2		54.3	51.2	52.2	52.5	
	Group 3		50.0	47.4	47.7	48.4	
Ave. By Group	Group 1	52.2	53.5	52.5	52.3	52.6	51.1
	Group 2	52.7	53.3	52.2	52.3	52.6	
	Group 3	47.7	48.9	47.8	47.8	48.1	
Average		50.9	51.9	50.9	50.8	51.1	

¹: 6 to 60 minutes²: Advance preemption warning time

TABLE C-11 Average Delay by Group (Analysis Period¹; Pedestrian Phase Active Scenario; and Fixed Train Arrival Time)

	Train Group	TPS0 (sec/veh)	TPS1 (sec/veh)	TPS2 (sec/veh)	TPS3 (sec/veh)	Average
Average By Group	Group 1	52.2	53.5	52.5	52.3	52.7
	Group 2	52.7	53.3	52.2	52.3	52.6
	Group 3	47.7	48.9	47.8	47.8	48.2
Average		50.9	51.9	50.9	50.8	51.1

¹: 6 to 60 minutes

In all of the TPS algorithms, Group 3 has the smallest delay with an average of 48.2 sec/veh, and Group 1 has the largest delay with an average of 52.7 sec/veh. The difference in delay between Group 1 and Group 3 was 4.5 sec/veh for the TPS0 algorithm, 4.6 sec/veh for the TPS1 algorithm, 4.7 sec/veh for the TPS2 algorithm, and 4.5 sec/veh for the TPS3 algorithm. Interestingly, the average delay of Group 2 is almost the same as the average delay of Group 1, even though the average train speed of Group 2 at FM 2818 is 11 km/h higher than that of Group 1 as mentioned in Section 6.1.

TABLE C-12 Results of Duncan Test between Train Speed Groups (Analysis Period¹; Pedestrian Phase Active Scenario; and Fixed Train Arrival Time)

Group Comparison		Mean (sec/veh)		Test Statistic	Critical Value	Result
		1 st Group	2 nd Group			
Group3	Group1	48.2	52.7	4.60	0.81	Reject H ₀ ²
Group3	Group2	48.2	52.6	4.44	0.78	Reject H ₀
Group2	Group1	52.6	52.7	0.15	0.78	Do not Reject H ₀

¹: 6 to 60 minutes

²: Statistically different between two means at 0.01 level of significance

It was found that the delay in Group 3 is smaller than the delay in Groups 1 and 2 and that the delay in Group 1 is the same as the delay in Group 2. Therefore, it is difficult to

conclude that there is a relationship between the train speed and the intersection delay for evaluation of the analysis period.

C.2.3.3 Delay Comparison Period; Pedestrian Phase Inactive Scenario

TABLE C-13 Average Delay by Group and APWT (Delay Comparison Period¹; Pedestrian Phase Inactive Scenario; and Fixed Train Arrival Time)

APWT ²	Train Group	TPS0 (sec/veh)	TPS1 (sec/veh)	TPS2 (sec/veh)	TPS3 (sec/veh)	Ave. By Group	Ave.
40	Group 1	55.6	55.6	55.6	55.6	55.6	49.7
	Group 2	49.1	49.1	49.1	49.1	49.1	
	Group 3	44.6	44.6	44.6	44.6	44.6	
50	Group 1		58.4	58.4	57.7	58.2	51.0
	Group 2		49.9	49.9	49.4	49.7	
	Group 3		45.3	45.3	44.6	45.1	
60	Group 1		57.3	57.5	57.6	57.4	50.6
	Group 2		49.1	49.1	49.3	49.1	
	Group 3		45.3	45.3	44.8	45.1	
70	Group 1		55.0	55.3	55.2	55.2	49.1
	Group 2		47.7	47.7	48.9	48.1	
	Group 3		43.9	43.9	44.0	44.0	
80	Group 1		54.7	55.2	54.2	54.7	48.4
	Group 2		46.7	46.7	47.4	46.9	
	Group 3		43.3	43.3	43.6	43.4	
90	Group 1		53.9	53.9	53.0	53.6	47.5
	Group 2		46.3	46.2	46.1	46.2	
	Group 3		42.9	42.9	42.7	42.8	
100	Group 1		54.6	54.0	52.9	53.8	47.5
	Group 2		46.6	45.6	45.4	45.9	
	Group 3		43.6	42.9	42.3	42.9	
110	Group 1		55.2	54.5	53.1	54.3	48.2
	Group 2		49.5	45.9	45.4	46.9	
	Group 3		44.6	43.0	42.3	43.3	
120	Group 1		54.9	54.0	53.6	54.1	48.3
	Group 2		49.4	45.9	45.3	46.9	
	Group 3		46.2	42.9	42.5	43.9	
Ave. By Group	Group 1	55.6	55.5	55.4	54.8	55.3	49.1
	Group 2	49.1	48.2	47.3	47.4	48.0	
	Group 3	44.6	44.4	43.8	43.5	44.1	
Average		49.7	49.4	48.8	48.5	49.1	

¹: 600 to 1320 seconds²: Advance preemption warning time

C.2.3.4 Analysis Period; Pedestrian Phase Inactive Scenario

TABLE C-14 Average Delay by Group and APWT (Analysis Period¹; Pedestrian Phase Inactive Scenario; and Fixed Train Arrival Time)

APWT ²	Train Group	TPS0 (sec/veh)	TPS1 (sec/veh)	TPS2 (sec/veh)	TPS3 (sec/veh)	Ave. By Group	Ave.
40	Group 1	43.8	43.8	43.8	43.8	43.8	42.5
	Group 2	43.3	43.3	43.3	43.3	43.3	
	Group 3	40.4	40.4	40.4	40.4	40.4	
50	Group 1		44.5	44.5	44.2	44.4	42.8
	Group 2		43.6	43.6	43.3	43.5	
	Group 3		40.5	40.5	40.4	40.5	
60	Group 1		44.1	44.1	44.3	44.2	42.6
	Group 2		43.1	43.1	43.3	43.1	
	Group 3		40.6	40.6	40.5	40.5	
70	Group 1		43.5	43.6	43.7	43.6	42.4
	Group 2		42.8	42.8	43.7	43.1	
	Group 3		40.5	40.5	40.4	40.5	
80	Group 1		43.4	43.5	43.5	43.5	42.3
	Group 2		43.1	43.1	43.1	43.1	
	Group 3		40.4	40.4	40.4	40.4	
90	Group 1		43.5	43.6	43.3	43.4	42.1
	Group 2		42.4	42.4	42.8	42.5	
	Group 3		40.6	40.6	40.0	40.4	
100	Group 1		43.7	43.6	43.3	43.5	42.1
	Group 2		42.5	42.4	42.5	42.5	
	Group 3		40.5	40.4	40.1	40.3	
110	Group 1		43.6	43.6	43.3	43.5	42.2
	Group 2		43.5	42.4	42.2	42.7	
	Group 3		40.5	40.5	40.1	40.4	
120	Group 1		43.6	43.5	43.6	43.5	42.3
	Group 2		43.5	42.4	42.4	42.8	
	Group 3		41.3	40.1	40.1	40.5	
Ave. By Group	Group 1	43.8	43.7	43.7	43.7	43.7	42.4
	Group 2	43.3	43.1	42.8	42.9	43.0	
	Group 3	40.4	40.6	40.4	40.3	40.4	
Average		42.5	42.5	42.3	42.3	42.4	

¹: 6 to 60 minutes²: Advance preemption warning time

TABLE C-15 Average Delay by Group (Analysis Period¹; Pedestrian Phase Inactive Scenario; and Fixed Train Arrival Time)

	Train Group	TPS0 (sec/veh)	TPS1 (sec/veh)	TPS2 (sec/veh)	TPS3 (sec/veh)	Average
Average By Group	Group 1	43.8	43.7	43.7	43.7	43.7
	Group 2	43.3	43.1	42.8	42.9	43.0
	Group 3	40.4	40.6	40.4	40.3	40.4
Average		42.5	42.5	42.3	42.3	42.4

¹: 6 to 60 minutes

Although the delay is lessened in the pedestrian phase inactive scenario compared to the pedestrian phase active scenario, the trend is the same as the pedestrian phase active scenario. In all of the TPS algorithms, Group 3 has the smallest delay with an average of 40.4 sec/veh, and Group 1 has the largest delay with an average of 43.7 sec/veh. The difference in delay between Groups 1 and 3 was 3.4 sec/veh for the TPS0 algorithm, 3.1 sec/veh for the TPS1 algorithm, 3.3 sec/veh for the TPS2 algorithm, and 3.4 sec/veh for the TPS3 algorithm for the pedestrian phase inactive scenario. It also was found that the average delay of Group 2 is only 0.7 sec/veh smaller than that of Group 1, even though the average train speed of Group 2 is 11 km/h higher than that of Group 1.

TABLE C-16 Results of Duncan Test between Train Speed Groups (Analysis Period¹; Pedestrian Phase Inactive Scenario; and Fixed Train Arrival Time)

Group Comparison		Mean (sec/veh)		Test Statistic	Critical Value	Result
		1 st Group	2 nd Group			
Group3	Group1	40.4	43.7	3.27	0.49	Reject H ₀ ²
Group3	Group2	40.4	43.0	2.54	0.47	Reject H ₀
Group2	Group1	43.0	43.7	0.74	0.47	Reject H ₀

¹: 6 to 60 minutes

²: Statistically different between two means at 0.01 level of significance

It was found that the delay in Group 3 is smaller than the delay in Groups 1 and 2, and the delay in Group 2 is smaller than the delay in Group 1 for the pedestrian phase inactive scenario. Therefore, it can be concluded that as train speed increases, the intersection is operated more efficiently for the pedestrian phase inactive scenario.

APPENDIX D**RANDOM TRAIN ARRIVAL TIME**

D.1 TRUNCATION OF PEDESTRIAN CLEARANCE INTERVAL RESULTS

A preemption will be initiated any time in the cycle. Considering the simulation period and the analysis periods, trains are designed to arrive at the crossing between 845 and 966 seconds. The simulation period, the analysis period, and the train arrival time range at the crossing are shown in Figure D-1. This is to evaluate the effect of the TPS3 algorithm under the normal operating condition.

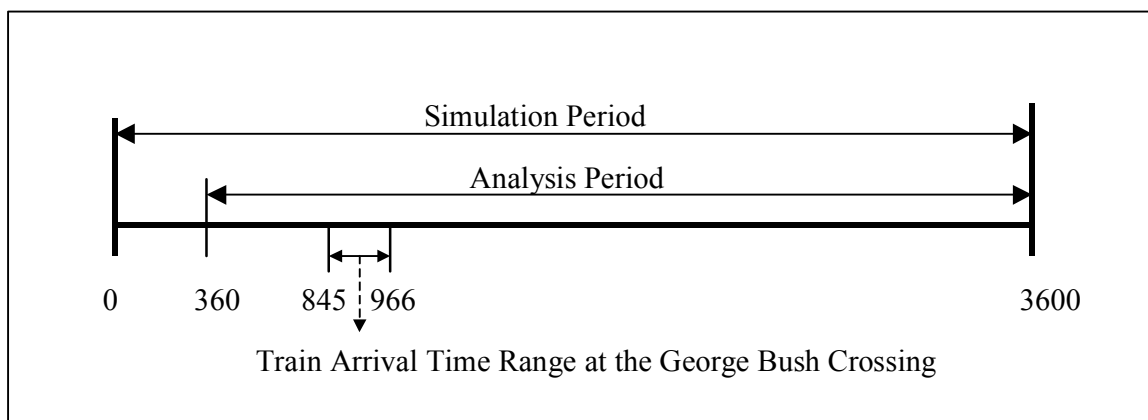


FIGURE D-1 Time Frame for Analysis Period and Train Arrival Time Range at the Crossing during Simulation for Random Train Arrival Time

The truncation number and abbreviation time of the pedestrian clearance interval also were measured to evaluate the safety of the intersection at the onset of preemption for each TPS algorithm. The results for the pedestrian phase active scenario are shown for each of the advance preemption warning times in Table D-1.

TABLE D-1 Number of Pedestrian Phase Truncations and Average Phase Abbreviation Time at the Onset of Preemption for Pedestrian Phase Active Scenario and Random Train Arrival Time

APWT*	TPS0 (sec/veh)	TPS1 (sec/veh)	TPS2 (sec/veh)	TPS3 (sec/veh)
	36(7)			
40		36(7)	36(7)	36(7)
50		33(7)	33(7)	35(7)
60		25(5)	25(5)	27(6)
70		7(4)	7(4)	18(5)
80		1(1)	1(1)	6(3)
90		0(0)	0(0)	0(0)
100		0(0)	0(0)	0(0)
110		0(0)	0(0)	0(0)
120		1(3)	2(3)	0(0)

*: Advance preemption warning time

(): Seconds of phase abbreviation.

Based on these results, once the APWT is 90 seconds or more, truncation does not occur except with the TPS1 and TPS2 algorithms at the APWT value of 120 seconds. However, in the worst case, that is, simulations that are designed to initiate preemption during a pedestrian clearance phase, the truncation still occurred 1 and 5 times out of 90 trains for the TPS1 and TPS2 algorithm, respectively. Even if the number of truncations decreased under the normal operating condition, the APWT should be decided based on the worst case. Therefore, the conclusion is the same as in Section 6.2, that is, at least the APWT value of 100 seconds with the TPS3 algorithm should be provided to eliminate the possibility of truncation of the pedestrian clearance time.

Even if there is no pedestrian volume in the simulations, because the coordinated signal timing is operated, the pedestrian phase corresponding to the coordinated phases are provided automatically whenever the coordinated phases are active, regardless of pedestrian calls. Therefore, the truncation of the pedestrian clearance interval can occur at the onset of preemption, even if these truncations do not affect the safety problem.

The truncation number and abbreviation time of the pedestrian clearance interval for the pedestrian phase inactive scenario are shown for each of the APWTs in Table D-2.

TABLE D-2 Number of Pedestrian Phase Truncations and Average Phase Abbreviation Time at the Onset of Preemption for Pedestrian Phase Inactive Scenario and Random Train Arrival Time

APWT*	TPS0 (sec/veh)	TPS1 (sec/veh)	TPS2 (sec/veh)	TPS3 (sec/veh)
	28(8)			
40		28(8)	28(8)	28(8)
50		27(7)	27(7)	28(7)
60		16(5)	16(5)	21(6)
70		6(2)	6(2)	12(4)
80		1(1)	1(1)	5(1)
90		0(0)	0(0)	0(0)
100		0(0)	0(0)	0(0)
110		0(0)	0(0)	0(0)
120		0(0)	0(0)	0(0)

*: Advance preemption warning time

(): Seconds of phase abbreviation

D.2 DELAY RESULTS

D.2.1 Effect of the TPS Algorithms

D.2.1.1 Delay Comparison Period; Pedestrian Phase Active Scenario

The average delay during the delay comparison period for the pedestrian phase active scenario is shown in Table D-3.

TABLE D-3 Average Delay (Delay Comparison Period¹; Pedestrian Phase Active Scenario; and Random Train Arrival Time)

APWT ²	TPS0 (sec/veh)	TPS1 (sec/veh)	TPS2 (sec/veh)	TPS3 (sec/veh)
	54.0			
40		54.0	54.0	54.0
50		54.3	54.3	54.1
60		54.0	54.0	54.1
70		53.7	53.8	53.8
80		53.8	53.8	53.6
90		54.1	53.4	53.1
100		54.8	53.1	52.4
110		56.3	52.9	51.5
120		56.0	52.5	51.1
Mean	54.0	54.6	53.5	53.1

¹: 600 to 1320 seconds

²: Advance preemption warning time

Bold: Minimum delay for each TPS algorithm

The best TPS3 algorithm delay (51.1 sec/veh) was 2.9, 2.6, and 1.4 seconds lower than the best delay identified for the TPS0, TPS1, and TPS2 algorithms, respectively. Therefore, when the TPS3 algorithm is applied with an APWT value of 120 seconds, the intersection can be operated safely and efficiently showing improvement of 2.9 sec/veh compared to the TPS0 algorithm and 2.6 sec/veh compared to the TPS1 algorithm during the delay comparison period.

The graph of delay versus APWT during the delay comparison period for the pedestrian volume is shown in Figure D-2.

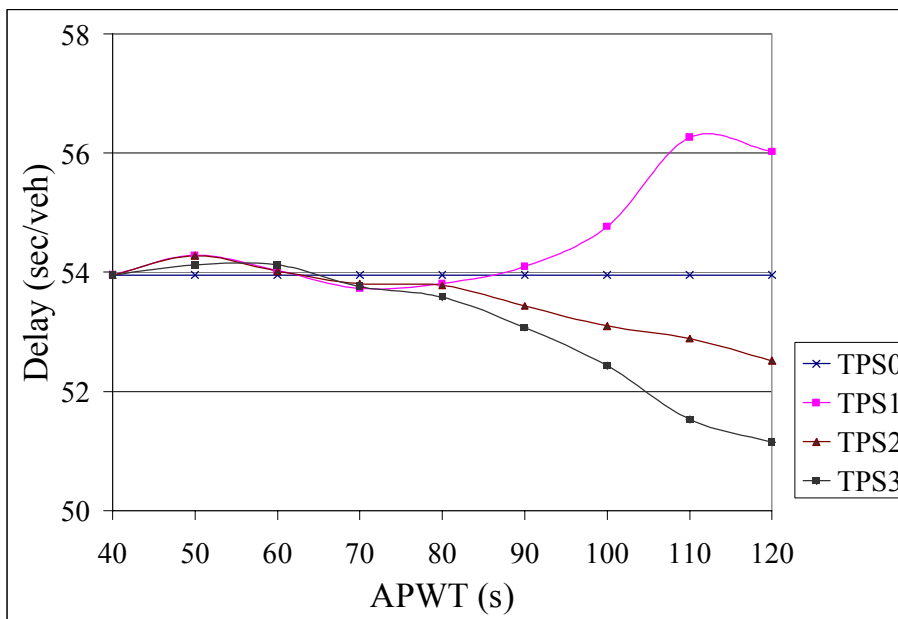


FIGURE D-2 Average Delay versus APWT for each TPS Algorithm (Delay Comparison Period; Pedestrian Phase Active Scenario; and Random Train Arrival Time)

Duncan's multiple range test was performed to compare each pair among the four TPS algorithms. Experimentwise error rate was set to 0.06, which means that the common level of significance per test is 0.01. The results of the delay comparison period for the pedestrian phase active scenario are shown in Table D-4. The table only shows the test results having a statistical difference between the TPS algorithms.

TABLE D-4 Results of Duncan Test between TPS Algorithms (Delay Comparison Period¹; Pedestrian Phase Active Scenario; and Random Train Arrival Time)

APWT ²	Algorithm Comparison		Mean (sec/veh)		Test Statistic	Critical Value	Result
	Algo.1	Algo.2	Algo.1	Algo.2			
90	TPS3	TPS1	53.1	54.1	1.03	0.82	Reject H ₀ ³
	TPS3	TPS0	53.1	54.0	0.89	0.80	Reject H ₀
100	TPS3	TPS1	52.4	54.8	2.34	1.03	Reject H ₀
	TPS3	TPS0	52.4	54.0	1.52	1.00	Reject H ₀
	TPS2	TPS1	53.1	54.8	1.67	1.00	Reject H ₀
110	TPS3	TPS1	51.5	56.3	4.74	1.28	Reject H ₀
	TPS3	TPS0	51.5	54.0	2.43	1.24	Reject H ₀
	TPS3	TPS2	51.5	52.9	1.36	1.19	Reject H ₀
	TPS2	TPS1	52.9	56.3	3.38	1.24	Reject H ₀
	TPS0	TPS1	54.0	56.3	2.31	1.19	Reject H ₀
120	TPS3	TPS1	51.1	56.0	4.87	1.43	Reject H ₀
	TPS3	TPS0	51.1	54.0	2.80	1.39	Reject H ₀
	TPS3	TPS2	51.1	52.5	1.37	1.34	Reject H ₀
	TPS2	TPS1	52.5	56.0	3.51	1.39	Reject H ₀
	TPS2	TPS0	52.5	54.0	1.44	1.34	Reject H ₀
	TPS0	TPS1	54.0	56.0	2.07	1.34	Reject H ₀

¹: 600 to 1320 seconds

²: Advance preemption warning time

³: Statistically different between two means at 0.01 level of significance

It was found that the delay in the TPS3 algorithm is smaller than the delay in the TPS0 and TPS1 algorithms at APWT values of 90, 100, 110, and 120 seconds. It also was found that the best delay in the TPS3 algorithm was smaller statistically at the 0.06 level of significance than the best delay in the TPS0, TPS1, and TPS2 algorithms, respectively. Therefore, it can be concluded that for the pedestrian phase active scenario the TPS3 algorithm with an APWT value of 120 seconds is the best operation strategy for both safety and efficiency. Moreover, the TPS3 algorithm still has a benefit in terms of delay in the normal operation case. These results can be interpreted that the TPS3 algorithm has a benefit by reducing the delay even at the condition where there is no safety problem.

D.2.1.2 Analysis Period; Pedestrian Phase Active Scenario

The average delay during the analysis period for the pedestrian phase active scenario is shown in Table D-5.

TABLE D-5 Average Delay (Analysis Period¹; Pedestrian Phase Active Scenario; and Random Train Arrival Time)

APWT ²	TPS0 (sec/veh)	TPS1 (sec/veh)	TPS2 (sec/veh)	TPS3 (sec/veh)
	51.3			
40		51.3	51.3	51.3
50		51.4	51.3	51.1
60		51.2	51.3	51.3
70		51.0	51.1	51.2
80		51.0	51.0	51.0
90		51.2	51.0	50.6
100		51.9	51.2	50.7
110		52.1	50.7	50.3
120		51.6	50.5	50.2
Mean	51.3	51.4	51.0	50.9

¹: 6 to 60 minutes

²: Advance preemption warning time

Bold: Minimum delay for each TPS algorithm

It can be seen that the average delay for the base case (TPS0) was 51.3 sec/veh. As shown in Table D-1 there was also a safety problem in 36 of 90 simulations. When the TPS1 algorithm was used, the smallest average delay was 51.0 sec/veh and occurred at the APWT values of 70 and 80 seconds. However, for this situation there was a safety problem in 7 and 1 out of the 90 preemption cases, respectively, as shown in Table D-1. When the TPS2 algorithm was used, the smallest average delay was 50.5 sec/veh and occurred at an APWT value of 120 seconds. However, there was still a safety problem in 2 out of 90 preemption cases. The minimum delay for the analysis period was found as 50.2 sec/veh with the TPS3 algorithm at an APWT value of 120 seconds. Therefore, when the TPS3 algorithm is applied with an APWT value of 120 seconds, the

intersection can be operated safely and efficiently showing improvement of 1.1 sec/veh compared to the TPS0 algorithm, 0.8 sec/veh in delay compared to the TPS1 algorithm, and 0.3 sec/veh in delay compared to the TPS2 algorithm.

The graph of delay versus APWT during the analysis period for the pedestrian volume is shown in Figure D-3.

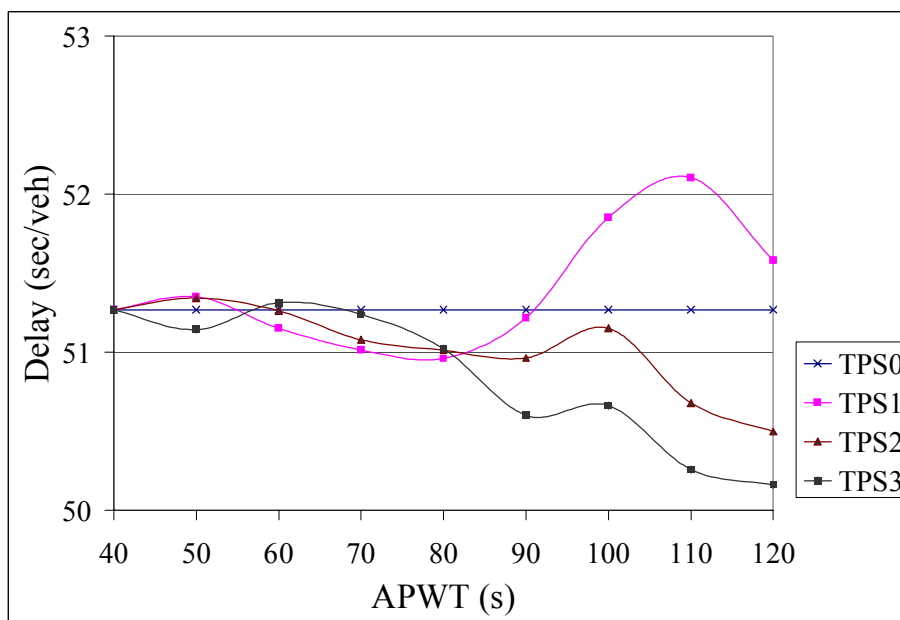


FIGURE D-3 Average Delay versus APWT for Each TPS Algorithm (Analysis Period; Pedestrian Phase Active Scenario; and Random Train Arrival Time)

Duncan's multiple range test was performed to compare each pair among the four TPS algorithms. Experimentwise error rate was set to 0.06, which means that the common level of significance per test is 0.01. The results of the analysis period at the pedestrian phase active scenario are shown in Table D-6. The table also shows only the test results having a statistical difference between TPS algorithms.

TABLE D-6 Results of Duncan Test between TPS Algorithms (Analysis Period¹; Pedestrian Phase Active Scenario; and Random Train Arrival Time)

APWT ²	Algorithm Comparison		Mean (sec/veh)		Test Statistic	Critical Value	Result
	Algo.1	Algo.2	Algo.1	Algo.2			
100	TPS3	TPS1	50.7	51.9	1.19	0.97	Reject H ₀ ³
110	TPS3	TPS1	50.3	52.1	1.84	0.98	Reject H ₀
	TPS3	TPS0	50.3	51.3	1.01	0.95	Reject H ₀
	TPS2	TPS1	50.7	52.1	1.42	0.95	Reject H ₀
120	TPS3	TPS1	50.2	51.6	1.42	1.04	Reject H ₀
	TPS3	TPS0	50.2	51.3	1.11	1.01	Reject H ₀
	TPS2	TPS1	50.5	51.6	1.08	1.01	Reject H ₀

¹: 6 to 60 minutes

²: Advance preemption warning time

³: Statistically different between two means at 0.01 level of significance

As expected, fewer differences between the TPS algorithms were detected during the analysis period than during the delay comparison period. It was found that the delay in the TPS3 algorithm is smaller than the delay in the TPS0 algorithm at APWT values of 110 and 120 seconds and is smaller than the delay in the TPS1 at APWT values of 100, 110, and 120 seconds. It also was found that the delay in the best TPS3 algorithm is not different statistically at the 0.06 level of significance from the smallest delay identified for the TPS1 algorithm; however, it is smaller than the delay for the TPS0 algorithm. Therefore, the same conclusion to the delay comparison period can be induced, that is, the TPS3 algorithm has a benefit by reducing the delay even in the normal operation case.

D.2.1.3 Delay Comparison Period; Pedestrian Phase Inactive Scenario

The average delay during the delay comparison period for the pedestrian phase inactive scenario is shown in Table D-7.

TABLE D-7 Average Delay (Delay Comparison Period¹; Pedestrian Phase Inactive Scenario; and Random Train Arrival Time)

APWT ²	TPS0 (sec/veh)	TPS1 (sec/veh)	TPS2 (sec/veh)	TPS3 (sec/veh)
	48.9			
40		48.9	48.9	48.9
50		49.4	49.4	49.1
60		49.4	49.4	49.1
70		48.8	49.0	48.8
80		48.7	48.8	48.5
90		48.2	47.9	48.1
100		47.7	47.4	47.5
110		47.8	47.0	46.8
120		47.7	46.3	46.2
Mean	48.9	48.5	48.2	48.1

¹: 600 to 1320 seconds

²: Advance preemption warning time

Bold: Minimum delay for each TPS algorithm

When the preemption was operated without a TPS algorithm, the average delay was 48.9 sec/veh. When the TPS1 algorithm was used, the smallest average delay was 47.7 sec/veh and occurred at APWT values of 100 and 120 seconds. When the TPS2 algorithm was used, the smallest average delay was 46.3 sec/veh and occurred at an APWT value of 120 seconds. When the TPS3 algorithm was applied with an APWT value of 120 seconds, the minimum average delay was 46.2 sec/veh. Therefore, the best TPS3 algorithm delay was 2.7, 1.5, and 0.1 seconds lower than the best delay identified for the TPS0, TPS1, and TPS2 algorithms, respectively.

The graph of delay versus APWT during the delay comparison period for the pedestrian phase inactive scenario is shown in Figure D-4.

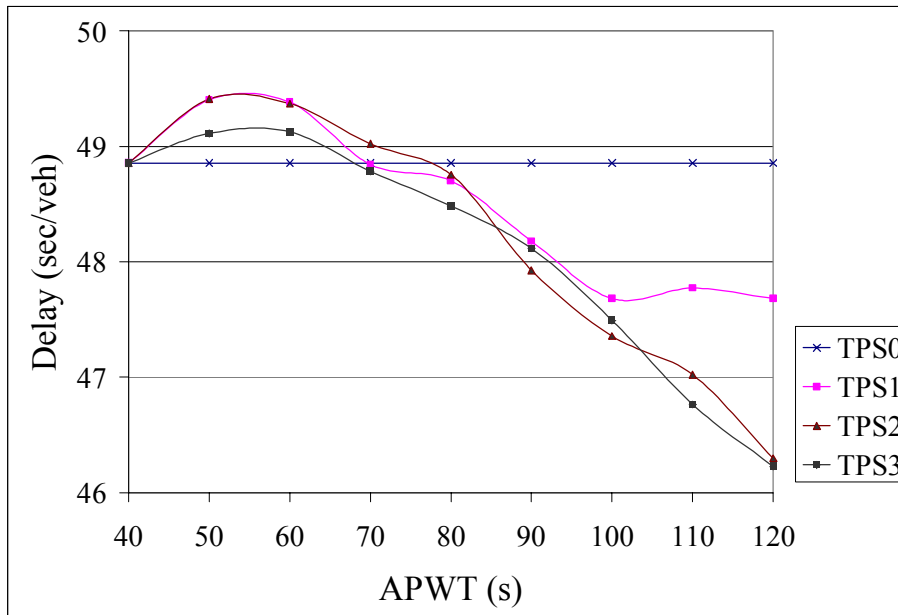


FIGURE D-4 Average Delay versus APWT for Each TPS Algorithm (Delay Comparison Period; Pedestrian Phase Inactive Scenario; and Random Train Arrival Time)

Duncan's multiple range test was performed to compare each pair among the four TPS algorithms. Experimentwise error rate was set to 0.06, which means that the common level of significance per test is 0.01. The results of the delay comparison period at the pedestrian phase inactive scenario are shown in Table D-8. The table also shows only the test results having a statistical difference between TPS algorithms.

TABLE D-8 Results of Duncan Test between TPS Algorithms (Delay Comparison Period¹; Pedestrian Phase Inactive Scenario; and Random Train Arrival Time)

APWT ²	Algorithm Comparison		Mean (sec/veh)		Test Statistic	Critical Value	Result
	Algo.1	Algo.2	Algo.1	Algo.2			
50	TPS0	TPS2	48.9	49.4	0.55	0.38	Reject H ₀
	TPS0	TPS1	48.9	49.4	0.55	0.37	Reject H ₀
90	TPS2	TPS0	47.9	48.9	0.93	0.74	Reject H ₀
	TPS3	TPS0	48.1	48.9	0.74	0.72	Reject H ₀
100	TPS2	TPS0	47.4	48.9	1.50	0.86	Reject H ₀
	TPS3	TPS0	47.5	48.9	1.36	0.83	Reject H ₀
	TPS1	TPS0	47.7	48.9	1.18	0.80	Reject H ₀
110	TPS3	TPS0	46.8	48.9	2.09	1.00	Reject H ₀
	TPS3	TPS1	46.8	47.8	1.01	0.97	Reject H ₀
	TPS2	TPS0	47.0	48.9	1.83	0.97	Reject H ₀
	TPS1	TPS0	47.8	48.9	1.08	0.94	Reject H ₀
120	TPS3	TPS0	46.2	48.9	2.63	1.00	Reject H ₀
	TPS3	TPS1	46.2	47.7	1.45	0.98	Reject H ₀
	TPS2	TPS0	46.3	48.9	2.56	0.98	Reject H ₀
	TPS2	TPS1	46.3	47.7	1.38	0.94	Reject H ₀
	TPS1	TPS0	47.7	48.9	1.17	0.94	Reject H ₀

¹: 600 to 1320 seconds

²: Advance preemption warning time

³: Statistically different between two means at 0.01 level of significance

It was found that the delay in the TPS3 algorithm is smaller than the delay in the TPS0 algorithm at APWT values of 90, 100, 110, and 120 seconds and smaller than the delay in the TPS1 algorithm at APWT values of 110 and 120 seconds. It also was found that the best delay in the TPS3 algorithm was smaller than the delay for the TPS0 algorithm and the best delay identified for the TPS1 algorithm statistically at the 0.06 level of significance. The delay in the TPS3 algorithm with an APWT value of 120 seconds decreased compared to the delay for the TPS0 algorithm and the best delay identified for the TPS1 algorithm. Therefore, it can be concluded that for the pedestrian phase inactive scenario the TPS3 algorithm with an APWT value of 120 seconds is the best operation strategy for efficiency. Conclusively, even if a preemption is initiated during

the period that does not serve a pedestrian clearance phase, the TPS3 algorithm still has a benefit in terms of delay.

D.2.1.4 Analysis Period; Pedestrian Phase Inactive Scenario

The average delay during the analysis period for the pedestrian phase inactive scenario is shown in Table D-9.

TABLE D-9 Average Delay (Analysis Period¹; Pedestrian Phase Inactive Scenario; and Random Train Arrival Time)

APWT ²	TPS0 (sec/veh)	TPS1 (sec/veh)	TPS2 (sec/veh)	TPS3 (sec/veh)
	42.7			
40		42.7	42.7	42.7
50		42.8	42.8	42.7
60		42.7	42.6	42.7
70		42.7	42.6	42.6
80		42.7	42.8	42.5
90		42.6	42.5	42.5
100		42.5	42.3	42.4
110		42.6	42.2	42.3
120		42.6	42.1	42.1
Mean	42.7	42.7	42.5	42.5

¹: 6 to 60 minutes

²: Advance preemption warning time

Bold: Minimum delay for each TPS algorithm

For the pedestrian phase inactive scenario, the difference in delay between the TPS algorithms was reduced compared to the pedestrian phase active scenario. The average delay for the base case (TPS0) was 42.7 sec/veh and there was no safety problem at all because there was no pedestrian. When the TPS1 algorithm was used, the smallest average delay was 42.5 sec/veh and occurred at an APWT value of 100 seconds. When the TPS2 algorithm was used, the minimum average delay was 42.1 sec/veh and occurred at an APWT value of 120 seconds. When the TPS3 algorithm was applied with an APWT value of 120 seconds, delay was the same as the TPS2 algorithm applied with

an APWT value of 120 seconds. Therefore, when the TPS2 or TPS3 algorithm was applied with an APWT value of 120 seconds, delay was improved by 0.6 sec/veh compared to the TPS0 algorithm, and 0.4 sec/veh compared to the TPS1 algorithm. Therefore, it can be concluded that the effect of the TPS algorithms and the APWT on delay decreases considerably when there is no pedestrian in the intersection.

The graph of delay versus APWT during the analysis period for the no-pedestrian volume is shown in Figure D-5.

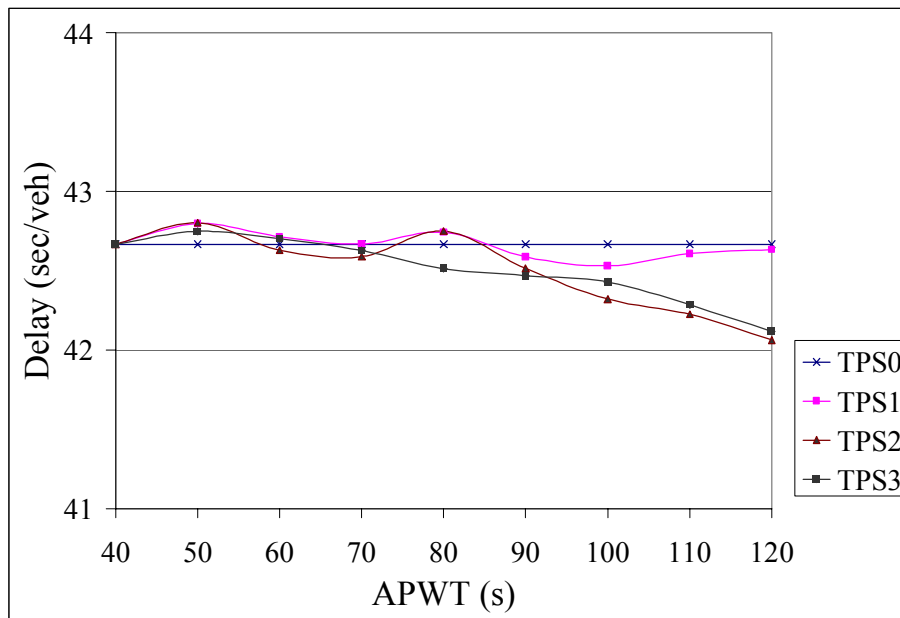


FIGURE D-5 Average Delay versus APWT for Each TPS Algorithm (Analysis Period; Pedestrian Phase Inactive Scenario; and Random Train Arrival Time)

Duncan's multiple range test was performed to compare each pair among the four TPS algorithms. Experimentwise error rate was set to 0.06, which means that the common level of significance per test is 0.01. The results of the analysis period at the pedestrian

phase inactive scenario are shown in Table D-10. The table also shows only the test results having a statistical difference between TPS algorithms.

TABLE D-10 Results of Duncan Test between TPS Algorithms (Analysis Period¹; Pedestrian Phase Inactive Scenario; and Random Train Arrival Time)

APWT ²	Algorithm Comparison		Mean (sec/veh)		Test Statistic	Critical Value	Result
	Algo.1	Algo.2	Algo.1	Algo.2			
120	TPS2	TPS0	42.1	42.7	0.60	0.55	Reject H ₀ ³
	TPS2	TPS1	42.1	42.6	0.57	0.53	Reject H ₀
	TPS3	TPS0	42.1	42.7	0.55	0.53	Reject H ₀
	TPS3	TPS1	42.1	42.6	0.52	0.51	Reject H ₀

¹: 6 to 60 minutes

²: Advance preemption warning time

³: Statistically different between two means at 0.01 level of significance

When there is no pedestrian volume, a difference in delay between the TPS algorithms occurred only at an APWT value of 120 seconds. Although the delay in the TPS2 and TPS3 algorithms is smaller than the delay in the TPS0 and TPS1 algorithms, there are no differences in delay between the TPS2 and TPS3 algorithms and between the TPS0 and TPS1 algorithms. It also was found that the best delay in the TPS3 algorithm is smaller statistically at the 0.06 level of significance than the delay in the TPS0 algorithm; however, it is not different from the delay in the TPS1 algorithm. Therefore, it can be concluded that even if the effect of the TPS algorithms and the APWT on delay decreases considerably when there is no pedestrian in the intersection, the TPS3 algorithm with an APWT value of 120 seconds can decrease the delay compared to the TPS0 algorithms even at the condition where there is no safety problem originally.

D.2.2 Effect of Pedestrians

When pedestrian volume was 400 ped/h, the average delays were 51.3, 51.4, 51.0, and 50.9 sec/veh for TPS0, TPS1, TPS2, and TPS3, respectively. However, when there was no pedestrian in the intersection, delay decreased to 42.7, 42.7, 42.5, and 42.5 sec/veh for TPS0, TPS1, TPS2, and TPS3, respectively, like the worst case in Section 6.2.

To check statistically the difference between the pedestrian volume levels, a paired t-test was performed at the 0.05 significance level. The null hypotheses and alternative hypotheses were set as $H_0: \text{Delay}_{400\text{ped/h}} = \text{Delay}_{0\text{ped/h}}$ and $H_1: \text{Delay}_{400\text{ped/h}} > \text{Delay}_{0\text{ped/h}}$, respectively. The results for both the analysis period and the delay comparison period are shown in Table D-11.

TABLE D-11 Results of Paired t-Test between Two Pedestrian Volumes for Random Train Arrival Time

	Pedestrian Scenario Comparison		Mean (sec/veh)		Test Statistic	Critical Value	Result
			400 ped/h	0 ped/h			
Analysis Period ¹	400 ped/h	0 ped/h	51.1	42.6	93.16	1.96	Reject H_0 ³
Comparison Period ²	400 ped/h	0 ped/h	53.7	48.3	81.07	1.96	Reject H_0

¹: 6 to 60 minutes

²: 600 to 1320 seconds

³: Statistically different between two means at 0.05 level of significance

It can be concluded that the delay in the simulation with the pedestrian phase active scenario is greater than the delay in the simulation with the pedestrian phase inactive scenario for both the analysis and delay comparison periods. As seen in the means and the test statistics, pedestrians can have a significant effect on the delay performance of the intersection. The main cause of the difference is the same as the case that is illustrated in Section 6.2.

D.2.3 Effect of Train Speed Profile

D.2.3.1 Delay Comparison Period; Pedestrian Phase Active Scenario

The average delay by train speed groups is shown in Table D-12 during the delay comparison period for the pedestrian phase active scenarios. The detailed results of the average delay depending on APWT also are shown in Table D-13.

TABLE D-12 Average Delay by Group (Delay Comparison Period¹; Pedestrian Phase Active Scenario; and Random Train Arrival Time)

	Train Group	TPS0 (sec/veh)	TPS1 (sec/veh)	TPS2 (sec/veh)	TPS3 (sec/veh)	Average
Average By Group	Group 1	58.3	59.4	58.4	57.6	58.4
	Group 2	52.9	53.2	52.6	52.2	52.7
	Group 3	50.6	51.1	49.6	49.4	50.2
Average		54.0	54.6	53.5	53.1	53.8

¹: 600 to 1320 seconds

In all of the TPS algorithms, Group 3 has the smallest delay with an average of 50.2 sec/veh and Group 1 has the largest delay with an average of 58.4 sec/veh. The difference in delay between Group 1 and Group 3 was 7.7 sec/veh for the TPS0 algorithm, 8.3 sec/veh for the TPS1 algorithm, 8.8 sec/veh for the TPS2 algorithm, and 8.2 sec/veh for the TPS3 algorithm for the pedestrian phase active scenario.

TABLE D-13 Average Delay by Group and APWT (Delay Comparison Period¹; Pedestrian Phase Active Scenario; and Random Train Arrival Time)

APWT ²	Train Group	TPS0 (sec/veh)	TPS1 (sec/veh)	TPS2 (sec/veh)	TPS3 (sec/veh)	Ave. By Group	Ave.
40	Group 1	58.3	58.3	58.3	58.3	58.3	54.0
	Group 2	52.9	52.9	52.9	52.9	52.9	
	Group 3	50.6	50.6	50.6	50.6	50.6	
50	Group 1		59.2	59.2	58.9	59.1	54.2
	Group 2		52.8	52.8	52.9	52.8	
	Group 3		50.8	50.8	50.6	50.7	
60	Group 1		59.2	59.2	59.1	59.2	54.1
	Group 2		52.6	52.4	52.8	52.6	
	Group 3		50.4	50.5	50.4	50.4	
70	Group 1		58.7	58.7	58.7	58.7	53.8
	Group 2		52.5	52.6	52.7	52.6	
	Group 3		50.0	50.1	49.9	50.0	
80	Group 1		58.9	58.8	58.3	58.7	53.7
	Group 2		52.6	52.7	52.8	52.7	
	Group 3		49.9	49.9	49.7	49.8	
90	Group 1		59.2	58.2	57.4	58.3	53.5
	Group 2		53.1	52.9	52.4	52.8	
	Group 3		50.1	49.1	49.4	49.5	
100	Group 1		59.6	57.8	56.2	57.9	53.4
	Group 2		53.6	52.8	52.0	52.8	
	Group 3		51.1	48.7	49.1	49.6	
110	Group 1		60.9	57.9	55.7	58.2	53.6
	Group 2		54.6	52.1	50.9	52.5	
	Group 3		53.3	48.6	48.0	50.0	
120	Group 1		60.7	57.3	56.2	58.1	53.2
	Group 2		53.9	51.8	50.2	52.0	
	Group 3		53.4	48.4	47.1	49.6	
Ave. By Group	Group 1	58.3	59.4	58.4	57.6	58.4	53.8
	Group 2	52.9	53.2	52.6	52.2	52.7	
	Group 3	50.6	51.1	49.6	49.4	50.2	
Average		54.0	54.6	53.5	53.1	53.8	

¹: 600 to 1320 seconds

²: Advance preemption warning time

To check statistically the difference among the train speed groups, Duncan's multiple range test was performed. Experimentwise error rate was set to 0.03, which means that the common level of significance per test is 0.01. The results are shown in Table C-14.

TABLE D-14 Results of Duncan Test between Train Speed Groups (Delay Comparison Period¹; Pedestrian Phase Active Scenario; and Random Train Arrival Time)

Group Comparison		Mean (sec/veh)		Test Statistic	Critical Value	Result
		1 st Group	2 nd Group			
Group3	Group1	50.1	58.5	8.42	0.81	Reject H ₀ ²
Group3	Group2	50.1	52.7	2.60	0.78	Reject H ₀
Group2	Group1	52.7	58.5	5.82	0.78	Reject H ₀

¹: 600 to 1320 seconds,

²: Statistically different between two means at 0.01 level of significance

It was found that the delay in Group 3 is smaller than the delay in Groups 1 and 2 and that the delay in Group 2 is smaller than the delay in Group 1. Therefore, it can be concluded that as train speed increases, the intersection is operated better for the pedestrian phase active scenario during the delay comparison period.

D.2.3.2 Analysis Period; Pedestrian Phase Active Scenario

The average delay by train speed groups is shown in Table D-15 during the analysis period for the pedestrian phase active scenarios. The detailed results of the average delay depending on APWT also are shown in Table D-16.

TABLE D-15 Average Delay by Group (Analysis Period¹; Pedestrian Phase Active Scenario; and Random Train Arrival Time)

	Train Group	TPS0 (sec/veh)	TPS1 (sec/veh)	TPS2 (sec/veh)	TPS3 (sec/veh)	Average
Average By Group	Group 1	52.9	53.2	53.0	52.9	53.0
	Group 2	51.8	51.9	51.7	51.4	51.7
	Group 3	49.0	49.0	48.4	48.2	48.7
Average		51.3	51.4	51.0	50.9	51.1

¹: 6 to 60 minutes

In all of the TPS algorithms, Group 3 has the smallest delay with an average of 48.7 sec/veh and Group 1 has the largest delay with an average of 53.0 sec/veh. The difference in delay between Group 1 and Group 3 was 3.9 sec/veh for the TPS0 algorithm, 4.2 sec/veh for the TPS1 algorithm, 4.6 sec/veh for the TPS2 algorithm, and 4.7 sec/veh for the TPS3 algorithm.

TABLE D-16 Average Delay by Group and APWT (Analysis Period¹; Pedestrian Phase Active Scenario; and Random Train Arrival Time)

APWT ²	Train Group	TPS0 (sec/veh)	TPS1 (sec/veh)	TPS2 (sec/veh)	TPS3 (sec/veh)	Ave. By Group	Ave.
40	Group 1	52.9	52.9	52.9	52.9	52.9	51.3
	Group 2	51.8	51.8	51.8	51.8	51.8	
	Group 3	49.0	49.0	49.0	49.0	49.0	
50	Group 1		53.1	53.1	52.5	52.9	51.3
	Group 2		52.0	51.9	51.9	51.9	
	Group 3		49.0	49.0	49.0	49.0	
60	Group 1		53.2	53.3	53.3	53.2	51.2
	Group 2		51.7	51.8	51.8	51.8	
	Group 3		48.6	48.7	48.8	48.7	
70	Group 1		52.9	52.7	53.2	53.0	51.1
	Group 2		51.5	51.7	51.6	51.6	
	Group 3		48.6	48.8	48.9	48.8	
80	Group 1		53.6	53.0	53.2	53.3	51.0
	Group 2		51.1	51.6	51.4	51.4	
	Group 3		48.2	48.5	48.5	48.4	
90	Group 1		53.6	53.1	52.9	53.2	50.9
	Group 2		51.9	52.0	51.2	51.7	
	Group 3		48.1	47.8	47.8	47.9	
100	Group 1		53.7	53.6	53.2	53.5	51.2
	Group 2		52.7	52.3	51.3	52.1	
	Group 3		49.2	47.6	47.5	48.1	
110	Group 1		53.7	53.3	52.7	53.2	51.0
	Group 2		52.2	50.8	50.8	51.3	
	Group 3		50.4	47.9	47.3	48.5	
120	Group 1		52.5	52.3	52.6	52.5	50.7
	Group 2		52.3	51.3	50.7	51.4	
	Group 3		49.9	47.9	47.3	48.4	
Ave. By Group	Group 1	52.9	53.2	53.0	52.9	53.0	51.1
	Group 2	51.8	51.9	51.7	51.4	51.7	
	Group 3	49.0	49.0	48.4	48.2	48.7	
Average		51.3	51.4	51.0	50.9	51.1	

¹: 6 to 60 minutes

²: Advance preemption warning time

To check statistically the difference among the train speed groups, Duncan's multiple range test was performed. Experimentwise error rate was set to 0.03, which means that the common level of significance per test is 0.01. The results are shown in Table D-17.

TABLE D-17 Results of Duncan Test between Train Speed Groups (Analysis Period¹; Pedestrian Phase Active Scenario; and Random Train Arrival Time)

Group Comparison		Mean (sec/veh)		Test Statistic	Critical Value	Result
		1 st Group	2 nd Group			
Group3	Group1	48.6	53.1	4.52	0.94	Reject H ₀ ²
Group3	Group2	48.6	51.7	3.12	0.90	Reject H ₀
Group2	Group1	51.7	53.1	1.40	0.90	Reject H ₀

¹: 6 to 60 minutes,

²: Statistically different between two means at 0.01 level of significance

It was found that the delay in Group 3 is smaller than the delay in Groups 1 and 2 and that the delay in Group 2 is smaller than the delay in Group 1. Therefore, the same conclusion to the delay comparison period can be induced, that is, as train speed increases, the intersection is operated better for the pedestrian phase active scenario

D.2.3.3 Delay Comparison Period; Pedestrian Phase Inactive Scenario

When there is no pedestrian in the intersection, the effect of train speed also was evaluated. The average delay by train speed groups is shown in Table D-18 during the delay comparison period for the pedestrian phase inactive scenario. The detailed results of the average delay depending on APWT also are shown in Table D-19.

TABLE D-18 Average Delay by Group (Delay Comparison Period¹; Pedestrian Phase Inactive Scenario; and Random Train Arrival Time)

	Train Group	TPS0 (sec/veh)	TPS1 (sec/veh)	TPS2 (sec/veh)	TPS3 (sec/veh)	Average
Average By Group	Group 1	52.8	52.8	52.7	52.2	52.6
	Group 2	48.2	47.8	47.4	47.4	47.7
	Group 3	45.6	44.9	44.5	44.7	45.0
Average		48.9	48.5	48.2	48.1	48.4

¹: 600 to 1320 seconds

Although the delay is lessened for the pedestrian phase inactive scenario compared to the pedestrian phase active scenario, the trend is the same for the pedestrian phase active scenario. In all of the TPS algorithms, Group 3 has the smallest delay with an average of 45.0 sec/veh and Group 1 has the largest delay with an average of 52.6 sec/veh. The difference in delay between Group 1 and Group 3 was 7.2 sec/veh for the TPS0 algorithm, 7.9 sec/veh for the TPS1 algorithm, 8.2 sec/veh for the TPS2 algorithm, and 7.5 sec/veh for the TPS3 algorithm for the pedestrian phase inactive scenario.

TABLE D-19 Average Delay by Group and APWT (Delay Comparison Period¹; Pedestrian Phase Inactive Scenario; and Random Train Arrival Time)

APWT ²	Train Group	TPS0 (sec/veh)	TPS1 (sec/veh)	TPS2 (sec/veh)	TPS3 (sec/veh)	Ave. By Group	Ave.
40	Group 1	52.8	52.8	52.8	52.8	52.8	48.9
	Group 2	48.2	48.2	48.2	48.2	48.2	
	Group 3	45.6	45.6	45.6	45.6	45.6	
50	Group 1		54.0	54.0	53.6	53.9	49.3
	Group 2		48.3	48.3	48.2	48.2	
	Group 3		45.9	45.9	45.6	45.8	
60	Group 1		53.8	53.8	53.8	53.8	49.3
	Group 2		48.4	48.3	48.2	48.3	
	Group 3		45.9	46.0	45.4	45.8	
70	Group 1		53.2	53.6	53.0	53.3	48.9
	Group 2		48.3	48.3	48.3	48.3	
	Group 3		45.0	45.2	45.1	45.1	
80	Group 1		53.3	53.5	52.5	53.1	48.6
	Group 2		48.1	48.0	48.0	48.0	
	Group 3		44.8	44.8	45.0	44.8	
90	Group 1		52.4	52.3	52.0	52.2	48.1
	Group 2		47.8	47.3	47.5	47.5	
	Group 3		44.3	44.2	44.8	44.5	
100	Group 1		51.6	51.6	51.0	51.4	47.5
	Group 2		47.5	46.9	46.7	47.0	
	Group 3		44.0	43.5	44.8	44.1	
110	Group 1		52.2	51.7	50.8	51.6	47.2
	Group 2		46.8	46.2	46.1	46.4	
	Group 3		44.4	43.1	43.4	43.6	
120	Group 1		52.1	50.8	50.6	51.2	46.7
	Group 2		46.5	45.5	45.4	45.8	
	Group 3		44.5	42.6	42.7	43.3	
Ave. By Group	Group 1	52.8	52.8	52.7	52.2	52.6	48.4
	Group 2	48.2	47.8	47.4	47.4	47.7	
	Group 3	45.6	44.9	44.5	44.7	45.0	
Average		48.9	48.5	48.2	48.1	48.4	

¹: 600 to 1320 seconds

²: Advance preemption warning time

To check statistically the difference among the train speed groups, Duncan's multiple range test also was performed. Experimentwise error rate was set to 0.03, which means that the common level of significance per test is 0.01. The results are shown in Table D-20.

TABLE D-20 Results of Duncan Test between Train Speed Groups (Delay Comparison Period¹; Pedestrian Phase Inactive Scenario; and Random Train Arrival Time)

Group Comparison		Mean (sec/veh)		Test Statistic	Critical Value	Result
		1 st Group	2 nd Group			
Group3	Group1	44.8	52.6	7.81	0.78	Reject H ₀ ²
Group3	Group2	44.8	47.6	2.79	0.75	Reject H ₀
Group2	Group1	47.6	52.6	5.02	0.75	Reject H ₀

¹: 600 to 1320 seconds

²: Statistically different between two means at 0.01 level of significance

It was found that the delay in Group 3 is smaller than the delay in Groups 1 and 2, and the delay in Group 2 is smaller than the delay in Group 1 for the pedestrian phase inactive scenario. Therefore, it also can be concluded that as train speed increases, the intersection is operated more efficiently for the pedestrian phase inactive scenario.

D.2.3.4 Analysis Comparison Period; Pedestrian Phase Inactive Scenario

The average delay by train speed groups is shown in Table D-21 during the analysis period for the pedestrian phase inactive scenarios. The detailed results of the average delay depending on APWT also are shown in Table D-22.

TABLE D-21 Average Delay by Group (Analysis Period¹; Pedestrian Phase Inactive Scenario; and Random Train Arrival Time)

	Train Group	TPS0 (sec/veh)	TPS1 (sec/veh)	TPS2 (sec/veh)	TPS3 (sec/veh)	Average
Average By Group	Group 1	44.4	44.2	44.0	44.0	44.2
	Group 2	42.6	42.9	42.7	42.7	42.7
	Group 3	41.0	40.9	40.8	40.8	40.9
Average		42.7	42.7	42.5	42.5	42.6

¹: 6 to 60 minutes

In all of the TPS algorithms, Group 3 has the smallest delay with an average of 40.9 sec/veh and Group 1 has the largest delay with an average of 44.2 sec/veh. The difference in delay between Group 1 and Group 3 was 3.4 sec/veh for the TPS0 algorithm, 3.3 sec/veh for the TPS1 algorithm, 3.2 sec/veh for the TPS2 algorithm, and 3.2 sec/veh for the TPS3 algorithm for the pedestrian phase inactive scenario.

TABLE D-22 Average Delay by Group and APWT (Analysis Period¹; Pedestrian Phase Inactive Scenario; and Random Train Arrival Time)

APWT ²	Train Group	TPS0 (sec/veh)	TPS1 (sec/veh)	TPS2 (sec/veh)	TPS3 (sec/veh)	Ave. By Group	Ave.
40	Group 1	44.4	44.4	44.4	44.4	44.4	42.7
	Group 2	42.6	42.6	42.6	42.6	42.6	
	Group 3	41.0	41.0	41.0	41.0	41.0	
50	Group 1		44.7	44.7	44.7	44.7	42.8
	Group 2		42.6	42.6	42.6	42.6	
	Group 3		41.1	41.1	41.0	41.0	
60	Group 1		44.2	44.2	44.5	44.3	42.7
	Group 2		42.8	42.7	42.6	42.7	
	Group 3		41.1	41.1	41.0	41.1	
70	Group 1		44.1	44.0	44.0	44.0	42.6
	Group 2		43.0	42.9	43.0	43.0	
	Group 3		40.8	40.9	40.9	40.9	
80	Group 1		44.2	44.1	43.9	44.0	42.7
	Group 2		43.0	43.0	42.7	42.9	
	Group 3		41.1	41.1	41.0	41.1	
90	Group 1		44.0	43.9	44.1	44.0	42.5
	Group 2		43.1	42.9	42.5	42.9	
	Group 3		40.7	40.7	40.8	40.7	
100	Group 1		43.8	43.6	43.9	43.8	42.4
	Group 2		43.0	42.8	42.7	42.8	
	Group 3		40.8	40.6	40.7	40.7	
110	Group 1		44.1	43.8	43.5	43.8	42.4
	Group 2		43.0	42.5	42.9	42.8	
	Group 3		40.8	40.4	40.5	40.5	
120	Group 1		44.1	43.4	43.3	43.6	42.3
	Group 2		42.8	42.4	42.5	42.6	
	Group 3		41.0	40.4	40.5	40.6	
Ave. By Group	Group 1	44.4	44.2	44.0	44.0	44.2	42.6
	Group 2	42.6	42.9	42.7	42.7	42.7	
	Group 3	41.0	40.9	40.8	40.8	40.9	
Average		42.7	42.7	42.5	42.5	42.6	

¹: 6 to 60 minutes

²: Advance preemption warning time

To check statistically the difference among the train speed groups, Duncan's multiple range test also was performed. Experimentwise error rate was set to 0.03, which means that the common level of significance per test is 0.01. The results are shown in Table D-23.

TABLE D-23 Results of Duncan Test between Train Speed Groups (Analysis Period¹; Pedestrian Phase Inactive Scenario; and Random Train Arrival Time)

Group Comparison		Mean (sec/veh)		Test Statistic	Critical Value	Result
		1 st Group	2 nd Group			
Group3	Group1	40.9	44.1	3.24	0.57	Reject H ₀ ²
Group3	Group2	40.9	42.7	1.89	0.55	Reject H ₀
Group2	Group1	42.7	44.1	1.34	0.55	Reject H ₀

¹: 6 to 60 minutes

²: Statistically different between two means at 0.01 level of significance

It was found that the delay in Group 3 is smaller than the delay in Groups 1 and 2, and the delay in Group 2 is smaller than the delay in Group 1 for the pedestrian phase inactive scenario. Therefore, the same conclusion to the delay comparison period can be induced, that is, as train speed increases, the intersection is operated more efficiently for the pedestrian phase inactive scenario

D.3 CONCLUDING REMARKS

In the simulation under the normal operation condition instead of the worst condition, which is the case where the pedestrian clearance phase is active at the onset of preemption in every simulation, the effect of the TPS3 algorithm on delay was almost same. That is, in both situations the TPS3 algorithm produced a minimum delay. Therefore, no matter when a preemption is initiated during a cycle, the TPS3 algorithm can operate the intersection without a safety problem and at the same time decrease the intersection delay.

VITA

HANSEON CHO

Texas Transportation Institute, Texas A&M University System

PERMANENT ADDRESS

Dong-A 3th APT. 305-1403, Yumchang-Dong Kangseo-Ku Seoul, 157-862, Republic of Korea.

EDUCATION

Ph.D., Civil Engineering, Texas A & M University, College Station, December 2003.

M.S., Transportation Engineering, Ajou University, Suwon, Korea, February 1995.

B.S., Industrial Engineering, Ajou University, Suwon, Korea, February 1993.

PUBLICATIONS & PRESENTATIONS

- Cho, H. and L.R. Rilett, "Forecasting Train Travel Time," Preprint 03-3918, Transportation Research Board 82nd Annual Meeting, Presented at conference. Recommended for Publication in Transportation Research Record, Washington, D.C., January, 2003.
- Cho, H. and L.R. Rilett, "Forecasting Train Arrival Time at Highway-Railroad Grade Crossings using Artificial Neural Networks," *Proceedings of the 7th International Conference on Applications of Advanced Technology in Transportation Conference*, Boston, Mass., August 2002, pp. 852-860.
- Wooldridge, M.D., D.B. Fambro, M.A. Brewer, R.J. Engelbrecht, S.R. Harry, and H. Cho. *Issues Related to Design of At-Grade Intersections Near Highway-Railroad Grade Crossings*, PSR 1845-S. Project No. 1845. Texas Transportation Institute, College Station, Tex., August 2001.
- Wooldridge, M.D., D.B. Fambro, M.A. Brewer, R.J. Engelbrecht, S.R. Harry, and H. Cho. *At-Grade Intersections Near Highway-Railroad Grade Crossings*, Research Report 1845-2. Texas Transportation Institute, College Station, Tex., August 2001.
- Wooldridge, M.D., D.B. Fambro, M.A. Brewer, R.J. Engelbrecht, S.R. Harry, and H. Cho. *Design Guidelines for At-Grade Intersections Near Highway-Railroad Grade Crossings*, Research Report 1845-3. Texas Transportation Institute, College Station, Tex., November 2000.